ENHANCING THE DELIVERY OF ONCOLYTIC VACCINIA VIRUS TO THE TUMORS OF HOSTS WITH PRE-EXISTING IMMUNITY

Laura Evgin

Thesis submitted to the

Faculty of Graduate and Postdoctoral Studies

in partial fulfillment of the requirements

for the Doctorate of Philosophy in Biochemistry

Department of Biochemistry, Microbiology & Immunology

Faculty of Medicine

University of Ottawa

Abstract

Oncolytic viruses (OVs) have begun to show their promise in the clinical setting, however these results have been predominantly associated with loco-regional administration of virus. The treatment of metastatic disease necessitates a systemic approach to virus delivery. The circulatory system, though, is a hostile environment for viruses and the advantages associated with intravenous (IV) delivery come at a heavy cost that must be understood and brokered. Pre-existing immunity, specifically through the function of antibody and complement, poses a significant hurdle to the IV delivery of infectious virus to dispersed tumor beds. This is of particular importance for therapeutic vaccinia viruses as a majority of today's cancer patients were vaccinated during the smallpox eradication campaign. *In vitro* neutralization assays of oncolytic vaccinia virus demonstrated that the antibodies elicited from smallpox vaccination, and also the anamnestic response in patients undergoing Pexa-Vec treatment, was minimally neutralizing in the absence of functional complement. Accordingly, in a Fischer rat model, complement depletion stabilized virus in the blood of pre-immunized hosts and correlated with improved delivery to mammary adenocarcinoma tumors. Complement depletion additionally enhanced infection of tumors following direct intratumoral injection of virus. The feasibility and safety of using a complement inhibitor, CP40, was tested in a cynomolgus macaque model. Immune animals saw an average 10-fold increase in infectious virus titer at an early point after the infusion, and a prolongation of the time during which infectious virus was still detectable in the blood. We have also demonstrated that vaccinia virus engages in promiscuous interactions with cells in the blood and that these interactions may be partially complement-dependent. Additionally,

we have translated this complement inhibition approach to other OV candidates and found that reovirus, measles virus and a virus pseudotyped with the LCMV glycoprotein all elicit antibodies, that to some degree, are dependent on complement activation to neutralize their target viruses. We show here that capitalizing on the complement dependence of anti-viral antibody with adjunct complement inhibitors may increase the effective dose to enable successful delivery of multiple rounds of OV in immune hosts.

Acknowledgements

I would like to thank my supervisor and mentor, Dr. John Bell for his support and faith in my abilities, the inspiration to pursue impactful clinical questions, and for providing me with amazing opportunities, including the tremendous experience to work with a non-human primate model. I would also like to thank Dr. Andrea McCart for hosting me in her lab and supporting the macaque experiment. I am very grateful to Dr. Sergio Acuna and Stacey Avery for their assistance during my time in Toronto. I would like to recognize the collaborative spirit of Dr. John Lambris who saw the value in our experiments and provided us with as much CP40 as we needed.

Special thanks to Christiano and Theresa for easing the process of working with rats and mice. To Dr. Harry Atkins and Dr. Robin Parks, thank you for your critical analysis and insightful experimental suggestions.

A sincere thank you to my friends and colleagues, Carolina, Monique, Vicki, and Chantal who have assisted with experiments and provided much thoughtful reflection, both scientific and otherwise. Thank you to Brian and Marie Claude for their careful edits of this thesis.

Lastly, I am grateful to my parents for their encouragement and for showing me that growth and success are only achieved by hard work. To my best friend and partner, Alex, your patience, understanding and confidence in me have been a remarkable source of strength.

Table of Contents

List of Abbreviations

5-FC	5-fluorocytosine
5-FU	5-fluorouracil
aHUS	Atypical hemolytic-uremic syndrome
ANOVA	Analysis of variance
BSA	Body surface area
CAF	Cancer associated fibroblast
CAR	Coxsackievirus and adenovirus receptor
CD	Cluster of differentiation
CDC	Centers for disease control
CPA	Cyclophosphamide
CR	Complement receptor
CRP	C reactive protein
CPT-11	Camptothecin-11 (irintotecan)
CTL	Cytotoxic lymphocyte
CTLA-4	Cytotoxic T-lymphocyte-associated protein-4
CVF	Cobra venom factor
DNA	Deoxyribonucleic acid
DC	Dendritic cell
EDTA	Ethylenediaminetetraacetic acid
EGFR	Epidermal growth factor receptor
ELISA	Enzyme-linked immunosorbent assay
EMT	Epithelial-mesenchymal transition
EOI	End of infusion
FACS	Fluorescence-activated cell sorting
FGF	Fibroblast growth factor
GM-CSF	Granulocyte-macrophage colony-stimulating factor
HIV	Human immunodeficiency virus
HLA	Human leukocyte antigen

HMGB-1	High-mobility group protein B1
HSP-70	Heat shock protein 70
HSV	Herpes simplex virus
IFN	Interferon
IHC	Immunohistochemistry
IL	Interleukin
IV	Intravenous
KC	Kuppfer cell
LCMV	Lymphocytic choriomeningitis virus
LDLR	Low-density lipoprotein receptor
MAC	Membrane attack complex
MASP	Mannan-binding lectin serine protease
MAVS	Mitochondrial antiviral-signaling protein
MBL	Mannan-binding lectin
MCP-1	Monocyte chemoattractant protein-1
MHC	Major histocompatibility complex
MG1	Maraba virus with point mutations in the M and G genes
MOI	Multiplicity of infection
MRB	Maraba virus
MVA	Modified vaccinia virus Ankara
MV-NIS	Measles virus encoding the sodium iodine symporter
NDV	Newcastle disease virus
NHP	Non-human primate
NIS	Sodium iodine symporter
NK	Natural killer (cell)
OV	Oncolytic virus
PBMC	Peripheral blood mononucleated cell
PBS	Phosphate buffered saline
PD-1	Programmed cell death protein 1

PD-L1	Programmed death-ligand 1
PDGF	Platelet-derived growth factor
Pexa-Vec	Pexastimogene devacirepvec
PFU	Plaque forming units
PMNC	Polymorphonuclear cell
PNH	Paroxysmal nocturnal hemoglobinuria
qPCR	Quantitative polymerase chain reaction
RECIST	Response Evaluation Criteria In Solid Tumors
RNA	Ribonucleic acid
SD	Standard deviation
SPECT-CT	Single-photon emission computerized tomography
TGF β	Transforming growth factor β
TK	Thymidine kinase
TLR	Toll-like receptor
T-Vec	Talimogene laherparepvec
VCP	Vaccinia virus complement control protein
VEGF	Vascular endothelial growth factor
VGF	Vaccinia growth factor
VSV	Vesicular stomatitis virus
VVdd	Vaccinia virus double deleted (TK and VGF genes)
WR	Western reserve strain vaccinia virus

List of Figures

List of Tables

1. Introduction

Preface

The clinical translation of oncolytic virotherapy has experienced success with intratumoral delivery, however the effective employment of systemically delivered oncolytic viruses (OVs) has been slower. A comprehensive understanding of the way in which OVs interact with blood components is necessary to develop strategies to efficiently deliver them to tumor beds. Therefore, the focus of this research project has been to develop the understanding of how OVs interact with blood components and the role of these interactions in viral neutralization. The sections that follow will describe how OVs are well-suited to take on the challenges of tumor debulking and the concomitant elicitation of an anti-tumoral immune response, and outline the current understanding of how these viruses interact with complement, antibodies, and circulating immune cells in the blood.

1.1 The heterogeneity and complexity of cancer

Carcinogenesis is a dynamic and multi-factorial process that is fundamentally a genetic disease, driven by mutation, epigenetic reprogramming, and supported by microenvironmental stromal remodeling. The collective impact of hereditary germ line defects and/or acquired somatic alterations to oncogenes, tumor-suppressor genes and stability genes all contribute to the growth of a cancer(1). Hanahan and Weinberg have defined the properties conferred by these alterations as the hallmarks of cancer, which

include the ability to sustain chronic proliferation and enable replicative immortality, independently of growth suppressors and apoptotic cues. This umbrella term also defines that neoplastic cells acquire invasive and metastatic properties and the ability to induce angiogenesis. Recently, two emerging hallmarks have been defined: the reprogramming of cellular metabolism and the ability to evade immunologic destruction in part via a process termed immunoediting(2, 3).

Genetic lesions can produce heterogeneity in both space and time to generate a dynamic and moving therapeutic target. In some disease states, for example colorectal cancer, the gene and growth pathway alterations that drive the transition from normal epithelium to invasive carcinoma follow a defined pattern and have been temporally mapped(4). Substantial genetic heterogeneity can also occur within the three-dimensional space of a single tumor, and can by phylogenetically mapped as in cases of renal carcinomas and associated metastatic sites(5). The resulting diverse genetic landscape maintains growth and drives the selective pressure that yields therapeutic resistance.

Cancer is a disease of genomic disfunction, and genes can become dysregulated at many levels. Integrated responses to extra- and intra-cellular signals are mediated by transcription factors whose actions are dependent on the accessibility of their target gene sequences. The configuration of chromatin structure, at the level of both DNA and histones is governed by epigenetic modifications. Both the distribution of marks as well as the activity of histone-modifying enzymes play key roles in the etiology and maintenance of the cancer cell phenotype and provide therapeutic targets(6). For example, mutations of the histone methyltransferase *MLL2* occurs in 32% of diffuse large B-cell lymphoma and close to 90% of cases of follicular lymphoma(7). Increasing

understanding of the epigenetic landscape of cancer has propelled the development of several classes of epigenetic cancer therapies including the approved DNA methyltransferase inhibitor, Azacitidine, and the histone deacetylase inhibitor, Vorinostat.(8).

Multiple genetically stable stromal cells that make up the complex architecture of the tumor sustain and enable the hallmark capabilities of the evolving tumor compartment. The congregation of players engaging in heterotypic communication includes the broad categories of cancer-associated fibroblasts (CAFs), infiltrating immune cells and angiogenic vascular cells. Through the secretion of growth factors such as VEGF, TGF-β, FGFs, PDGF, as well as many others, CAFs are able to orchestrate angiogenesis, support tumor cell proliferation and via the pleotropic factor TGF-β, induce an epithelial-mesenchymal transition (EMT) to support an invasive phenotype, and promote an immune suppressive microenvironment(9).

Infiltrating innate and adaptive immune cells have both pro-inflammatory and immune suppressive functions and the balance between these opposing functions determines the outcome of the tumor. Notably, myeloid derived suppressor cells and M2 polarized macrophages suppress T cell activation and proliferation, antigen presentation and support the recruitment of T regulatory cells(10). Natural killer (NK) cells and cytotoxic T cells have the capacity to destroy malignant cells, however they can also drive selection for cells capable of immune escape. For example, cytotoxic T cell engagement with MHC class I presenting an altered protein peptide, with the appropriate co-stimulation, can lead to target cell killing. However, between 40-90% of human tumors have lost HLA class I protein expression(11). According to the missing self

hypothesis, this loss of expression should target MHC class I null cells for NK cell mediated destruction(12, 13). In turn tumor cells have been reported to shed expression of ligands of the NK activating receptor NKG2D via a micro-RNA dependent mechanism (3, 14). This interplay is thus a race between immune effector cells to detect and eradicate and the tumor that must effectively camouflage itself in order to persist.

Immune cells, CAFs and tumor cells themselves contribute to the recruitment of endothelial cells and pericytes required to transport the blood supply of oxygen and nutrients and evacuate waste. This also becomes an important route for the dissemination of cancer cells and the subsequent establishment of metastatic foci(9).

Tumors possess a plethora of diverse genetic lesions that can be additionally regulated by epigenetic mechanisms and stromal cell interactions. It is evident that cancer treatment necessitates comprehensive multi-modality approaches to reduce tumor bulk and elicit immune surveillance.

1.2 Replicating oncolytic viruses

1.2.1 Cancer cells are inherently sensitive to viral infection

Oncolytic virotherapy is being developed using viruses from many families, nine of which are currently being tested clinically: *Adenoviridae, Picornaviridae, Herpesviridae, Paramyxoviridae, Parvoviridae, Reoviridae, Poxviridae, Retroviridae* and *Rhabdoviridae*(15). Some viruses have been found to have natural tropism for cancer cells, whereas others have been engineered to be tumor-tropic at the level of cellular

entry or intracellular replication, whereby the dysregulated signalling pathways in neoplastic cells complement the requirements for replication.

Many of the characteristics of a favourable viral replication niche are in fact hallmarks of neoplastic development(16). The most fundamental hallmark of cancer is sustained proliferation. Aberrant signalling via the epidermal growth factor receptor (EGFR) and through the PI3K/AKT axis or Ras-MEK-MAPK pathway occurs with overwhelming frequency and promote cell proliferation, cell survival, and metastasis(17). Not only does vaccinia virus have natural tropism for cells with EGFR activation(18), it also encodes a viral protein, vaccinia growth factor (VGF) that binds EGFR to condition neighbouring cells to be primed for infection(18, 19). Disruption of this family of pathways also renders cells hypersensitive to OVs such as myxoma virus, reovirus and herpes simplex virus (HSV)(20–22). Checkpoint proteins that regulate cell cycle progression are commonly disrupted to maintain chronic proliferation. In a wild-type viral infection, the adenovirus E1A protein activates proliferation by binding to and abrogating the effect of the retinoblastoma protein family(23). Similarly, the E1B viral protein interferes with p53-mediated cell cycle arrest. Both of these genes become dispensable in malignant cells with defects in these pathways. In contrast, the deletion of *E1A* and *E1B* restricts adenovirus replication in normal cells(24). The corollary to chronic proliferation is altered metabolism and elevated levels of cellular building blocks such as nucleotides. Both vaccinia virus and herpesvirus encode thymide kinase analogs, which render the virus selective for highly proliferative cells when deleted. Inactivation of this gene product has been used in the clinical candidate Pexa-Vec (pexastimogene devacirepvec)(25).

The anti-viral response is often dysregulated in cancer. In fact, over 80% of a panel of cells from the NCI60 cell bank were found to have a defect in type I interferon (IFN) signalling(26). The reason underlying this seemingly extensive incompatibility of neoplastic development and type I IFN signalling may be partially attributed to immunoediting, as well as the ability of IFNs to inhibit angiogenesis or induce cell cycle arrest(16, 27–29). This vulnerability to viral infection of cancerous cells can be exploited by a number of OVs. Newcastle disease virus (NDV), an avian paramyxovirus, has evolved a STAT inhibitor, however the binding affinity of the protein is restricted to avian cells. As such, this virus is naturally tumor-tropic as it is only able to replicate in human cells in which type I IFN signalling is disrupted(30). Similarly, the rhabdoviruses such as vesicular stomatitis virus (VSV) and maraba virus have had mutations engineered into their matrix (M) proteins, which have rendered the virus defective for blocking the IFN response(26, 31). The predilection of VSV for cancer cells will be further explored in section 1.4.

Lastly, the selectivity of OVs may be predicated on the overexpression of a viral receptor on transformed cells. Nectin-like molecule-5, the poliovirus receptor, is in fact a tumor antigen and its expression is restricted to malignant tissue such as gliomas as well as colorectal, breast, lung, and hepatocellular carcinomas(32). The increase in expression of the complement regulatory protein CD46 has been implicated as a mechanism of resistance against complement attack and has been associated with malignancy of many cell types(33). Accordingly, measles virus uses CD46 for attachment and entry and provides the basis for its oncolytic selectively(34). The selectivity of a number of other oncolytic viruses is also established by receptor expression(16).

1.2.2 Mechanisms of oncolytic virotherapy

The class of replicating OV therapeutics was originally chosen for their ability to selectively replicate in and kill neoplastic cells, yielding not only tumor destruction but also the amplification of the active "drug." Beyond this initial premise, novel intrinsic mechanisms of action have been discovered and engineering has endowed OVs with a broad array of capabilities. In this respect, OVs with multiple mechanisms of action are well-suited to treat the heterogenous nature of tumors, as well as target other cellular compartments of the tumor microenvironment.

The infection of tumor vasculature by oncolytic vaccinia virus and VSV is an intrinsic viral property that has been demonstrated in both pre-clinical and clinical settings. This has been shown to be associated with an activated endothelial cell state induced by treatment with VEGF or FGF-2(35). Infection leads to an inflammatory response whereby the neutrophil-dependent initiation of micro-clots within tumor blood vessels is observed. The concomitant vascular collapse that leads to decreased tumor proliferation and extensive apoptosis has been termed the "bystander killing of tumors"(36, 37). This phenomenon has been observed clinically, whereby patients with hepatocellular carcinoma exhibited intratumoral vascular disruption and decreased perfusion of tumors following Pexa-Vec treatment(35).

Perhaps one of the most important mechanisms of OV therapy is the engagement of the immune system to recognize and target tumor antigens that were subject to immune tolerance and located in immune suppressive microenvironments. Ideally, this may aid in tumor clearance and protect from future recurrence(38). Oncolytic virus

infection of tumor cells with measles or HSV-1 induces immunogenic cell death characterized by the release of alarmins such as HMGB-1 and HSP-70 as well as pro-inflammatory cytokines such as type I IFNs, IL-6 and RANTES(39, 40). Moreover, the importance of the detection of viral pathogen- associated molecular patterns by toll-like receptors (TLRs) was evidenced by a loss of therapeutic efficacy with oncolytic VSV in MyD88 null mice(41). Correspondingly, OV infection of tumor cells *in vitro* also increases phagocytosis by dendritic cells and stimulates maturation and cross presentation to T cells(42, 43). In pre-clinical models, OVs such as reovirus or HSV have been shown to generate T cell responses to tumor antigens(44, 45). Clinically, this has translated into the observation of increased lymphocytic infiltration to tumors from patients following treatment with Pexa-Vec and objective responses to both injected and non-injected lesions(46, 47). The generation of antibodies against tumor atigens additionally suggests that OVs can act as vectors inducing *in situ* tumor vaccination(48).

The capacity to engineer OVs to express therapeutic transgenes offers an opportunity to enhance their innate capabilities as well as provide novel effector mechanisms. In order to maximize their cytolytic effects in malignant cells, pro-drug converting enzymes have been encoded in OVs. Several examples include cytosine deaminase which converts the prodrug 5-fluorocytosine (5-FC) to 5-fluorouracil (5-FU), CYP2B1 which hydrolyzes cyclophosphamide to an active form, and carboxylesterase which converts irinotecan (CPT-11) to its active metabolite SN-38. Improved cell killing was reported with these engineered viruses in combination with their respective drug counterparts compared to parental virus alone in infected and surrounding non-infected cells(49, 50). Similarly, the sodium iodide symporter (NIS) has been used to increase

uptake of radioiodine by infected cells as an adjuvant treatment and also for non-invasive imaging by SPECT-CT(51, 52).

Not only are OVs immune-stimulatory by nature, they can encode cytokines or tumor-associated antigens to elicit potent anti-tumor adaptive immune responses. In particular, both the vaccinia virus and herpesvirus respective lead clinical candidates, Pexa-Vec and T-Vec (Talimogene laherparepvec), in addition to numerous other OVs, encode the cytokine granulocyte-macrophage colony-stimulating factor (GM-CSF)(53). GM-CSF has been shown to exert pleiotropic effects on immune cell populations, including inducing the proliferation, differentiation, and activation of antigen presenting cells(54). A study comparing oncolytic measles virus expressing GM-CSF with its parental strain demonstrated an improved cell-mediated tumor-specific immune response, an increased number of tumor-infiltrating $CD3^+$ lymphocytes, and corresponding delayed tumor progression and improved survival associated with the cytokine(55). Similarly, adenoviral vectors expressing mouse GM-CSF, compared to the species-restricted human homolog, showed better tumor control and increased numbers of $CD11c^+$ cells in tumor-draining lymph nodes(56). In this manner, GM-CSF expressed by infected tumor cells was able to stimulate the proliferation and maturation of host antigen-presenting cells such as dendritic cells and macrophages(56). Several other cytokines and chemokines have also been expressed by OVs including IFN β, IFN γ, IL 12, and CCL 3 and CCL 5(53). While encoding tumor antigens in rhabdoviruses has been met with limited success, their use in a heterologous prime-boost setting in combination with an adenoviral vector encoding the same antigen has demonstrated tremendous potential. This strategy has been exemplified with the human dopachrome tautomerase tumor-

associated antigen expressed by an adenoviral vector in combination with either VSV or maraba virus vectors and was shown to induce strong anti-tumor T cell responses with a central memory phenotype and extend survival(57–59).

Importantly, OVs have been shown to provide additive or synergistic effects when used in combination with approved forms of therapeutics such as chemotherapy and radiation therapy, or more recently, immune checkpoint blockade. Notably, external beam radiotherapy mediated an increase of cellular GADD34 tumor cell expression and was associated with increased viral titers of HSV and improved cytotoxicity. The viral γ34.5 gene, which has been deleted in many oncolytic HSV derivatives, can be functionally replaced with GADD34(60, 61). Similarly, increased tumor cell death was observed with oncolytic vaccinia virus in combination with radiation therapy specifically in BRAF mutant cells. This was associated with attenuation of JNK and p38 as well as phosphorylation of ERK MAPK(62). While reovirus has been shown to have limited lytic capacity, it maintains potent immune-stimulatory properties(44). In this respect, its immune effects are being tested clinically in combination with chemotherapeutics. In pre-clinical testing reovirus was shown to induce synergistic cell killing with taxanes. As such, clinical trials have been designed to test Reolysin in combination with docetaxel, carboplatin and paclitaxel chemotherapy(63–65). Recently, oncolytic NDV and measles virus have been tested in pre-clinical models in combination with immune checkpoint blockade inhibitory antibodies against PD-L1 and CTLA-4. When NDV was administered directly to a subcutaneous tumor in combination with a systemic dose of anti-CTLA-4, an increase in $CD8^+$ and $CD4^+$, effector but not regulatory, tumor infiltrating T cells was observed and associated with tumor regression. Notably, pre-

existing, non-virally injected tumors without distant virus spread also regressed and experienced an increased infiltration of tumor-specific lymphocytes(66). Likewise, both CTLA-4 and PD-L1 inhibitory antibodies have been cloned into oncolytic measles virus and have been shown to increase tumor infiltration of $CD8^+$ cytolytic but not $Foxp3^+$ regulatory T cells, and induce a high frequency of complete tumor remission(67).

The list of combinations is extensive and provides an additional dimension to oncolytic virotherapy. While engineering a virus to express a transgene provides local elevated concentrations within the tumor microenvironment, adjunct regional or systemic administration of the same drug allows for specific control over the dosage and timing. Each approach has benefits and pitfalls and must be carefully understood and tailored to each combination to maximize therapeutic efficacy and maintain safety.

1.3 Oncolytic Vaccinia virus

Vaccinia virus is the prototypic member of the genus *Orthopoxvirus* and of the larger family *Poxviridae*. Other members of the genus include cowpox, mousepox (ectromelia), monkeypox and variola virus. Vaccinia virus's immunologic cross-reactivity enabled its use in the smallpox vaccination campaign. Vaccinia virus is morphologically characterized as a large brick-shaped membrane-bound particle ranging from 200-400 nm in length(68). The virus has a linear double stranded DNA genome of approximately 200 kb that encodes 118 early, 53 intermediate and 38 late genes(69). There are two distinct infectious virus particle types: the mature virion (intracellular mature virus; IMV) and the wrapped virion (extracellular enveloped virus or cell-associated enveloped virus; EEV, CEV). The mature virion form is the most prevalent

form of viral progeny and remains in the cytoplasm until it is liberated by cell lysis. The wrapped virion, in contrast, acquires an additional two membranes from the trans-golgi or endosomal network and is able to exit the cell via membrane fusion. At least 20 proteins have been associated with the mature virion membrane and an additional six with the wrapped virion. Four viral proteins are responsible for cellular attachment, and three of these are known to bind to ubiquitously expressed glycosaminoglycans such as laminin, heparin and chondroitin. An additional 11-12 proteins comprise the entry-fusion complex. Entry of the viral core requires membrane fusion with either the plasma or endocytic membrane(70).

Several characteristics make vaccinia virus particularly suitable as an OV. Due to its use as the smallpox vaccine, the safety profile of the virus has been extensively characterized. Severe complications are rare and prognostic factors for adverse events as well as clinical management have been thoroughly delineated(71). Since the virus promiscuously enters diverse cell types, oncolytic vaccinia virus may be used for the treatment of cancer from many origins. The virus replicates exclusively within the cytoplasm, thereby precluding any risk of integration of viral DNA into the host cell genome(72). Moreover, due to the large size of the genome, vaccinia virus can easily accommodate numerous transgenes (up to 25kb) without compromising viral replication(73). Lastly, the virus is known to be robustly immunogenic, as evidenced by its use as a vaccine platform for numerous purposes such as encoding tumor antigens such as NY-ESO-1 as well as HIV antigens(74–77). Together, vaccinia virus enables a targeted and robustly immune-stimulatory approach to treatment within the constraints of important safety parameters.

Several strains of vaccinia virus have been developed through genetic engineering to have increased oncolytic tropism. Three strains have been tested clinically, with Pexa-Vec, JX594 (Sillajen, formerly Jennerex Biotherapeutics; Transgene) emerging as the most clinically advanced candidate. Pexa-Vec is a Wyeth strain (Dryvax) derivative that has an engineered disruption in the thymidine kinase (TK) gene and encodes GM-CSF and the lac-Z marker transgene. The replication of this virus is restricted to cells with activated EGFR/Ras pathway signaling and elevated cellular TK levels(78). A closely related strain, Western Reserve (WR), which was produced through the passage of the Wyeth strain in mice, has also produced oncolytic derivatives(79). The double deleted Vaccinia virus (VVdd) carries mutations in both the *TK* and *VGF* genes and was demonstrated to be safe in mouse and non-human primate models(80, 81). The wild type WR strain, relative to its parental strain Wyeth, has shown increased replicative capacity in tumor cells. VVdd armed with GM-CSF has demonstrated robust tumor control and the generation of tumor-specific cytotoxic T lymphocytes (CTL) in pre-clinical rabbit models(82, 83). A first-in-man study of VVdd (JX929) recently reported safety and replication in injected and some non-injected tumors, however induced only minimal clinical benefit(84). Finally, GL-ONC-1 (GLV-1h68) is a Lister strain derivative being developed by Genelux as a diagnostic and therapeutic agent. In this respect, the virus carries three imaging genes, Renilla luciferase–Aequorea green fluorescent protein fusion, β-galactosidase, and β-glucuronidase, that have been inserted into the F14.5L, J2R (encoding TK), and A56R (encoding hemagglutinin) loci, respectively(85, 86). The virus has oncolytic activity in a wide range of cancers and several phase I/II clinical trials

for numerous indications have been initiated, however the findings from these trials have not yet been reported(87, 88).

1.4 Oncolytic rhabdoviruses

The *Rhabdoviridae* family are enveloped viruses with a linear, negative-sense single-stranded RNA genome. Both the VSV and maraba viruses are members of the *Vesiculovirus* genus, while their close relative, rabies virus, is a member of the *Lyssavirus* genus. These viruses all share a characteristic bullet-shaped morphology (100-430 nm long and 45-100 nm in diameter) (89). Both the VSV and maraba viruses have small 11kb genomes(31). The genome encodes five genes in the order $3'$ *N-P-M-G-L* $5'$: nucleoprotein (N), phosphoprotein (P), matrix (M), glycoprotein (G) and polymerase (L). The virus membrane is studded with trimers of the viral glycoprotein. Internally, the RNA is bound by the N protein, in complex with the L and P proteins. The M protein bridges the nucleocapsid and envelope bound G(89). The LDL receptor serves as the cellular receptor for VSV and its ubiquitous expression profile enables the virus's broad tropism(90). VSV is an insect-borne virus that infects rodents as well as cattle, horses and swine, and humans in rare instances(91). In humans, the disease has been characterized as producing acute mild to severe flu-like symptoms that are often typical of a viral prodrome: fever, chills, myalgia, anorexia, headache, pharyngitis, and nausea or vomiting(92).

The prototypical rhabdovirus, VSV, Indiana strain, was initially discovered to have oncolytic properties whereby IFN signaling established the basis of its restriction

from non-transformed cells(93). This specificity was further refined with the introduction of a deletion of the methionine in the position 51 of the matrix protein that restricted the virus to cells with defective IFN signaling. The matrix protein blocks the nuclear export of mRNA, and in this way prevents anti-viral mRNA translation, a function that is blocked upon deletion of the methionine at position 51. VSVΔ51 was shown to induce oncolysis in the majority of cell lines tested from the NCI60 cell panel and induce cures in mice with either subcutaneous or lung tumors(26). More recently, a screen of the rhabdovirus family identified new oncolytic candidates, including maraba virus. This virus was isolated from sandflies in Brazil(94). Additional mutations in the M protein L123W and the G protein Q242R defined the new front-runner virus as MG1. Notably, the *in vitro* therapeutic index and efficacy in mouse tumor models of MG1 was found to be significantly greater than VSVΔ51(31).

1.5 Clinical experience with the administration of oncolytic viruses

Primary tumors can be treated focally, however, disseminated, metastatic or hematologic disease requires systemic treatment. Depending on the organ(s) affected and staging of the disease, either intratumoral (IT) or intravenous (IV) administration have been chosen for clinical evaluation. The Pexa-Vec candidate has undergone phase I and II testing, being administered both systemically and via direct intratumoral injection and will be further described in the following section. The clinical investigation of a VSV derivative expressing human IFN β administered intratumorally to hepatocellular carcinoma has begun, however results have not yet been reported(88). Oncolytic

rhabdoviruses have largely only been investigated in pre-clinical models to date but have explored both routes of administration. Other advanced OV clinical candidates have been tested in defined routes of administration. T-Vec (Amgen, previously OncoVEX) has recently been reported to have achieved its primary endpoint of improvement in durable response rate following intratumoral injection in advanced stage melanoma(95). In the setting of intravenous administration, MV-NIS is being evaluated in a dose escalation trial (1×10^6 to a maximum of 1×10^{11} $TCID_{50}$). Interim results document the durable complete remission at all disease sites in one patient and a partial response in a second patient treated at the highest dose level(96). Reolysin (Oncolytics Biotech Inc.) is also being tested primarily in the setting of systemic delivery. Probing for the expression of reovirus proteins in post-treatment metastatic melanoma biopsies by immunohistochemistry has validated the successful delivery of virus(97).

Pexa-Vec, has been administered intratumorally in several phase I and II trials for liver cancer as well as metastatic melanoma. Biopsy samples demonstrated increased necrosis, lymphocyte infiltration, and pockets of infection as determined by immunohistochemistry. Correspondingly, the re-emergence of genomes in the blood and expression of the transgene GM-CSF were observed several days after injection. Antibodies against the virus and the transgene β-galactosidase were also noted(46, 98). Objective responses were observed in both injected and non-injected tumors(98). Notably, when patients were randomized to compare outcomes with low-dose (1×10^8 plaque forming units; pfu) and high-dose (1×10^9 pfu) virus treatment, survival was significantly correlated with dose (14.1 months compared to 6.7 months on the high and low dose treatments, respectively) (99).

Pexa-Vec, was also tested in a phase I trial in which the virus was administered intravenously to 23 patients with advanced treatment- refractory solid tumors(100). A dose escalation ladder (1 x 10^5 pfu/kg to 3 x 10^7 pfu/kg) was followed in order to establish the safety and pharmacokinetics of the virus. The virus was well tolerated; patients exhibited flu-like symptoms, however no dose-limiting toxicities were observed. Delivery of the virus to the tumor was established by qPCR and IHC of biopsies obtained eight to 10 days following the infusion of virus. With the exception of one patient treated at a dose of approximately 2 x 10^8 pfu, delivery was confirmed by qPCR or IHC at doses at or above 1 x 10^9 pfu. Replication of the virus in the tumor was established from granular cytoplasmic staining indicative of viral factories observed by IHC. Additionally, the expression of the transgenes β-galactosidase and GM-CSF was observed, thereby confirming replication. Dose-dependent anti-tumoral effects were observed as measured by Choi and RECIST disease control criteria(100).

1.6 Barriers to the systemic administration of oncolytic viruses in the blood

The potential therapeutic efficacy induced by OVs is only as good as our ability to deliver them to tumors. Successful delivery first necessitates viral stability in the face of antibodies, natural or IgG, and complement. These opsonins that decorate the surface of the virus also play an important role in sequestration by the liver and spleen, through the use of Fc receptors, complement receptors and scavenger receptors(88). The virus must also evade neutralization or clearance by blood cells as well as non-specific uptake by non-neoplastic tissue. Importantly, these barriers are a dynamic and interconnected system whose humoral and cellular arms dramatically change over the course of multiple

treatment cycles. Encouragingly, however, the clinical results with IV administered Pexa-Vec suggests that one or a number of these barriers can be saturated in order to allow for the delivery of infectious virus particles to tumors.

1.6.1 Complement activation and neutralization

The complement system acts as a powerful first line of defense against invading pathogens through its ability to induce neutralization, target pathogens to antigen presenting cells, and initiate and facilitate adaptive immunity(101). There are three recognized activating enzyme cascades that converge on the cleavage of C3 and lead to the terminal pathway: the classical pathway, the mannose-binding lectin pathway (MBL) and the alternative pathway; however novel activation pathways have also been identified(102). The complement cascade is schematized in Figure 1.1. The classical pathway is initiated by antibody, specifically IgM or certain IgG isotypes, binding to target antigen. This interaction recruits C1q and its associated partners C1s and C1r, which leads to the cleavage of C4 and C2 to form the classical pathway convertase C4bC2a. Alternatively, MBL and ficolins can bind to carbohydrate moieties on the surface of microorganisms and recruit MBL-associated serine proteases (MASPs), which cleave C4 and C2 to generate the C4bC2a convertase. The alternative pathway is constitutively active as C3 spontaneously hydrolyzes to produce C3a and C3b. The deposition of C3b on the surface of a target triggers interaction with factor B and subsequently factor D, resulting in the formation of C3bBb, the alternative pathway convertase. The alternative pathway also acts as an important feedback loop to amplify complement activation by the other two pathways. The binding of C3b to a C3 convertase results in the formation of the C5 convertase, which recruits components C6-C9 to

produce the membrane attack complex (MAC)(102). Through the cleavage of C3 and C5, two important anaphylatoxins are produced: C3a and C5a. These peptide fragments act as chemoattractants for phagocytic cells including monocytes and neutrophils, and induce vasodilation and histamine release(103). In this manner, the complement system acts as an important link between the innate and adaptive immune systems. Complement is understood to act as a natural adjuvant for B cells since ligation of CR2 with the associated B cell receptor (BCR) and CD19 lowers the activation threshold, enabling opsonized antigen at either low concentration or with low avidity for the BCR to induce activation(104). The T cell compartment is also regulated by complement, both through the interaction of antigen presenting cells with complement-coated targets to regulate antigen uptake and co-stimulatory molecule expression, as well as through direct interaction with CR1, CD46 and the C5aR(102, 105, 106). Innate anti-viral mechanisms can also be activated in infected cells where complement components have been internalized. It has been shown that complement-coated intracellular pathogens, such as adenovirus, induce NFκB activation via mitochondrial antiviral signaling (MAVS) and target the pathogen to proteasomal degradation. Correspondingly, infected cells up-regulate activating NKG2D ligands and MHC class I and release pro-inflammatory cytokines(107). Notably, this study demonstrated that enveloped viruses did not induce a similar mechanism, and complement induced cellular immunity may therefore only be pertinent to some OVs. The complement system provides several layers of mechanisms to neutralize and clear viruses while stimulating anti-viral immunity.

Figure 1.1. Simplified complement cascade schematic

Complement is activated by one of three activations pathways (Classical, Lectin or Alternative) and is mediated by the binding of pattern recognition molecules (ie C1q or MBL) to their cognate motifs (ie IgG-antigen complex or mannose). The three pathways converge on the formation of a C3 convertase, which cleaves C3 to C3a and C3b. The C3b and C3 convertase molecules combine to produce a C5 convertase complex and lead to the Terminal pathway and the ultimate formation of the membrane attack complex (MAC). The molecules outlined in red are important targets to inhibit to determine the relative importance of each pathway.

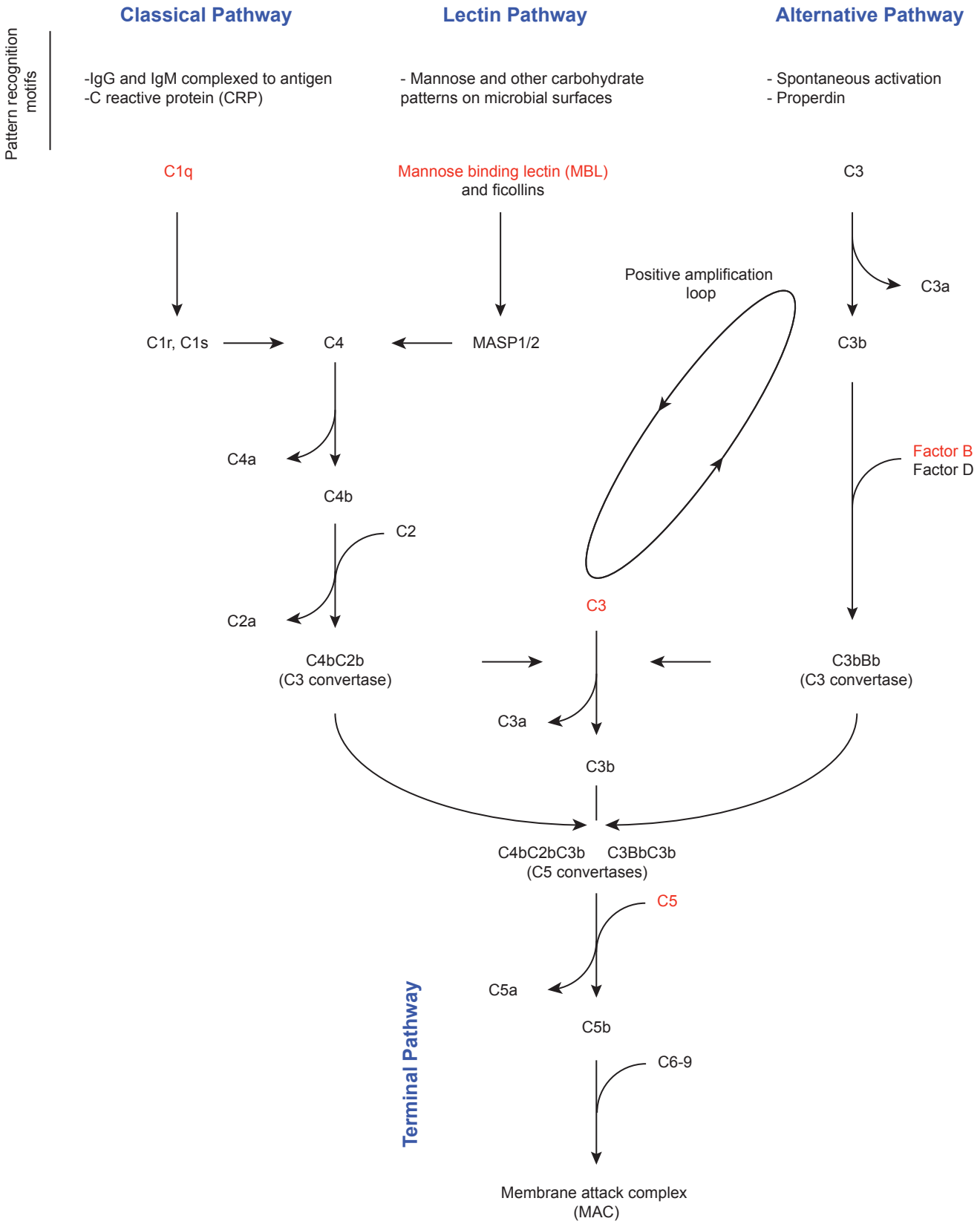
Classical Pathway
Lectin Pathway
Alternative Pathway
Pattern recognition motifs
-IgG and IgM complexed to antigen
-C reactive protein (CRP)
- Mannose and other carbohydrate patterns on microbial surfaces
- Spontaneous activation
- Properdin
C1q
Mannose binding lectin (MBL) and ficollins
C3
Positive amplification loop
C3a
C1r, C1s
C4
MASP1/2
C3b
C4a
C4b
Factor B
Factor D
C2
C2a
C3
C4bC2b (C3 convertase)
C3bBb (C3 convertase)
C3a
C3b
C4bC2bC3b C3BbC3b (C5 convertases)
C5
C5a
C5b
Terminal Pathway
C6-9
Membrane attack complex (MAC)

1.6.3 Complement and oncolytic viruses

The best indication that complement plays an important role in the vaccinia virus life cycle is that it has naturally evolved two mechanisms by which it can avoid complement-mediated neutralization. The mature virion is exquisitely sensitive to neutralization by complement, however the wrapped virion is conferred protection by the host complement regulatory proteins embedded in its additional membrane(108). While some vaccinia virus strains such as International Health Department-J (IHD-J) have specific mutations that increase the production of the wrapped virion, such as the K151E mutation in the A34R protein, the Wyeth strain does not carry any wrapped virion enhancing mutations and therefore primarily produces mature virion progeny(109, 110). Although the wrapped virion is less sensitive to complement, the combination of complement and neutralizing antibodies can significantly reduce infectivity(111–113). Vaccinia virus also encodes a complement decoy receptor, vaccinia complement control protein (VCP). This protein has been shown to protect viral particles from neutralization *in vitro* via the inhibition of both C3 and C4 and consequently, *in vivo*, dampens the resulting antibody and T cell responses(108, 114, 115).

Several studies have reported conflicting information regarding which complement pathways are important for orthopoxvirus neutralization by complement. Murine models using ectromelia virus have shown that the classical and the alternative pathways of complement activation play important roles in viral neutralization *in vitro* and in survival upon viral challenge in mice(116). Using human sera genetically deficient in selective complement components, it has been shown that vaccinia is sensitive to inactivation by the early components of the pathway. Specifically, plaque reduction

assays demonstrated that serum deficient of C5 and C6 neutralized the virus to a similar degree to complement-competent serum, indicating that the terminal pathway was not required for vaccinia neutralization(117). More recently, however, it was demonstrated that C5 inhibition with eculizumab could prevent complement-mediated viral neutralization(118).

It has been demonstrated that VSV is also very sensitive to complement-mediated neutralization. Classical pathway activation initiated by the binding of natural antibody, IgM, to the virion leads to viral lysis(119, 120). Notably, although the G protein of the maraba virus is approximately 80% homologous to the VSV G protein, maraba virus is less sensitive to neutralization by non-immune serum. Correspondingly, pseudotyping of VSV with maraba G protein confers some protection against complement-mediated neutralization(121). These results suggest that a high affinity epitope on the VSV G protein for IgM is not present on the maraba G protein.

1.6.4 Therapeutic targeting of complement

Complement-associated pathophysiology has been implicated in autoimmune, inflammatory, hematological and neurodegenerative diseases, as well as ischemia/reperfusion injury, sepsis and transplantation(122). This range of associated diseases and conditions requires that diverse and tailored therapeutic strategies must be employed for each indication. Several classes of therapeutics are currently in various stages of development, however few have been approved for clinical use. The two clinically approved complement inhibitors are the C1 esterase inhibitor, (trade names Cinryze, Berinert, Ruconest) and the monoclonal antibody targeting C5, eculizumab

(trade name Soliris; Alexion Pharmaceuticals, Inc.). The C1 esterase inhibitor is primarily used for the treatment of hereditary angioedema, a genetic disease characterized by the swelling of subcutaneous tissue caused by the deficiency of this protein. Beyond this primary indication, the C1 esterase inhibitor has demonstrated efficacy in other disease models and clinical trials have been initiated for its use in attenuating thrombo-inflammatory responses in trauma and kidney transplantation(122, 123). Eculizumab binds to C5 to prevent its activation by the C5 convertase and the subsequent production of the anaphylatoxin C5a and the MAC. It is currently used to treat paroxysmal nocturnal hemoglobinuria (PNH) and atypical hemolytic uremic syndrome (aHUS), where it has been shown to prevent erythrocyte lysis and improve renal function, respectively(123).

Cobra venom factor (CVF), isolated from the cobra species Naja naja, can be safely administered to laboratory animals to deplete complement. The crystal structure has been elucidated and demonstrates extensive structural homology between CVF and C3. It is able to form a fluid phase CVF,Bb convertase, which utilizes factor B and factor D and rapidly activates and consumes C3 and C5. CVF administration, depending on dosing, can deplete C3 to low or undetectable levels of hemolytic activity for 2-3 days. The protein, however, is extremely immunogenic and limits repeat administration(124). The only known side effect from the exhaustive activation of complement by CVF is transient neutrophil-mediated inflammatory lung injury induced by C5a(125).

The serine protease inhibitor nafamostat mesilate (Futhan, FUT-175) was shown to possess activity against the C1r and C1s subunits of the classical pathway, as well as factor B and D of the alternative pathway(126). This compound has been used both *in vitro* and in pre-clinical models to inhibit complement(126–128). It is currently being

developed by Torii Pharmaceuticals for acute pancreatitis for its ability to reduce complement-mediated systemic inflammation as well as its non-specific protease inhibitory capacity(123, 129).

Compstatin was identified from a phage display library for its ability to bind to human and non-human primate C3 and C3b(130). The crystal structure of C3 in complex with Compstatin has demonstrated that it sterically hinders the interaction of C3 with its convertase(131). Through targeting the hub protein C3, Compstatin quenches all three activation pathways and further downstream the formation of the anaphylatoxins C3a and C5a and the membrane attack complex. Novel analogs have been generated with improved pharmacokinetic and pharmacodynamic properties, with CP40 emerging as the lead clinical candidate(132, 133). Compstatin analogs are being developed in preclinical models for a variety of indications including, hemodialysis, sepsis, transplantation and PNH, and have undergone phase II clinical testing for age-related macular degeneration(123, 133).

1.6.4 The antibody response

Antibody can be pre-existing as a result of the virus in question being a natural contagion (HSV and reovirus) or as a result of a vaccination campaign (vaccinia virus and measles virus). Humoral immunity will either develop or be boosted throughout the course of treatment and mount an increasing barrier in multi-dosing treatment scenarios. The neutralization capacity of antiviral antibodies is not limited to the inhibition of viral attachment and entry to target cells. Antibody-bound virus can be targeted for clearance via opsonophagocytosis by antigen presenting cells(134). Perhaps as a last resort

mechanism, the intracellular sensing of antibody-coated viruses via TRIM21 targets the virus to proteolysis and activates anti-viral signaling cascades(135).

The smallpox vaccination campaign utilizing vaccinia virus ended in Canada in 1972 and naturally occurring smallpox disease was eradicated worldwide by 1977(136). It was previously generally accepted that vaccination would not be protective long term, and it is currently reported by the Center for Disease Control (CDC) that protection from smallpox persists for 3 to 5 years(137, 138). However, several groups have reported very long lasting cellular and humoral immunity to the smallpox vaccination. Several studies have demonstrated long-lived antibody with weak neutralizing or no neutralizing capacity. Notably, it was shown that greater than 90% of donors that were vaccinated 25-75 years prior to the study had maintained humoral and/or cellular immunity or both(139). Specifically, antibodies to the wrapped virion proteins B5 or A33, the mature virion proteins A27 and L1, or the secreted protein VCP have been demonstrated by ELISA or immunoblot(140, 141). Antibodies elicited by smallpox vaccination against the mature virion proteins H3, D8, L1, D13 and A14 have been shown to possess moderate neutralizing capacity under conditions designed to maximize neutralization(142). Long-lived B cells have also been reported by ELISPOT, however only have weak neutralizing ability(143, 144). Several reports published during the time when smallpox vaccination was ongoing suggested that the neutralizing effects of antibodies induced by the smallpox vaccine were considerably enhanced by complement(145–147). There have been no recent reports, however, of long-lasting, robustly neutralizing, complement-dependent human anti-vaccinia antibodies. Therefore, the degree of protective immunity that is

directed against vaccinia virus and how this may impact the systemic delivery of virus remains unclear.

Epidemiologic studies document pockets in Central and South America where VSV is endemic in livestock and wildlife and that human populations living in close proximity have variable degrees of seropositivity(148, 149). Sporadic outbreaks in livestock have also occurred in the United States(150). Correlated human disease has only rarely been reported and was associated with some degree of contact with infected animals(92). The seroprevalence of VSV antibodies in the general population is thought to be very low(151). Despite the sparse reports of VSV antibodies in humans, a much better understanding comes from mouse models. VSV infection stimulates a robust neutralizing response against the G protein with very rapid kinetics in mice(152). As an OV, VSV can be administered systemically to subcutaneous tumors in naïve mice, such that a sufficient dose to effectuate therapeutic advantage is delivered. In immunized mice, however, circulating antibodies completely abrogated the delivery of infectious particles(153, 154). The robust antibody response to VSV therefore precludes multiple systemic dosing regimens and necessitates additional adjunct therapy to prevent neutralization. The infection of humans or animals with the maraba virus has not been reported(155).

1.6.5 Cellular interactions of oncolytic viruses

The interaction of viruses with blood cells is likely context- and concentration-dependent. In the context of an infusion of oncolytic vaccinia virus, the effect of cellular interaction on neutralization and clearance is unknown. The *in vitro* studies of vaccinia virus interaction with immune cells that transit in the blood are numerous, however do

not mimic the dose, the role of the presence of complement and antibodies, or the strain and engineered mutations or transgenes of OVs. Vaccinia was found to preferentially bind to and infect human antigen-presenting cells, specifically monocytes and B cells to a greater degree than other peripheral blood mononuclear cells (PBMCs), however the replication in these cell types was abortive(156–158). Interestingly, vaccinia was found to productively infect activated human T cells, but not unstimulated T cells, as measured by viral genome quantification and late gene expression(157). These interactions were also investigated in murine cells, where the vaccinia strain modified vaccinia Ankara (MVA) was found to preferentially, yet abortively, infect dendritic cells (DCs), macrophages and B cells. The infected DCs were found to mature, produce IFN α, and then undergo apoptosis(159). In fact, various strains of vaccinia have been shown to abortively infect human dendritic cells and induce apoptosis(160–163). Vaccinia interferes with DC maturation, as shown by reduced expression of DC maturation markers and ability to activate and induce T cell proliferation(162, 163). Other groups have also shown that human macrophages, B and T cells may undergo apoptosis following infection with vaccinia(164, 165). The importance of context is underscored by the demonstration that human neutrophils take up vaccinia in a serum-dependent manner. Using electron micrographs, it has been shown that both intact and partially degraded particles exist in phagolysosomes in neutrophils, from which infectious virus could be recovered(166). While some previous interactions with complement and cells have been documented, none have reported generating their results under conditions that mimic systemic delivery with Pexa-Vec: low multiplicity of infection (MOI), Wyeth strain virus with appropriate genetic modifications, in the presence of complement and antibodies.

Several reports have demonstrated that OVs engage in interactions with cells in the blood that are both beneficial and detrimental to the delivery of virus. Notably, protective blood cell carriage has been shown in pre-clinical models and clinical correlative assays with reovirus. This hitchhiking phenomenon was observed in the mononuclear and granulocyte fractions as well as the platelet cell compartment and is thought to protect the virus against neutralizing antibodies(167–169). Conversely, adenovirus has been found to associate with human erythrocytes via the coxsackie adenovirus receptor (CAR) and complement receptor 1 (CR1). *In vitro*, this interaction precluded infectivity of target tumor cells and studies with NOD-SCID mice demonstrated that these interactions sequester the virus in the bloodstream and prevent extravasation(170).

1.7 Barriers in the tumor microenvironment

Oncolytic viruses arriving at the site of a tumor still face additional barriers to infectivity. Extravasation is facilitated by "leaky" neoplastic vasculature, but the passive diffusion of virions is limited by elevated interstitial fluid pressure. The increased interstitial fluid pressure is the result of extracellular matrix deposits, heterogeneous blood supply, lack of lymphatic flow, and dense tumoral and stromal cellularity(171, 172). Several approaches including the administration of permeability factors such as VEGF or TNF-α, as well as the engineering of viruses to express matrix-degrading proteins have been met with only moderate success(172, 173). Additionally, serous fluid and resident immune cells present the same barriers that were encountered in the blood. In fact, complement plays an important role in the neoplastic process. Perhaps the role of

complement in cancer is best interpreted through the theory of cancer immunoediting. Although there is no direct evidence that nascent tumors can be eliminated by complement, there is considerable support that there is selective pressure to develop mechanisms to evade complement-mediated destruction(174). Membrane complement regulatory proteins such as CD55, CD46, and CD59 have been reported at elevated levels on a diverse array of cancer cell types relative to the normal tissue from which they evolve(33). In addition, clinical studies have reported elevated levels of complement activation products such as C3a in the serum of breast(175) and colorectal(176) cancer patients. A result of such studies has been to suggest the use of C3a in a panel of biomarkers that will influence prognosis(177). One interesting study of the ascitic fluid of ovarian cancer patients documented elevated levels of C3a relative to normal sera, and isolated malignant cells with C1q and C3 activation product deposits but not C5b-9, suggesting control of complement activation at the cell surface(178).

Once cells have developed a reduced sensitivity to complement, chronic inflammation, in contrast to acute inflammation, has many tumor-promoting effects. Notably, subcutaneous tumor growth of a syngeneic cell line was impaired in C3 null mice, and moreover, wild type animals have elevated levels of C3 degradation products have been observed near the vasculature of tumors(179). Complement has been implicated in the shaping of the tumor microenvironment through immunoregulation, the promotion of angiogenesis and the promotion of mitogenic signaling. Specifically, complement activation and the generation of C5a led to the recruitment of myeloid derived suppressor cells (MDSCs) which in turn impaired the cytotoxic T cell response through the production of reactive oxygen and nitrogen species(179). The role of

complement has been well established as an angiogenic driver in disease states other than cancer, including the pathologic neovascularization in age-related macular degeneration(180). Consistent with this, when TgMISIIR-TAg transgenic mice that develop epithelial ovarian cancer with 100% penetrance were crossed with either C3 or C5aR knock out mice, tumor growth was dramatically impaired; the tumors that did develop were small and poorly vascularized. This was attributed to functional impairment of endothelial cells, whereby tube formation was shown to be C5a dependent(181). Additionally, deposition of sublytic concentrations of terminal complement complexes was found to stimulate proliferation through both the Ras and MAPK signaling pathways(182). Similarly, a wide variety of cancer cells express C3, and this has been found to activate an autocrine loop whereby engagement of the C3a and C5a receptors activated the PI3K/Akt pathway and stimulated cell proliferation(183).

1.8 Strategies to evade neutralization and improve delivery

Numerous strategies have been investigated to evade the barriers presented to systemic delivery. The use of hydrophilic polymers like polyethylene glycol (PEG) were pioneered with adenovirus initially with the aim of de-targeting the virus from hepatocytes(184, 185). It has since been demonstrated to prevent the CR1 and CAR-mediated interactions of adenovirus with erythrocytes(170). More recently, this approach has been adapted to VSV, where in a pre-immune murine model it provided protection in the blood from antibodies, increased accumulation of viral genomes in tumors, and reduced hepatotoxicity as measured by serum concentration of liver enzymes, suggesting viral de-targeting from the liver(154). This strategy however requires extensive post-

production modification and additional engineering to retarget the virus. This approach has not yet been taken into clinical trials.

Similarly, several groups have generated pseudotyped viruses to avoid neutralizing antibodies. Vaccination against Edmonston vaccine strain measles in the general population poses a considerable challenge to the systemic administration of this virus. Pseudotyping measles with the canine distemper virus envelope glycoproteins fusion (F) and hemagglutinin (H) produced a new virus that was not neutralized by anti-measles antibodies. However, in order to retain neoplastic cellular tropism, a single chain antibody to carcinoembryonic antigen was engineered on the extracellular terminus of the attachment glycoprotein hemagglutinin(186). Pseudotyped VSVs have also been generated to avoid IgM-induced neutralization by complement and neutralizing IgG. The closely related maraba virus's G protein was also exchanged for the VSV G protein, which conferred significant protection against complement(121). The lymphocytic choriomeningitis virus (LCMV) G protein was also swapped with VSV G protein to produce an interesting phenotype in mice. The non-cytopathic LCMV is well known to generate neutralizing antibody responses that are extremely late, being observed 50–80 days after infection in the mouse model(187). A study in which the glycoproteins of VSV and LCMV were swapped determined that the kinetics of protective antibodies were determined exclusively by the viral surface glycoprotein, and not by the virus backbone(152). Building on this, the model antigen OVA was introduced into VSV expressing parental G protein or the LCMV G protein. In contrast to the parental strain that was hampered by neutralizing antibodies, the pseudotyped virus could repeatedly boost the CTL response against ovalbumin(188). With the exception of the LCMV G

protein being a unique case, pseudotyping is not a method to prevent the generation of an antibody response, but rather to bypass a pre-existing one. This advantage, however, is offset by potential changes in virus attachment and tropism and must be brokered with additional engineering strategies.

The loading of carrier cells with OVs has been a very popular strategy to prevent neutralization and the platform has been developed with an extensive list of viruses, including adenovirus, VSV, measles virus, HSV, vaccinia virus, reovirus and NDV(189). The ability of some cell types in the blood to act as natural carrier cells for reovirus has been observed in patients treated with Reolysin, however the *ex vivo* loading of cells for use as delivery vehicles has been limited to pre-clinical models(169). The ideal cell protects the viral cargo from neutralization and directs the virus to the tumor, in addition to having a favorable safety profile, and as a bonus has its own anti-tumor activity. Three classes of cells have primarily been investigated: transformed cells, immune cells and progenitor cells. In contrast to the scenario where the virus is administered into the blood and only a minority remains infectious as it reaches the tumor, carrier cells ideally can dose-amplify in permissive transformed cells en route to the tumor. To this end MM1 cells, a myeloma cell line, were loaded with MV-NIS and were shown to home to the bone marrow and infect the pre-established disease in passively immunized mice(190). Similarly, the leukemic cell line L1210 loaded with VSV was shown to deliver virus to subcutaneous tumors in pre-immune animals(153). Safeguards must be put in place to mitigate the risk of tumorigenesis by cells that escape virus-mediated cell death such as irradiation or the inclusion of suicide genes(189). Several immune cell types have been used whereby virus is either internalized or remains surface adsorbed. Antigen-specific T

cells loaded with VSV as well as cytokine induced killer cells (CIK) loaded with vaccinia virus deliver virus in addition to having cell-mediated cytotoxic activity(191, 192). Mesenchymal stem cells (MSCs) naturally home to inflammation, stress, and tissue injury, often characteristics of the tumor microenvironment. MSCs loaded with measles virus were able to transfer virus to ovarian tumor xenografts via cell-to-cell heterofusion in both measles naïve and passively immunized mice, which led to enhanced survival(193).

The pharmacologic immune suppression of neutralizing factors has been used to increase delivery of OVs to tumors and to aid in their replication and spread. Cyclophosphamide (CPA) is used commonly as a chemotherapeutic and immunosuppressive agent due to its ability to kill proliferating lymphocytes, including NK, T and B cells. As such, high doses of CPA have been used in combination with numerous viruses to reduce titers of both natural antibodies and neutralizing antibodies(194). CVF and CPA were used to deplete complement and IgM, respectively, in HSV-1 naïve rats and their use increased infection of orthotopic brain tumors following a systemic administration of HSV and provided survival advantage(195). High dose CPA in combination with systemic reovirus also substantially increased anti-tumor effects, but induced severe toxicity. In contrast, low dose metronomic CPA induced an incomplete depression of neutralizing antibodies, but improved efficacy compared to virus alone with the added benefit of reduced toxicity(196). Another report suggested that metronomic CPA has been associated with the depletion of regulatory T cells and the restoration of NK and T cell effector functions; a mechanism that may have supported the anti-neoplastic effects observed(197).

In the context of the vaccinia derivative VVdd, several immune suppressive drugs frequently used in the setting of transplantation (CellCept, Solu-Medrol and FK-506) were tested alongside CPA and CVF for their ability to increase delivery to MC38 tumors in pre-immune mice. The cocktail was only able to increase delivery of virus via a local intra-peritoneal administration, and not via the IV route. Notably, a marked increase in the infiltration of M2-polarized macrophages and MDSCs into the tumor microenvironment was observed(198). While this immune suppressive microenvironment was credited for the increase in viral replication and survival duration, all the animals still succumbed to their disease. Immune suppression comes at a heavy cost of perhaps preventing the recruitment of infiltrating lymphocytes and the production of pro-inflammatory cytokines that would lead to the generation of an adaptive anti-tumor immune response.

The immune system presents two faces to oncolytic virotherapy. First, in its capacity to protect against invading pathogens, it serves to limit the replication and spread of the OV and stem its 'oncolytic' potential. Conversely, the immune stimulatory response in the tumor microenvironment may provide enough danger signals to generate a $CD4^+$ or $CD8^+$ T cell response against tumor antigens to advance the ultimate goal of eradicating the tumor. Any intervention seeking to inhibit the factors leading to viral neutralization must be carefully designed in terms of its safety, specificity, dosage and duration in order to maximize both the oncolytic effect and its immune-stimulatory corollary effects.

1.9 Rationale, Hypothesis and Objectives

1.9.1 Rationale

Clinical experience with the local administration of Pexa-Vec has demonstrated that favourable patient outcomes are associated with elevated doses of virus. The phase I IV dose escalation trial with Pexa-Vec showed that virus can be safely delivered systemically to tumor tissue, even in the face of pre-existing immunity from smallpox vaccination. However, delivery was only observed if a critical threshold dose of virus was administered. The relatively short-term responses that were reported do not come close to demonstrating this to be efficacious at treating either the primary tumor or metastatic disease. Moving forward, it will be necessary to provide adjunct therapy to increase the effective dose that is delivered to tumors. Against this background, we sought to characterize the nature of the barriers to systemic delivery of oncolytic vaccinia virus in the blood with respect to their mechanism and magnitude of neutralization.

1.9.2 Objectives

A. Develop an *in vitro* system that reconstitutes all the components of human blood in their active states to determine their impact on virus infectivity.
B. Determine the relative impacts of complement, antibodies and cellular interactions on the infectivity of vaccinia virus in human blood *in vitro*.
C. Find an *in vivo* model that recapitulates the neutralization effects observed in human blood *in vitro*.

These first objectives enabled us to identify which factors were most important and to formulate a testable hypothesis as to how to increase the effective dose of administered virus. The overarching hypothesis was that complement played a key role in the antibody-mediated neutralization of oncolytic vaccinia virus in the blood stream and that its inhibition would improve viral stability and increase delivery. This was further explored in the subsequent objectives:

D. Model the delivery of virus to a tumor in an *in vivo* model and test the validity of complement inhibition to increase delivery.
E. Test the feasibility and safety of transient complement inhibition with a clinical candidate complement inhibitor.
F. Investigate the role that complement plays in shaping the cellular associations with which vaccinia virus engages.
G. Determine the translational ability of complement inhibition to other clinical candidate OVs.

2. Materials and Methods

Cell culture and virus. The U2OS, Vero, L929, CT26 LacZ and HeLa cell lines were purchased from the American Type Culture Collection (Manassas, VA) and maintained in complete Dulbecco's Modified Eagle's medium (HyClone, Logan, UT) supplemented with 10% fetal bovine serum (HyClone, Logan, UT). The 13762 MAT B III rat mammary adenocarcinoma cell line was purchased from the American Type Culture Collection and maintained in McCoy's 5A medium modified (ATCC, Manassas, VA) supplemented with 10% fetal bovine serum (HyClone, Logan, UT). The oncolytic vaccinia virus Wyeth strain TK^- gfp was previously described(18, 25). The oncolytic vaccinia virus WR VVdd firefly luciferase was previously described(199). HSV-1 (ICP0 null mutant n212)(200, 201) was a gift from Dr. Karen Mossman, McMaster University. Reolysin was a gift from Dr. Patrick Lee (Dalhousie University). Measles Edmonston was purchased from American Type Culture Collection (Manassas, VA). The oncolytic version of maraba virus, named MG1, was previously described(31). The maraba virus pseudotyped with the LCMV glycoprotein was cloned by the lab of Dr. David Stojdl.

Human blood neutralization experiments This study protocol was approved by the Ottawa Hospital Research Ethics Board and all volunteers gave informed consent. Human blood was collected from healthy donors by venipuncture into glass serum collection vacutainer tubes (BD Bioscience) and treated immediately with Refludan at a final concentration of 50 μg/mL. Blood was centrifuged at 800 x g for 10 minutes to obtain plasma. Plasma aliquots were incubated for 30 minutes at 56^{o}C to inactivate complement. Blood or fractions thereof were incubated for one hour at 37^{o}C with

vaccinia virus at range of doses between 2 x 10^4 - 2 x 10^7 pfu/mL. The infectious virus remaining was quantified by plaque assay on U2OS cells. To investigate the complement pathway, the Compstatin analog CP40(132) or the inactive control peptide (D-Tyr-Ile-Cys-Sar-Val-Asp-Trp-Ala-His-Trp(1-Me)-Gln-Arg-Cys-N-Me-Ile-NH2) (kindly provided by Dr. John Lambris, University of Pennsylvania) was pre-incubated for 15 minutes at 37^{o}C at a final concentration of 25μM prior to virus inoculation. The serine protease inhibitor FUT-175 (Futhan, nafamostat mesilate) (BD Biosciences, Mississauga, ON) was used at a final concentration of 50 μg/mL. Alternatively, the neutralizing monoclonal antibodies 3F8(202) mouse anti-human MBL, P1H10 mouse anti-human C1q (kindly provided by Dr. Greg Stahl, Harvard) or 1379 mouse-anti human Factor B(203) (kindly provided by Dr. Joshua Thurman, University of Colorado) or Eculizumab were pre-incubated for 15 minutes at 37^{o}C with plasma at concentrations of 60 μg/mL, 100 μg/mL or 500 μg/mL 50 μg/mL, respectively.

In order to assess anti-vaccinia antibodies from hyper-immune individuals, remaining serum was collected from patients enrolled in JX594-CRC019 (Clinical trial registration IDNCT01394939). This study protocol was approved by the Ottawa Hospital Research Ethics Board and all patients gave informed consent. The serum was heat inactivated and combined with serum free DMEM or plasma collected from a naïve donor as a source of complement and incubated with vaccinia at a ratio of 2 x 10^5 pfu/mL. The infectious virus remaining was quantified by plaque assay on U2OS cells.

Neutralization of MG1, HSV-1, reovirus and measles Edmonston were performed at concentrations ranging from of 2 x 10^4 - 2 x 10^7 pfu/mL. Plasma samples were incubated with CP40 (25 μM) or DMEM for 15 minutes at 37^{o}C prior to a one hour

incubation at 37°C in the presence of virus. MG1, HSV-1 and measles were titered on Vero cells and reovirus was titered on L929 cells. Anti-herpes simplex virus type 1 (HSV1) IgG and IgM human ELISA kits (Abcam, Cambridge MA) were used to validate serologic status.

Fluorochrome linked immunoassay (FLISA) Activation of the MBL-dependent lectin pathway was assessed in human serum incubated with mAb 3F8 at 10 μg/mL as previously described(204). This assay was performed by Margaret Morrissey and Dr. Greg Stahl (Center for Experimental Therapeutics and Reperfusion Injury, Harvard Institutes of Medicine, Boston, MA, USA) on our behalf.

Sucrose gradient separation of viral proteins Vaccinia virus was incubated with PBS, detergent (1% Triton X-100) or plasma from an immune donor at a concentration of 2 x 10^7 pfu/mL for one hour at 37°C. Samples were overlaid on continuous 5-75% sucrose gradients and centrifuged at 25000 rpm in an SW41Ti rotor for 35 minutes at 4°C. The gradient was collected in 16 fractions.

Immunoblotting Plasma or viral proteins were resolved on 4-12% SDS PAGE polyacrylamide gels (BioRad, Hercules, CA) and transferred to nitrocellulose membranes (Amersham GE Healthcare Lifesciences, Baie d'Urfe QC). Membranes were incubated for one hour at room temperature or at 4°C overnight with the following antibodies and dilutions: 1:100 rabbit anti-rat C3 (Cedarlane, Burlington, ON; CL7334AP); rabbit polyclonal antibody to Vaccinia (Quartett, Berlin, Germany; 1220100715). Membranes

were incubated with goat anti-rabbit horseradish peroxidase-conjugated IgG (Jackson ImmunoResearch Laboratories, Inc.) for one hour at room temperature. The peroxidase-conjugated goat anti-mouse complement C3 antibody (MP Biomedicals, Cappel, Solon, OH) was used at 1:10 000. Proteins were detected using Supersignal West Pico chemiluminescent substrate (Pierce Biotechnology, Rockford, IL) followed by exposure to X-ray film (Fuji Photo Film Co, LTD, Tokyo, Japan).

Human cell association studies

In vitro cell association

Blood was collected from a healthy naïve human donor and incubated with vaccinia virus at a concentration of 1 x 10^8 pfu/mL for one hour at 37^{o}C. Blood was diluted and incubated with PE conjugated antibodies (anti-CD19 clone LT19, CD15 clone VIMC6, CD14 clone TUK4, CD3 clone BW264/56 from Miltenyi Biotec or anti CD45-PE-Cy5, clone HI30 eBioscience). Approximately 5 x 10^6 cells were sorted on a Beckman-Coulter MoFlo cytometer (DakoCytomation) by the OHRI Stem Core laboratory. Sorted populations were subjected to plaque assay on U2OS cells as well as DNA extraction (DNeasy kit, Qiagen) and qPCR using primers against the viral E3L gene.

Futhan pre-treated human blood was incubated with 2 x 10^5 pfu/mL of vaccinia virus for 1h at 37^{o}C. Alternatively, blood was pre-treated with CP40 and incubated with 2 x 10^5 pfu/mL of vaccinia virus for 1h at 37^{o}C. Blood was centrifuged at 600-800 g to separate plasma from compacted cells. Plasma and whole blood were titered. For the Futhan experiment, the hematocrit was not measured and estimated to be 0.45. For CP40

experiment, microhematocrit capillary tubes (Fisher Scientific) were centrifuged for 10 minutes and hematocrit measured for each donor. The whole blood and plasma titers and genomic content were determined by plaque assay and qPCR, respectively. The proportion of virus in the plasma was used to calculate the remaining virus associated with the cellular fraction.

In vivo cell association

Two patients were treated as part of a phase 2a trial in which they received 1 x 10^9 pfu of Pexa- Vec over a one hour IV infusion (Clinical trial registration number NCT01329809). Blood samples were collected at various time points after the infusion and overlaid on a Lympholyte Poly cell separation media (Cedarlane), to isolate plasma, polymorphonuclear cells (PMNCs), periphereal blood mononuclear cells (PBMCs) and red blood cells (RBCs). The total genomes in each respective component was also quantified by qPCR using primers for the vaccinia virus E3L gene and for isolated cells, normalized to the β actin gene.

Animal Studies

Ex vivo neutralization experiments

Serum from guinea pig, hamster (Syrian Gold), rat (Sprague Dawley) and rabbit (New Zealand White) were purchased from Innovative Research Biologicals (MI, USA). Serum samples were left untouched or heat inactivated (56^{o}C for 30 minutes) and

incubated with vaccinia virus at a ratio of 2 x 10^5 pfu/mL for one hour at 37^{o}C. Remaining infectious virus was quantified by plaque assay.

Blood was collected from healthy cynomolgus macaques using the anticoagulant Refludan (50 μg/mL). Blood or plasma was incubated with vaccinia virus at 2 x 10^5 pfu/mL. Immune serum from rhesus macaques infected with 1x 10^9 pfu VVdd was collected between day 80 and 90 post infection and used as a source of antibody and was combined at a ratio of 4:1 plasma to heat inactivated immune serum. Futhan was added to a final concentration of 50 or 250 μg/mL. For the validation of animals treated in the study, plasma was heat inactivated and combined with plasma from a naïve animal as a source of complement (ratio 5:1 naïve plasma to heat inactivated plasma). Samples were incubated for one hour at 37^{o}C and infectious virus remaining was quantified by plaque assay.

Balb/c mouse model

Female Balb/c mice weighing (6-8 weeks of age) were obtained from Charles River (Wilmington, MA). All animals were housed in pathogen-free conditions and all studies conducted were in accordance with the guidelines of the Animal Care Veterinary Service facility of the University of Ottawa. Mouse plasma was collected from animals vaccinated with 1 x 107 pfu of vaccinia virus. Blood was collected by cardiac puncture and used immediately for *in vitro* neutralization assays. Blood was treated with Refludan (50 μg/mL). Blood was centrifuged at 800 x g and plasma was heat inactivated (56^{o}C for 30 minutes) or treated with Futhan (50 μg/mL). Tumors were established by injecting 1 x 10^6 CT26 Lac Z cells subcutaneously. Animals were depleted of complement using 4.5 U

of cobra venom factor (CVF) (Quidel, San Diego, CA). Animals were vaccinated (days 0,8) and treated (day 35) with 1 x 10^7 pfu of vaccinia (Western reserve, VVdd, expressing Firefly Luciferase) administered intravenously. Luminescence imaging was performed 48 hours post IV virus administration using the IVIS imaging System Series 200 (Xenogen Corporation). Data acquisition and analysis was performed using Living Image v2.5 software. Tumours were homogenized and infectious virus was quantified by plaque assay.

Rat model

Female F344 Fischer rats weighing 100-150g were purchased from Charles River (Wilmington, MA). All animals were housed in pathogen-free conditions and all studies conducted were in accordance with the guidelines of the Animal Care Veterinary Service facility of the University of Ottawa. Animals were vaccinated with 1 x 10^7 pfu of vaccinia virus or MG1 or MRB LCMV G. Tumors were established by injecting 5 x 10^5-1 x 10^6 13762 MATBIII cells subcutaneously bilaterally in the left and right flanks or 3 x 10^5 cells IV by tail vein injection. Tumors were treated IV with 1 x 10^8 pfu of vaccinia virus and 10 minutes or 24 hours post infection, the animals were sacrificed and the tumors resected. Alternatively, tumors were also treated with an intratumoral injection of 1 x 10^7 pfu of vaccinia virus and animals were sacrificed either 24 or 48 hours after administration. Following the same schedule, animals were also treated with 1 x 10^8 pfu of MG1 or MRB LCMV G intravenously or 1 x 10^7 pfu intratumorally. Blood was collected by cardiac puncture into EDTA vacutainer tubes for analysis of *in vivo* neutralization. Alternatively, blood was collected with serum tubes and treated with

Refludan to assess *in vitro* neutralization. For the depletion of complement, 35U of CVF (Quidel, San Diego, CA) was administered intraperitoneally 24 hours prior to virus delivery. A second dose of 35 U was administered intraperitoneally 24 hours after virus if animals were to be sacrificed 48 hours after virus administration. Tumors and livers were collected and immediately frozen. Tissues were homogenized in PBS and titered on U2OS cells. Tumor length and width was measured by calipers and tumor volume calculated using the formula $V=(L \times W^2)/2$, where L is the long side.

Cynomolgus macaque model

Healthy male and female cynomolgus macaques weighing 3 to 6 kg were obtained from Primus BioResources (Vaudreuil-Dorion QC) and Charles River (Montreal, QC). All NHP studies were performed under a protocol approved by the Animal Resource Centre, University Health Network, Toronto, ON, Canada.

To facilitate intravenous injection and blood sampling, a vascular access port was surgically implanted into the right flank with the venous line inserted into the right femoral/iliac vein. Animals were allowed to recover from surgery for several weeks prior to the initiation of the study. Macaques were randomized across schedule groups such that a male and female were assigned to each group. Animals received two doses of vaccinia virus (1×10^8 pfu infused over 30 minutes) in the naïve setting (day 0 and day 2), a booster dose (1×10^8 pfu infused over 30 minutes) two months after their first two doses, and two doses in the immune setting (day 0, day 2), four months after their initial doses. According to their group schedule, animals received a bolus dose of CP40 (2mg/kg) immediately prior to their virus infusion either on day 0 or day 2. One female

animal was used to validate the initial dose, but not did receive CP40 in the naïve setting. She was boosted and subsequently received virus alone and in combination with CP40 in the immune setting.

Blood samples were collected immediately before and at various time points after the infusion of virus (end of infusion, + 5 min, + 10 min, + 30 min, + 2h, + 5h). EDTA treated whole blood samples were frozen for subsequent analysis by qPCR and titration of infectious virus on U2OS cells. EDTA and Refludan treated blood samples were centrifuged at 800 g for 5 minutes to obtain plasma, and immediately frozen until further analysis. PBMCs were isolated by overlaying blood diluted 1:1 with HBSS on Ficoll Paque and centrifuged for 400 g for 35 min. The granulocyte fraction was isolated from the bottom fraction of the Ficoll separation by overlaying it on 6% Dextran. The leukocyte rich supernatant was subjected to ACK lysis to remove any RBCs. The population of cells in each isolation was analyzed using the Drew Hemavet 950FS Multispecies Hematology Analyser (Drew Scientific Inc, Waterbury, CT, USA). Frozen cell samples were analyzed by plaque assay on U2OS cells and qPCR against the E3L gene.

Temperature was measured rectally immediately before and at various time points after the infusion of virus (end of infusion, + 5 min, + 10 min, + 30 min, + 2h, + 5h). Fever was designated as a temperature of 39.8°C and above. CBC profiles were determined using a Drew Hemavet 950FS on samples collected immediately before the infusion of virus, at the end of the infusion, + 2h and + 5h after the infusion. Blood biochemistry was analyzed using a Vetscan VS2 Chemistry Analyzer (Abaxis, Union City, CA, USA) on samples collected immediately before the infusion of virus, at the end

of the infusion, + 2h and + 5h after the infusion. Measurements were obtained for alanine aminotransferase (ALT), alkaline phosphatase (ALP), amylase, blood urea nitrogen, creatinine, total bilirubin, albumin, total protein, globulin, glucose, sodium, potassium, phosphate, and calcium.

Alternative pathway hemolytic assay Blood was collected and treated with Refludan (50 ug/mL), centrifuged to collect plasma (800g) and frozen immediately. To assess hemolytic activity, rabbit erythrocytes (Complement Technology, TX USA) were incubated with plasma at a concentration corresponding to 70% lysis (7 μL of 1:1 diluted plasma) in GVB^{++} (Complement Technology, Texas, USA) and optical absorbance measured at 410 nm using a Multiskan Ascent (Thermo Labsystems, Mississauga, ON). The percent inhibition of complement activity was calculated relative to the corresponding sample collected prior to CP40 administration.

Cytokine array A MILLIPLEX MAP non-human primate magnetic bead cytokine array (Millipore, Bedford MA) was performed according to the manufacturer's instructions by the Princess Margaret Genomics Centre, Toronto ON. Samples were quantified with a Luminex 100 and data was analyzed using Bio-plex Manager 6.0. OBS concentrations were measured in pg/mL.

qPCR DNA was isolated from whole blood collected in EDTA tubes, liver, or tumor samples using the DNeasy kit (Qiagen, Germantown, MD) according to the manufacture's protocol. Quantitative PCR was performed on viral DNA extracted from

whole blood or tissues using the SYBR Green PCR Master Mix (Qiagen, Germantown MD) on a RotorGene RG3000A (Corbett Research). Primers targeting the E3L gene were used to quantify viral genomes (TCCGTCGATGTCTACACAGG; ATGTATCCCGCGAAAAATCA). DNA isolated from purified viral stock was used as a standard where molecular weight was used to give an estimate of the number of copies per μg of DNA. Primers targeting the human β actin gene were used to normalize E3L signals when a given number of cells was used (AGGTATCCTGACCCTGAAGT, AGGTCTCAAACATGATCTGG).

Statistics Where possible, statistical analyses were performed on log transformed values. When data points fell below the limit of detection, the value of half the limit of detection was used for statistical comparisons, however was reported as ND (not detected) for graphical purposes. Statistical analyses were performed using GraphPad Prism and the R statistical software. Two-tailed unpaired student's t tests were performed for the comparison of two groups and one-way ANOVAs employed for the comparison of multiple independent groups. Linear mixed effects models were fitted for experiments with repeated measures data using treatment condition, vaccination status or time point as fixed effects, and donor as the random effect. Model fit was compared for models generated using pooled or unpooled levels of fixed effects to determine statistical significance. *p*-values of < 0.05 were considered significant *$p \leq 0.05$, **$p \leq 0.01$, ***$p < 0.001$, ****$p < 0.0001$.

3. Results

3.1 Human complement, antibodies and vaccinia virus

As part of the phase I dose escalation clinical trial where patients were treated with IV Pexa-Vec (clinical trials registration number NCT00625456), we received and quantified the infectious virus in the blood of three patients treated at the dose of 1 x 10^9 pfu (Figure 3.1). At the end of the one hour infusion, we recovered a mean of 6 x 10^2 pfu/mL or approximately 3 x 10^6 pfu in an estimated blood volume of 5L. This corresponds to nearly 0.3% of the total dose of virus. Infectious virus was cleared quickly from the circulation, and 30 minutes post infusion, virus was only detectable in the blood of one of the three patients. Although viral delivery was confirmed by immunohistochemistry or qPCR in tumor biopsies taken 8-10 days post infusion, the therapeutic response rate was moderate(100).

3.1.1 Human complement and antibodies lead to profound neutralization of vaccinia virus in vitro

As a first step to understanding the relative impact of the factors leading to a loss of infectious virus in the blood, we assessed *in vitro* the neutralization of a prototype of the clinical Pexa-Vec virus in blood or fractions thereof that was collected from healthy human donors. Donors were stratified into naïve and vaccinated categories based on age (date of birth relative to 1972), the presence of a vaccination scar, and self-reported immunization history. Both genders were sampled equally (48% female, 52% male). A concentration of 2 x 10^5 pfu/mL was used to mimic the clinical dose of 1 x 10^9 pfu in an estimated blood volume of approximately 5L that was required to achieve delivery(100).

Figure 3.1. Infectious virus in the blood after an intravenous dose of Pexa-Vec

Blood samples were collected from three patients that were treated at the dose of 1 x 10^9 pfu as part of a phase one clinical trial (clinical trials registration number NCT00625456). Infectious virus was quantified by plaque assay**.** Data is represented as group means ±SD. Each dot represents a patient. ND, not detected; NC, not collected. The number of patients from which virus was not detected or for which blood was not collected is indicated in parentheses.

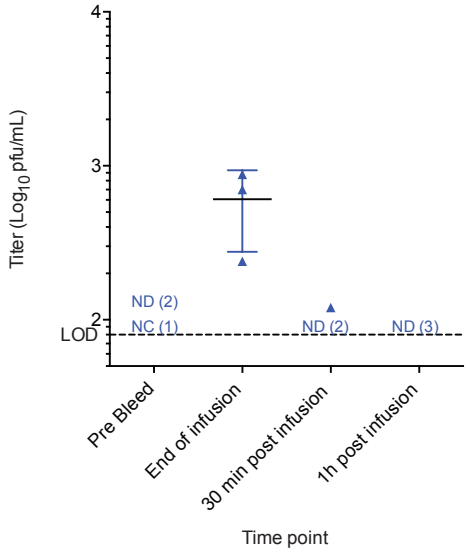
4
3
2
LOD
Titer (Log10 pfu/mL)
ND (2)
NC (1)
ND (2)
ND (3)
Pre Bleed
End of infusion
30 min post infusion
1h post infusion
Time point

The anti-coagulant Refludan was used as it does not interfere with the complement cascade as do EDTA, citrate and heparin(205). As shown in Figure 3.2A, we observed similar levels of recovery in whole blood and plasma samples from both naïve and vaccinated donors. This suggested to us that the factors leading to the greatest loss of infectivity were plasma components. As was consistent with previous findings(108), vaccinia virus was shown to be sensitive to complement in naïve plasma samples, leading to the loss of up to approximately 90% of infectivity. This viral neutralization could be prevented using heat treatment as a method to inactivate complement. We observed robust neutralization of vaccinia virus in blood and plasma samples from vaccinated individuals with up to 99% of infectivity lost. Interestingly, we saw that the effect of the long-lived antibodies was almost completely abrogated when complement was inactivated, whereby heat inactivation of plasma from immunized individuals restored infectivity to 20% of maximum. We confirmed our findings with respect to complement with two complement inhibitors: CP40 and Futhan. Using the C3 – specific peptide, CP40, and an inactive peptide as a control, we demonstrated that vaccinia virus neutralization by antibodies was entirely dependent on complement activation (Figure 3.2B). Indeed, CP40 pre-treatment of plasma led to virus recovery from samples from immune individuals that was not statistically different from naïve donors. Using the serine protease inhibitor Futhan, we also demonstrated that complement inhibition could prevent viral neutralization in naïve and immune plasma (Figure 3.2C). These findings led us to ask whether this complement dependence of antibody was unique to individuals that had been vaccinated several decades ago or if it would hold true in the anamnestic antibody response. To this end, we collected serum samples from patients involved in a

Pexa-Vec clinical trial (clinical trials registration number IDNCT01394939), both prior to their first treatment with virus, and two weeks after their first treatment. This serum was heat inactivated to specifically assess the antibodies and was combined with plasma from a naïve donor as a replenished source of complement. The serum collected prior to Pexa-Vec treatment contained pre-existing antibodies that were exclusively complement-dependent. The anamnestic antibodies that were produced two weeks after treatment possessed a moderately increased capacity to neutralize vaccinia virus in the absence of complement, however, was profoundly neutralizing in the presence of replenished complement. Importantly, complement-enhanced neutralization could be prevented if plasma samples were pre-treated with the complement inhibitor CP40 (Figure 3.2D).

Clinically, dose escalation identified a breakthrough dose where intravenously delivered virus was detected in biopsied tumor samples(100). We sought to characterize vaccinia virus neutralization at doses above and below this concentration (2×10^4 pfu/ml – 2×10^7 pfu/mL). In plasma from naïve donors (Figure 3.3A), the effect of complement could be saturated at doses of 2×10^6 pfu/mL or higher. If plasma samples were pre-treated with CP40, however, nearly all the virus could be recovered at all dose levels. In vaccinated plasma samples (Figure 3.3B), a threshold effect was observed whereby between 0.1 and 1% of virus was recovered at dose levels between 2×10^4 and 2×10^6 pfu/mL. However, at the dose of 2×10^7 pfu/mL, a significant increase in recovery was observed. Consistent with our previous results, significantly elevated levels of infectious virus could be recovered at all doses if complement was inhibited with CP40.

Figure 3.2. Human complement and antibody lead to the neutralization of vaccinia virus

(A) Assessment of vaccinia virus neutralization *in vitro* in human blood samples from vaccinia naïve or immunized healthy donors. Infectious virus was quantified by plaque assay following a one hour incubation at 37^{o}C at the concentration of 2 x 10^5 pfu/mL in whole blood, plasma or heat inactivated plasma. (n=4-5 donors per immune status) This panel represents pooled data from several experiments. (B) Plasma samples were heat inactivated or treated with CP40 (25μM) or the inactive peptide control prior to incubation with vaccinia virus (2 x 10^5 pfu/mL). (n=3 donors per immune status) (C) Plasma samples were heat inactivated or treated with Futhan (50 μg/mL) prior to incubation with vaccinia virus. (2 x 10^5 pfu/mL). (n=3 donors per immune status) (D) Heat inactivated serum samples from four patients enrolled in a Pexa-Vec clinical trial (clinical trials registration number IDNCT01394939) was combined with plasma from a naïve donor as a source of complement. Naïve plasma was pre-treated with CP40 (as described in B) when noted. Virus was incubated with complement and antibody at a concentration of 2 x 10^5 pfu/mL. Data are represented as group means ±SD. Each dot represents a donor. (*** p<0.001, ** $p < 0.01$, * $p < 0.05$, ^{ns} $p > 0.05$).

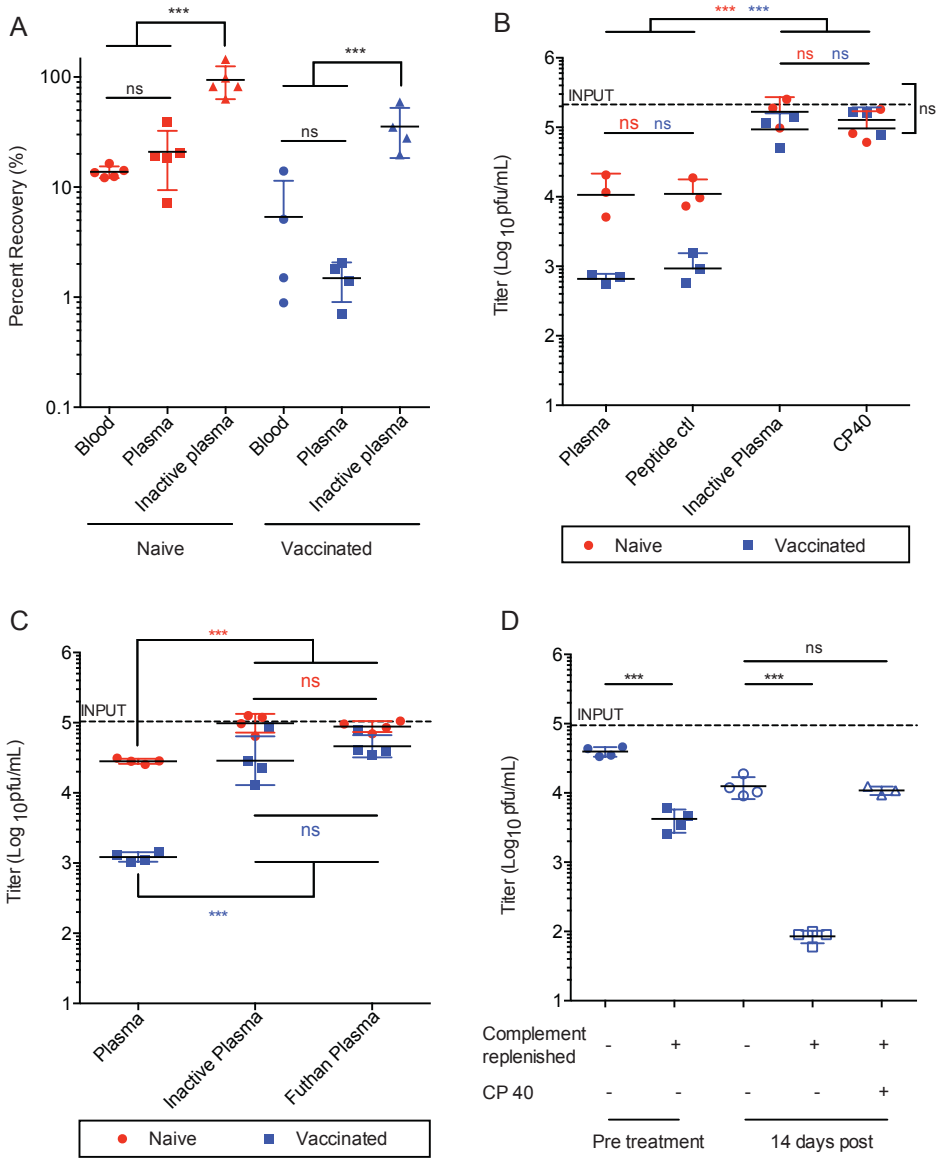
A
***
***
ns
ns
100
10
1
0.1
Percent Recovery (%)
Blood
Plasma
Inactive plasma
Blood
Plasma
Inactive plasma
Naive
Vaccinated
B
*** ***
ns ns
INPUT
ns ns
ns
6
5
4
3
2
1
Titer (Log 10 pfu/mL)
Plasma
Peptide ctl
Inactive Plasma
CP40
Naive
Vaccinated
C
***
ns
INPUT
ns
***
6
5
4
3
2
1
Titer (Log 10pfu/mL)
Plasma
Inactive Plasma
Futhan Plasma
Naive
Vaccinated
D
ns
***
***
INPUT
6
5
4
3
2
1
Titer (Log10 pfu/mL)
Complement replenished
- + - + +
CP 40
- - - - +
Pre treatment
14 days post

Figure 3.3. Virus neutralization by antibody and complement can be overcome at elevated concentrations of virus

Vaccinia virus neutralization in naïve (A) or vaccinated (B) plasma at virus concentrations ranging from 2 x 10^4 pfu/mL to 2 x 10^7 pfu/mL after a one hour incubation at 37^{o}C. Plasma was pre-treated with CP40 (25μM) when noted. (n=3 donors per immune status). Data are represented as group means ±SD. Each dot represents a donor. The number of donors from which virus was not detected (ND) is indicated in parentheses. The comparisons between plasma and plasma pre-treated with CP40 at each dose are indicated by (‡ $p<0.001$, † $p < 0.01$, § $p < 0.05$, ^{ns} $p > 0.05$). All other statistical comparisons are indicated by (*** $p<0.001$, ** $p < 0.01$, * $p < 0.05$, ^{ns} $p > 0.05$).

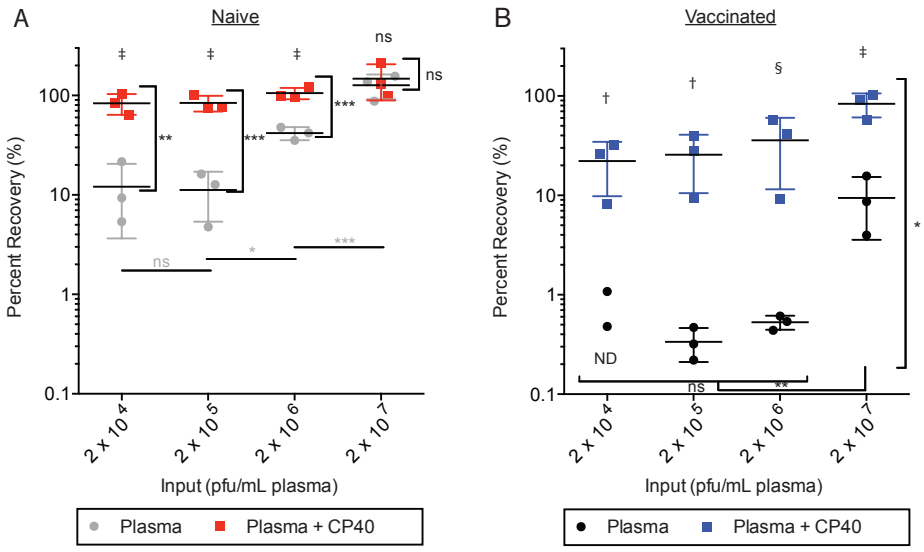
A
Naive
B
Vaccinated
Percent Recovery (%)
100
10
1
0.1
ns
*
**
***
†
‡
§
ND
2 x 10 4
2 x 10 5
2 x 10 6
2 x 10 7
Input (pfu/mL plasma)
Plasma
Plasma + CP40

To assess the relative importance of particular pathways of the complement cascade on viral neutralization, we employed antibodies to selectively block the function of key complement components (illustrated in Figure 3.4A). In naïve plasma samples, we observed complete viral recovery when either the classical or alternative pathways were inhibited, thereby underscoring their importance (Figure 3.4B). Although the MBL antibody produced a statistically significant increase in recovery, the effect size was very small relative to the increase in virus recovery observed when the classical or alternative pathways were inhibited. In plasma samples from vaccinated donors, we observed incomplete but statistically significant increases in recovery with classical and alterative pathway inhibition (Figure 3.4C). Specifically, we observed a 3-fold and 13-fold increase with the anti-C1q and anti-Factor B antibodies, respectively. Recovery of infectious virus was maximized when these pathways were inhibited in combination (38 fold increase in titer), thereby highlighting the role of the alternative pathway as a positive amplification loop for the other two pathways. In samples from vaccinated donors, inhibition of the MBL pathway did not increase viral recovery. The efficacy of the MBL antibody was validated in an MBL binding assay whereby anti-MBL treated serum was assessed for its ability to activate complement by mannan (Figure 3.4D).

The clinically approved monoclonal antibody, eculizumab, directed against C5, was used to inhibit the terminal pathway. In both naïve and immune plasma, inhibition of the terminal pathway abrogated virtually all the viral neutralization, leading to a mean 7-fold and 52-fold increase in titer, respectively (Figure 3.4E). In an alternative method to assess the involvement of the terminal pathway and the MAC, we carried out sucrose density centrifugation of virus incubated with detergent, plasma or saline. While native,

intact, particles subjected to centrifugation were observed by immunoblot to be present in fractions 12 and 13, detergent or plasma treated virus was detected in fractions 1-4 in addition to fractions 12 and 13 (Figure 3.4F). These observations were consistent with complement and antibody-mediated virolysis by the MAC.

Figure 3.4. Mechanistic characterization of complement and antibody mediated neutralization of Vaccinia virus.

(A) Complement pathway schematic with targets of inhibitory antibodies. Complement activation pathway dissection is shown in naïve (B) or immune (C) plasma. Selective inhibition of the various pathways of the complement cascade demonstrates their contribution to viral neutralization. Plasma from naïve and immune donors was pre-treated with 500 μg/mL anti-Factor B or 100 μg/mL anti-C1q or 60 μg/mL anti-MBL antibodies to allow for binding. Vaccinia virus neutralization over the course of a one hour incubation at $37^{o}C$ (2×10^{5} pfu/mL) was subsequently assessed by plaque assay. (n=3 per immune status with the exception of naïve eculizumab samples (n=2). Data are represented as group means ±SD, Each dot represents a donor. (*** $p<0.001$, ** $p < 0.01$, * $p < 0.05$, ^{ns} $p > 0.05$). (D) Validation of functionality of the anti-MBL antibody. MBL dependent C3 deposition was measured in the presence or absence of the anti-MBL antibody(10ug/ml) by absorbance at 405 nm. (n=2 donors). (E) Plasma from naïve and immune donors was pre-treated with 50 μg/mL of eculizumab (anti-C5) and neutralization over the course of a one hour incubation at $37^{o}C$ (2×10^{5} pfu/mL) was subsequently assessed by plaque assay. (F) Loss of virus particle density is observed by sucrose gradient separation of vaccinia antigens. Continuous sucrose gradients (5%-75%) were overlaid with vaccinia virus treated with PBS, Triton or immune plasma at a concentration of 2×10^{7} pfu/mL. Fractions were collected and assayed by immunblot blot for vaccinia proteins using the polyclonal Quartett antibody.

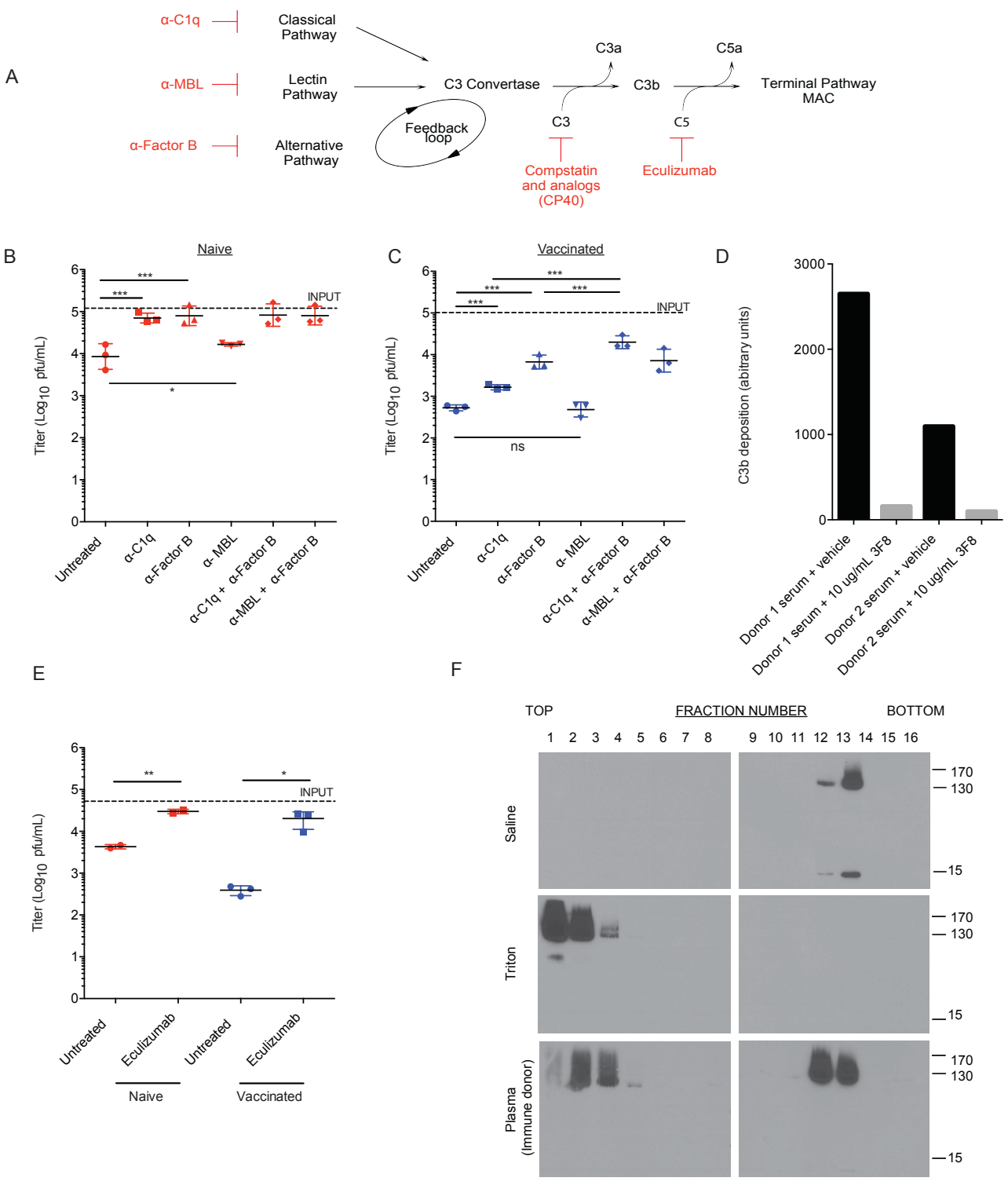
A
α-C1q
α-MBL
α-Factor B
Classical Pathway
Lectin Pathway
Alternative Pathway
Feedback loop
C3 Convertase
C3a
C5a
C3b
C3
C5
Terminal Pathway MAC
Compstatin and analogs (CP40)
Eculizumab
B
Naive
Titer (Log10 pfu/mL)
INPUT
Untreated
α-C1q
α-Factor B
α- MBL
α-C1q + α-Factor B
α-MBL + α-Factor B
C
Vaccinated
ns
D
C3b deposition (abitrary units)
Donor 1 serum + vehicle
Donor 1 serum + 10 ug/mL 3F8
Donor 2 serum + vehicle
Donor 2 serum + 10 ug/mL 3F8
E
Eculizumab
Naive
Vaccinated
F
TOP
FRACTION NUMBER
BOTTOM
Saline
Triton
Plasma (Immune donor)
170
130
15

3.2 Discerning appropriate models for the in vivo study of vaccinia virus neutralization by complement and antibodies

3.2.1 The mouse model is not a suitable surrogate to represent human antibody and complement-mediated neutralization of vaccinia virus

We explored the validity of the mouse model to replicate the findings observed with human complement and anti-vaccinia virus antibodies. An *ex vivo* neutralization assay was performed with fresh mouse plasma from a naïve animal or an animal vaccinated one month prior to the terminal bleed (Figure 3.5A). In naïve plasma, complement inhibition had no effect on the virus recovered. While reduced viral recovery was observed from vaccinated plasma, antibody-mediated neutralization was not enhanced by complement. To assess virus delivery to tumors in the presence or absence of complement and antibody, we pursued a model whereby virus was administered intravenously to tumor bearing mice (Figure 3.5B). Only tumors from naïve animals contained infectious virus 48 hours post-administration, as was also observed by imaging of the Firefly luciferase transgene (Figures 3.5C, D). The dose of cobra venom factor used to deplete complement was validated by immunoblot against the mouse C3 protein (Figure 3.5E). While C3 degradation products could be detected in plasma (lower band) from all mice, full length C3 could not be detected in CVF treated mice (upper band).

The inability of mouse plasma to fully recapitulate the neutralizing effects seen in human plasma led us to explore other small animal models. To this end, we obtained serum from guinea pig, hamster, rat and rabbit and assessed the sensitivity of vaccinia virus to complement of these species relative to human complement. We observed similar degrees of complement dependent neutralization (input dose 2 x 10^5 pfu/mL) in both rat and rabbit serum, but not guinea pig

Figure 3.5. Mouse complement and antibody do not work together to neutralize vaccinia virus

(A) Ex vivo neutralization of vaccinia virus by plasma from naïve or vaccinated Balb/c mice (1x 10^7 pfu virus one month prior). Refludan was used to anti-coagulate blood (50 ug/mL). Plasma was heat inactivated or pre-treated with Futhan (50 ug/mL). Virus was incubated with plasma for one hour at 37^{o}C at a ratio of approximately 2 x 10^5 pfu/mL and quantified by plaque assay. (n=1 mouse/immune status). Data is represented as technical replicates ±SD. According to the schedule in (B), animals were vaccinated and treated with 1 x 10^7 pfu of vaccinia (Western reserve, VVdd, expressing Firefly Luciferase). Animals were depleted of complement with 4.5 U of CVF. Viral delivery to subcutaneous tumors following an intravenous bolus dose of vaccinia virus (1 x 10^7 pfu) was measured by plaque assay (C) as well as by luminescence measured by an IVIS imaging system following an intraperitoneal injection of luciferin (D). (n=5 mice per group). The number of mice from which virus was not detected (ND) is indicated in parentheses. (E) Plasma from mice that were treated with 4.5 U CVF as well as untreated control animals was collected and immunoblot analysis using a polyclonal antibody to mouse complement C3 specific was performed. (n=2 mice per group)

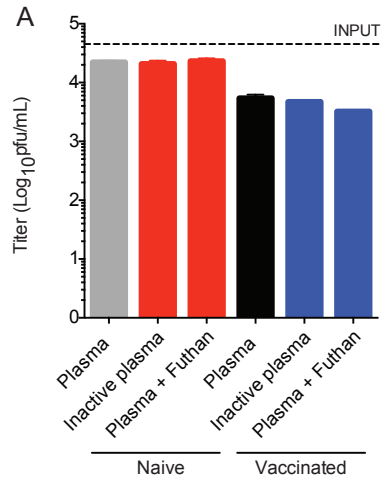
A
INPUT
Titer (Log10pfu/mL)
5
4
3
2
1
0
Plasma
Inactive plasma
Plasma + Futhan
Plasma
Inactive plasma
Plasma + Futhan
Naive
Vaccinated

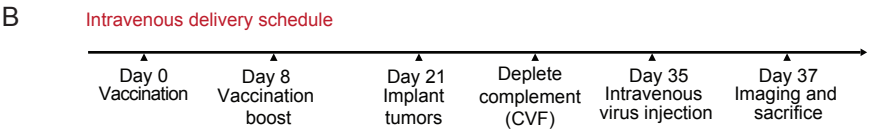
B
Intravenous delivery schedule
Day 0
Vaccination
Day 8
Vaccination
boost
Day 21
Implant
tumors
Deplete
complement
(CVF)
Day 35
Intravenous
virus injection
Day 37
Imaging and
sacrifice

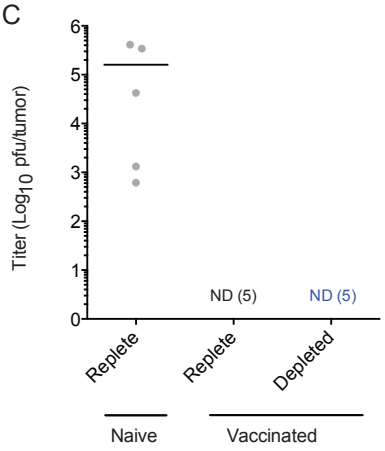
C
Titer (Log10 pfu/tumor)
6
5
4
3
2
1
0
ND (5)
ND (5)
Replete
Replete
Depleted
Naive
Vaccinated

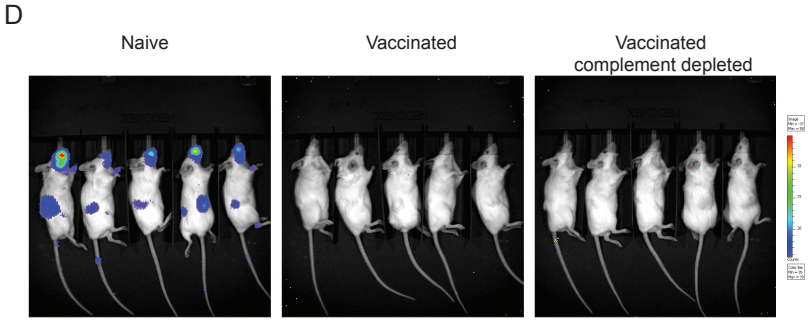
D
Naive
Vaccinated
Vaccinated
complement depleted

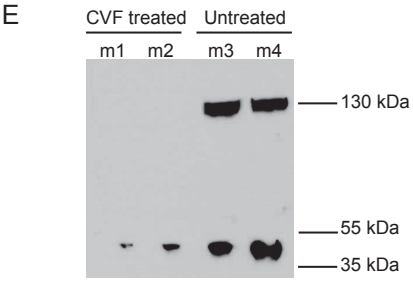
E
CVF treated
Untreated
m1
m2
m3
m4
130 kDa
55 kDa
35 kDa

or hamster (Figure 3.6A). We went on to explore the antibody profile generated in Fischer F344 rats to which the 13762 MAT B III mammary adenocarcinoma cell line is syngeneic. Rats were left naïve or vaccinated with 1 x 10^7 pfu of vaccinia virus intravenously and/or depleted of complement with 35U CVF. Since the inhibitor CP40 is specific to human and non-human primate C3(132), we resorted to using CVF in our rat model to manipulate complement. Animals were terminally bled and virus neutralization was assessed *ex vivo* in untouched or heat-inactivated plasma (Figure 3.6B). Again, similarly to the neutralization seen in human plasma, complement mediated neutralization of vaccinia virus was observed in naïve plasma. Importantly, the antibodies generated against the virus were only modestly neutralizing when complement was inhibited. The viral recovery was very similar between heat inactivated plasma and plasma from complement depleted animals, thereby functionally validating the complement depletion. Complement depletion at the dose of 35 U was also assessed by immunoblot using an antibody against rat C3 (Figure 3.6C). C3 degradation products could be detected in plasma (lower band) from all rats, full length C3 could not be detected in CVF treated rat (upper band).

3.2.2 Complement depletion in immune Fischer rats enhances delivery and infection of tumors

We assessed the impact of complement depletion in immune rats on the stability of infectious virus in the blood and delivery to tumors, as outlined in (Figure 3.7A). At a very early time point after intravenous virus administration (10 minutes), we recovered

Figure 3.6. The rat is an appropriate model for the study of complement and antibody mediated neutralization of vaccinia virus

(A) The ability of serum from guinea pig, hamster (Syrian Gold), rat (Sprague Dawley) and rabbit (New Zealand White) to neutralize vaccinia virus was tested alongside naïve human plasma. Vaccinia virus was incubated with untouched or heat-inactivated serum at a concentration of 2 x 10^5 pfu/mL for one hour at 37^{o}C and subsequently quantified by plaque assay. Data is represented as technical replicate means ±SD. (B) *In vitro* neutralization of vaccinia virus with Fischer rat plasma. Animals were vaccinated with 1 x 10^7 pfu intravenously and or depleted of complement with 35U CVF. Blood was collected 24 hours after complement depletion. Vaccinia virus was incubated with untouched or heat inactivated plasma (2 x 10^5 pfu/mL) and quantified by plaque assay. (n=2 rats/treatment group) Data are represented as group means ±SD. Each dot represents a rat. (*** $p<0.001$, ^{ns} $p > 0.05$). **(C)** Plasma samples collected 24 hours post CVF treatment (35U) was analyzed by immunoblot using an antibody against C3. (n=4 rats per group).

A

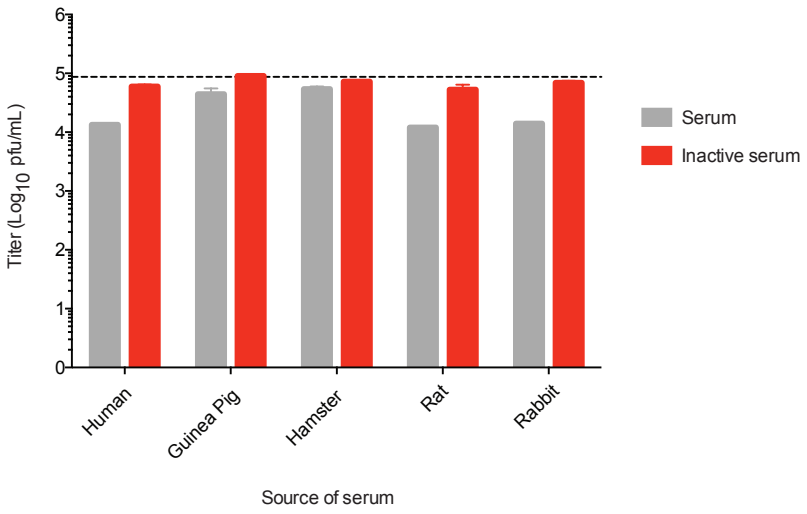
Titer (Log10 pfu/mL)
0
1
2
3
4
5
6
Human
Guinea Pig
Hamster
Rat
Rabbit
Source of serum
Serum
Inactive serum

B

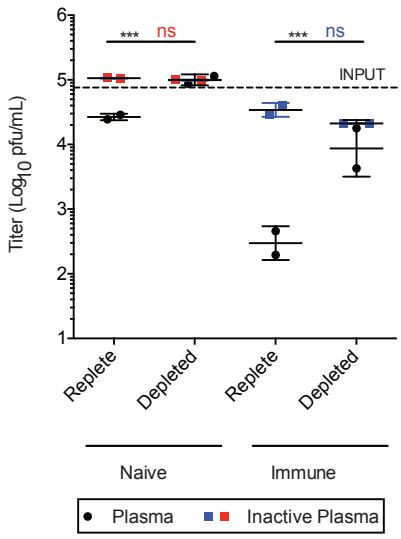
Titer (Log10 pfu/mL)
1
2
3
4
5
6
*** ns
*** ns
INPUT
Replete
Depleted
Replete
Depleted
Naive
Immune
Plasma
Inactive Plasma

C

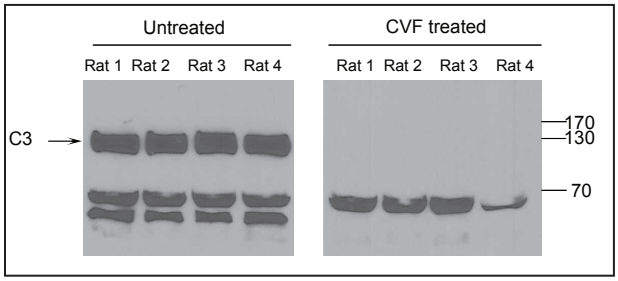
Untreated
CVF treated
Rat 1 Rat 2 Rat 3 Rat 4
Rat 1 Rat 2 Rat 3 Rat 4
C3
170
130
70

approximately 100-fold more infectious virus from the blood of complement-depleted animals relative to their complement-replete counterparts (Figure 3.7B). At the same time point, a concomitant increase was observed in infectious virus in the subcutaneous tumors of complement-depleted animals (Figure 3.7C). To better understand the increase in titer that was observed, vaccinia virus genomes were quantified in blood, tumor, and liver samples by quantitative real-time PCR (qPCR) using primers against the viral E3L gene. Although a substantial increase was observed in the number of infectious particles in each organ when complement was depleted, the number of total genomes experienced minor changes. This pattern suggested that complement depletion reduced viral neutralization, but did not change the distribution of the virus (Figure 3.7D). Indeed, complement depletion did not appear to alter the rapid non-specific clearance to a great degree, however it increased the proportion of the dose that accumulates in the tumor that remains infectious. Viral recovery from tumors implanted both subcutaneously and in the lungs was assessed at a longer time point: 24 hours post intravenous virus administration. Notably, infectious virus was only recovered from subcutaneous tumors or lung tumors if the animal was depleted of complement at the time of virus administration (Figure 3.7E). Similarly to the increase in titer observed in the blood and tumors, a corresponding increase in viral titer was observed in the liver 10 minutes post tail vein injection of virus (Figure 3.7F). However, infectious virus could not be recovered from the liver 24 hours after injection whether the animal was depleted of complement or not, suggesting that complement depletion did not increase the infection of normal tissue.

Figure 3.7. Complement depletion in vaccinia virus immune Fischer rats leads to improved delivery and infection of tumors

Vaccinia virus (1 x 10^8 pfu) was delivered intravenously to Fischer rats bearing bilateral 13762 MATBIII tumors, according the schedule in (A). As per the treatment groups, rats were vaccinated intravenously with 1 x 10^7 pfu or depleted of complement with 35 U of CVF. Infectious virus in the blood (B) and in subcutaneous tumors (C) ten minutes post virus administration was quantified by plaque assay. (n=3-4 rats per group) (D) The fold change in titer and total genome content of blood, subcutaneous tumors and liver is expressed as the ratio of complement depleted relative to complement-replete samples. (E) Subcutaneous and lung tumor titers 24 hours after an intravenous dose of oncolytic vaccinia virus at 1 x 10^8 pfu. (n=7-8 per group). (F) Ten minutes or 24h after intravenous virus delivery, animals were sacrificed and livers were analyzed for virus content by plaque assay. (n=3-4 per group). Data are represented as group means ±SD, Each dot represents a rat. The number of rats from which virus was not detected (ND) is indicated in parentheses. (*** $p<0.001$, ** $p < 0.01$, * $p < 0.05$, ^{ns} $p > 0.05$).

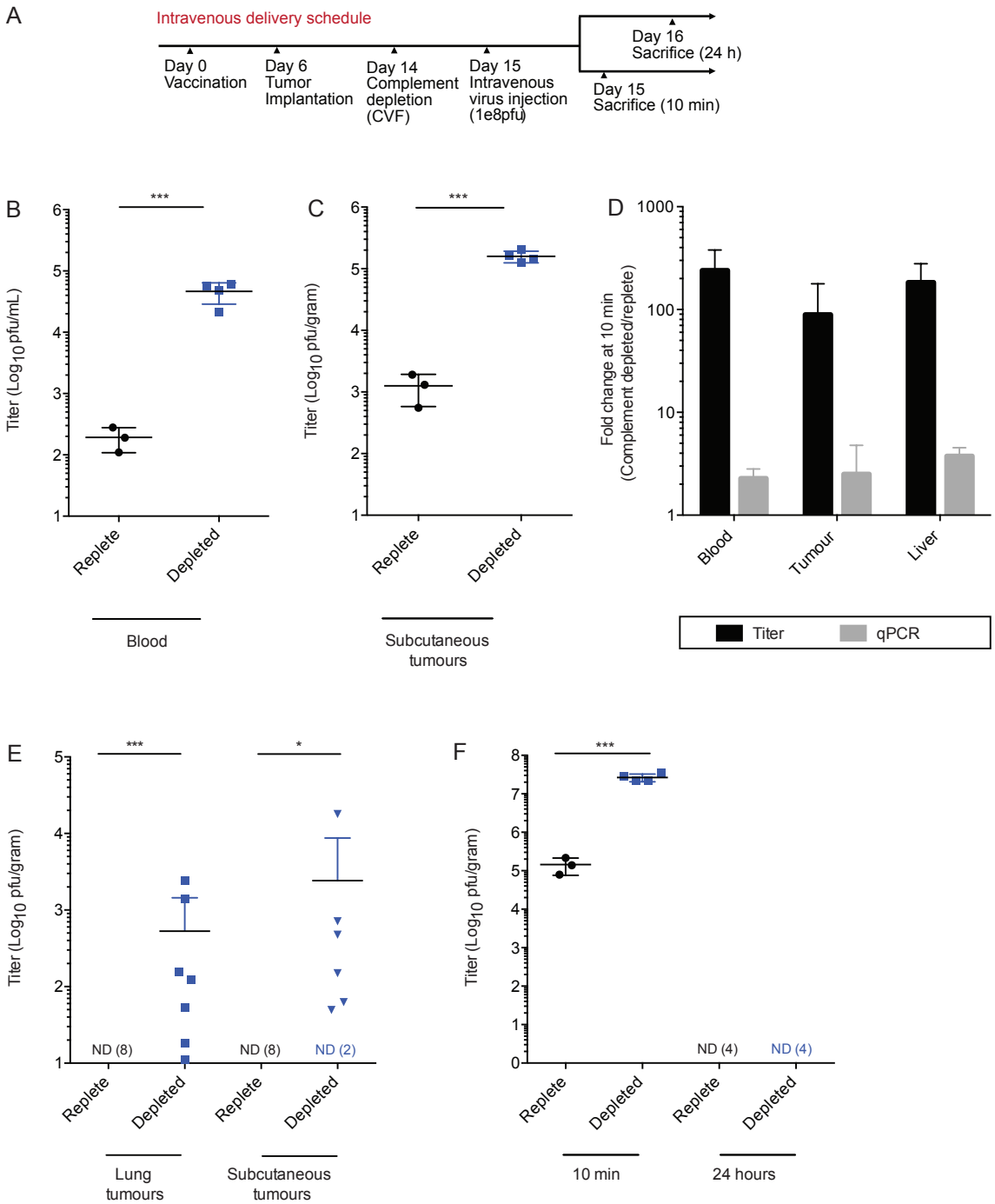
A
Intravenous delivery schedule
Day 0
Vaccination
Day 6
Tumor
Implantation
Day 14
Complement
depletion
(CVF)
Day 15
Intravenous
virus injection
(1e8pfu)
Day 16
Sacrifice (24 h)
Day 15
Sacrifice (10 min)
B
Titer (Log10 pfu/mL)
***
Replete
Depleted
Blood
C
Titer (Log10 pfu/gram)
***
Replete
Depleted
Subcutaneous
tumours
D
Fold change at 10 min
(Complement depleted/replete)
Blood
Tumour
Liver
Titer
qPCR
E
Titer (Log10 pfu/gram)
***
*
ND (8)
ND (8)
ND (2)
Replete
Depleted
Replete
Depleted
Lung
tumours
Subcutaneous
tumours
F
Titer (Log10 pfu/gram)
***
ND (4)
ND (4)
Replete
Depleted
Replete
Depleted
10 min
24 hours

Naïve animals were treated according to the schedules outlined in Figure 3.8 A and D. Unlike in the vaccinated animals, changes in viral stability in the blood of complement replete or depleted naïve animals at an early time point (5 min post injection) were not observed (Figure 3.8B). Genome quantification in the blood of these animals did not reveal a significant change due to complement depletion (Figure 3.8C). Similarly, when virus was administered to virus-naïve tumor bearing rats, infectious virus was equally recovered from the tumors of complement-depleted or complement-replete animals 48 hours post injection (Figure 3.8E).

The increased delivery of infectious virus to subcutaneous tumors in immune animals led us to investigate whether this would have therapeutic benefit and slow tumor growth. Animals were treated according to the schedule in Figure 3.9A, where they were received vaccinia virus or PBS with or without complement depletion. Tumor volume was followed for two weeks after implantation. Comparison of the treatment groups suggested no significant difference between any of the groups (Figure 3.9B).

In light of the clinical preference for regional over systemic administration of virus, we sought to determine if the infection following direct intratumoral injection of virus into subcutaneous tumors would also benefit from complement depletion. Animals were treated according to the schedule in Figure 3.10A and sacrificed either 24 or 48 hours after virus injection. Tumors from immunized and complement depleted animals were found to contain an average of 20 and 117 fold more infectious virus 24 and 48 hours post-injection, respectively (Figure 3.10B). In keeping with the previous results in naïve rats, complement depletion did not increase the infection of tumors in naïve rats following intratumoral administration of virus.

Figure 3.8. Complement depletion in vaccinia virus naïve Fischer rats does not change virus stability in the blood nor infection of tumors

Vaccinia virus (1 x 10^8 pfu) was delivered intravenously to Fischer rats bearing bilateral 13762 MATBIII tumors, according the schedule in (A). As per the treatment groups, rats were depleted of complement with 35 U of CVF. Infectious virus in the blood five minutes after intravenous virus administration as measured by plaque assay (B) and qPCR quantification of viral genomes using primers against the E3L gene (C) (n=3-4 rats per group) . Naïve rats bearing bilateral tumors were treated according to the schedule in (D). Delivery of virus to subcutaneous tumors as measured by plaque assay 48 hours after virus administration (E). (n=3-4 per group). Data are represented as group means ±SD, Each dot represents a rat. (^{ns} $p > 0.05$).

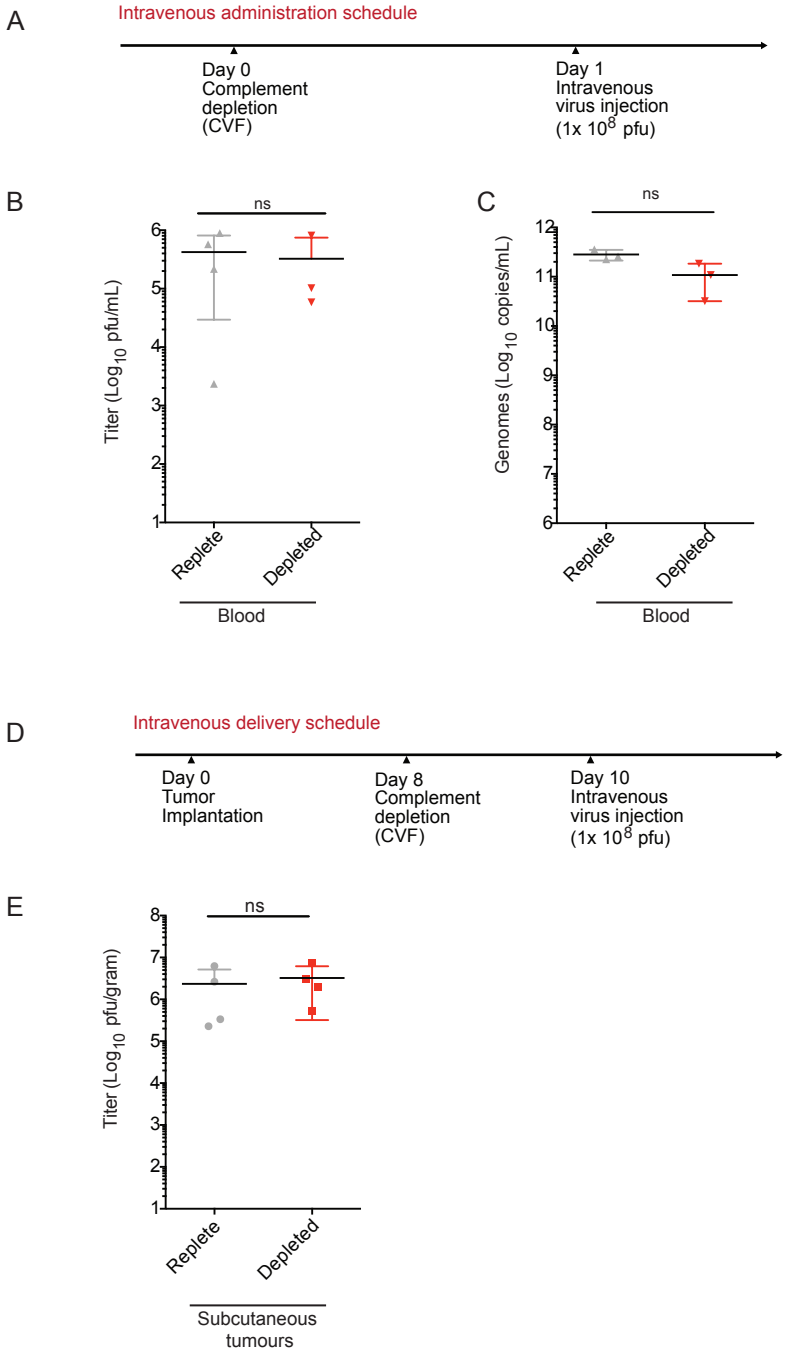
A
Intravenous administration schedule
Day 0
Complement
depletion
(CVF)
Day 1
Intravenous
virus injection
(1x 10^8 pfu)
B
ns
Titer (Log10 pfu/mL)
Replete
Depleted
Blood
C
ns
Genomes (Log10 copies/mL)
Replete
Depleted
Blood
D
Intravenous delivery schedule
Day 0
Tumor
Implantation
Day 8
Complement
depletion
(CVF)
Day 10
Intravenous
virus injection
(1x 10^8 pfu)
E
ns
Titer (Log10 pfu/gram)
Replete
Depleted
Subcutaneous
tumours

Figure 3.9. Intravenous virus treatment does not impact the growth rate of subcutaneous mammary adenocarcinoma tumors in Fischer rats.

1 x 10^6 13762 MAT B III cells were implanted subcutaneously bilaterally and treated according to the schedule in (A) with 1 x 10^8 pfu intravenously with or without CVF treatment (35 U). Tumor burden was determined by caliper measurement and was determined to be not significantly different between groups by one-way ANOVA (^{ns} $p > 0.05$). Volume was calculated using the formula $V= (L \times W^2)/2$, where L is the larger value. (n=3 rats per group).

A

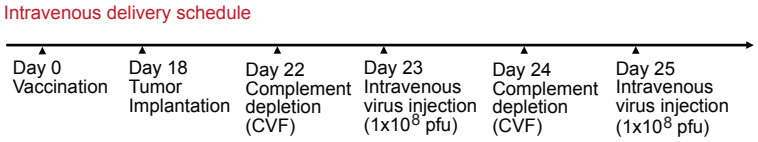
Intravenous delivery schedule
Day 0
Vaccination
Day 18
Tumor
Implantation
Day 22
Complement
depletion
(CVF)
Day 23
Intravenous
virus injection
(1x10^8 pfu)
Day 24
Complement
depletion
(CVF)
Day 25
Intravenous
virus injection
(1x10^8 pfu)

B

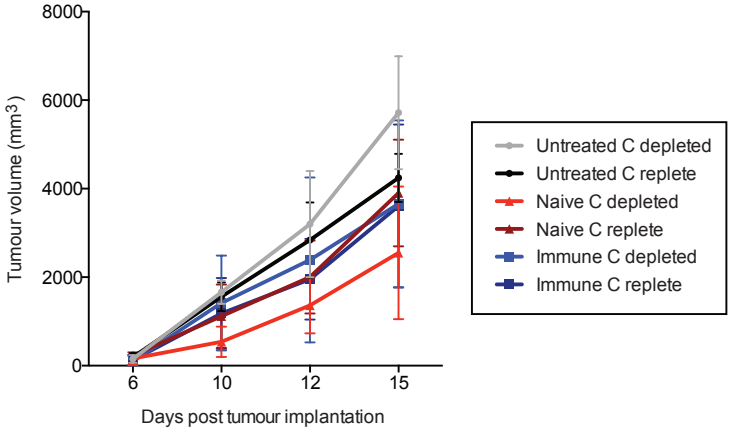
8000
6000
4000
2000
0
Tumour volume (mm3)
6
10
12
15
Days post tumour implantation
Untreated C depleted
Untreated C replete
Naive C depleted
Naive C replete
Immune C depleted
Immune C replete

Figure 3.10. Complement depletion improved infection of tumors following local administration in immune rats

Vaccinia virus (1 x 10^7 pfu) was delivered intratumorally to Fischer rats bearing bilateral 13762 MAT B III tumors, according to the schedule in (A). As per the treatment groups, rats were vaccinated intravenously with 1 x 10^7 pfu and or depleted of complement with 35 U of CVF. (B) Subcutaneous tumor titers are shown for animals sacrificed 24 and 48 hours post virus administration. (n=4 per group) Data are represented as group means ±SD, Each dot represents a rat. (** $p < 0.01$, * $p < 0.05$, ^{ns} $p > 0.05$).

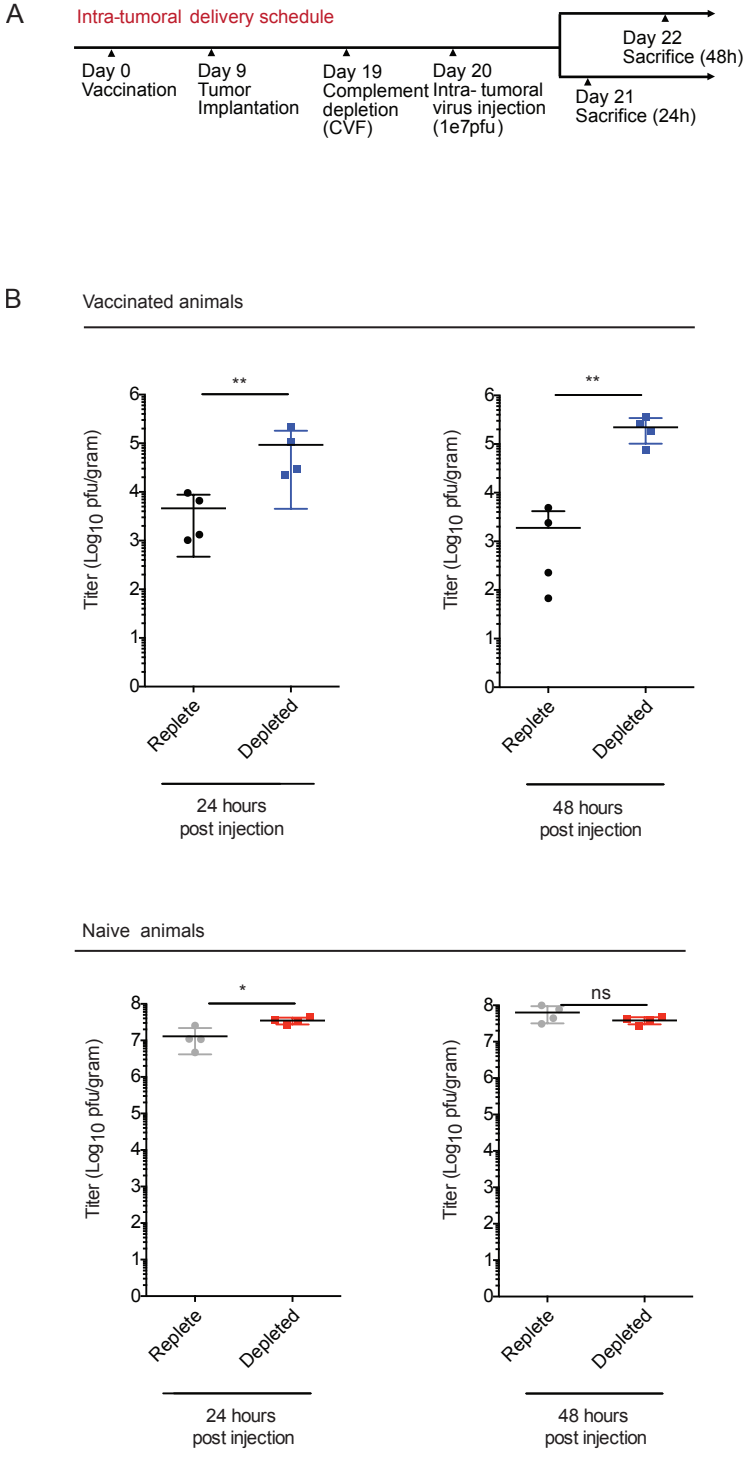
A
Intra-tumoral delivery schedule
Day 0
Vaccination
Day 9
Tumor
Implantation
Day 19
Complement
depletion
(CVF)
Day 20
Intra- tumoral
virus injection
(1e7pfu)
Day 21
Sacrifice (24h)
Day 22
Sacrifice (48h)
B
Vaccinated animals
Titer (Log10 pfu/gram)
**
Replete
Depleted
24 hours
post injection
48 hours
post injection
Naive animals
*
ns

3.2.3 Testing the feasibility and safety of the clinical candidate inhibitor CP40 in conjunction with an infusion of vaccinia virus in a NHP model

After the success of complement inhibition *in vitro* and complement depletion in the immune rat model, we wanted to investigate whether this phenomenon could be replicated with the clinical candidate complement inhibitor CP40 *in vivo*. Due to the primate specific binding of CP40, we investigated the potential of employing a cynomolgus macaque model. Two preliminary *in vitro* neutralization experiments were performed to assess the sensitivity of vaccinia virus to cynomolgus macaque complement and the dependence of anti-vaccinia antibodies on complement activation. A first experiment investigated neutralization of vaccinia virus in blood, plasma or heat inactivated plasma collected from a virus naïve macaque *in vitro*. We observed similar levels of neutralization between whole blood and plasma fractions and viral neutralization that was abrogated upon complement inactivation by heat treatment (Figure 3.11A). We then went on to look at neutralization *in vitro* in blood or plasma in the context of an exogenous source of anti-vaccinia antibody and a complement inhibitor. Heat inactivated serum from a previous experiment from a rhesus macaque treated with 1 x 10^9 pfu of VVdd via an intraperitoneal catheter approximately 3 months prior to blood collection was used as a source of antibody. Blood, plasma or heat-inactivated plasma was combined with the complement inhibitor Futhan (250 μg/mL for all samples with the exception of plasma where it was used at 50 μg/mL) or heat inactivated serum (final dilution 1:4). The addition of Futhan to blood or plasma substantially increased viral recovery, underscoring the importance of complement-mediated neutralization of vaccinia virus (Figure 3.11B). The addition of anti-viral antibodies in the presence of functional complement was able to completely prevent the recovery of infectious virus.

Importantly, in the absence of functional complement (ie Futhan treated plasma/blood or heat inactivated plasma), these antibodies induced only moderate viral neutralization.

These initial experiments verified that the model was appropriate and led us to design an experiment to test the feasibility and safety of transient complement inhibition with CP40 and its impact on the half-life of infectious virus in the blood after an infusion of vaccinia virus. Four animals were used in the main study and one animal used to test that the dose was sufficient to detect infectious virus in the blood after the infusion. We designed the experiment to maximize the number of treatment conditions that we could assess while minimizing the number of animals. As outlined in Figure 3.12A all the animals in the main study received 5 doses of virus as an intravenous infusion (1×10^8 pfu vaccinia virus over 30 minutes). The first two doses were administered within the same week to assess the naïve animals: one dose was given as single agent virus, and the other with a bolus dose of CP40 (2mg/kg) immediately prior to virus. The doses of virus were given in this short interval so that both doses would be given prior to the generation of antibody(206). The animals received a boost of virus close to three months later. Approximately four months after their first virus treatments, all the animals, with the test dose animal included, received two doses of vaccinia in the same week, with one dose given as single agent virus, and the other with a bolus dose of CP40 to test the feasibility of complement inhibition in the virus immune state. Again, the two doses were

Figure 3.11. The cynomolgus macaque model recapitulates the sensitivity of vaccinia virus that was observed to human antibody and complement.

Two independent validation experiments were performed to test the appropriateness of the cynomolgus macaque model. Blood was collected from a healthy cynomolgus macaque and anticoagulated with Refludan (50 μg/mL). The neutralization of vaccinia virus was evaluated in blood, plasma or heat inactivated plasma after a one hour incubation at 37^{o}C (A). The effect of complement and antibody were further explored in (B) with the use of Futhan (250 μg/mL for all samples with the exception of plasma where it was used at 50 μg/mL) and exogenous antibody (heat inactivated serum, final dilution 1:4) from previously treated macaques. Data is represented as technical replicate means ±SD. ND, not detected.

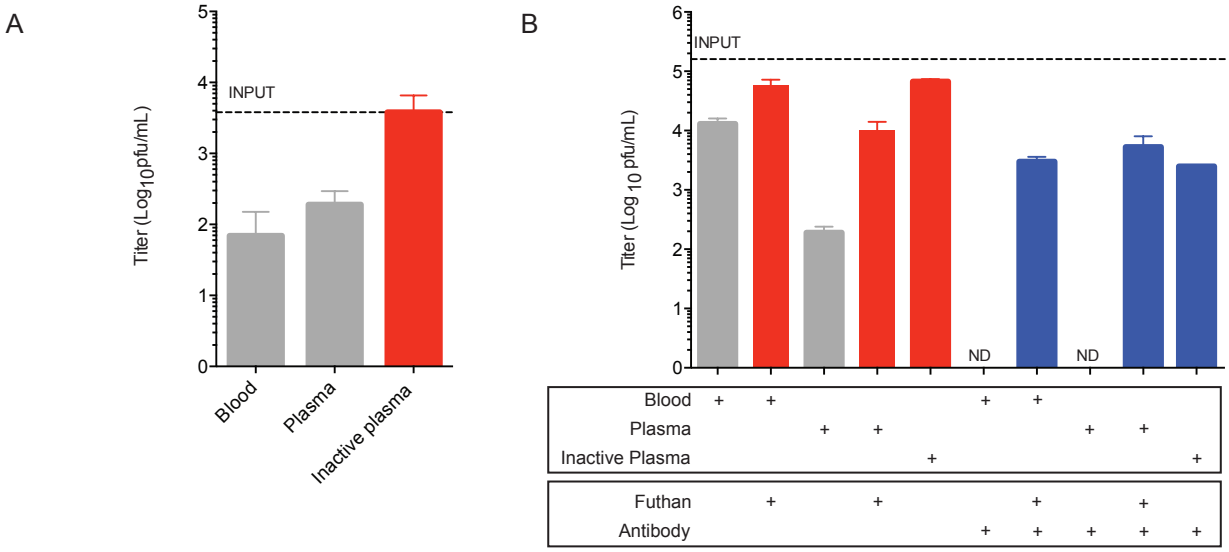
A
Titer (Log10pfu/mL)
INPUT
Blood
Plasma
Inactive plasma
B
Titer (Log 10 pfu/mL)
INPUT
ND
ND
Blood
Plasma
Inactive Plasma
Futhan
Antibody

given two days apart to ensure that they would be administered in the context of the same amount of anti-viral antibodies. The animals were divided into two treatment schedules such that half of them would receive virus as a single agent as the first treatment, and the other group would receive a CP40 bolus prior to virus as their first treatment. We did not observe any differences that would suggest that the order of treatment produces artifacts that impacted our assessment of viral stability in the blood.

As previously done with human plasma (Figure 3.2), we validated that all the animals used in our study generated anti-viral antibodies that were almost exclusively neutralizing in the presence of complement in an *in vitro* neutralization assay (Figure 3.12B).

As the primary objective of the study was to assess the impact of complement inhibition on viral stability in the blood, we collected blood samples at the end of the infusion (EOI) and various time points after to assess infectious virus and total virus by plaque assay and qPCR, respectively. The average viral titers for all the animals is represented in Figure 3.13A and data for each individual animal is depicted in Figure 3.13B. While we did not observe a significant difference in the viral titer when the animals were pre-treated with CP40 in the naïve state, profound changes were observed with CP40 pre-treatment when the animals were immune to the virus. Relative to when they were naïve, peak blood titers in immune animals at the end of the infusion were reduced (mean titer 9.82 x 10^2 pfu/mL) and infectious virus fell below the limit of detection quickly. With CP40 pre-treatment, however, the peak titer at the end of the infusion was significantly elevated (mean titer 9.23 x 10^3pfu/mL; mean increase 9.93-fold) and approached the titer that was detected when the animal was naïve. At the end of

Figure 3.12. Experimental outline for the cynomolgus macaque model

(A) Animals were treated according to the treatment schedule. Vaccinia virus (1×10^8 pfu) was infused using a venous line over the course of 30 minutes. As per the treatment schedules, animals received a bolus intravenous dose of CP40 (2mg/kg) immediately prior to virus treatment. (B) Heat inactivated plasma collected from animals when they were naïve or immune to the virus was combined with an exogenous source of complement (plasma from a naïve animal) and neutralization of vaccinia virus was assessed *in vitro* at 2×10^5 pfu/mL after a one hour incubation at 37^oC. (n=4) Data are represented as group means ±SD. Each dot represents a macaque. (*** $p<0.001$)

A

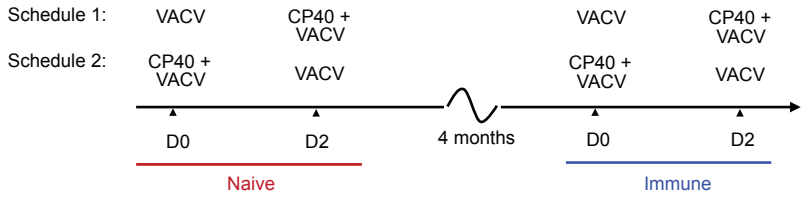
Schedule 1:
VACV
CP40 + VACV
VACV
CP40 + VACV
Schedule 2:
CP40 + VACV
VACV
CP40 + VACV
VACV
D0
D2
4 months
D0
D2
Naive
Immune

B

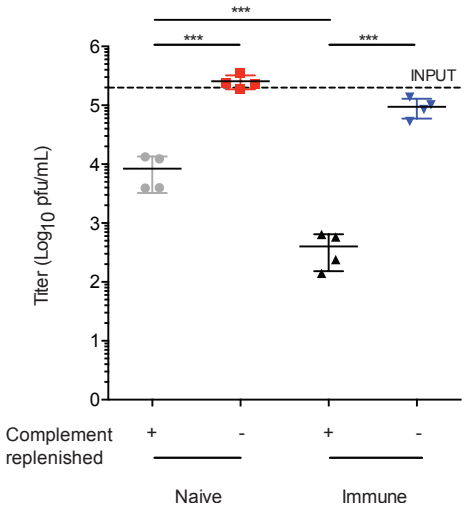
***
***
***
INPUT
Titer (Log10 pfu/mL)
0
1
2
3
4
5
6
Complement replenished
+
-
+
-
Naive
Immune

the infusion, in naïve animals, approximately 8% of the input virus was recovered by plaque assay, while in immune animals 0.2% was recovered. If CP40 was used, the average proportion of the input that remained in circulation was approximately 1.9%. Moreover, the time after the infusion during which infectious virus was detectable was prolonged with CP40 pre-treatment in all immune animals. These trends, albeit slightly different in each outbred animal, are consistent across all tested animals. In contrast to the robust changes observed in viral titer, the concentration of genomes was not significantly affected in CP40 pre-treated animals, irrespective of immune status (Figure 3.14 A, B). This observation was consistent with the rat model and indicated that complement did not have a substantial role in directing the clearance of viral particles from the circulation. The quantification of infectious virus and total virus in the blood of the test dose animal are shown in Appendix Figure 1 and are consistent with the trends observed in the other animals.

Although the dose of CP40 has been extensively tested in numerous non-human primate models, we verified that complement was inhibited by means of an alternative pathway hemolysis assay. We observed close to complete complement inhibition in all animals treated with CP40. The average data is shown in Figure 3.15 and individual animals shown in Appendix Figure 2. Since complement activation does not follow a linear relationship between the amount of complement protein present and the amount of lysis that is observed, an initial experiment was performed to determine the volume of plasma to use to give optimal sensitivity of the assay. A specified volume of plasma from each animal and time point was incubated with rabbit erythrocytes, and using a standard curve, the volume equivalents of complement activity were calculated. These values were

Figure 3.13. Complement inhibition in a cynomolgus macaque model stabilizes vaccinia virus in the blood of immune animals

Infectious virus in the blood was measured by plaque assay on samples collected at various time points after the end of the infusion (EOI). (A) Mean blood titers for all naïve and immune are represented as group means ±SD. (n=4) (B) Titers for individual animals are represented as technical replicate means ±SD. ND, not detected, LOD, limit of detection (*** $p<0.001$, ^{ns} $p > 0.05$).

A

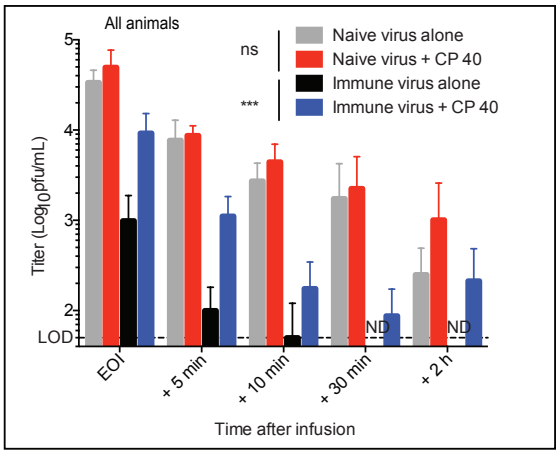

B

Naive time point

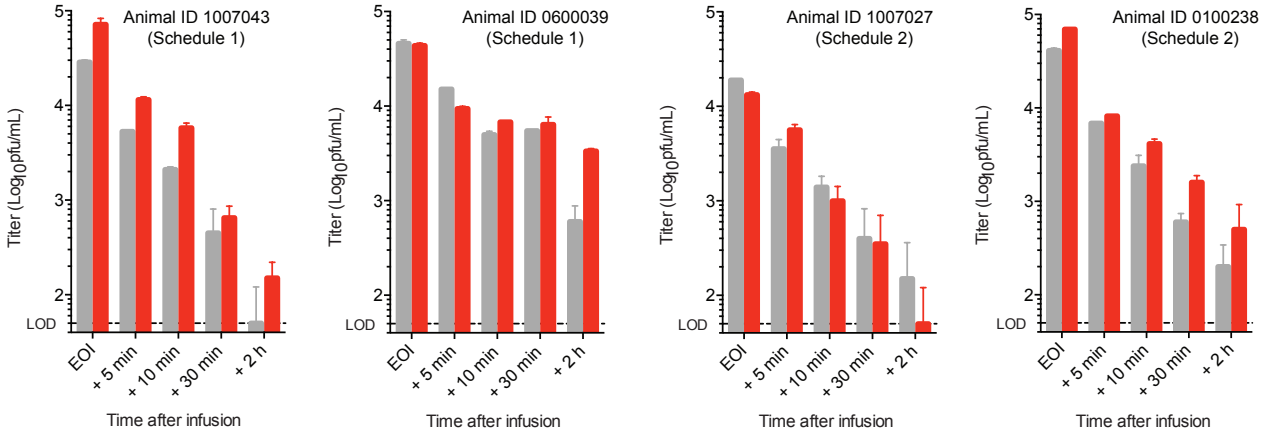

Immune time point

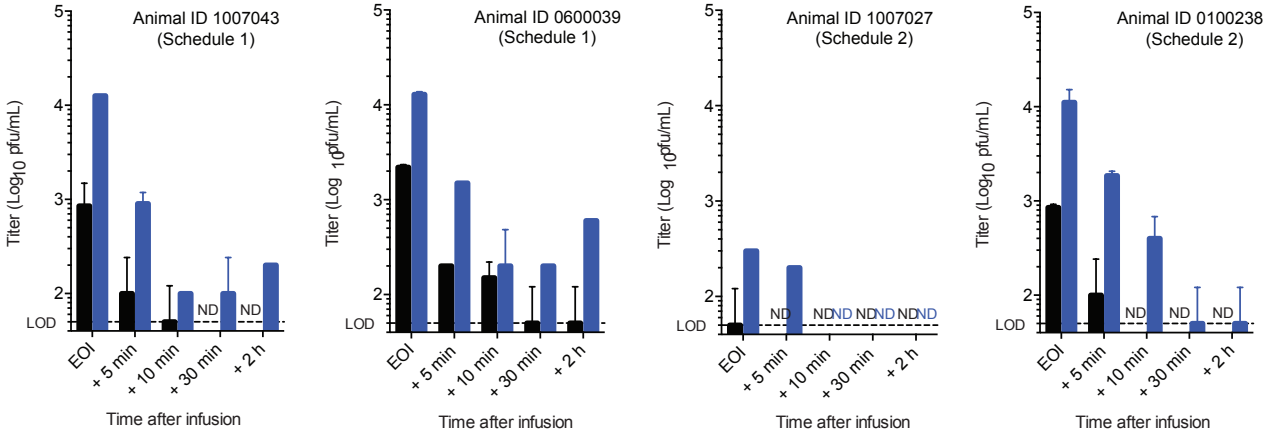

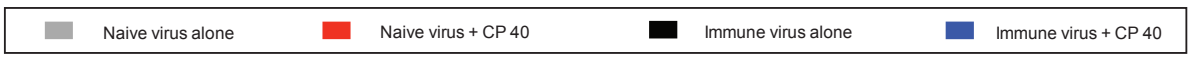

Figure 3.14. Complement inhibition does not change the rate of clearance of viral genomes from the circulation.

Genome content of blood collected at various time points after the end of the infusion (EOI), as measured by qPCR using primers against the viral gene E3L. (A) Mean genome concentrations in the blood for all naïve and immune animals are represented as group means ±SD. (n=4) The blood genome concentrations for individual animals are shown in (B) and are represented as technical replicate means ±SD. (^{ns} $p > 0.05$).

A

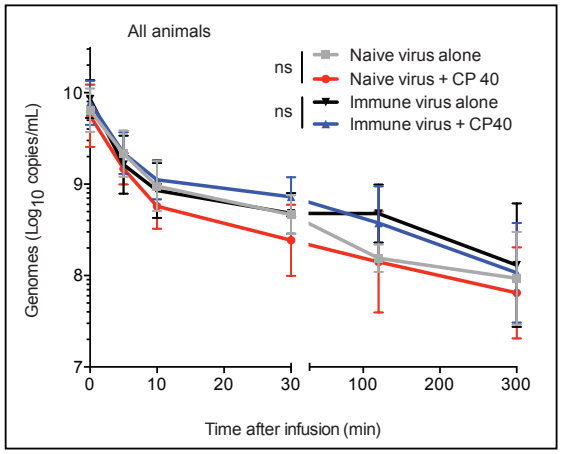

B Naive time point

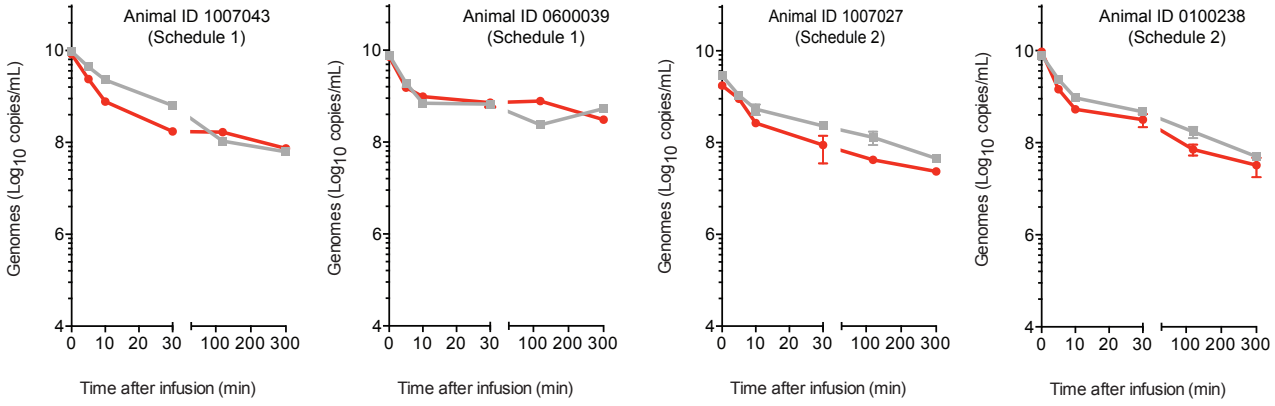

Immune time point

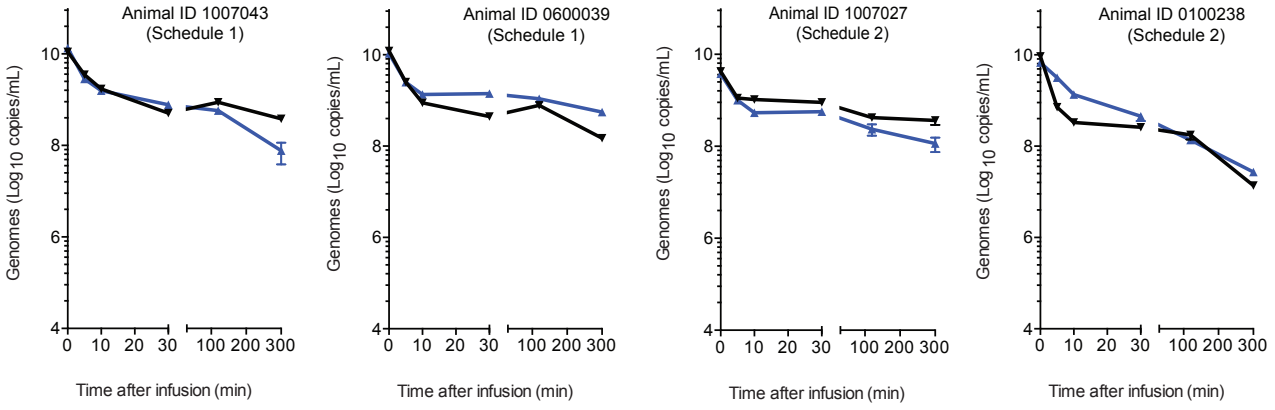

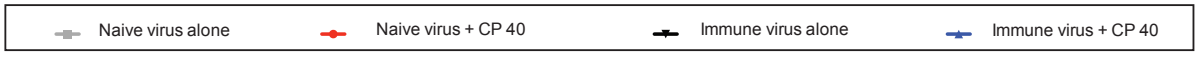

Figure 3.15. CP40 inhibited complement activation

To assess hemolytic activity, rabbit erythrocytes were incubated for 30 minutes at 37^{o}C with plasma collected at various time points on the day of infusion prior to and after the the end of the infusion (EOI) at a concentration corresponding to 70% lysis. The percent inhibition of complement activity was calculated relative to a sample collected from the same animal prior to CP40 administration. The group mean inhibition is shown ±SD. (n=4) (*** $p<0.001$).

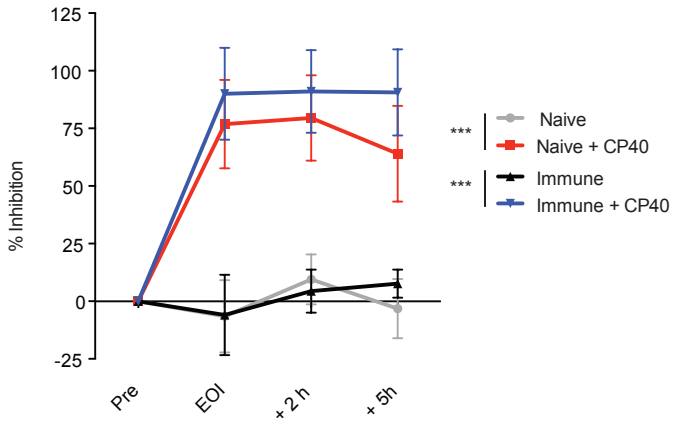
125
100
75
50
25
0
-25
% Inhibition
Pre
EOI
+2 h
+5h
***
Naive
Naive + CP40
***
Immune
Immune + CP40

used to calculate the percent inhibition of complement observed in samples collected after the blood draw prior to any treatment. This optimization is illustrated in Appendix Figure 2.

Animals were monitored daily throughout the experiment to assess their activity level and food consumption. We evaluated blood chemistry at several time points before and after infusion, and did not observe any indication of renal, hepatic or pancreatic dysfunction. We also performed a hematologic analysis on the days of infusion, and while we observed transient changes in lymphocyte, neutrophil and monocyte counts, they were drug independent (Figure 3.16). Rectal temperature was measured at several time points and was deemed to be a fever if it reached the threshold of 39.8^{o}C. We observed mild fevers in some naïve animals, however the incidence of fever on the day of infusion was not increased by complement inhibition. Fevers were treated with acetaminophen as soon as the temperature threshold was reached. Fevers were not observed in immune animals on the day of infusion (Table 3.1). Pock lesions were observed in naïve animals but not immune animals and resolved without complication.

We performed a cytokine array on plasma collected prior to the infusion as well as two and five hours post infusion. The concentration of 23 cytokines was assessed in samples from three animals (two animals from schedule 2, and one animal from schedule 1). The analysis was complicated by the time frame of repeat dosing with or without CP40 and some cytokines did not return to baseline prior to the second infusion. However, there is not sufficient evidence to suggest that complement inhibition definitively modified pro or anti-inflammatory cytokine profiles. Three important pro-inflammatory cytokines, IFN γ, TNF α and IL 1β are shown in Figure 3.17 and do

Figure 3.16. Complete blood cell counts for animals on the day of infusion

CBC profiles were determined for blood samples taken prior to treatment and various time points after the end of the infusion (EOI). Absolute counts (K/μL) and percent of leukocytes (%) are reported as means ±SD. K, one thousand cells (n=4 animals).

Complete blood cell counts for naive animals

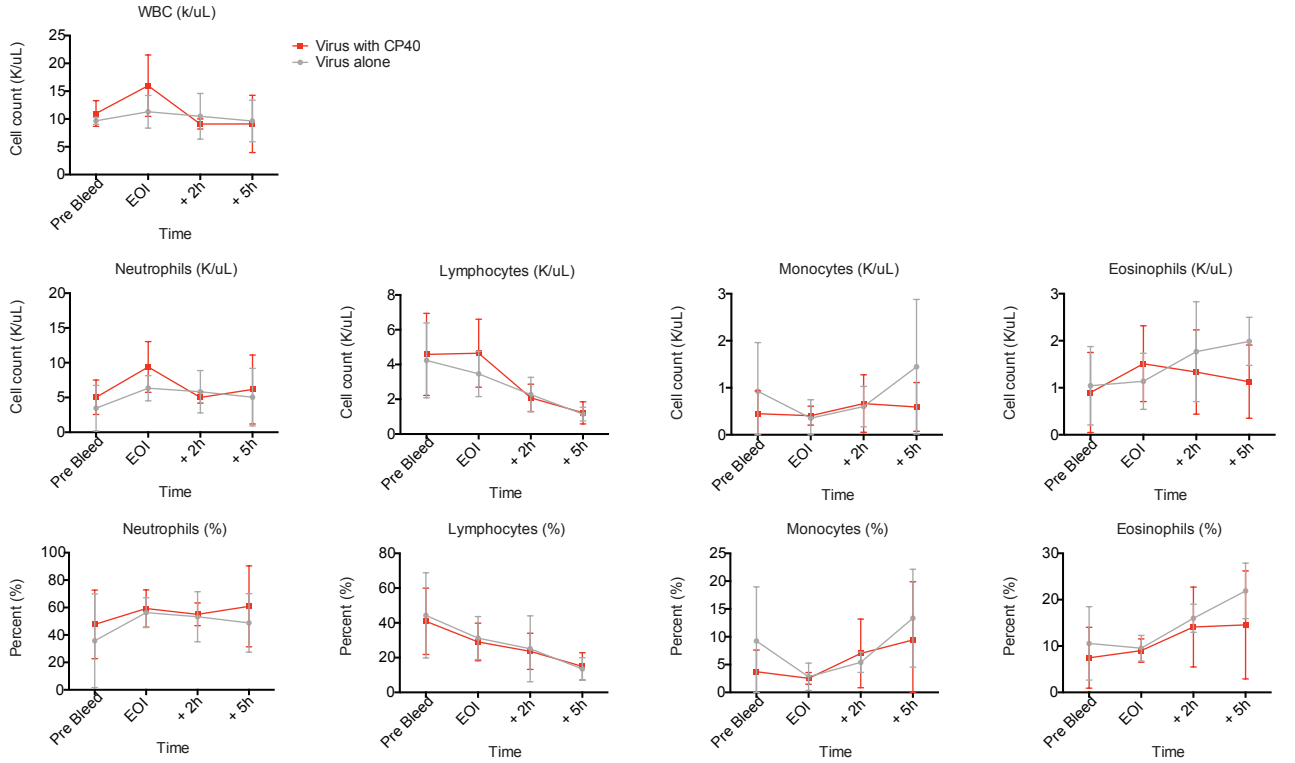

Complete blood cell counts for immune animals

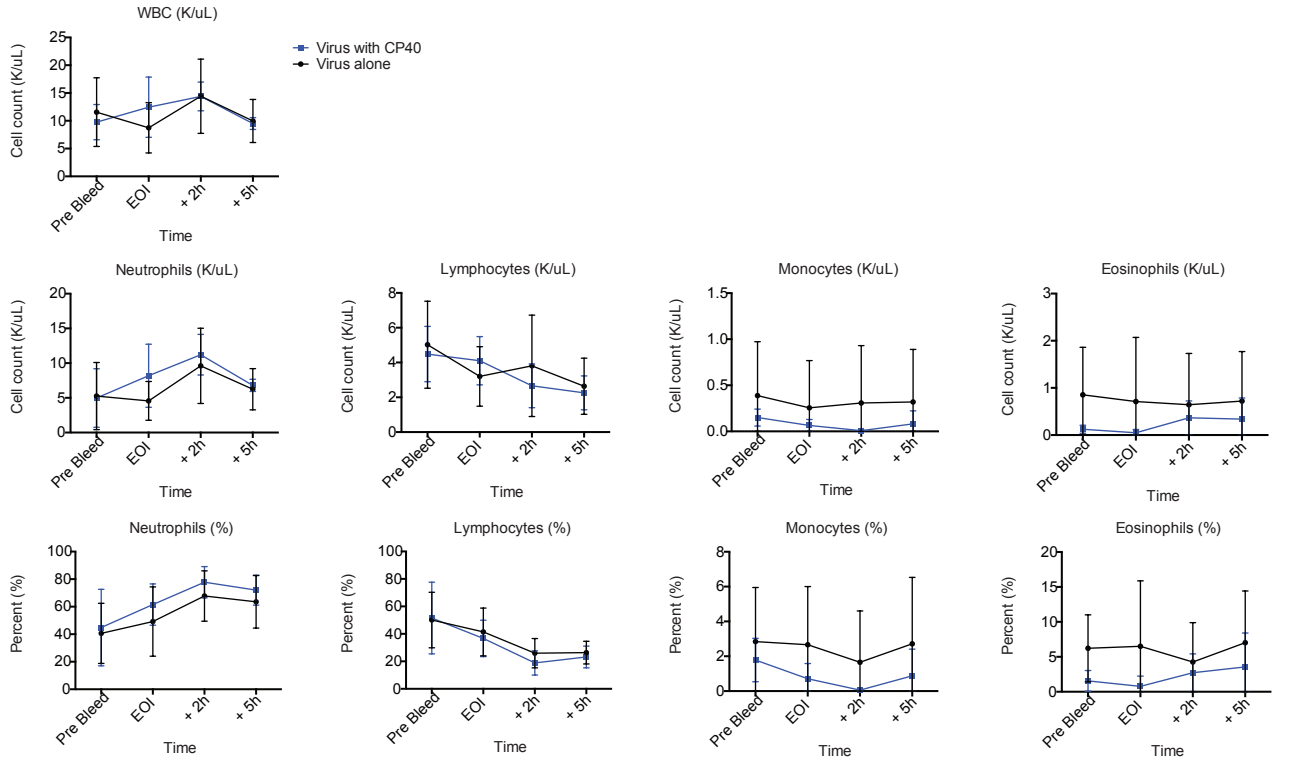

Table 3.1. Fever incidence on the day of infusion

Rectal temperature was measured prior to infusion and up to five hours after virus treatment. The temperature threshold for a fever was designated as 39.8^{o}C. Y, yes, N, no.

Animal ID	Schedule	Naive		Immune	
		Virus alone	Virus + CP40	Virus alone	Virus + CP40
0600039	1	N	N	N	N
1007043	1	Y	Y	N	N
1007027	2	Y	N	N	N
0100238	2	Y	N	N	N

not appear to be exacerbated or diminished specifically by virus alone or in combination with CP40. Cytokine expression cascades are tightly regulated, and mechanisms of negative regulation that curb the magnitude and duration of responses have been well characterized(207). In this respect, Figure 3.18 depicts two cytokines, IL 6 and MCP-1, which appear to be elevated on the first day (day 0) of virus administration and unresponsive on the second day (day 2), regardless of which treatment is first. This effect also seems to be independent of immune status or complement. Nonetheless, all the animals seem to behave slightly differently and there are exceptions to these trends. The profile of the additional cytokines assayed is shown in Appendix Figure 3.

Figure 3.17. Pro-inflammatory cytokine production is not exacerbated with CP40 treatment

Blood samples were collected prior to treatment, and 2 and 5 hours after the end of the infusion. The plasma from these samples was analyzed for a panel of cytokines. Here shown are three pro-inflammatory cytokines: IFNγ, TNFα and IL-1β. Each connected set of data points represents an animal. Each grey dotted box represents an infusion day. (n=3 animals)

Interferon γ

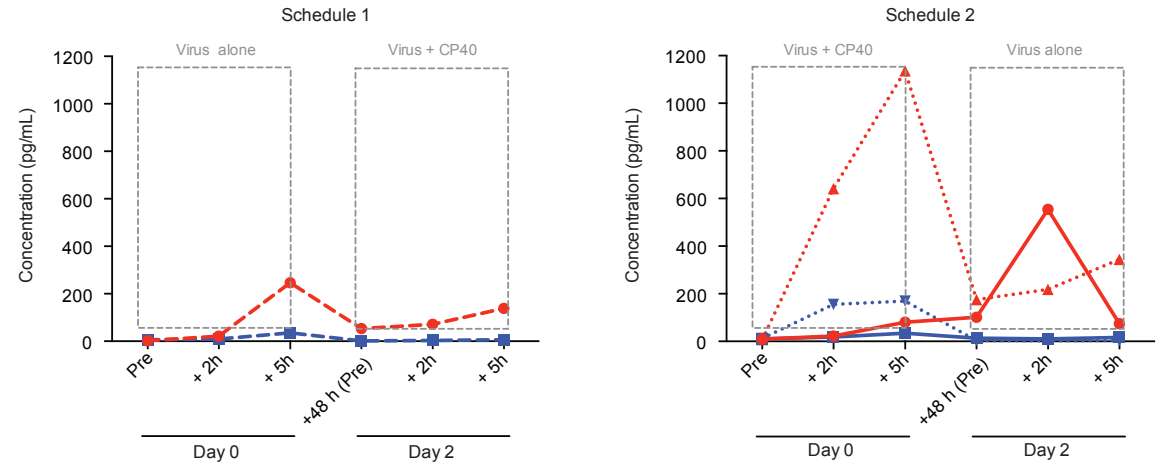

TNFα

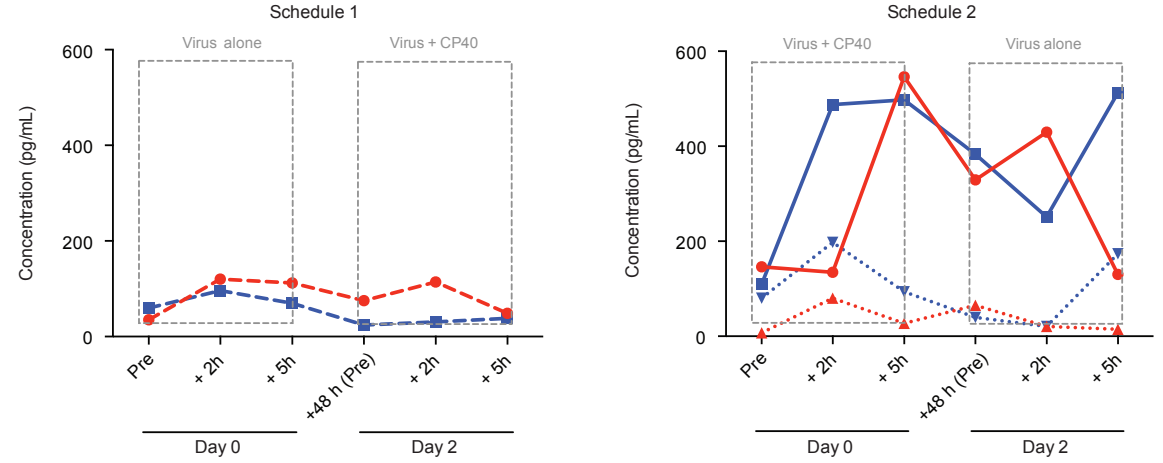

IL 1 β

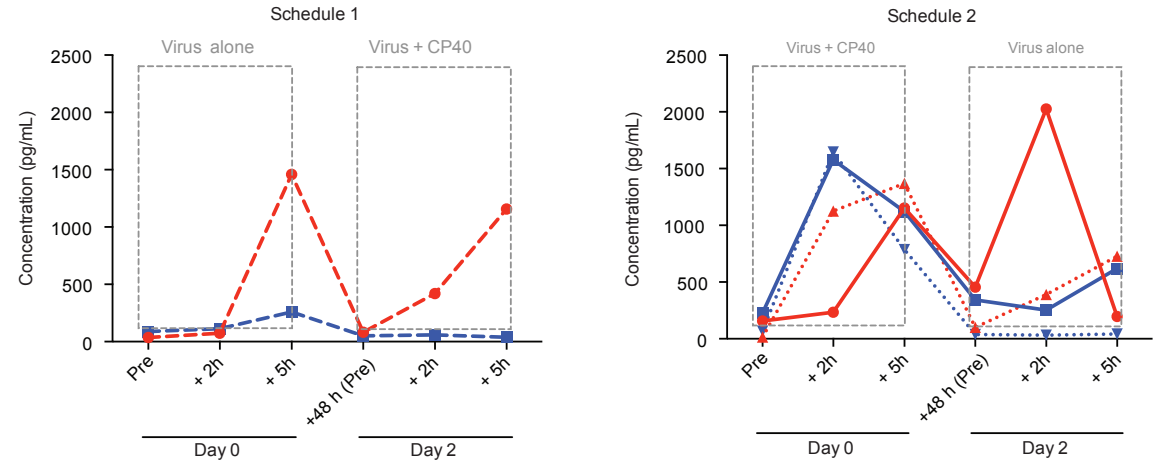

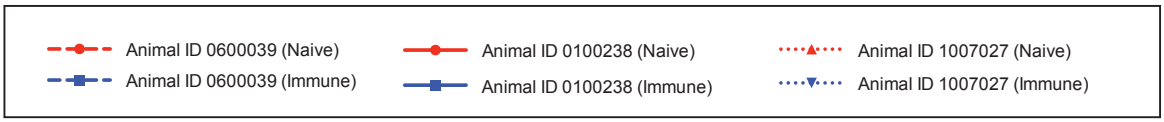

Figure 3.18. Negative regulation of cytokines on day 2

Blood samples were collected prior to treatment, and 2 and 5 hours after the end of the infusion. The plasma from these samples was analyzed for a panel of cytokines. Here shown is the expression of two cytokines, IL 6 and MCP-1, that were elevated upon first treatment (day 0) but that may be under the regulation of a negative feedback mechanism for the second treatment (day 2). Each connected set of data points represents an animal. Each grey dotted box represents an infusion day. (n=3 animals)

IL 6

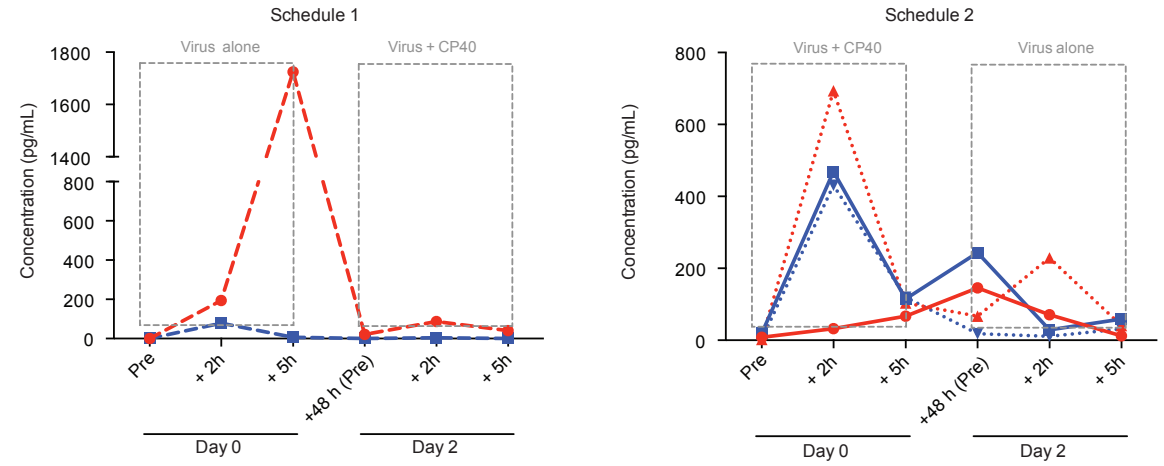
Schedule 1
Virus alone
Virus + CP40
Concentration (pg/mL)
1800
1600
1400
800
600
400
200
0
Pre
+ 2h
+ 5h
+48 h (Pre)
+ 2h
+ 5h
Day 0
Day 2
Schedule 2
Virus + CP40
Virus alone
800
600
400
200
0

MCP-1

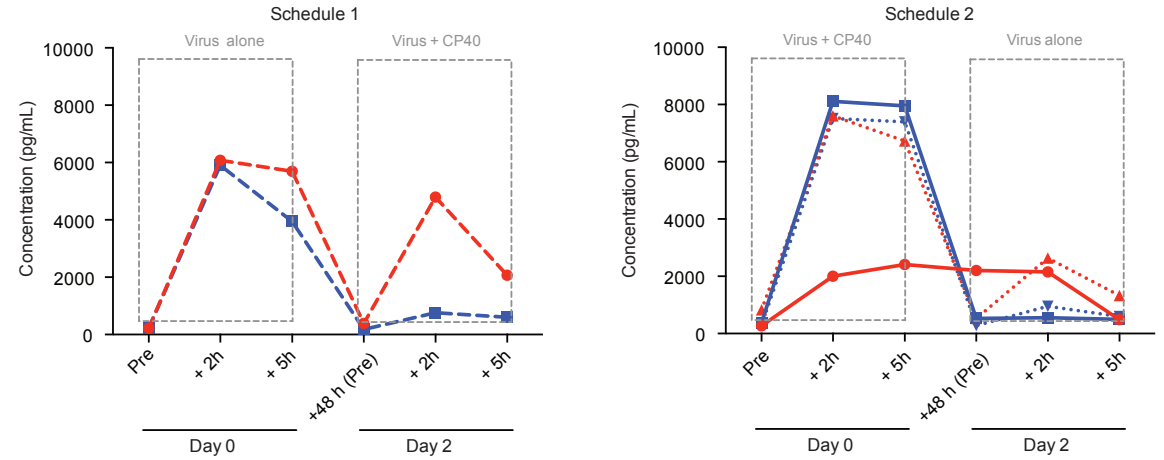
Schedule 1
Virus alone
Virus + CP40
Concentration (pg/mL)
10000
8000
6000
4000
2000
0
Pre
+ 2h
+ 5h
+48 h (Pre)
+ 2h
+ 5h
Day 0
Day 2
Schedule 2
Virus + CP40
Virus alone

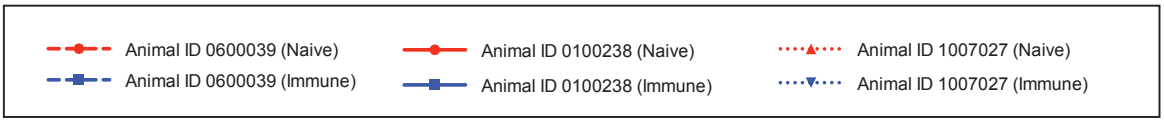
Animal ID 0600039 (Naive)
Animal ID 0600039 (Immune)
Animal ID 0100238 (Naive)
Animal ID 0100238 (Immune)
Animal ID 1007027 (Naive)
Animal ID 1007027 (Immune)

3.3 The cellular interactions of vaccinia virus

In the following sections, we sought to characterize the localization of vaccinia virus in the blood amongst either the cellular or plasma compartments, and in some instances, to characterize the interaction with particular cell types. We pursued some of this characterization in the presence or absence of active complement.

3.3.1 Vaccinia virus engages in numerous cellular interactions in the blood

Our first set of experiments investigated the preferential cellular associations of vaccinia virus in the presence of complement. Blood from a naïve donor was collected using the anticoagulant Refludan (50 μg/mL) and incubated with virus at a concentration of 1 x 10^8 pfu/mL of blood for an hour at 37^{o}C. Specific cell types were stained with antibodies and separated by fluorescence activated cell sorting (FACS). This high concentration of virus was used to ensure that we could recover a sufficient amount of cell-associated virus without sorting a prohibitively high number of cells. The infectious virus and total virus associated with each cell type was quantified by plaque assay and by qPCR using primers against the viral E3L gene, respectively. We observed a clear affinity for leukocytes over erythrocytes (Figure 3.19A). Per cell, there was an approximate 1000 fold increased association of both infectious virus and total virus with $CD45^+$ cells over $CD45^-$ cells. Looking more closely at the white blood cell compartment, we were able to recover infectious virus from T cells, monocytes, B cells and granulocyte populations. Per cell, a preferential association was observed with monocytes, granulocytes and B cells over T cells, as measured by qPCR. More infectious

virus was also recovered from these cell types relative to T cells (Figure 3.19B). The ratio of total virus to infectious virus was similar for all cell types.

We obtained blood from two patients from a clinical trial where 1 x 10^9 pfu of Pexa-Vec was administered intravenously (Clinical trial registration number NCT01329809). We quantified genomes in the blood and plasma from these samples using primers against the E3L gene. We also separated polymorphonuclear cells (PMNCs), peripheral blood mononuclear cells (PBMCs) and erythrocytes using density centrifugation and determined viral association by qPCR using the E3L primers and normalized to β actin. We observed a slow clearance rate of genomes from the blood that was still relatively elevated eight hours post infusion (Figure 3.20A). The majority of virus was cell associated, as measured by the genomes in the plasma per milliliter of whole blood (panel B). Additionally, the clearance rate of genomes from the plasma was much more rapid than was observed in the blood, suggesting that virus that persisted in the blood remained cell associated and not in the plasma compartment. We observed viral association with both PMNCs and PBMCs that persisted throughout the day of infusion (panels C and D). Moreover, virus that was detected in the blood on days subsequent to the infusion was cell associated, and not in the plasma. It was unclear whether there was a preference for PBMCs or PMNCs for natural cell carriage on day of infusion or days following the infusion. We also observed an affinity for leukocytes over erythrocytes as was consistent with our *in vitro* spike experiment (panel E). Similar trends were observed between both patients.

We next evaluated how the compartmentalization of vaccinia virus between the plasma and cellular fractions is impacted by complement. This was first performed *in*

vitro in blood collected from healthy naïve and vaccinated donors. Both CP40 and Futhan were used to inhibit complement (Figures 3.21 A and B, respectively) and very similar effects were observed with both inhibitors. In both naïve and vaccinated donors, we observed a predominance of cell associated infectious virus in the presence of active complement. When complement was inhibited with either compound, we observed an increase in the recovery of infectious virus from the plasma. Total genome quantification was performed by qPCR on the whole blood and the plasma fraction and the proportion of genomes in the plasma and cellular fractions calculated (panel A, bottom). By qPCR, we observed a re-localization of virus particles away from the cells and toward the plasma when complement was inhibited. Altogether this suggests that complement inhibition not only reduces the number of cell associated virus particles, and also reduces neutralization in the plasma.

We performed the same analysis on blood from the cynomolgus macaques infused with virus either with or without CP40 at the end of the infusion time point. Similarly to the observations made in human samples, infectious virus was preferentially associated with the cellular fraction in naïve animals (approximately 93-97%) and in immune animals, infectious virus was exclusively recovered from the cellular fraction (Figure 3.22). When complement was inhibited with CP40, we observed an increase in the infectious virus in the plasma of naïve animals, and were also able to recover infectious virus from the plasma of immune animals. These trends were mirrored by the observations made with regard to genome localization as measured by qPCR (Figure 3.23). Again, these results reflect reduced complement mediated cellular associations

Figure 3.19. Assessment of the preferential interactions of vaccinia virus in blood

Vaccinia virus was incubated with blood from a single healthy naïve donor at a concentration of 1 x 10^8 pfu/mL for one hour at 37^{o}C. Cells were isolated by FACS and titered and assessed by qPCR to determine the number of infectious particles and genomes per 1 x 10^6 cells. (A) Virus association with erythrocytes and leukocytes as measured by the expression of CD45. (B) Virus associations with T cells, monocytes, granulocytes, and B cells as separated by FACS using the CD3, CD14, CD15 and CD19 markers, respectively.

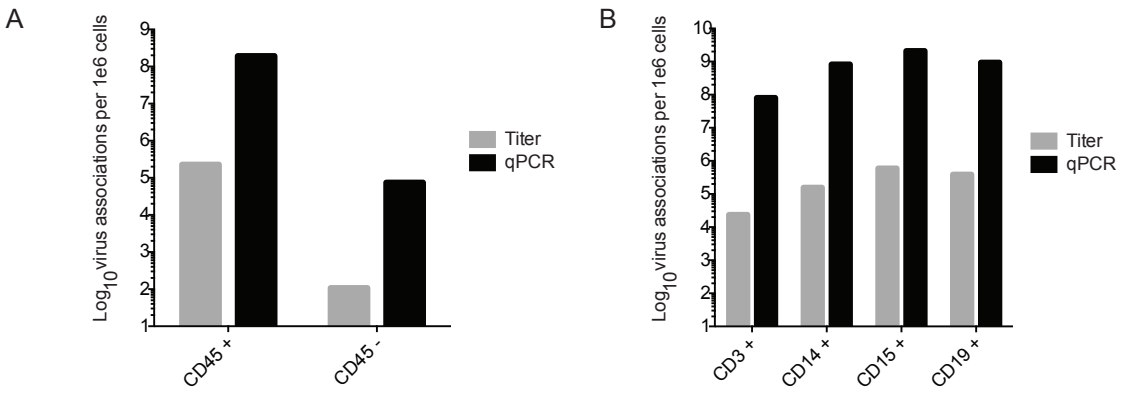
A
Log10 virus associations per 1e6 cells
9
8
7
6
5
4
3
2
1
CD45 +
CD45 -
Titer
qPCR
B
Log10 virus associations per 1e6 cells
10
9
8
7
6
5
4
3
2
1
CD3 +
CD14 +
CD15 +
CD19 +
Titer
qPCR

Figure 3.20. Viral genomes in the blood of two patients treated intravenously with Pexa-Vec

Blood was collected on the day of infusion and subsequently up to day 14 or 15 after infusion for two patients treated with 1 x 10^9 pfu intravenously as a part of a Pexa Vec clinical trial (Clinical trial registration number NCT01329809). Virus content in blood, plasma or associated with particular cell types isolated by density centrifugation was assessed by qPCR using primers against the viral gene E3L. D, day post infusion.

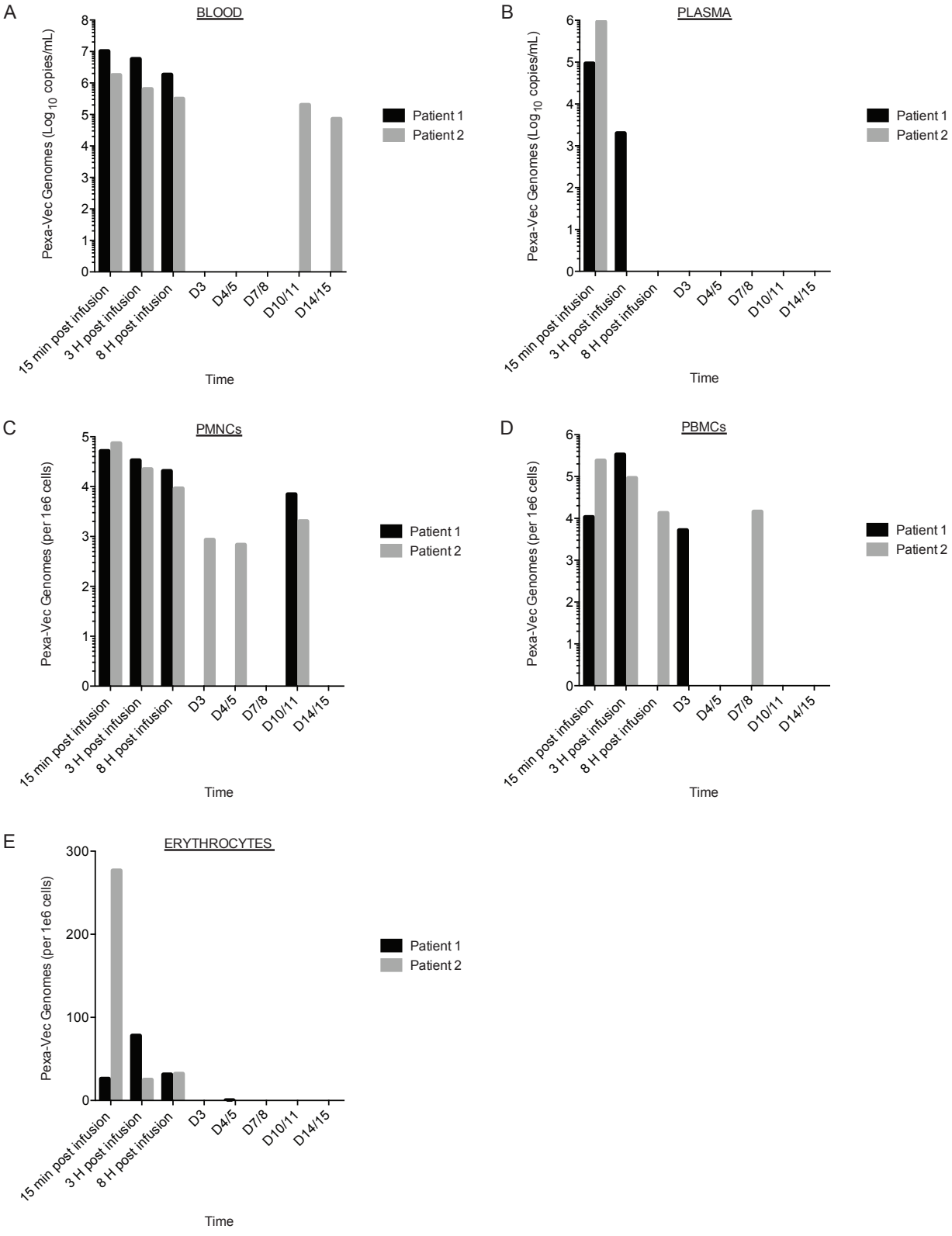
A
BLOOD
Pexa-Vec Genomes (Log10 copies/mL)
Patient 1
Patient 2
15 min post infusion
3 H post infusion
8 H post infusion
D3
D4/5
D7/8
D10/11
D14/15
Time
B
PLASMA
Pexa-Vec Genomes (Log10 copies/mL)
Patient 1
Patient 2
Time
C
PMNCs
Pexa-Vec Genomes (per 1e6 cells)
Patient 1
Patient 2
Time
D
PBMCs
Pexa-Vec Genomes (per 1e6 cells)
Patient 1
Patient 2
Time
E
ERYTHROCYTES
Pexa-Vec Genomes (per 1e6 cells)
Patient 1
Patient 2
Time

(likely through complement receptors) and a reduction of neutralization in the plasma. The specific cell types that are affected are however unknown.

Complement inhibition also changed the nature of the association of vaccinia virus with PBMCs and PMNCs. We isolated these cell types from blood collected at the end of the infusion though density centrifugation and dextrose sedimentation of erythrocytes and assessed infectious virus and total virus association by plaque assay and qPCR, respectively. We observed a significant increase in the total number of particles (mean 10 fold increase) as well as in the number of infectious particles associated with PBMCs (mean 15 fold increase) isolated from macaques pre-treated with CP40 relative to when they were administered virus as a single agent (Figure 3.24 A, C). Although there was a trend for some animals to see a decrease in total and infectious virus association with the PMNC population, this was not consistent for all animals and was not statistically significant (Figure 3.24 B, D). The average purity of the isolation of the PBMCs and PMNCs pool is shown in panels E and F, respectively. The purity of the PBMC isolation was higher than the PMNCs and may partially account for the inconsistent results observed within the PMNC fraction.

Figure 3.21. Virus compartmentalization in the absence and presence of active complement

Vaccinia virus was incubated with blood from naïve or vaccinated donors for one hour at 37^{o}C. Blood and plasma were titered to quantify infectious virus (panels with blue bars). Virus in the plasma is plotted as a proportion of the whole blood titer. Complement was manipulated with CP40 (A) or Futhan (B). Samples were additionally subjected to qPCR to quantify genomes associated with the plasma compartment and plotted as a proportion of the whole blood genome content (panels with red bars). While hematocrit was measured for samples in the CP40 experiment, hematocrit was estimated to be 0.45 (208) in the Futhan experiment. Each blood donor is plotted individually.

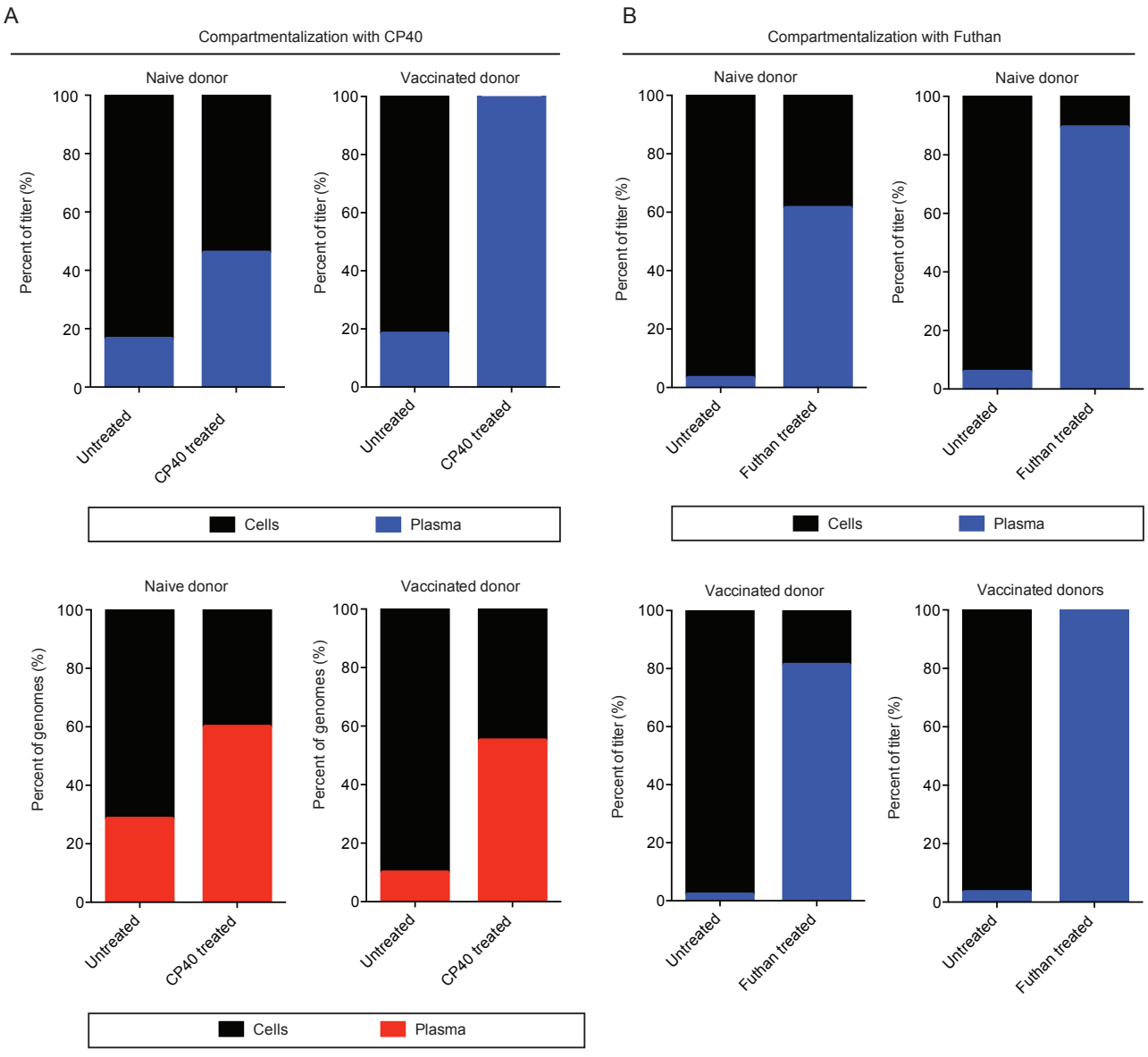
A
Compartmentalization with CP40
Naive donor
Vaccinated donor
Percent of titer (%)
Percent of genomes (%)
100
80
60
40
20
0
Untreated
CP40 treated
Cells
Plasma
B
Compartmentalization with Futhan
Naive donor
Naive donor
Vaccinated donor
Vaccinated donors
Futhan treated

Figure 3.22. Compartmentalization of infectious virus in the blood at the end of the infusion

Infectious virus in the blood and plasma at the end of the infusion was quantified by plaque assay. The proportion of infectious virus associated with the plasma compartment calculated from the plasma and whole blood titers using the hematocrit values for each animal. The individual animals are plotted separately. (n=5 animals)

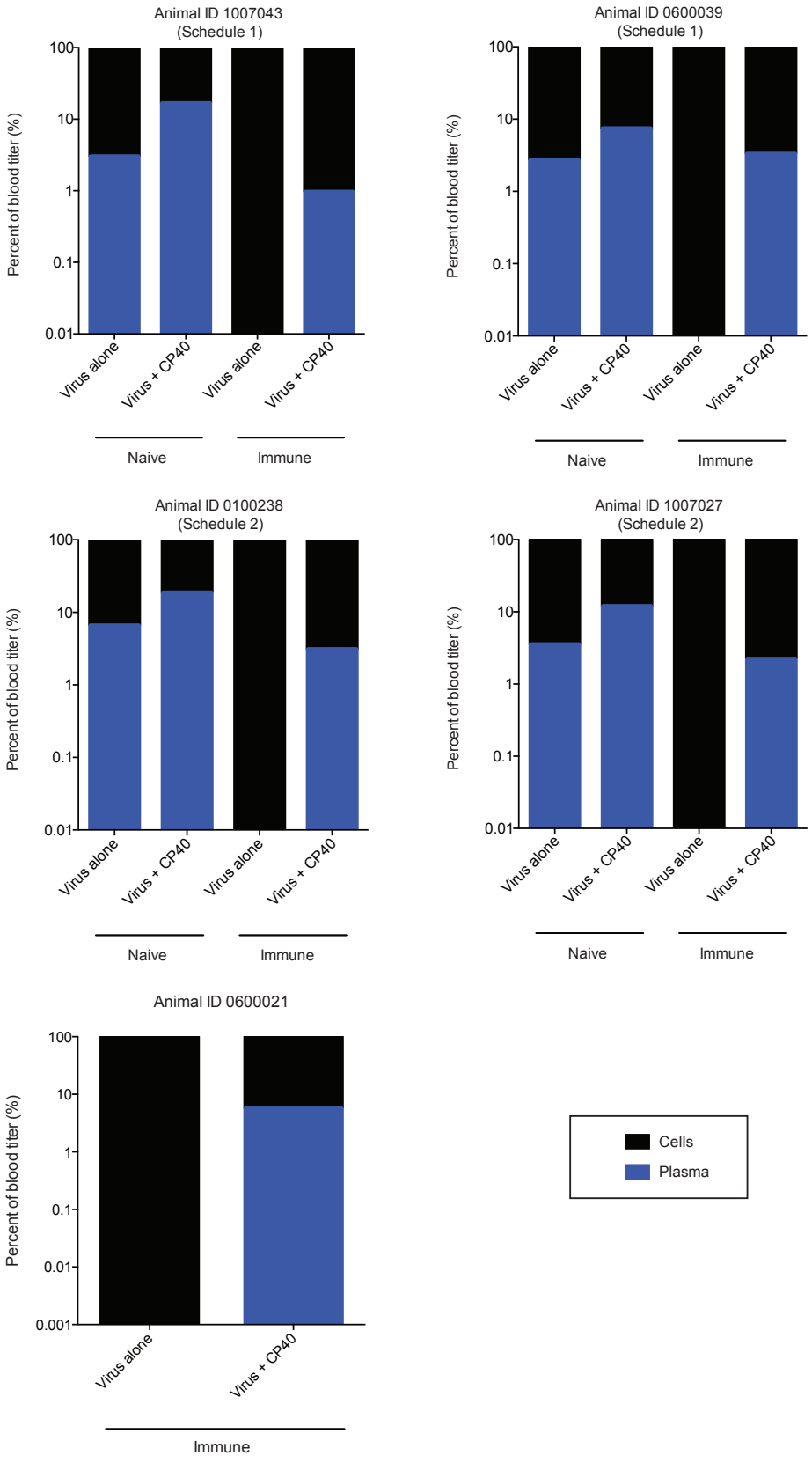
Animal ID 1007043
(Schedule 1)
Percent of blood titer (%)
100
10
1
0.1
0.01
Virus alone
Virus + CP40
Virus alone
Virus + CP40
Naive
Immune
Animal ID 0600039
(Schedule 1)
Percent of blood titer (%)
100
10
1
0.1
0.01
Virus alone
Virus + CP40
Virus alone
Virus + CP40
Naive
Immune
Animal ID 0100238
(Schedule 2)
Percent of blood titer (%)
100
10
1
0.1
0.01
Virus alone
Virus + CP40
Virus alone
Virus + CP40
Naive
Immune
Animal ID 1007027
(Schedule 2)
Percent of blood titer (%)
100
10
1
0.1
0.01
Virus alone
Virus + CP40
Virus alone
Virus + CP40
Naive
Immune
Animal ID 0600021
Percent of blood titer (%)
100
10
1
0.1
0.01
0.001
Virus alone
Virus + CP40
Immune
Cells
Plasma

Figure 3.23. Compartmentalization of total genomes in the blood at the end of the infusion

Genomes in the blood and plasma at the end of the infusion was quantified by qPCR using primers specific to the viral E3L gene. The proportion of genomes associated with the plasma compartment calculated using the plasma and whole blood concentration and the hematocrit values for each animal. The individual animals are plotted separately. (n=5 animals)

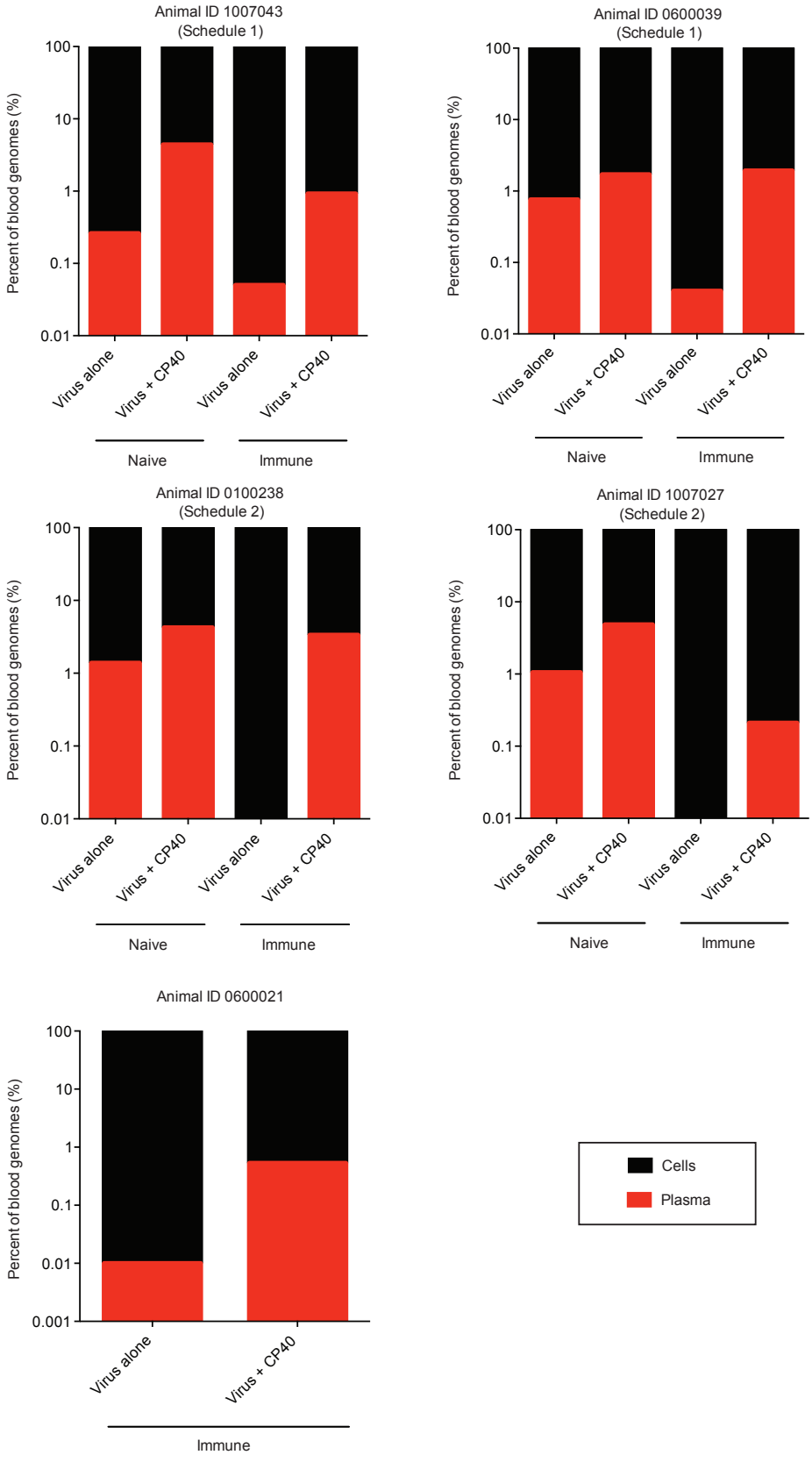
Animal ID 1007043
(Schedule 1)
Percent of blood genomes (%)
100
10
1
0.1
0.01
Virus alone
Virus + CP40
Virus alone
Virus + CP40
Naive
Immune
Animal ID 0600039
(Schedule 1)
Percent of blood genomes (%)
100
10
1
0.1
0.01
Virus alone
Virus + CP40
Virus alone
Virus + CP40
Naive
Immune
Animal ID 0100238
(Schedule 2)
Percent of blood genomes (%)
100
10
1
0.1
0.01
Virus alone
Virus + CP40
Virus alone
Virus + CP40
Naive
Immune
Animal ID 1007027
(Schedule 2)
Percent of blood genomes (%)
100
10
1
0.1
0.01
Virus alone
Virus + CP40
Virus alone
Virus + CP40
Naive
Immune
Animal ID 0600021
Percent of blood genomes (%)
100
10
1
0.1
0.01
0.001
Virus alone
Virus + CP40
Immune
Cells
Plasma

Figure 3.24. Infectious and total virus associated with PBMCs and PMNCs of NHPs at the end of the infusion

Blood collected at the end of the infusion was subjected to density centrifugation and dextrose sedimentation of erythrocytes to isolate PBMCs and PMNCs for the immune time point only. These cell isolations were assessed for infectious virus and total virus content by plaque assay (A, B) and qPCR (C,D), respectively. Each animal is represented by a set of connected dots. (*** $p<0.001$, ** $p < 0.01$, * $p < 0.05$, ^{ns} $p > 0.05$). Cell isolates were analyzed using the Drew Hemavet 950FS to validate the purity of the cellular isolations (E,F).

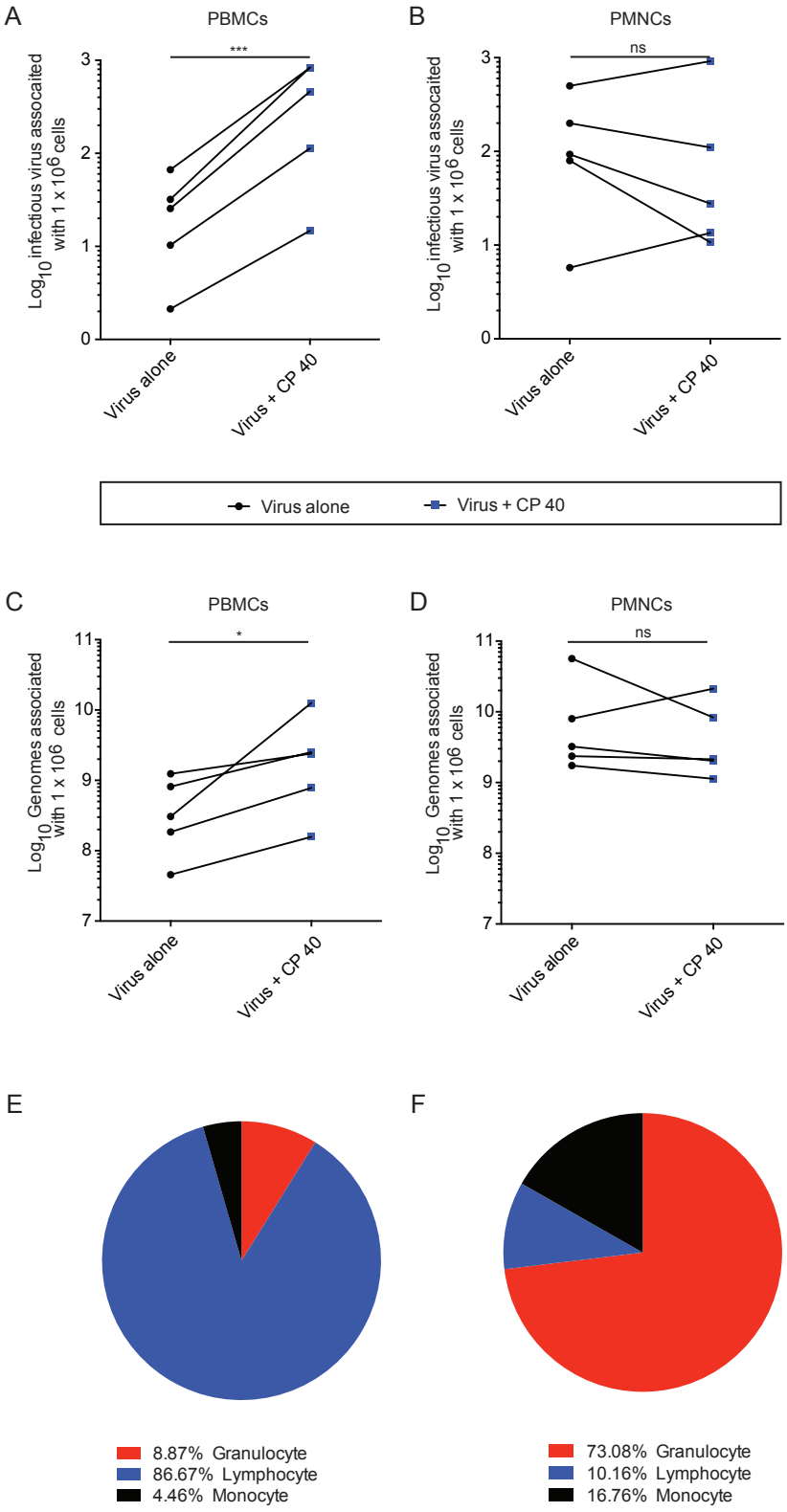
A
PBMCs
***
Log10 infectious virus assocaited with 1 x 10^6 cells
3
2
1
0
Virus alone
Virus + CP 40
B
PMNCs
ns
Log10 infectious virus assocaited with 1 x 10^6 cells
3
2
1
0
Virus alone
Virus + CP 40
Virus alone
Virus + CP 40
C
PBMCs
*
Log10 Genomes associated with 1 x 10^6 cells
11
10
9
8
7
Virus alone
Virus + CP 40
D
PMNCs
ns
Log10 Genomes associated with 1 x 10^6 cells
11
10
9
8
7
Virus alone
Virus + CP 40
E
8.87% Granulocyte
86.67% Lymphocyte
4.46% Monocyte
F
73.08% Granulocyte
10.16% Lymphocyte
16.76% Monocyte

3.4 Complement, antibodies and other oncolytic virus candidates

3.4.1 Complement inhibition reduces in vitro neutralization of clinical candidate OVs

We sought to determine the impact of complement inhibition on other clinical candidate oncolytic viruses. In the same manner as performed with vaccinia virus, the *in vitro* neutralization of MG1, reovirus, HSV-1 and measles Edmonston was assessed across a range of input doses in the presence or absence of the complement inhibitor CP40 (Figure 3.25) As was consistent with previously published results(121), MG1 was shown to be sensitive to complement, and neutralization was reversed upon complement inhibition (panel A). Reovirus was moderately neutralized by complement and this could be reversed with CP40 (panel B). Due to the elevated level of seropositivty in the population(209), the three donors have likely been previously exposed to reovirus. However, this remains unconfirmed. The saturation effect observed with vaccinia virus was not seen across the range of doses analyzed with MG1 or reovirus. Donors were stratified into HSV-1 seropositive or negative groups based on an ELISA for IgG specific to HSV-1 (panel F). In seronegative plasma, there was a significant increase in viral recovery with complement inhibition, as has been previously documented (panel C)(195). In contrast to vaccinia virus, the antibodies specific to HSV-1 were neutralizing independently of complement. There was, however, a significant increase in the proportion of infectious virus recovered above doses of 2×10^4 pfu/mL, independent of complement (panel D). Lastly, all donors analyzed were vaccinated against measles and were considered to be seropositive. Measles Edmonston was shown to be very sensitive to complement and antibody (panel E). A clear biologic trend was associated with

complement inhibition, in particular at the highest dose level tested, however due to the variability within the donors, it was not statistically significant. This effect was dose dependent as elevated doses of virus were required to observe the effect induced by complement inhibition.

3.4.2 Complement inhibition with oncolytic rhabdoviruses in the Fischer rat model

Since there is no human reservoir of pre-existing immunity to maraba virus, we investigated the sensitivity of the maraba vector MG1 and also the maraba (MRB) vector that had been pseudotyped LCMV glycoprotein to the rat model. Naïve rats, or vaccinated animals (1 x 10^7 pfu IV) were treated or not with CVF and terminally bled. Blood was anti-coagulated with Refludan and viral neutralization assessed *in vitro* in blood, plasma or heat-inactivated plasma. In blood or plasma from complement-replete naïve rats, we observed complement dependent neutralization of MG1 that was prevented if the rats were depleted of complement with CVF (Figure 3.26A). MG1 was robustly neutralized in samples from animals vaccinated against the virus and only a moderate increase in viral recovery was observed if complement was inactivated by heat or depleted *in vivo*. In contrast to the delayed neutralizing antibody response that has been reported in response to the LCMV glycoprotein in mice(188, 210), an early robust antibody response was observed in blood and plasma from the vaccinated rat (Figure 3.26B). Notably, this neutralization was only observed if complement was intact. Neutralization was observed in blood and plasma from the complement-replete rat and abrogated if plasma was heat inactivated or if samples were sourced from animals treated with CVF.

Figure 3.25. Neutralization of MG1, reovirus, HSV-1 and measles Edmonston by complement and antibody

MG1 (A), reovirus (B) HSV-1 (C,D) and measles Edmonston (E) were incubated with plasma from healthy human donors at virus concentrations ranging from 2 x 10^4 pfu/mL to 2 x 10^7 pfu/mL. Plasma was pre-treated with CP40 (25μM) when noted. (n=3 donors per immune status). The number of donors from which virus was not detected (ND) is indicated in parentheses. The comparisons between plasma and plasma + CP40 at each dose are indicated by (‡ $p<0.001$, † $p < 0.01$, § $p < 0.05$, ^{ns} $p > 0.05$). All other statistical comparisons are indicated by (*** $p<0.001$, ** $p < 0.01$, * $p < 0.05$, ^{ns} $p > 0.05$). (F) Serologic status of blood donors was determined using an ELISA measuring IgG specific to HSV-1.

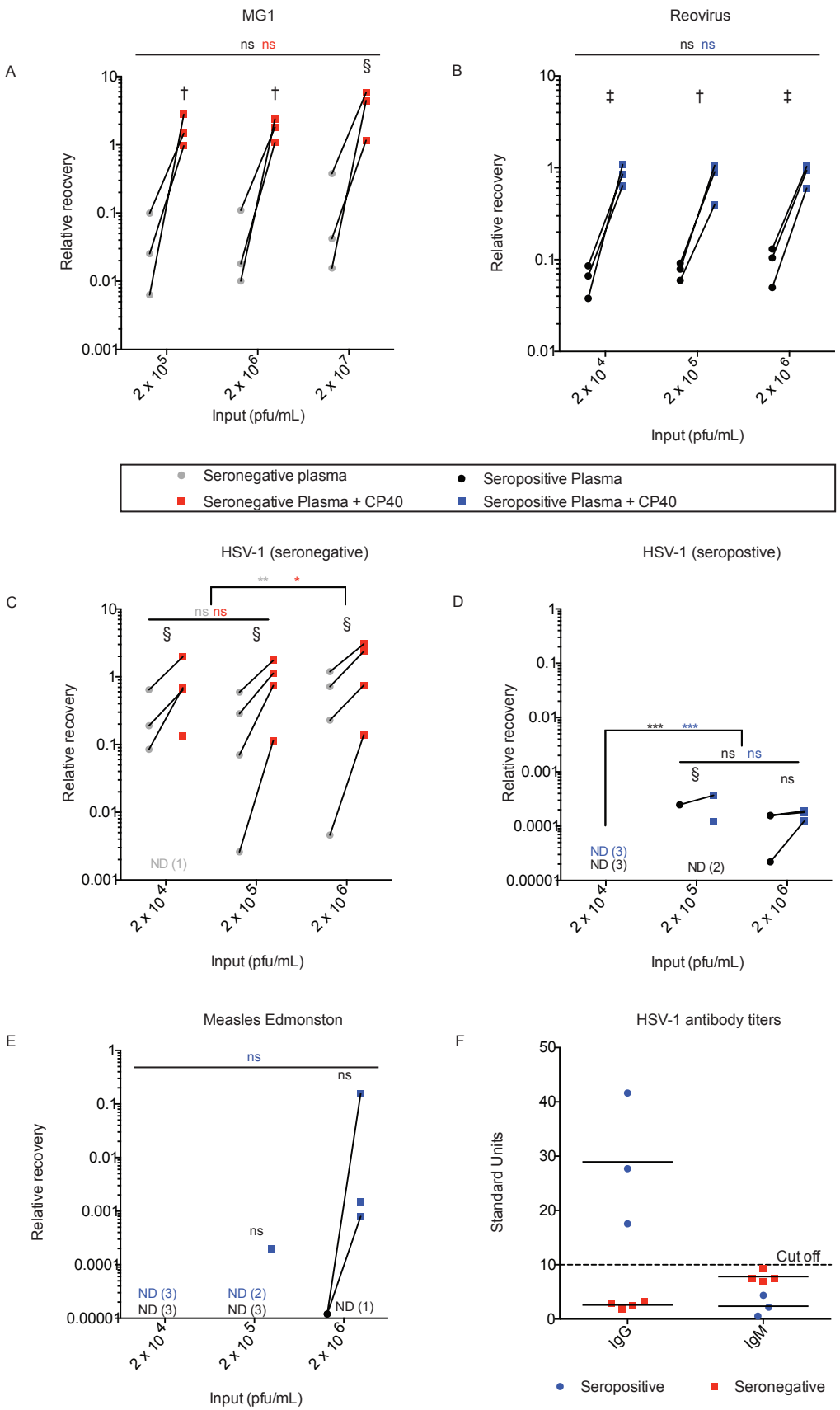
A
MG1
ns ns
§
†
†
10
1
0.1
0.01
0.001
Relative reocvery
2 x 10^5
2 x 10^6
2 x 10^7
Input (pfu/mL)
B
Reovirus
ns ns
‡
†
‡
10
1
0.1
0.01
Relative recovery
2 x 10^4
2 x 10^5
2 x 10^6
Input (pfu/mL)
Seronegative plasma
Seronegative Plasma + CP40
Seropositive Plasma
Seropositive Plasma + CP40
C
HSV-1 (seronegative)
** *
ns ns
§
§
§
10
1
0.1
0.01
0.001
Relative recovery
ND (1)
2 x 10^4
2 x 10^5
2 x 10^6
Input (pfu/mL)
D
HSV-1 (seropostive)
1
0.1
0.01
0.001
0.0001
0.00001
Relative recovery
*** ***
ns ns
§
ns
ND (3)
ND (3)
ND (2)
2 x 10^4
2 x 10^5
2 x 10^6
Input (pfu/mL)
E
Measles Edmonston
ns
ns
1
0.1
0.01
0.001
0.0001
0.00001
Relative recovery
ns
ND (3)
ND (3)
ND (2)
ND (3)
ND (1)
2 x 10^4
2 x 10^5
2 x 10^6
Input (pfu/mL)
F
HSV-1 antibody titers
50
40
30
20
10
0
Standard Units
Cut off
IgG
IgM
Seropositive
Seronegative

Figure 3.26. MG1 and MRB LCMV G neutralization by antibody and complement

Ex vivo neutralization of MG1(A) or MRB LCMV G (B) with rat blood, plasma or heat inactivated plasma. Rats were vaccinated with 1 x 10^7 pfu intravenously two weeks prior to the terminal blood, and or depleted of complement with 35 U CVF the day prior to the bleed. One rat per immune/complement status was used and data is expressed as the technical replicates ±SD. Left panels demonstrate titer values, and the right panels show the fold change in titer (complement depleted: complement replete).

A Neutralization of MG1 *in vivo*

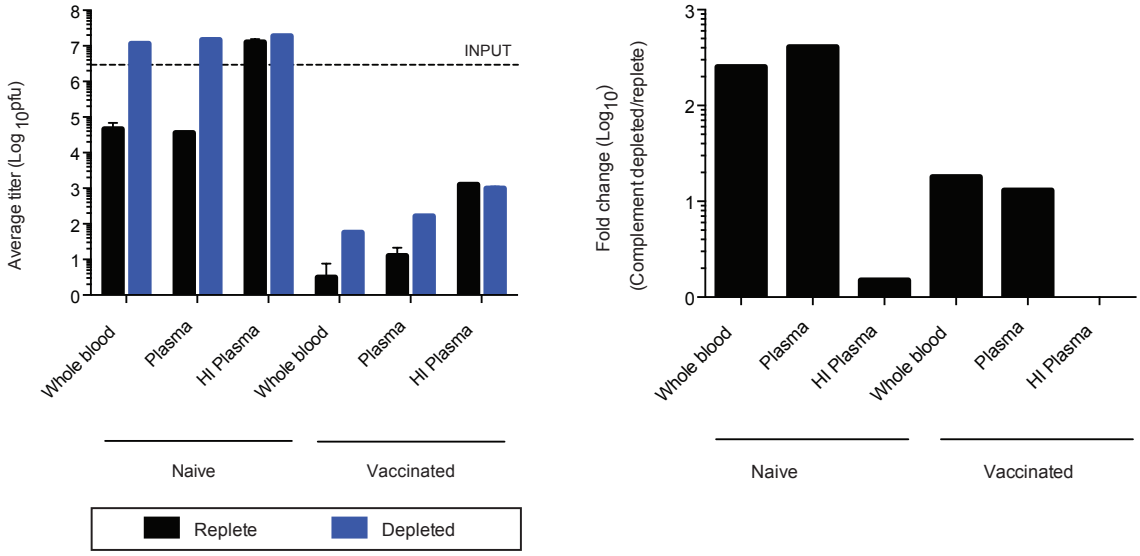

B Neutralization of MRB LCMV G *in vivo*

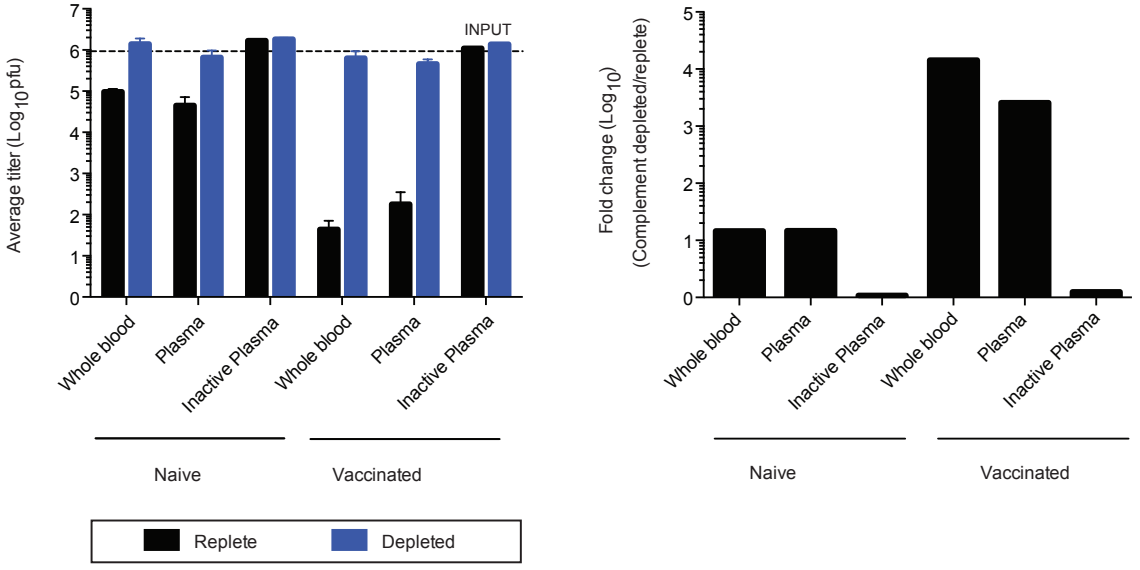

The LCMV G pseudotyped maraba virus behaved similarly to vaccinia virus in response to complement and generated a similar profile of anti-viral antibody. We therefore sought to test whether complement inhibition would ameliorate viral stability in the blood of vaccinated animals and if it would increase the effective dose that infects a tumor. Animals were vaccinated and treated with MG1 or MRB LCMV G according to the schedule in Figure 3.27A. Rats were treated intravenously with virus and infectious virus in the blood and tumors 10 minutes post-tail vein injection was quantified by plaque assay. We observed a significant increase in infectious virus recovery from the blood of MRB LCMV G immune animals if they were complement depleted (Figure 3.27B). We also observed a significant increase in viral recovery from the blood of MRB LCMV G naïve complement depleted rats relative to their complement-replete counterparts. These findings translated to a significant increase in infectious virus recovered from subcutaneous tumors in MRB LCMV G immune animals and a trend toward increased recovery in tumors of naïve animals that was associated with complement depletion (Figure 3.27C). In contrast to maraba virus pseudotyped with the LCMV G, neither in immune or naïve animals did we observe any benefit from complement depletion on stability of MG1 in the blood or delivery to tumors (Figure 3.27D, E).

The effect of complement depletion was also assessed in the context of a local administration of virus. Rats were vaccinated and treated according to the schedule in Figure 3.28A. Complement depletion increased MRB LCMV G recovery from tumors from immune rats, but not naïve rats following an intratumoral injection of virus (Figure 3.28B). Consistent with the study on viral stability in the blood, the antibodies against MG1 neutralized the virus independently of complement to prevent infection of tumors.

Complement depletion also did not aid in the infection of MG1 of subcutaneous tumors in naïve animals (Figure 3.28C).

Figure 3.27. Complement depletion improves the stability and delivery of MRB LCMV G but not MG1 in immunized animals

MG1 (4 x 10^7 pfu) or MRB LCMV G (4 x 10^8 pfu) was delivered intravenously to Fischer rats bearing bilateral 13762 MATBIII tumors, according the schedule in (A). As per the treatment groups, rats were vaccinated intravenously with 1 x 10^7 pfu and or depleted of complement with 35 U of CVF. Infectious virus in the blood (B, D) and in subcutaneous tumors (C,E) ten minutes post virus administration was quantified by plaque assay. (n=3-4 rats per group). Data are represented as group means ±SD. Each dot represents a rat. The number of rats from which virus was not detected (ND) is indicated in parentheses. (*** p<0.001, ** $p < 0.01$, * $p < 0.05$, ^{ns} $p > 0.05$).

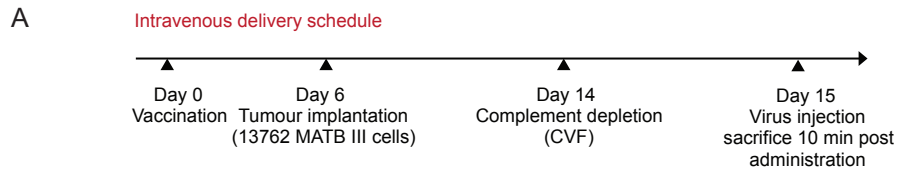

Intravenous delivery of MRB LCMV G

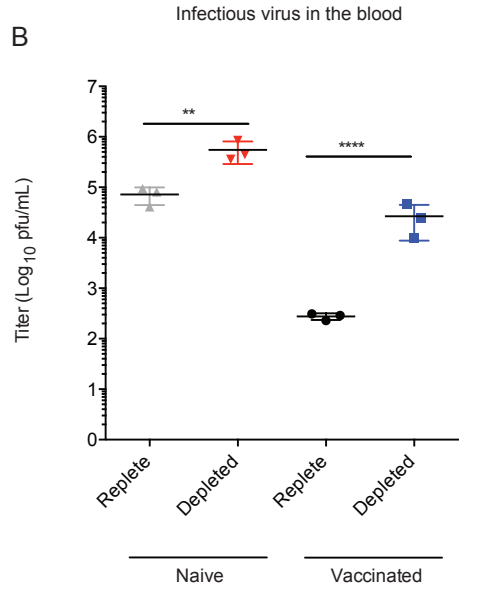

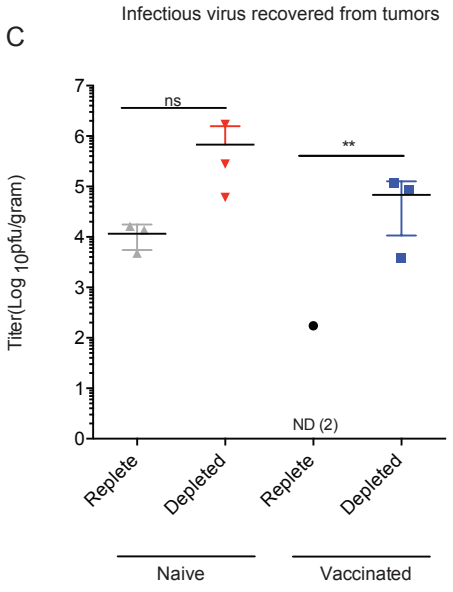

Intravenous delivery of MG1

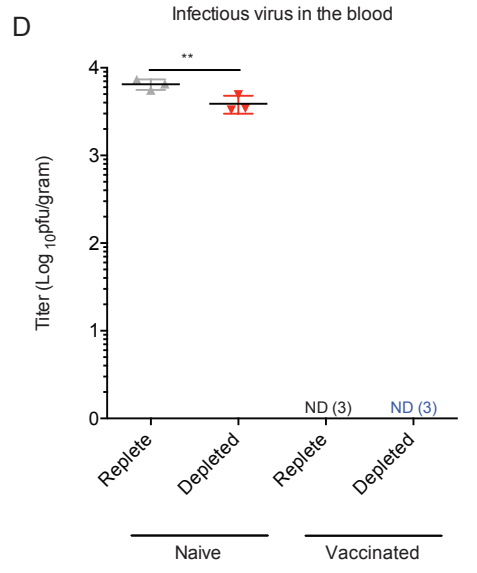

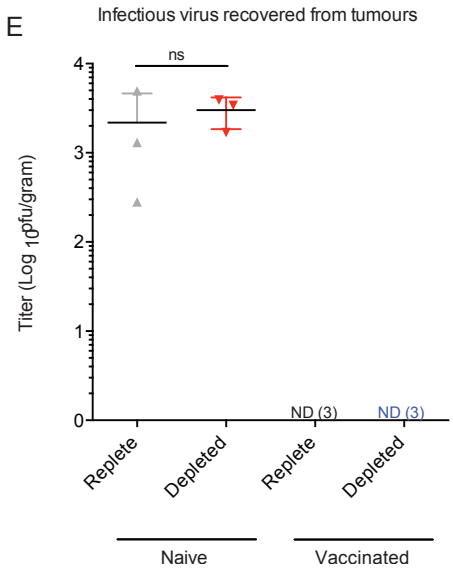

Figure 3.28. Complement depletion improved infection of tumors following local administration of MRB LCMV G but not MG1 in immune rats

(A) As per the treatment groups, rats were vaccinated intravenously with 1 x 10^7 pfu and or depleted of complement with 35 U CVF. The dose of 1 x 10^7 pfu MRB LCMV G (B) or MG1 (C) was delivered intratumorally to Fischer rats bearing bilateral 13762 MATBIII tumors. Subcutaneous tumor titers are shown for animals sacrificed 24 hours post virus administration. (n=4 per group) Data are represented as group means ±SD, Each dot represents a rat. The number of rats from which virus was not detected (ND) is indicated in parentheses. (* $p < 0.05$, ^{ns} $p > 0.05$).

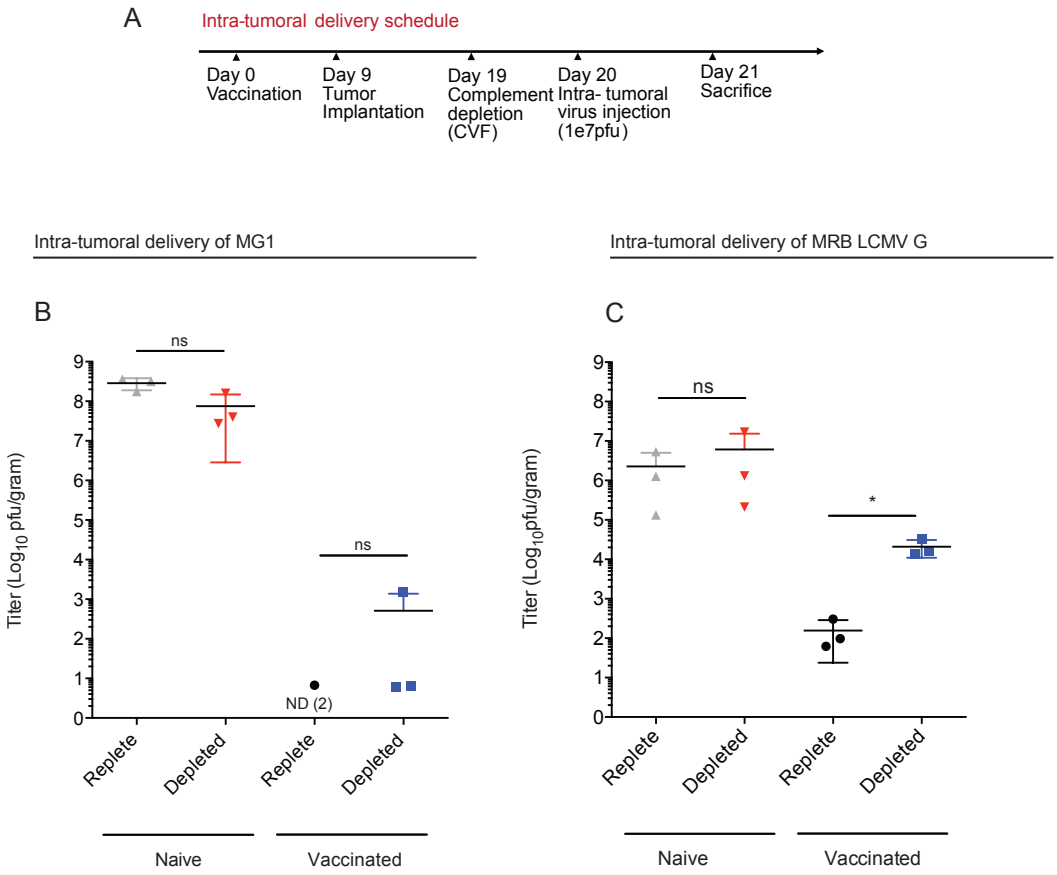
A
Intra-tumoral delivery schedule
Day 0
Vaccination
Day 9
Tumor
Implantation
Day 19
Complement
depletion
(CVF)
Day 20
Intra- tumoral
virus injection
(1e7pfu)
Day 21
Sacrifice
Intra-tumoral delivery of MG1
Intra-tumoral delivery of MRB LCMV G
B
C
Titer (Log10 pfu/gram)
ns
ns
ND (2)
*
Replete
Depleted
Replete
Depleted
Naive
Vaccinated

4. Discussion

The ability of oncolytic vaccinia virus to induce tumor regression has been shown in clinical trials where the virus was administered locally by intratumoral injection. Correspondingly, survival duration in response to Pexa-Vec was related to dose: the median survival associated with a dose of 1 x 10^9 pfu was 14.1 months compared 6.7 months for the patient group treated with 1 x 10^8 pfu(99). In the Pexa-Vec phase I IV trial, virus delivery to tumors by systemic administration was observed above a critical threshold dose and was associated with moderate anti-tumor effects as measured by RECIST or modified Choi criteria(100). The clinical evidence demonstrates that the best tumor responses are associated with higher doses of virus. Importantly, the threshold for delivery does not equate to the dose required to induce a substantial therapeutic benefit. It is therefore imperative to increase the effective dose of virus that is administered systemically. This prompted the question as to which factors in the blood were responsible for neutralization, and how we could manipulate them to mitigate their neutralizing effects. Throughout the work presented in this dissertation, we have sought to understand the mechanisms involved in viral neutralization and clearance. With a better understanding of this phenomenon, we have developed a strategy to increase the infectious half-life of vaccinia virus in the blood that we have proven in two pre-clinical animal models.

4.1 The complement dependence of human anti-vaccinia antibodies to neutralize the virus provides a window of opportunity to bypass pre-existing immunity

It has previously been shown that vaccinia virus, and in particular the mature virion, is sensitive to complement(108). It has also been shown as long as 60 years ago that a heat-labile serum factor potentiated the effect of antibody against variola virus(146). Nonetheless, post-vaccination era assessment of anti-vaccinia neutralizing antibodies has largely ignored the effect of complement. We show here that the long-lived antibody response that is residual from smallpox vaccination retains a robust ability to induce neutralization that is dependent on complement activation. Moreover, the anamnestic antibody response induced following treatment with Pexa-Vec also exhibits this dependence on complement. We have revealed this phenomenon using three methods to inhibit complement: heat inactivation, a non-specific serine protease inhibitor, Futhan, and a highly specific C3 inhibitory binding peptide, CP40 (Figure 3.2).

Through the adaptations that it has acquired, the virus provides insight into its intrinsic vulnerability to complement. Firstly, the virus encodes a secreted protein, VCP, that prevents the formation of the C3 convertase (211), suggesting that complement plays an important role in the microenvironment of the infection. Secondly, vaccinia virus has evolved the ability to produce two distinct virions, of which the wrapped virion is uniquely suited to travel in the blood due to its resistance to complement conferred by the incorporation of host cell surface complement regulatory proteins in its outer membrane(108). Although both these adaptations may improve the chances of virus spread once a primary infection has been established, they do not aid the stability of an infusion of virus comprised of mature virions.

Analogous to the pharmacokinetic barrier to infection of tumor sites observed clinically(100), we also observed a saturation effect on viral neutralization in plasma *in vitro*. We saw that the effect of complement could be overcome in naïve plasma with increasing concentrations of virus (Figure 3.3A). In immune plasma, we observed a threshold of neutralization whereby at a dose of 2 x 10^7pfu/mL, a significantly greater proportion of infectious virus could be recovered (Figure 3.3B). This is consistent with what is known about IgM and IgG binding to antigen. IgM exists in a polymeric state (either pentameric or hexameric) and the binding site for C1q only becomes accessible once IgM is complexed to an antigen(212, 213). Monomeric IgG, on the other hand, has an exposed C1q binding site on its Fc tail, but the binding affinity is too low to allow for adequate binding. Hexameric IgG aggregates however bind C1q with high avidity to activate complement(214). In naïve plasma, we could dilute the number of pattern recognition molecules among virions to reduce virus neutralization. In immune plasma, the stoichiometry of one C1q molecule binding to the interface of six interacting Fc tails(214) is met with decreasing frequency at higher concentrations of virus. Within this model, it should be hypothesized that a point would be reached where the anti-viral IgG is distributed amongst too many virus particles and does not meet the stoichiometric requirement to bind C1q. This concentration was found to be 2 x 10^7 pfu/mL. Although this provides interesting biological information about vaccinia virus and its neutralization by complement and antibodies, this threshold dose is relevant only to human plasma *in vitro*. In fact, the threshold dose was clinically reached at 1 x 10^9 pfu, which can be scaled down to 2 x 10^5 pfu/mL based on an estimated blood volume of 5L. It would be interesting to repeat this experimental setup with whole blood, in addition to plasma, to

compare both thresholds. Due to the accessibility of antibody to the virus or perhaps protective interactions with cells, this threshold may be substantially different in whole blood. This particular threshold effect would also have been very interesting to explore *in vivo* in the rat model.

We observed considerable virus neutralization in naïve human plasma *in vitro*. This was in contrast to both our rat model and non-human primate model where we did not observe a change in viral stability *in vivo* when complement was depleted or inhibited, respectively. *In vitro* complement activation occurs spontaneously(215) and produces the artifact of overestimating the effect of the alternative pathway. It is best to describe the *in vitro* neutralization as a measure of the sensitivity of the virus to these factors, but does not reflect the levels of activation *in vivo*. This likely inflated the threshold effect and contributed to the difference in neutralization thresholds demonstrated clinically and in our *in vitro* experiments.

4.2 Choosing appropriate targets for complement modulation and suitable inhibitors with desirable characteristics

Based on previous work with vaccinia virus and complement, it was unclear which specific players were involved in viral neutralization, and as a result, which therapeutic tools may be of use. We have identified that the classical and alternative pathways play important roles in viral neutralization in both naïve and immune human plasma (Figure 3.4). Moreover, the alternative pathway acts as a positive amplification loop to the activation initiated by the classical pathway. Inhibition of the MBL pathway did not have an important impact on virus recovery. While early literature shows that C5

and C6 deficient serum can neutralize vaccinia virus(117), recent evidence with eculizumab now shows that the terminal pathway is important(118). Our neutralization assay with eculizumab and our sucrose gradient density experiment both support vaccinia virus virolysis by the MAC (Figure 3.4).

The inhibition of complement for the purpose of increasing the delivery of virus does not come without risk. Using the surrogate poxvirus ectromelia, C3 null mice were found to be more susceptible to morbidity and mortality at lower doses of virus than their congenic counterparts. Moreover, elevated titers of virus were recovered from all major organs and was associated with extensive liver necrosis(116). We feel that it is important that we exert strict functional and temporal control over the method of complement inhibition. For this reason, a pharmacological approach that can induce transient complement inhibition is much preferred to the genetic manipulation of the virus to confer complement resistance.

The Compstatin family of analogs, represented by CP40, which we used extensively in this study, may be an ideal pharmacophore to use in combination with oncolytic vaccinia virus. Since CP40 binds to the C3 molecule, it is able to quench initiation of the complement cascade by all three pathways and prevent the formation of the MAC(132). We have shown that classical and alternative pathways lead to the terminal pathway activation and in this respect, this inhibitor satisfies the requirement for preventing neutralization. Considerable effort has been put into the generation of analogs of the original Compstatin molecule that now have subnanomolar binding affinity and enhanced pharmacokinetic properties(216). CP40 has a half-life of 11.8 hours when administered as a bolus intravenous dose to cynomolgus macaques at 2mg/kg(132). The

small peptide is eliminated by proteolytic cleavage in the blood and liver, as well as filtration from the kidney(217). Pharmacokinetic assessment of CP40, as well as other Compstatin analogs, defines a biphasic elimination profile characterized by rapid initial elimination, followed by a slow log linear terminal phase that is highly dependent on the binding affinity for C3(132). This profile ensures that complement can be inhibited on the day of virus administration but that complement activity will rebound by the time that the first waves of virus replication begin to emerge 12-24 hours after infection(68).

Aside from preventing neutralization, blocking C3 cleavage also precludes the formation of the anaphylatoxins C3a and C5a. These molecules act as powerful pro-inflammatory mediators that have pleotropic functions including the stimulation of vasodilation, chemotaxis, and activation and stimulation of leukocyte effector functions (for example neutrophil phagocytosis)(218, 219). While vasodilation would be predicted to enhance viral delivery, pro-inflammatory cytokine production may help to promote early clearance of the virus, and more acutely, induce pyrexia and therefore may be involved in some of the side effects seen in patients. This angle has not been explored throughout the work presented here, however it is relevant and would be interesting to explore as more complement inhibitors become clinically available.

Looking at the two complement inhibitors that are currently on the market, the C1 esterase inhibitor would likely not be a good candidate since inhibition of the classical pathway in our *in vitro* assay only demonstrated partial reduction of neutralization in immune plasma. Eculizumab has the ability to prevent vaccinia virus neutralization through the inhibition of the terminal pathway, however this humanized monoclonal antibody has a very long half-life(220). The extended half-life does not meet our need to

transiently inhibit complement and poses an important safety risk. A single-chain variable fragment form of eculizumab, pexelizumab (Alexion Pharmaceuticals), has a half-life of 4.5h that may be more appropriate, however is no longer in development(123, 221). Neither of these two inhibitors is as suitable as CP40.

4.3 The mouse provides an inadequate model to investigate the systemic delivery of oncolytic vaccinia virus

It has been shown that the complement system of all inbred mouse strains possesses low hemolytic activity relative to that of rats or humans(222). This may be at least partially attributed to a C4 polymorphism that precludes the formation of a functional C5 convertase(223). It has also recently been reported that mouse serum, but not human or rat serum, contains an unspecified classical pathway inhibitor that is able to inhibit IgG-dependent complement-mediated cytotoxicity(224). These differences between human and mouse serum render mouse complement unable to accurately reflect antibody-mediated activation of the classical pathway and the subsequent virolysis induced by the terminal pathway that was observed in human blood samples. The results from our experiment where we assessed vaccinia virus neutralization in naïve or immune mouse plasma are therefore consistent with previously published knowledge regarding mouse complement (Figure 3.5A). We also showed that complement depletion with CVF does not aid in the delivery of vaccinia virus to tumors, or their infection, in the murine model (Figure 3.5C,D). Our experiment is also consistent with previously published results that showed that CVF did not increase the amount of virus recovered from tumors of animals that were immune to vaccinia virus(198). Due to the limitations of the mouse model with regard to complement, as well as the greater resemblance of the profile of rat

antibody and complement mediated neutralization of vaccinia (Figure 3.6), we believe that the rat model has greater predictive value for the preclinical development of oncolytic vaccinia virus.

4.4 Antibodies targeting vaccinia virus mature virion epitopes

A very recently published study looked at the ability of mouse monoclonal antibodies targeting the L1, D8, H3, and A27 mature virion membrane proteins to neutralize vaccinia virus(225). It was shown that the majority of the L1 antibody clones were neutralizing independently of complement. In contrast, the antibodies targeting the D8, H3 and A27 surface proteins were virtually non-neutralizing in the absence of rabbit complement, but induced a strong neutralizing effect in the presence of supplemented complement. This is particularly interesting in the context of a study published by the same group a couple years prior that showed that the H3 viral protein is the immunodominant epitope in humans, and the L1, which is co-immunodominant in mice, is a less common target(142). The predominance of human anti-vaccinia antibodies to target non-neutralizing epitopes supports the profile of complement fixing antibodies that we observed in human plasma (Figure 3.2). This finding also helps to explain why mouse immune plasma is neutralizing in the absence of complement. The requirement of complement to aid the D8, H3, and A27 targeting antibodies is partially explained by their function. These proteins play a redundant role in mediating cellular attachment. As a result, high concentrations of antibody are necessary to saturate these sites. In contrast, the L1 is an important part of the entry-fusion complex and its blockade may prevent cellular entry(225).

4.5 Thoughts on choosing appropriate animals models

Choosing appropriate animal models is critical to the ability to test hypotheses generated from human samples *in vitro* and to produce results that will be clinically relevant. Ultimately no pre-clinical animal model is a human and while some aspects may be the best approximation, cognizance of the differences can help us to interpret the results generated from these models.

As a precursor to therapeutic efficacy, the virus must remain non-neutralized in the bloodstream long enough to reach and infect its site of action, tumor beds. This means that the virus must evade numerous immune mechanisms that tag invading microbes for phagocytic uptake and destruction. This begins with opsonization: the binding of antibodies and subsequently complement components to the surface of the antigen with the purpose of increasing visibility to phagocytic cells(226). Complement receptors bind to C3 fragments and have unique expression profiles and functions: CR1 is expressed on eyrthrocytes, monocytes, neutrophils and macrophages, and acts as an important immune adherence receptor, CR2 is expressed on B cells and lowers the activation threshold for the B cell receptor, and CR3 and CR4 have broad expression patterns and a variety of functions(227).

Notably, the capture of immune complexes by CR1 on erythrocytes is thought to be of primary importance in the filtration of pathogens by liver macrophages(228). Opsonized virus travels to the spleen and liver, either bound by cells or free in suspension, where it is taken up by resident macrophages. Blood is circulated to the spleen via the splenic artery, and branches into venous sinuses where macrophages and B cells of the marginal zone that express a variety of complement receptors and Fc

receptors filter antigens(229, 230). In the liver, virus in the blood flows though the sinusoidal circulation and interacts with liver sinusoidal endothelial cells (LSECs) and Kupffer cells (KCs) located in the vasculature which serve as immune sentinels to detect and capture blood pathogens(231). While LSECs express a limited repertoire of scavenger and Fc receptors, KCs express several classes of Fc receptors, complement receptors, and importantly CrIg, a new class of complement receptor that binds C3b and iC3b and is required for efficient phagocytosis of complement C3-opsonized particles(231, 232).

Our rat studies have underscored the importance of liver mediated removal of virus, as noted by quantification of virus in the liver. Close to two orders of magnitude of additional infectious virus was found in the liver relative to the tumor on a per gram basis 10 minutes post injection. However, none of this virus remained infectious 24 hours post administration (Figure 3.7F). Although we have not explored the aspect of viral administration that deals with removal from the blood in this study, we wish to highlight some of the previously reported differences between the species used in our experiments and humans.

Notable differences exist between the functionality of the human and mouse complement systems and this was discussed in the previous section. While this may impact the load of infectious virus in the blood, presumably the viral particles are still opsonized. In the blood, the array of leukocytes with which the virus can interact is dramatically different in rodents and primates. While the majority of blood leukocytes in rodents are represented by lymphocytes (close to 80%), this is reversed in primates where neutrophils represent an equal or greater proportion as lymphocytes (Table 4.1). These

cells types express a different selection of complement and Fc receptors and their relative abundance likely influences the interaction patterns of the virus in the blood.

In addition, genetic divergence has occurred between complement receptors of rodents and primates. CR1 expressed on erythrocytes in primates serves as the primary immune adherence receptor to deliver pathogens to the liver and spleen. In contrast, in rodents, CR1 and CR2 are splice variants of the same gene and CR1 expression is restricted to B cells and follicular dendritic cells(233). To compensate, rodents utilize platelet-associated Factor H to remove opsonized particles(234). Along these same lines, rodent KCs express CRIg and CR3 while primate KCs additionally express CR1 and CR4(227). This differential expression likely impacts how virus is taken up by the liver, but has not been characterized.

From the perspective of the whole organism, the physiology of rodents, non-human primates, and humans is quite different in terms of size, blood volume, and cardiac output. These differences are outlined in Table 4.1. A comparison of the cardiac output to blood volume ratio suggests that five blood volumes are circulated in the rat during the time required for the circulation of one human blood volume. Blood pathogens with more exposure to the liver, as well as every other organ, will likely be cleared more rapidly from the circulation. Extrapolation from rats to humans may cause us to overestimate the rate at which virus is cleared from the blood of an organism.

Table 4.1. Physiological and hematologic comparison of humans with animal models

Values for various physiological parameters and hematologic parameters are indicated with source references are indicated in shaded rows.

	Human (adult)	Rat	Mouse	Macaque
Physiologic parameters				
Estimated average weight (kg)	60	0.15	0.02	3
	(235)	(235)	(235)	(235)
Body surface area (m^2)	1.6	0.025	0.007	0.24
	(235)	(235)	(235)	(235)
Cardiac output (CO)(mL/min)	5000	51	11	340
	(236)	(237)	(238)	(239)
Total blood volume (TBV) (mL)	5000	10 (64 ml/kg)	1.6 (80 mL/kg)	200 (65.5ml/kg)
	(236)	(240)	(236)	(241)
Estimated blood volume circulations per minute (CO/TBV)	1	5	7	1.7
Hematologic composition (%)				
Neutrophils	40-70	14	14.8	46.6
Lymphocytes	22-44	83	80.6	46.0
Monocytes	4-11	3	0.8	6.4
Eosinophils	0-8	1	3.0	0.8
Basophils	0-3	0	0.2	0.2
	(242)	(243)	(244)	(245)

Body surface area (BSA) relationships between species reflect to a sufficient degree oxygen utilization, caloric expenditure, metabolic activity, blood volume, and renal function, and was adequate to translate dosing with chemotherapeutics(235, 246). However, it does not provide an accurate reflection of the complexity of differences previously outlined and their interaction with actively replicating viruses. To illustrate this point, we can consider the dose of 2 $x10^9$ pfu of vaccinia virus which is the maximum feasible dose given intravenously in humans(100), and 1 x 10^9 pfu of vaccinia virus to be the maximum tolerated dose (MTD) given intratumorally (98), and scale down to the rat or mouse using the BSA ratio. The equivalent dose would be 1 x 10^7 pfu in rats or 4 x 10^6 pfu in mice. By comparison, mice treated intraperitoneally with VVdd all survived a dose of 1 x 10^9 pfu(81). The MTD across species is quite disparate given their size, and as a result, important physiological differences will likely make the *in vivo* comparative study of neutralizing factors and their potential thresholds of activity difficult.

To add to this complicated picture, technical restrictions limit the procedures that can be feasibly performed. Although it is easy to perform a slow infusion of virus in humans, and albeit with a shorter duration in NHP models, this is considerably more difficult in rodent models. In rodents, bolus injections are favored since slow infusions necessitate anesthesia. Clinically however, slow infusion has been the preferred method of administration since bolus dosing can produce numerous acute adverse events(247–249). How the rate of infusion impacts complement activation and liver clearance is of particular relevance, but a largely unexplored phenomenon with oncolytic viruses in pre-clinical animal models.

4.6 Complement manipulation in the rat model underscores the dependence of anti-vaccinia antibodies on complement activation

Contrary to our findings with the mouse model, the neutralization of vaccinia virus by complement and antibodies in rats closely mirrored our observations with human complement and antibodies (Figures 3.2, 3.5 and 3.6). This similarity enabled us to investigate how complement depletion impacted viral stability in blood and delivery to tumors in immunized animals. Complement inhibition in immune rats substantially increased the stability of the virus in the presence of anti-viral antibodies and increased the proportion of virus that remained infectious when delivered to tumors (Figure 3.7). The *in vitro* neutralization assays demonstrated that complement inhibition could render anti-vaccinia antibodies nearly non-neutralizing. Despite the robust enhancement of virus stability and infectivity of tumors associated with complement depletion in the rat, we still observed a difference between the naïve and immune complement depleted rats in blood and tumor titers (Figures 3.7 B,C compared to Figure 3.8 B,E and Figure 3.10).

There are a couple of hypotheses that may help to explain these differences. Despite seeing an almost complete reduction in C3 levels in the plasma (Figure 3.6C), it is possible that there remains a basal amount of C3 that is below the detection limit of the Western blot and that is still able to enhance the effect of anti-viral antibodies. In line with this idea is the fact that transgenic mice that constitutively express CVF, despite having very low C3 levels, do not have a tendency to develop infections, and have a normal lifespan, in contrast with C3 null mice, suggesting that there is some remaining C3(124). Nonetheless, the Fc portion of the antibody may help to induce receptor mediated phagocytosis of the virus, and cellular immunity remains intact such that that

antibodies bound to infected cells can still activate antibody-dependent cell-mediated cytotoxicity (ADCC), and T cells directed against the virus help to quell virus infection.

We did not observe overt signs of pathology in either naïve or immune complement-depleted rats treated with virus. This can be interpreted as a sign that we have not substantially impaired the ability of the animal to deal with the infection. We could not recover infectious virus from the liver 24h post-infection, a disease site where inflammation and necrosis were observed with ectromelia(116), and also a site from which oncolytic vaccinia has been recovered in a rabbit model(83). As a next step, a more rigorous analysis of infectious virus biodistribution and pathogenesis by histological examination would help to substantiate this claim.

We chose intravenous vaccination to mimic the scenario of multiple therapeutic intravenous doses of virus. However, this route of administration does not correlate with the first exposure for patients that were previously vaccinated against smallpox. The route of vaccination has been shown to be quite important in humans: scarification yielded a significantly higher neutralizing antibody titer than intramuscular inoculation(250). In mice, however, IV vaccination has been reported to elicit a similar if not moderately higher antibody titer than tail scarification(251). In our hands, we saw that the rat antibodies elicited against vaccinia virus by IV inoculation exhibited very similar functional characteristics to human antibodies generated from scarification (Figure 3.2 and 3.6B). It may yet be worthwhile to explore different routes of vaccination in the rat. Nonetheless, while the magnitude of response may differ between routes, based on our results, perhaps the dependence on complement does not.

Unexpectedly, complement depletion had a large magnitude of effect when virus was delivered directly into the tumor. By 24 hours post-virus infection, a time point that investigates only the first round of replication, we showed that we could substantially increase the initial infection of the tumor (Figure 3.10A). By 48 hours post-virus injection, we recovered close to 120 fold more infectious virus from the tumors of immune complement-depleted animals relative to their complement-replete counterparts (Figure 3.10B). The 48 hour time points suggests that complement depletion may have aided in the spread of the virus within the tumor. Clinically, direct intratumoral injection has been the preferred route of administration of virus since it was thought to circumvent the neutralizing factors in the blood. However, the tumor microenvironment can be a highly perfused region, and complement and antibodies clearly serve to limit the infection of the tumor. There is a wealth of evidence to support the important role of complement in the tumor microenvironment, and the neutralization of oncolytic viruses is a novel function to add to the compendium.

4.7 The cynomolgus macaque model offers an opportunity to assess the feasibility of using CP40 in combination with an infusion of oncolytic vaccinia virus

The study of CP40-mediated complement inhibition in a NHP model allowed us to determine whether complement inhibition could stabilize infectious virus in the blood of a pre-clinical model that is most analogous to humans. Our schedule with doses two days apart enabled us to make comparisons within the same immunologic time frame not only between animals, but also within the same animal. Although these animals were not tumor bearing, we believe that the greater bioavailability of infectious virus in the blood

would improve tumor infection. While we observed an increase in the infectious virus concentration the blood of all the immune animals, we acknowledge that the animals used in the study are outbred animals and we do not expect them to all behave identically. Interestingly, the level of antibody produced and the magnitude of cellular IFN γ, TNFα and IL 6 responses induced in humans receiving the smallpox vaccine have been associated with particular HLA genotypes(252). We believe that despite the differences seen between animals, the consistency of the trend adds strength to the rationale for using complement inhibitors during intravenous dosing of oncolytic viruses.

Complement has been described as a natural adjuvant to vaccination, working to lower the activation threshold of B cells through CR2 ligation(253). Correspondingly, HSV and influenza virus fail to mount antibody responses in C3, C4 and CR2 null mice(254, 255). With this in mind when designing our experiment, we wanted to ensure that all the animals would be exposed to complement-opsonized virus, mount a robust neutralizing antibody response, and could be used later as immune animals. This provided additional rationale to give the two doses of virus within a short time frame. This objective was satisfied since the macaques developed similar levels of antibody (Figure 3.12B). Additionally, we have no reason to believe based on these results, and the blood titers in Figure 3.13, that the scheduled order of treatments had any impact on the measure of the efficacy of this combinatorial approach.

We used a body surface area ratio to scale down the human dose of 1×10^9 pfu to a NHP equivalent dose(235). The proportion of infectious virus remaining in the blood at the end of the infusion is remarkably similar between the macaque model (Figure 3.13) and humans treated in the IV clinical trial (Figure 3.1). In the blood collected from the

Pexa-Vec clinical trial approximately 0.3% of the initial dose was detected at the end of the infusion. In the macaques, approximately 0.2% of the input dose remained in circulation in immune animals at the end of the infusion. If CP40 was administered prior to virus infusion, 1.9% of the input dose could be recovered. While these are approximations that do not account for the duration of infusion (humans were infused for one hour and not 30 minutes), among other factors, it does suggest that an increase in infectious virus of close to 10 fold could be achieved in humans.

4.8 The cynomolgus macaque model offers an opportunity to assess the safety of complement inhibition combination with an infusion of oncolytic vaccinia virus

It is particularly relevant to note that historically individuals with severe T cell abnormalities, but not those with agammaglobulinemia, developed generalized vaccinia virus infection following primary smallpox vaccination(256). This underscores the importance of cell-mediated immunity in the control of vaccinia virus. While anti-viral antibodies may prevent viral delivery, they may not be integral to controlling infection. Nonetheless, we believe that the safety of the approach lies in the transient nature of complement disruption with CP40.

Given the important role of complement and antibodies in the opsonization process and in the removal of blood-borne pathogens by the liver and spleen, it is surprising to see that the clearance rate of virus from the circulation, as measured by qPCR on blood samples (Figure 3.14), is the same for naïve and vaccinated animals with or without CP40 treatment. While on the one hand, this may be interpreted to serve as

another marker of safety since virus clearance from the blood was not impeded by complement inhibition. On the other hand, clearance from the blood may not be a relevant metric of uptake by the liver or spleen. Similar clearance kinetics could be a reflection of the virus's non-specific determinants for binding and cellular entry and suggests that the virus is taken up by all tissues that it encounters. In the immune setting, it is possible that Fc receptor expressing tissue resident macrophages could compensate for the lack of complement receptor mediated uptake. In the naïve setting however, virus could be freer to infect susceptible organs such as the skin. All the animals received virus both with and without CP40 treatment in a very short time frame, and all the animals developed pock lesions when they were naïve. Given the schedule, it is difficult to tease out if CP40 exacerbated the skin infection. We did not observe any lesions in immune animals. Protective resident memory $CD8^{+}$T cell immunity in the skin may also prevent the development of skin infection in immunized animals(257).

We hypothesized that since the anaphylatoxins C3a and C5a play an important role in the generation of inflammatory reactions(218), the abrogation of their production with CP40 would alter pro-inflammatory cytokine production. This suggestion is substantiated by a previously published *in vitro* experiment with human whole blood investigating the effect of Compstatin on the production of cytokines in response to baculoviruses. While substantial variability existed between blood donors, IL 6, IL 8 and TNF α were induced in response to virus, however were blunted if the samples were pretreated with Compstatin. Of the cytokines, IL 8 experienced the most robust inhibition with complement inhibition(258).

We did not observe a specific reduction or increase in the production of pro-inflammatory cytokines with complement inhibition (Figure 3.17). Unfortunately, we were limited to analyze samples from only three animals, we saw substantial differences between the outbred animals, and the levels of some cytokines had not returned to baseline by the time of the second infusion. These factors limit the conclusions that we can draw to broad strokes that are primarily hypothesis-generating. While we saw the predicted effects on live virus in the blood of immune animals with complement inhibition, we did not observe adverse signs of increased pro-inflammatory cytokine expression.

The intravenous Pexa-Vec clinical trial documented elevated levels of IFN γ, TNF α and IL 6 that increased acutely and peaked at 8 hours post-treatment. In addition, IL 10 increased between days 4-8(100). These results were reported in the text but not graphically, and there was no indication given of the magnitude of the response. Looking at mouse models, MCP-1, IFN γ, TNF α and IL 6 were all observed to increase and peak between 6 to 12 hours post intravenous injection of VVdd(199). An independent study showed IL 6 upregulation in the serum of mice treated intravenously with vaccinia in a manner that was dependent on the signaling of TLR 2 through MyD88. Concomitantly, it was also shown that *ex vivo* stimulation of dendritic cells with infectious or UV-inactivated vaccinia virus yielded very similar profiles of expression of IL 6, IL 1β, IL 12 and IFN β(259). This is interesting because it indicates that it is the total number of particles and not the infectious fraction that is of particular importance for acute phase cytokine production. This finding is consistent with our results, especially in the immune

condition where pro-inflammatory cytokine expression does not appear to be exacerbated with CP40(Figure 3.17).

A study of serum cytokines in primary or repeat vaccination with Dryvax (Wyeth strain vaccinia virus) demonstrated an interesting parallel(260). There are many differences between an intravenous dose of virus and virus administered percutaneously including the array of immune cells and organs that are exposed to the virus, and the time that it takes for replication to occur and produce a sufficient load of viral particles. Nonetheless, this study showed that IFN γ was substantially elevated in primary vaccine recipients and peaked between days 8 and 9, but was unresponsive in revaccinated individuals. Similarly, the magnitude of response of IFN γ in the NHP experiment in immune animals was also substantially lower than when the animals were naive (Figure 3.17). The mechanism underlying this difference is unknown.

The expression profile of some cytokines elicited by the second infusion of virus (day 2) appears to exhibit an altered hypo-responsive state, relative to the first infusion (day 0). This effect seems to be independent of CP40 and is particularly notable with MCP-1 (CCL2) and IL 6 (Figure 3.18). There may indeed be other cytokines that behave in this manner, including IL 10 (Appendix 3), however the trend is less clear and not observed in all the animals. There are three primary classes of inhibitors that negatively regulate cytokine expression following stimulation: tyrosine phosphatases (ie SHP-1), protein inhibitors of activated STATS (PIAS), and the suppressor of cytokine signaling (SOCS) which all serve to prevent cytokine receptor signal transduction through inhibition of the JAK/STAT axis(207). Specifically, the negative feedback loop mediated by the SOCS proteins is stimulated by a number of cytokines, including IL-2, IL-3, IL-4,

IL-6, IFN γ, G-CSF, and GM-CSF(261) and SOCS-3 has been documented to limit the expression of IL 6(262). MCP-1 has been reported to be regulated by SOCS-1(263, 264), and the MCP-1 promoter contains STAT binding sites(265). If it is indeed possible to induce a refractory state following a first infusion of virus, there are important consequences for OV treatment. Of particular interest is the resistance of SOCS-1 deficient mice to infection which was shown to be mediated by the inability of these mice to attenuate type I interferon signaling(266). This study showed that lower viral loads were detected in all the organs assayed of SOCS-1 deficient mice relative to their wild-type counterparts. If a second dose of oncolytic virus is administered during a refractory period while SOCS has extinguished JAK STAT signaling, it may be possible to increase virus infection. While this may increase the infection of some tumors, SOCS proteins have been reported to be silenced by hypermethylation in a number of cancers(267). Therefore, dosing during an altered responsiveness state may be an important safety concern as it could increase the infection of normal tissue. Lastly, the way in which this effect may sculpt anti-viral and anti-tumoral cellular immunity remains to be seen. The mechanism by which cytokines are negatively regulated after OV treatment has yet to be elucidated, however the SOCS proteins may be likely candidates. Based on our findings, we do not believe this phenomenon to be complement related.

4.9 Vaccinia engages in promiscuous cellular interactions

The experiments describing the way in which vaccinia virus interacts with cells in the blood are mostly hypothesis-generating, but suggest that vaccinia virus is predominantly cell-associated in the blood, and that some of the cellular interactions are

complement-mediated. Figure 3.19 presents a preliminary look at the association of vaccinia virus with specific cell types in the context of whole blood. We performed both qPCR and plaque assays on sorted cells to quantify the number of total particles, and the proportion of infectious particles associated with each cell type. This approach does not allow us to distinguish between virus that has entered a blood cell, produced progeny, and subsequently infected the monolayer to produce a plaque, and virus that has hitchhiked on the exterior of a blood cell and produced a plaque. In light of the dose escalation experiment in Figure 3.3, the virus concentration in the blood from a naïve donor used in this experiment would suggest that we would not observe virus neutralization. It is therefore not surprising that the ratio of infectious to total particles remains constant across cell types. So while this experiment provides information regarding the preferential interactions of the virus in the presence of complement, it does not inform us about which interactions may be protective against the effect of complement and that would lead to the recovery of infectious virus. It can be suggested that on a per cell basis, vaccinia virus was found to be more associated with phagocytic cell types that express high levels of complement receptors, compared to T cells. The association with neutrophils may be important given the large proportion of the leukocyte compartment that they represent (Table 4.1). To further explore this, it would be informative to perform the experiment in the opposite order, where the cells would be isolated first and incubated with virus (ideally in the presence of plasma with or without CP40). This would provide insight into which cells may act as productive cell carriers that can deliver infectious virus to target tumor tissue. The analysis of blood from patients treated intravenously with Pexa-Vec confirms preferential association with leukocytes over

erythrocytes on a per cell basis, and ubiquitous interactions with leukocytes (Figure 3.20).

Reovirus has been found to engage in protective interactions with blood cells in the presence of neutralizing antibodies. Specifically, T cells and dendritic cells have been shown to act as cell carriers in a murine model of melanoma(168) and lymphokine-activated killer cells and dendritic cells can protect the virus against human antibodies in ascites(268). Correlative assays from a Reolysin clinical trial demonstrated natural cell carriage whereby replication competent virus was recovered from PBMCs, granulocytes and platelets, but not from the plasma(169). The use of *ex vivo* loaded carrier cells poses several technical challenges in the clinic, so to improve upon natural cell carriage, a cytokine-conditioning regimen was subsequently developed to mobilize a population of tumor homing cells and enhance *in vivo* cell loading of reovirus. To this end, it was demonstrated that GMCSF mobilized $CD11b^+$ cells into tumors and as a result enhanced cell-associated virus delivery to tumors(269). One could envision a similar cytokine conditioning strategy for vaccinia virus, to increase the probability of virus interacting with a particular cell type that could home to tumors.

We also showed that complement inhibition seems to change the nature of the interaction with at least some cell types. *In vitro*, vaccinia virus preferentially associated with the cellular compartment in the presence of active complement, and when complement was inhibited, a shift in recovery was observed toward the plasma fraction (Figure 3.21). Importantly, this relocalization was observed with total virus, as measured by qPCR, and not just infectious virus. Given the importance of CR1 on erythrocytes to act as a mediator of immune adherence, it is tempting to think that this may be the

population responsible for the changes in compartmentalization seen in Figures 3.21, 3.22 and 3.23. Importantly, this same shift toward the plasma compartment was observed in macaque blood when the animals were pre-treated with CP40. Although we attempted to investigate vaccinia virus- erythrocyte association in the NHP experiment, the isolations were always considerably contaminated with leukocytes. There may have been a trend toward increased recovery from the erythrocyte compartment of animals treated with virus as a single agent (data not shown) although this remains very speculative and warrants a more direct investigation. We did not conclusively explore whether complement depletion altered the compartmentalization in the blood of rats. However, if this phenomenon is in fact related to CR1 binding on erythrocytes, due to the expression of the splice variant of CR1 described in section 4.5, we would not observe re-compartmentalization in the rats. Although the rat model provides a more accurate recapitulation of the effect of human complement and antibody, this may be an important difference.

4.10 Complement and antibody engage in the neutralization of other clinical candidate oncolytic viruses

Given our understanding of the phenotype of the antibody profile that vaccinia virus induced, we looked at whether neutralization by antibodies elicited by other oncolytic virus candidates is dependent on complement activation. We looked at the neutralization of HSV-1, reovirus, measles Edmonston, and MG1 *in vitro* in human plasma collected from healthy volunteers (Figure 3.25).

The glycoprotein C encoded by HSV has been shown to confer some protection to the virus by binding C3b and preventing its interaction with C5. However, this functionality has been demonstrated primarily *in vitro* at low concentrations of non-immune serum, and considerable virus neutralization could still occur at elevated concentrations of serum(270). In line with this demonstration of the sensitivity of HSV to complement, CVF pre-treatment has been shown to improve the systemic delivery of oncolytic HSV-1 to brain tumors in naïve rats(195). Here we also saw that HSV-1 is moderately neutralized by non-immune plasma. In contrast, plasma from immune individuals was strongly neutralizing, independent of complement activity. While complement modulation may aid the delivery of HSV-1 in naïve individuals, it will likely not improve delivery in immune individuals.

An age-dependent increase in reovirus-specific antibodies has been reported by two studies, where in a cohort of volunteers aged 20-29, upwards of 75% of individuals possessed reovirus specific IgG(271, 272). Although we did not validate the presence of anti-reovirus antibody, based on historical data it is likely that all three donors tested in our study were seropositive. We suggest that the anti-viral antibodies exhibit some degree of complement dependence. To substantiate our claims, a next step is nonetheless to validate that the donors did in fact possess anti-reovirus antibodies by ELISA or Western blot. An alternative explanation comes from a recent publication documenting that non-enveloped viruses carry complement proteins into the cytosol where C3 acts as both as a sensor to mediate an innate anti-viral response in the cell, and to target the virus to proteasome-mediated viral degradation(273). While this phenomenon has never been demonstrated to occur with reovirus, and it is uncertain that a broad array of cancer cell

types maintain functionality of this pathway, we suggest that complement inhibition may be of great clinical importance for oncolytic reovirus.

Measles vaccination has yielded very high seropositivity coverage in the general population and poses a significant barrier to the delivery of this virus. The neutralization of measles virus appears to be subject to a threshold effect, similarly to vaccinia. At the concentration of 2 x 10^6 pfu/mL and in the presence of the complement inhibitor CP40, elevated concentrations of virus could be recovered. There is a clear biological trend toward increased recovery of infectious virus. A more thorough examination of this effect is warranted, specifically through validation with more donors, higher concentrations of virus, and animal modeling. These findings are of particular interest in light of the recently reported interim clinical results with MV-NIS for the treatment of multiple myeloma. Of note, this is a patient population in which the levels of functional antibody titers were shown to be very low, and the two patients reported on, one of which experienced a durable complete remission, were seronegative (96). If the results with CP40 hold true in a larger cohort of donors, adjunct complement inhibition may be particularly useful for oncolytic measles virus and enable the treatment of measles vaccinated patients.

4.11 Characterization of the antibody profile to native and pseudotyped rhabdoviruses

Our data with MG1 in naïve human serum supports a previously published study(121). We observed virus neutralization in plasma from naïve donors that can likely be described as IgM-activated complement-mediated neutralization. Since this virus and also the LCMV pseudotyped maraba virus are not human pathogens, we vaccinated rats

and collected blood to assess *in vitro* whether complement-fixing antibodies were elicited. Similarly to the neutralizing antibody response elicited by VSV in mice(153), MG1 induced robustly neutralizing antibodies, the function of which was largely independent of complement (Figure 3.26A). Unexpectedly, given that the LCMV glycoprotein is well known for its inability to generate neutralizing antibodies early after vaccination in mice(274), we saw neutralization of the MRB LCMV G virus in immune plasma that was strictly dependent on complement activation (Figure 3.26B). Further exploration of these antibodies *in vivo* also substantiates that the anti-LCMV G antibody response was complement dependent (Figures 3.27, 3.28). Of note, the more appropriate control would have been the wild type maraba virus, even though it is not a therapeutic agent, since MG1 has a point mutation in the G protein(31). Clearly many questions remain outstanding to help explain this phenomenon, but the data suggests that pseudotyping a virus with the LCMV glycoprotein allows for the generation of a system in which the antibody profile can be modulated with complement inhibition.

This really prompts the question as to why some viruses elicit an antibody response that is dependent or not on the activity of complement. Antibody can render a virus neutralized either directly or indirectly. It can act through the binding of virion structures that preclude binding and entry to host cells, and can also bind surface determinants to activate complement and augment phagocytosis. Antibodies target numerous vaccinia virus mature virion proteins, however the glycoprotein is the only viral protein on the surface of the rhabdovirus virion. VSV G has been extensively characterized, and since it shares 80% homology with the maraba G(121), it can act as an appropriate surrogate comparator. Several factors have been identified that impact the

immunogenicity of viral surfaces, including the number and accessibility, organization, and glycosylation pattern of antigenic sites, and importantly, whether high-affinity V regions are frequently encoded in germline(187).

To address these criteria, it has been shown that swapping of the G proteins between the characteristically cytolytic VSV and latent non-cytolytic LCMV produces antibody responses typical of the parental virus glycoprotein and not the viral backbone. Additionally, it was shown that the highly repetitive, paracrystalline array of glycoproteins on the parental viruses was retained when the reciprocal pseudotyped viruses were generated(152). This organization is thought to favor the generation of a highly directed neutralizing antibody response toward the single accessible antigen(187). Looking at the B cell repertoire in mice, early antibodies against VSV have been shown to already possess high affinity, and over time and with somatic hypermutation, do no improve in affinity(275, 276). In contrast, early antibodies against LCMV in mice are non-neutralizing and affinity maturation is necessary to produce neutralizing antibodies(274). Arguably however, these phenotypes may be true only for natural reservoir hosts such as mice, since incidental hosts of LCMV such as primates possess completely different B cell repertoires. Importantly, the infection of mice with LCMV bears little resemblance to infection of primates, where the virus induces severe and sometimes fatal pathology and serves as a tool to study its arenavirus family member, the hemorrhagic fever inducing Lassa fever virus(277). To further illustrate the differences of the protective effects of antibodies, mice vaccinated with a vector expressing LCMV G have been shown to experience increased and accelerated mortality upon exposure to LCMV(278), whereas immunized macaques survived exposure to Lassa fever virus

infection without signs of disease(277, 279). While the effect seen in mice is the result of a complex interplay resulting in increased CTL-mediated immunopathology, this striking difference demonstrates once again the species differences. In humans, infection can range from sub-clinical to mild flu-like symptoms to meningitis and rarely encephalitis. Seroprevalence is thought to be low and is associated with exposure to either wild mice, or in rare cases, employee exposure to infected colonies in rodent breeding facilities(277, 280).

Looking at the mechanism of binding and entry provides insight into the potential targets of neutralizing antibodies. The VSV glycoprotein binds to its receptor, the LDL receptor(90), and is internalized by clathrin-mediated endocytosis(281). A large change in the conformation of the glycoprotein is driven by the low pH of the endosomal compartment and results in membrane fusion(282–284). LCMV binds to α-dystroglycan and cell entry occurs in a cholesterol-dependent, clathrin-independent, and caveolin-independent manner(285). The glycoprotein also undergoes a low pH-induced conformational change to induce fusion(286). From our data, we suggest that the anti-VSV antibodies likely restrict the interaction with the LDL receptor or lock the glycoprotein in the pre-fusion conformation and thus prevents the necessary low-pH induced structural transition required for fusion with the endocytic membrane. Neutralizing epitopes on the glycoprotein have been associated with fusion inhibition and have been associated with only moderate inhibition of binding(287). Nonetheless, the VSV receptor was identified only last year, now enabling studies to understand how neutralizing antibodies may interfere with its interaction with VSV G. In contrast, the early antibodies against the LCMV G likely binds locations of the glycoprotein in a

manner that does not interfere with binding to the cellular receptor or prevent the conformational change. The LCMV glycoprotein is comprised of two subunits: GP-1 and GP-2. Neutralizing antibodies that appear late in infection in mice are directed against a particular site on the GP-1 and prevent cellular entry through sterically blocking interaction with α-dystroglycan. Although early antibodies targeting this neutralizing epitope are detected in mice, they are of low affinity. GP-2 non-neutralizing antibodies achieve high titers early after infection(274). The GP-2 directed non-neutralizing antibodies may in fact be important mediators of complement activation.

Perhaps one of the most important differences between the mouse model where these viruses have best been described, and the rat model, is the complement system. It has been shown that early antibodies are generated in mice and while they are not neutralizing on their own(274), they very well may be complement fixing. We hypothesize that both mice and rats generate early antibodies against LCMV G, but that the low hemolytic activity of mouse complement may be responsible for the lack of functionality of antibodies in mice. In contrast, in rats these non-neutralizing antibodies can activate complement and lead to virolysis. To help substantiate this claim, we could perform an *in vitro* neutralization assay with antibodies derived from mouse and rat that is supplemented with active complement serum from either the same or opposite species. If this hypothesis is true, mouse antibodies should neutralize MRB LCMV G in the presence of rat complement but not mouse complement. Conversely, rat antibodies should be neutralizing in the presence of rat complement but not mouse complement. Passive immunization of rats with mouse anti-LCMV G antibodies would also provide evidence for this theory. The LCMV virus has coevolved with mice and the infection

phenotype may not translate to other species. It will be particularly important to validate the antibody phenotype in a non-human primate model.

General concluding thoughts

The primary objective of this work was to improve upon the understanding of neutralizing factors in the blood that reduce the delivery of infectious virus to the sites of tumor beds. Understanding of the way in which anti-vaccinia antibody functions suggested to us a therapeutic strategy to utilize complement inhibitors to improve the stability of oncolytic vaccinia virus in the blood of immune animals. Importantly, we have shown in two pre-clinical animal models that this approach is not only efficacious but also safe.

This work underscores the importance of choosing appropriate models and understanding the limits of the inferences that can be made from pre-clinical models to humans. While the mouse was most convenient and had been previously used for the modeling of intravenous delivery of OVs, it did not provide an accurate reflection of the human scenario. The rat and cynomolgus macaque models provided a better estimation of vaccinia virus neutralization by complement and antibody, but still differ from humans in numerous respects. Yet another manifestation of this idea is the dramatically different disease outcome in mice and primates when infected with LCMV. Importantly, the characteristics of the antibody generated in mice in response to LCMV infection likely does not model the antibody elicited by non-viral-host species. As a result, pseudotyping of a rhabdovirus with the LCMV glycoprotein may produce a non-neutralizing antibody phenotype in mice, however it is not necessarily translated to other species.

It is abundantly clear that the oncolytic virus platform has tremendous potential: its power sits at the convergence of the ability to initiate immune activation and induce tumor debulking in a self-amplifying manner. The unpredictability of patient responses in

the clinic underscores that we need more representative models and a better understanding of key determinants of infection and predictive biomarkers for efficacy. To fully capitalize on the prospect of the therapeutic class, clinicians and researchers will likely need an armory of viruses and adjunct therapeutics to aid in delivery, replication in heterogeneous cancerous cells, immune activation, and likely yet undiscovered combinations.

References

1. **Vogelstein B, Kinzler KW**. 2004. Cancer genes and the pathways they control. Nat. Med. **10**:789–99.

2. **Hanahan D, Weinberg RA**. 2011. Hallmarks of cancer: the next generation. Cell **144**:646–74.

3. **Vesely MD, Kershaw MH, Schreiber RD, Smyth MJ**. 2011. Natural innate and adaptive immunity to cancer. Annu. Rev. Immunol. **29**:235–71.

4. **Markowitz SD, Bertagnolli MM**. 2009. Molecular Basis of Colorectal Cancer. N. Engl. J. Med. **361**:2449–2460.

5. **Gerlinger M, Rowan AJ, Horswell S, Larkin J, Endesfelder D, Gronroos E, Martinez P, Matthews N, Stewart A, Tarpey P, Varela I, Phillimore B, Begum S, McDonald NQ, Butler A, Jones D, Raine K, Latimer C, Santos C, Nohadani M, Eklund A, Spencer-Dene B, Clark G, Pickering L, Stamp G, Gore M, Szallasi Z, Downward J, Futreal PA, Swanton C**. 2012. Intratumor Heterogeneity and Branched Evolution Revealed by Multiregion Sequencing. N. Engl. J. Med. **366**:883–892.

6. **Forbes NE, Abdelbary H, Lupien M, Bell JC, Diallo J-S**. 2013. Exploiting tumor epigenetics to improve oncolytic virotherapy. Front. Genet. **4**:184.

7. **Morin RD, Mendez-Lago M, Mungall AJ, Goya R, Mungall KL, Corbett RD, Johnson N a, Severson TM, Chiu R, Field M, Jackman S, Krzywinski M, Scott DW, Trinh DL, Tamura-Wells J, Li S, Firme MR, Rogic S, Griffith M, Chan S, Yakovenko O, Meyer IM, Zhao EY, Smailus D, Moksa M, Chittaranjan S, Rimsza L, Brooks-Wilson A, Spinelli JJ, Ben-Neriah S, Meissner B, Woolcock B, Boyle M, McDonald H, Tam A, Zhao Y, Delaney A, Zeng T, Tse K, Butterfield Y, Birol I, Holt R, Schein J, Horsman DE, Moore R, Jones SJM, Connors JM, Hirst M, Gascoyne RD, Marra MA**. 2011. Frequent mutation of histone-modifying genes in non-Hodgkin lymphoma. Nature **476**:298–303.

8. **Dawson MA, Kouzarides T**. 2012. Cancer epigenetics: from mechanism to therapy. Cell **150**:12–27.

9. **Hanahan D, Coussens LM**. 2012. Accessories to the crime: functions of cells recruited to the tumor microenvironment. Cancer Cell **21**:309–22.

10. **Quail DF, Joyce JA**. 2013. Microenvironmental regulation of tumor progression and metastasis. Nat. Med. **19**:1423–37.

11. **Dunn GP, Old LJ, Schreiber RD**. 2004. The three Es of cancer immunoediting. Annu. Rev. Immunol. **22**:329–60.

12. **Raulet DH**. 2006. Missing self recognition and self tolerance of natural killer (NK) cells. Semin. Immunol. **18**:145–50.

13. **Gross S, Walden P**. 2008. Immunosuppressive mechanisms in human tumors: why we still cannot cure cancer. Immunol. Lett. **116**:7–14.

14. **Stern-Ginossar N, Gur C, Biton M, Horwitz E, Elboim M, Stanietsky N, Mandelboim M, Mandelboim O**. 2008. Human microRNAs regulate stress-induced immune responses mediated by the receptor NKG2D. Nat. Immunol. **9**:1065–73.

15. **Miest TS, Cattaneo R**. 2014. New viruses for cancer therapy: meeting clinical needs. Nat. Rev. Microbiol. **12**:23–34.

16. **Ilkow CS, Swift SL, Bell JC, Diallo J-S**. 2014. From scourge to cure: tumour-selective viral pathogenesis as a new strategy against cancer. PLoS Pathog. **10**:e1003836.

17. **Roberts PJ, Der CJ**. 2007. Targeting the Raf-MEK-ERK mitogen-activated protein kinase cascade for the treatment of cancer. Oncogene **26**:3291–310.

18. **Parato KA, Breitbach CJ, Le Boeuf F, Wang J, Storbeck C, Ilkow C, Diallo J-S, Falls T, Burns J, Garcia V, Kanji F, Evgin L, Hu K, Paradis F, Knowles S, Hwang T-H, Vanderhyden BC, Auer R, Kirn DH, Bell JC**. 2012. The oncolytic poxvirus JX-594 selectively replicates in and destroys cancer cells driven by genetic pathways commonly activated in cancers. Mol. Ther. **20**:749–58.

19. **Twardzik DR, Brown JP, Ranchalis JE, Todaro GJ, Moss B**. 1985. Vaccinia virus-infected cells release a novel polypeptide functionally related to transforming and epidermal growth factors. Proc. Natl. Acad. Sci. U. S. A. **82**:5300–4.

20. **Stanford MM, McFadden G**. 2007. Myxoma virus and oncolytic virotherapy: a new biologic weapon in the war against cancer. Expert Opin. Biol. Ther. **7**:1415–25.

21. **Fu X, Tao L, Cai R, Prigge J, Zhang X**. 2006. A mutant type 2 herpes simplex virus deleted for the protein kinase domain of the ICP10 gene is a potent oncolytic virus. Mol. Ther. **13**:882–90.

22. **Marcato P, Shmulevitz M, Pan D, Stoltz D, Lee PW**. 2007. Ras transformation mediates reovirus oncolysis by enhancing virus uncoating, particle infectivity, and apoptosis-dependent release. Mol. Ther. **15**:1522–30.

23. **Zamanian M, La Thangue NB**. 1992. Adenovirus E1a prevents the retinoblastoma gene product from repressing the activity of a cellular transcription factor. EMBO J. **11**:2603–2610.

24. **Gomez-Manzano C, Balague C, Alemany R, Lemoine MG, Mitlianga P, Jiang H, Khan A, Alonso M, Lang FF, Conrad CA, Liu T-J, Bekele BN, Yung WKA, Fueyo J**. 2004. A novel E1A-E1B mutant adenovirus induces glioma regression in vivo. Oncogene **23**:1821–8.

25. **Kim JH, Oh JY, Park BH, Lee DE, Kim JS, Park HE, Roh MS, Je JE, Yoon JH, Thorne SH, Kirn D, Hwang TH**. 2006. Systemic armed oncolytic and immunologic therapy for cancer with JX-594, a targeted poxvirus expressing GM-CSF. Mol. Ther. **14**:361–70.

26. **Stojdl DF, Lichty BD, tenOever BR, Paterson JM, Power AT, Knowles S, Marius R, Reynard J, Poliquin L, Atkins H, Brown EG, Durbin RK, Durbin JE, Hiscott J, Bell JC**. 2003. VSV strains with defects in their ability to shutdown innate immunity are potent systemic anti-cancer agents. Cancer Cell **4**:263–75.

27. **Dunn GP, Bruce AT, Sheehan KCF, Shankaran V, Uppaluri R, Bui JD, Diamond MS, Koebel CM, Arthur C, White JM, Schreiber RD**. 2005. A critical function for type I interferons in cancer immunoediting. Nat. Immunol. **6**:722–9.

28. **Indraccolo S**. 2010. Interferon-alpha as angiogenesis inhibitor: learning from tumor models. Autoimmunity **43**:244–7.

29. **Subramaniam PS, Johnson HM**. 1997. A Role for the Cyclin-Dependent Kinase Inhibitor p21 in the Gi Cell Cycle Arrest Mediated by the Type I Interferons. J. Interferon Cytokine Res. **15**:11–15.

30. **Fiola C, Peeters B, Fournier P, Arnold A, Bucur M, Schirrmacher V**. 2006. Tumor selective replication of Newcastle disease virus: association with defects of tumor cells in antiviral defence. Int. J. Cancer **119**:328–38.

31. **Brun J, McManus D, Lefebvre C, Hu K, Falls T, Atkins H, Bell JC, McCart JA, Mahoney D, Stojdl DF**. 2010. Identification of genetically modified Maraba virus as an oncolytic rhabdovirus. Mol. Ther. **18**:1440–9.

32. **Goetz C, Dobrikova E, Shveygert M, Dobrikov M, Gromeier M**. 2011. Oncolytic poliovirus against malignant glioma. Futur. Med. **6**:1045–1058.

33. **Fishelson Z, Donin N, Zell S, Schultz S, M K**. 2003. Obstacles to cancer immunotherapy: expression of membrane complement regulatory proteins (mCRPs) in tumors. Mol. Immunol. **40**:109–123.

34. **Anderson BD, Nakamura T, Russell SJ, Peng K**. 2004. High CD46 Receptor Density Determines Preferential Killing of Tumor Cells by Oncolytic Measles Virus High CD46 Receptor Density Determines Preferential Killing of Tumor Cells by Oncolytic Measles Virus 4919–4926.

35. **Breitbach CJ, Arulanandam R, De Silva N, Thorne SH, Patt R, Daneshmand M, Moon A, Ilkow C, Burke J, Hwang T-H, Heo J, Cho M, Chen H, Angarita FA, Addison C, McCart JA, Bell JC, Kirn DH**. 2013. Oncolytic vaccinia virus disrupts tumor-associated vasculature in humans. Cancer Res. **73**:1265–75.

36. **Breitbach CJ, De Silva NS, Falls TJ, Aladl U, Evgin L, Paterson J, Sun YY, Roy DG, Rintoul JL, Daneshmand M, Parato K, Stanford MM, Lichty BD, Fenster A, Kirn D, Atkins H, Bell JC**. 2011. Targeting tumor vasculature with an oncolytic virus. Mol. Ther. **19**:886–94.

37. **Breitbach CJ, Paterson J, Lemay CG, Falls T, McGuire A, Parato KA, Stojdl DF, Daneshmand M, Speth K, Kirn DH, McCart JA, Atkins H, Bell JC**. 2007. Targeted inflammation during oncolytic virus therapy severely compromises tumor blood flow. Mol. Ther. **15**:1686–93.

38. **Mellman I, Coukos G, Dranoff G**. 2011. Cancer immunotherapy comes of age. Nature **480**:480–9.

39. **Donnelly OG, Errington-Mais F, Steele L, Hadac E, Jennings V, Scott K, Peach H, Phillips RM, Bond J, Pandha H, Harrington K, Vile R, Russell S, Selby P, Melcher AA**. 2013. Measles virus causes immunogenic cell death in human melanoma. Gene Ther. **20**:7–15.

40. **Workenhe ST, Simmons G, Pol JG, Lichty BD, Halford WP, Mossman KL**. 2014. Immunogenic HSV-mediated oncolysis shapes the antitumor immune response and contributes to therapeutic efficacy. Mol. Ther. **22**:123–31.

41. **Wongthida P, Diaz RM, Galivo F, Kottke T, Thompson J, Melcher AA, Vile R**. 2011. VSV oncolytic virotherapy in the B16 model depends upon intact MyD88 signaling. Mol. Ther. **19**:150–8.

42. **Moehler MH, Zeidler M, Wilsberg V, Cornelis JJ, Woelfel T, Rommelaere J, Galle PR, Heike M**. 2005. Parvovirus H-1-induced tumor cell death enhances human immune response in vitro via increased phagocytosis, maturation, and cross-presentation by dendritic cells. Hum. Gene Ther. **16**:996–1005.

43. **Gauvrit A, Brandler S, Sapede-Peroz C, Boisgerault N, Tangy F, Gregoire M**. 2008. Measles virus induces oncolysis of mesothelioma cells and allows dendritic cells to cross-prime tumor-specific CD8 response. Cancer Res. **68**:4882–92.

44. **Prestwich RJ, Ilett EJ, Errington F, Diaz RM, Steele LP, Kottke T, Thompson J, Galivo F, Harrington KJ, Pandha HS, Selby PJ, Vile RG, Melcher A**. 2009. Immune-mediated antitumor activity of reovirus is required for therapy and is independent of direct viral oncolysis and replication. Clin. Cancer Res. **15**:4374–81.

45. **Toda M, Rabkin SD, Kojima H, Martuza RL**. 1999. Herpes simplex virus as an in situ cancer vaccine for the induction of specific anti-tumor immunity. Hum. Gene Ther. **10**:385–93.

46. **Hwang T-H, Moon A, Burke J, Ribas A, Stephenson J, Breitbach CJ, Daneshmand M, De Silva N, Parato K, Diallo J-S, Lee Y-S, Liu T-C, Bell JC, Kirn DH**. 2011. A mechanistic proof-of-concept clinical trial with JX-594, a targeted multi-mechanistic oncolytic poxvirus, in patients with metastatic melanoma. Mol. Ther. **19**:1913–22.

47. **Kaufman HL, Bines SD**. 2010. OPTIM trial: a Phase III trial of an oncolytic herpes virus encoding GM-CSF for unresectable stage III or IV melanoma. Future Oncol. **6**:941–9.

48. **Kim MK, Breitbach CJ, Moon A, Heo J, Lee YK, Cho M, Lee JW, Kim S-G, Kang DH, Bell JC, Park BH, Kirn DH, Hwang T-H**. 2013. Oncolytic and immunotherapeutic vaccinia induces antibody-mediated complement-dependent cancer cell lysis in humans. Sci. Transl. Med. **5**:185ra63.

49. **Nakamura H, Mullen JT, Chandrasekhar S, Pawlik TM, Yoon SS, Tanabe KK**. 2001. Multimodality Therapy with a Replication-conditional Herpes Simplex Virus 1 Mutant that Expresses Yeast Cytosine Deaminase for Intratumoral Conversion of 5-Fluorocytosine to Multimodality Therapy with a Replication-conditional Herpes Simplex Virus 1 Mutan. Cancer Res. **61**:5447–5452.

50. **Tyminski E, Leroy S, Terada K, Finkelstein DM, Hyatt JL, Danks MK, Potter PM, Saeki Y, Chiocca EA**. 2005. Brain Tumor Oncolysis with Replication-Conditional Herpes Simplex Virus Type 1 Expressing the Prodrug-Activating Genes , CYP2B1 and Secreted Human Intestinal Carboxylesterase , in Combination with Cyclophosphamide and Irinotecan Combination with Cyclophos. Cancer Res. **65**:6850–6857.

51. **Hingorani M, White CL, Zaidi S, Pandha HS, Melcher AA, Bhide SA, Nutting CM, Syrigos KN, Vile RG, Vassaux G, Harrington KJ**. 2010. Therapeutic effect of sodium iodide symporter gene therapy combined with external beam radiotherapy and targeted drugs that inhibit DNA repair. Mol. Ther. **18**:1599–605.

52. **Reddi H V, Madde P, McDonough SJ, Trujillo MA, Morris JC, Myers RM, Peng KW, Russell SJ, McIver B, Eberhardt NL**. 2012. Preclinical efficacy of

the oncolytic measles virus expressing the sodium iodide symporter in iodine non-avid anaplastic thyroid cancer: a novel therapeutic agent allowing noninvasive imaging and radioiodine therapy. Cancer Gene Ther. **19**:659–65.

53. **Pol JG, Resseguier J, Lichty BD**. 2012. Oncolytic viruses : a step into cancer immunotherapy. Dovepress **2012:4**:1–21.

54. **Shi Y, Liu CH, Roberts AI, Das J, Xu G, Ren G, Zhang Y, Zhang L, Yuan ZR, Tan HSW, Das G, Devadas S**. 2006. Granulocyte-macrophage colony-stimulating factor (GM-CSF) and T-cell responses: what we do and don't know. Cell Res. **16**:126–33.

55. **Grossardt C, Engeland CE, Bossow S, Halama N, Zaoui K, Leber MF, Springfeld C, Jaeger D, von Kalle C, Ungerechts G**. 2013. Granulocyte-macrophage colony-stimulating factor-armed oncolytic measles virus is an effective therapeutic cancer vaccine. Hum. Gene Ther. **24**:644–54.

56. **Du T, Shi G, Li YM, Zhang JF, Tian HW, Wei YQ, Deng H, Yu DC**. 2014. Tumor-specific oncolytic adenoviruses expressing granulocyte macrophage colony-stimulating factor or anti-CTLA4 antibody for the treatment of cancers. Cancer Gene Ther. **21**:340–8.

57. **Pol JG, Zhang L, Bridle BW, Stephenson KB, Rességuier J, Hanson S, Chen L, Kazdhan N, Bramson JL, Stojdl DF, Wan Y, Lichty BD**. 2014. Maraba virus as a potent oncolytic vaccine vector. Mol. Ther. **22**:420–9.

58. **Bridle BW, Clouthier D, Zhang L, Pol J, Chen L, Lichty BD, Bramson JL, Wan Y**. 2013. Oncolytic vesicular stomatitis virus quantitatively and qualitatively improves primary CD8(+) T-cell responses to anticancer vaccines. Oncoimmunology **2**:e26013.

59. **Bridle BW, Boudreau JE, Lichty BD, Brunellière J, Stephenson K, Koshy S, Bramson JL, Wan Y**. 2009. Vesicular stomatitis virus as a novel cancer vaccine vector to prime antitumor immunity amenable to rapid boosting with adenovirus. Mol. Ther. **17**:1814–21.

60. **Chou J**. 1994. Herpes simplex virus 1 y134.5 gene function, which blocks the host response to infection, maps in the homologous domain of the genes expressed during growth arrest and DNA damage. Proc. Natl. Acad. Sci. U. S. A. **91**:5247–5251.

61. **Kim S-H, Wong RJ, Kooby D a, Carew JF, Adusumilli PS, Patel SG, Shah JP, Fong Y**. 2005. Combination of mutated herpes simplex virus type 1 (G207 virus) with radiation for the treatment of squamous cell carcinoma of the head and neck. Eur. J. Cancer **41**:313–22.

62. **Kyula JN, Khan A, Mansfield D, Karapanagiotou EM, McLaughlin M, Roulstone V, Zaidi S, Pencavel T, Touchefeu Y, Seth R, Chen NG, Yu YA, Zhang Q, Melcher A, Vile RG, Pandha HS, Ajaz M, Szalay A, Harrington KJ**. 2014. Synergistic cytotoxicity of radiation and oncolytic Lister strain vaccinia in (V600D/E)BRAF mutant melanoma depends on JNK and TNF-α signaling. Oncogene **33**:1700–12.

63. **Karapanagiotou EM, Roulstone V, Twigger K, Ball M, Tanay M, Nutting C, Newbold K, Gore ME, Larkin J, Syrigos KN, Coffey M, Thompson B, Mettinger K, Vile RG, Pandha HS, Hall GD, Melcher AA, Chester J, Harrington KJ**. 2012. Phase I/II trial of carboplatin and paclitaxel chemotherapy in combination with intravenous oncolytic reovirus in patients with advanced malignancies. Clin. Cancer Res. **18**:2080–9.

64. **Comins C, Spicer J, Protheroe A, Roulstone V, Twigger K, White CM, Vile R, Melcher AA, Coffey MC, Mettinger KL, Nuovo G, Cohn DE, Phelps M, Harrington KJ, Pandha HS**. 2010. REO-10: a phase I study of intravenous reovirus and docetaxel in patients with advanced cancer. Clin. Cancer Res. **16**:5564–72.

65. **Sei S, Mussio JK, Yang Q, Nagashima K, Parchment RE, Coffey MC, Shoemaker RH, Tomaszewski JE**. 2009. Synergistic antitumor activity of oncolytic reovirus and chemotherapeutic agents in non-small cell lung cancer cells. Mol. Cancer **8**:47.

66. **Zamarin D, Holmgaard RB, Subudhi SK, Park JS, Mansour M, Palese P, Merghoub T, Wolchok JD, Allison JP**. 2014. Localized oncolytic virotherapy overcomes systemic tumor resistance to immune checkpoint blockade immunotherapy. Sci. Transl. Med. **6**:226ra32.

67. **Engeland CE, Grossardt C, Veinalde R, Bossow S, Lutz D, Kaufmann JK, Shevchenko I, Umansky V, Nettelbeck DM, Weichert W, Jäger D, von Kalle C, Ungerechts G**. 2014. CTLA-4 and PD-L1 Checkpoint Blockade Enhances Oncolytic Measles Virus Therapy. Mol. Ther.

68. **Buller RM, Palumbo GJ**. 1991. Poxvirus pathogenesis. Microbiol. Rev. **55**:80–122.

69. **Yang Z, Reynolds SE, Martens C a, Bruno DP, Porcella SF, Moss B**. 2011. Expression profiling of the intermediate and late stages of poxvirus replication. J. Virol. **85**:9899–908.

70. **Moss B**. 2012. Poxvirus cell entry: how many proteins does it take? Viruses **4**:688–707.

71. Adverse Reactions Following Smallpox Vaccination Department of Health and Human Services; Centers for Disease Control and Prevention.

72. **Kirn DH, Thorne SH**. 2009. Targeted and armed oncolytic poxviruses: a novel multi-mechanistic therapeutic class for cancer. Nat. Rev. Cancer **9**:64–71.

73. **Smith GL, Moss B**. 1983. Infectious poxvirus vectors have capacity for at least 25000 base pairs of foreign DNA. Gene **25**:21–28.

74. **García-Arriaza J, Nájera JL, Gómez CE, Tewabe N, Sorzano COS, Calandra T, Roger T, Esteban M**. 2011. A candidate HIV/AIDS vaccine (MVA-B) lacking vaccinia virus gene C6L enhances memory HIV-1-specific T-cell responses. PLoS One **6**:e24244.

75. **Gómez CE, Nájera JL, Perdiguero B, García-Arriaza J, Sorzano COS, Jiménez V, González-Sanz R, Jiménez JL, Muñoz-Fernández MA, López Bernaldo de Quirós JC, Guardo AC, García F, Gatell JM, Plana M, Esteban M**. 2011. The HIV/AIDS vaccine candidate MVA-B administered as a single immunogen in humans triggers robust, polyfunctional, and selective effector memory T cell responses to HIV-1 antigens. J. Virol. **85**:11468–78.

76. **Gudmundsdotter L, Nilsson C, Brave A, Hejdeman B, Earl P, Moss B, Robb M, Cox J, Michael N, Marovich M, Biberfeld G, Sandström E, Wahren B**. 2009. Recombinant Modified Vaccinia Ankara (MVA) effectively boosts DNA-primed HIV-specific immune responses in humans despite pre-existing vaccinia immunity. Vaccine **27**:4468–74.

77. **Jäger E, Karbach J, Gnjatic S, Neumann A, Bender A, Valmori D, Ayyoub M, Ritter E, Ritter G, Jäger D, Panicali D, Hoffman E, Pan L, Oettgen H, Old LJ, Knuth A**. 2006. Recombinant vaccinia/fowlpox NY-ESO-1 vaccines induce both humoral and cellular NY-ESO-1-specific immune responses in cancer patients. Proc. Natl. Acad. Sci. U. S. A. **103**:14453–8.

78. **Parato K a, Breitbach CJ, Le Boeuf F, Wang J, Storbeck C, Ilkow C, Diallo J-S, Falls T, Burns J, Garcia V, Kanji F, Evgin L, Hu K, Paradis F, Knowles S, Hwang T-H, Vanderhyden BC, Auer R, Kirn DH, Bell JC**. 2012. The oncolytic poxvirus JX-594 selectively replicates in and destroys cancer cells driven by genetic pathways commonly activated in cancers. Mol. Ther. **20**:749–58.

79. **Guse K, Cerullo V, Hemminki A**. 2011. Oncolytic vaccinia virus for the treatment of cancer. Expert Opin. Biol. Ther. **11**:595–608.

80. **Naik AM, Chalikonda S, McCart JA, Xu H, Guo ZS, Langham G, Gardner D, Mocellin S, Lokshin AE, Moss B, Alexander HR, Bartlett DL**. 2006. Intravenous and isolated limb perfusion delivery of wild type and a tumor-

selective replicating mutant vaccinia virus in nonhuman primates. Hum. Gene Ther. **17**:31–45.

81. **McCart JA, Ward JM, Lee J, Hu Y, Alexander HR, Libutti SK, Moss B, Bartlett DL**. 2001. Systemic Cancer Therapy with a Tumor-selective Vaccinia Virus Mutant Lacking Thymidine Kinase and Vaccinia Growth Factor Genes Systemic Cancer Therapy with a Tumor-selective Vaccinia Virus Mutant Lacking Thymidine Kinase and Vaccinia Growth Factor Genes. Cancer Res. **61**:8751–8757.

82. **Thorne SH, Hwang T-HH, O'Gorman WE, Bartlett DL, Sei S, Kanji F, Brown C, Werier J, Cho J-H, Lee D-E, Wang Y, Bell J, Kirn DH**. 2007. Rational strain selection and engineering creates a broad-spectrum, systemically effective oncolytic poxvirus, JX-963. J. Clin. Invest. **117**:3350–8.

83. **Lee J-H, Roh M-S, Lee Y-K, Kim M-K, Han J-Y, Park B-H, Trown P, Kirn DH, Hwang T-H**. 2010. Oncolytic and immunostimulatory efficacy of a targeted oncolytic poxvirus expressing human GM-CSF following intravenous administration in a rabbit tumor model. Cancer Gene Ther. **17**:73–9.

84. **Zeh H, Downs-Canner S, McCart J, Guo Z, Rao U, Ramalingam L, Thorne S, Jones H, Kalinski P, Wieckowski E, O'Malley M, Daneshmand M, Hu K, Bell J, Hwang T, Moon A, Breitbach C, Kirn D, Bartlett D**. 2014. First-in-man Study of Western Reserve Strain Oncolytic Vaccinia Virus: Safety, Systemic Spread and Anti-tumor Activity. Mol. Ther.

85. **Qian Z, Liang C, Yu YA, Chen N, Dandekar T, Szalay AA**. 2009. The highly attenuated oncolytic recombinant vaccinia virus GLV-1h68: comparative genomic features and the contribution of F14.5L inactivation. Mol. Genet. genomics **282**:417–435.

86. **Zhang Q, Yu Y a, Wang E, Chen N, Danner RL, Munson PJ, Marincola FM, Szalay A a**. 2007. Eradication of solid human breast tumors in nude mice with an intravenously injected light-emitting oncolytic vaccinia virus. Cancer Res. **67**:10038–46.

87. **Ascierto ML, Worschech A, Yu Z, Adams S, Reinboth J, Chen NG, Pos Z, Roychoudhuri R, Di Pasquale G, Bedognetti D, Uccellini L, Rossano F, Ascierto P a, Stroncek DF, Restifo NP, Wang E, Szalay A a, Marincola FM**. 2011. Permissivity of the NCI-60 cancer cell lines to oncolytic Vaccinia Virus GLV-1h68. BMC Cancer **11**:451.

88. **Russell SJ, Peng K-W, Bell JC**. 2012. Oncolytic virotherapy. Nat. Biotechnol. **30**:658–70.

89. 2005. Virus Taxonomy VIIIth Report of the International Committee on Taxonomy of Viruses. Elsevier, London.

90. **Finkelshtein D, Werman A, Novick D, Barak S, Rubinstein M**. 2013. LDL receptor and its family members serve as the cellular receptors for vesicular stomatitis virus. Proc. Natl. Acad. Sci. U. S. A. **110**:7306–11.

91. **Lichty BD, Power AT, Stojdl DF, Bell JC**. 2004. Vesicular stomatitis virus: re-inventing the bullet. Trends Mol. Med. **10**:210–6.

92. **Fields BN, Hawkins K**. 1967. Human Infection with the Virus of Vesicuar Stomatitis During and Epizootic. N. Engl. J. Med. **277**.

93. **Stojdl DF, Lichty B, Knowles S, Marius R, Atkins H, Sonenberg N, Bell JC**. 2000. Exploiting tumor-specific defects in the interferon pathway with a previously unknown oncolytic virus. Nat. Med. **6**:821–5.

94. **Travassos APA, Rosa DA, Tesh RB, Travassos JF, Herve P, Main AJ, Joya L**. 1984. Carajas and maraba viruses, two new vesiculoviruses isolated from phlemotomine sand flies in Brazil. Am. J. Trop. Med. Hyg. **33**:999–1006.

95. **Ross MI, Andtbacka RHI, Puzanov I, Milhem MM, Collichio FA, Delman KA, Noyes DR, Zager JS, Cranmer LD, Spitler LE, Hsueh EC, Ollila DW, Amatruda T, Chen L, Gansert JL, Kaufman HL**. 2014. Patterns of durable response with intralesional talimogene laherparepvec (T-VEC) Results from a phase III trial in patients with stage IIIb-IV melanoma. J. Clin. Oncol. **32**.

96. **Russell SJ, Federspiel MJ, Peng K-W, Tong C, Dingli D, Morice WG, Lowe V, O'Connor MK, Kyle RA, Leung N, Buadi FK, Rajkumar SV, Gertz MA, Lacy MQ, Dispenzieri A**. 2014. Remission of disseminated cancer after systemic oncolytic virotherapy. Mayo Clin. Proc. **89**:926–33.

97. **Galanis E, Markovic SN, Suman VJ, Nuovo GJ, Vile RG, Kottke TJ, Nevala WK, Thompson MA, Lewis JE, Rumilla KM, Roulstone V, Harrington K, Linette GP, Maples WJ, Coffey M, Zwiebel J, Kendra K**. 2012. Phase II trial of intravenous administration of Reolysin(®) (Reovirus Serotype-3-dearing Strain) in patients with metastatic melanoma. Mol. Ther. **20**:1998–2003.

98. **Park B-H, Hwang T, Liu T-C, Sze DY, Kim J-S, Kwon H-C, Oh SY, Han S-Y, Yoon J-H, Hong S-H, Moon A, Speth K, Park C, Ahn Y-J, Daneshmand M, Rhee BG, Pinedo HM, Bell JC, Kirn DH**. 2008. Use of a targeted oncolytic poxvirus, JX-594, in patients with refractory primary or metastatic liver cancer: a phase I trial. Lancet Oncol. **9**:533–42.

99. **Heo J, Reid T, Ruo L, Breitbach CJ, Rose S, Bloomston M, Cho M, Lim HY, Chung HC, Kim CW, Burke J, Lencioni R, Hickman T, Moon A, Lee YS,**

Kim MK, Daneshmand M, Dubois K, Longpre L, Ngo M, Rooney C, Bell JC, Rhee B-G, Patt R, Hwang T-H, Kirn DH. 2013. Randomized dose-finding clinical trial of oncolytic immunotherapeutic vaccinia JX-594 in liver cancer. Nat. Med. **19**:329–36.

100. **Breitbach CJ, Burke J, Jonker D, Stephenson J, Haas AR, Chow LQM, Nieva J, Hwang T-H, Moon A, Patt R, Pelusio A, Le Boeuf F, Burns J, Evgin L, De Silva N, Cvancic S, Robertson T, Je J-E, Lee Y-S, Parato K, Diallo J-S, Fenster A, Daneshmand M, Bell JC, Kirn DH**. 2011. Intravenous delivery of a multi-mechanistic cancer-targeted oncolytic poxvirus in humans. Nature **477**:99–102.

101. **Ricklin D, Hajishengallis G, Yang K, Lambris JD**. 2010. Complement: a key system for immune surveillance and homeostasis. Nat. Immunol. **11**:785–97.

102. **Stoermer KA, Morrison TE**. 2011. Complement and viral pathogenesis. Virology **411**:362–373.

103. **Sarma JV, Ward PA**. 2010. The complement system. Cell Tissue Res. 227–235.

104. **Holers VM, Kulik L**. 2007. Complement receptor 2, natural antibodies and innate immunity: Inter-relationships in B cell selection and activation. Mol. Immunol. **44**:64–72.

105. **Dunkelberger JR, Song W-C**. 2010. Role and mechanism of action of complement in regulating T cell immunity. Mol. Immunol. **47**:2176–86.

106. **Sacks SH**. 2010. Complement fragments C3a and C5a: the salt and pepper of the immune response. Eur. J. Immunol. **40**:668–70.

107. **Tam JCH, Bidgood SR, McEwan WA, James LC**. 2014. Intracellular sensing of complement C3 activates cell autonomous immunity. Science (80-.). **345**:1256070.

108. **Vanderplasschen A, Mathew E, Hollinshead M, Sim RB, Smith GL**. 1998. Extracellular enveloped vaccinia virus is resistant to complement because of incorporation of host complement control proteins into its envelope. Proc. Natl. Acad. Sci. U. S. A. **95**:7544–9.

109. **Blasco R, Sisler JR, Moss B**. 1993. Dissociation of progeny vaccinia virus from the cell membrane is regulated by a viral envelope glycoprotein: effect of a point mutation in the lectin homology domain of the A34R gene. J. Virol. **67**:3319–25.

110. **McIntosh AA, Smith GL**. 1996. Vaccinia virus glycoprotein A34R is required for infectivity of extracellular enveloped virus. J. Virol. **70**.

111. **Law M, Smith GL**. 2001. Antibody neutralization of the extracellular enveloped form of vaccinia virus. Virology **280**:132–42.

112. **Benhnia MR-E-I, McCausland MM, Moyron J, Laudenslager J, Granger S, Rickert S, Koriazova L, Kubo R, Kato S, Crotty S**. 2009. Vaccinia virus extracellular enveloped virion neutralization in vitro and protection in vivo depend on complement. J. Virol. **83**:1201–15.

113. **Lustig S, Fogg C, Whitbeck JC, Moss B**. 2004. Synergistic neutralizing activities of antibodies to outer membrane proteins of the two infectious forms of vaccinia virus in the presence of complement. Virology **328**:30–5.

114. **Kotwal GJ, Isaacs SN, McKenzie R, Frank MM, Moss B**. 1990. Inhibition of the complement cascade by the major secretory protein of vaccinia virus. Science **250**:827–30.

115. **Girgis NM, Dehaven BC, Xiao Y, Alexander E, Viner KM, Isaacs SN**. 2011. The Vaccinia virus complement control protein modulates adaptive immune responses during infection. J. Virol. **85**:2547–56.

116. **Moulton EA, Atkinson JP, Buller RML**. 2008. Surviving mousepox infection requires the complement system. PLoS Pathog. **4**:e1000249.

117. **Leddy JP, Simons RL, Douglas RG**. 1977. Effect of Selective Complement Deficiency on the Rate of Neutralization of Enveloped Viruses by Human Sera. J. Immunol. **118**:28–34.

118. **Magge D, Guo ZS, O'Malley ME, Francis L, Ravindranathan R, Bartlett DL**. 2013. Inhibitors of C5 complement enhance vaccinia virus oncolysis. Cancer Gene Ther. **20**:342–50.

119. **Beebe DP, Cooper NR**. 1981. Neutralization of vesicular stomatitis virus (VSV) by human complement requires a natural IgM antibody present in human serum. J. Immunol. **126**:1562–8.

120. **Mills BJ, Beebe DP, Cooper NR**. 1979. Antibody-Independent Neutralization of Vesicular Stomatitis Virus by Human Complement : II . Formation of VSV-Lipoprotein Complexes in Human Serum and Complement-Dependent Viral Lysis. J. Immunol. **123**:2518–2524.

121. **Tesfay MZ, Ammayappan A, Federspiel MJ, Barber GN, Stojdl D, Peng K-W, Russell SJ**. 2014. Vesiculovirus neutralization by natural IgM and complement. J. Virol. **88**:6148–57.

122. **Ricklin D, Lambris JD**. 2013. Progress and Trends in Complement Therapeutics. Adv. Exp. Med. Biol. **735**:1–22.

123. **Ricklin D, Lambris JD**. 2013. Complement in immune and inflammatory disorders: therapeutic interventions. J. Immunol. **190**:3839–47.

124. **Vogel C-W, Fritzinger DC**. 2010. Cobra venom factor: Structure, function, and humanization for therapeutic complement depletion. Toxicon **56**:1198–222.

125. **Mulligan MS, Schmid E, Beck-Schimmer B, Till GO, Friedl HP, Brauer RB, Hugli TE, Miyasaka M, Warner RL, Johnson KJ, Ward PA**. 1996. Requirement and role of C5a in acute lung inflammatory injury in rats. J. Clin. Invest. **98**:503–12.

126. **Tagawa T**. 2011. Protease inhibitor nafamostat mesilate attenuates complement activation and improves function of xenografts in a discordant lung perfusion model. Xenotransplantation **18**:315–9.

127. **Inagi R, Miyata T, Maeda K, Sugiyama S, Miyama A, Nakashima I**. 1991. FUT-175 as a potent inhibitor of C5 / C3 convertase activity for production of C5a and C3a. Immunol. Lett. **27**:49–52.

128. **Issekutz AC, Roland DM, Patrick RA**. 1990. The effect of FUT-175 (nafamstat mesilate) on C3a, C4a and C5a generation in vitro and inflammatory reactions in vivo. Int. J. Immunopharmacol. **12**:1–9.

129. **Keck T, Balcom JH, Antoniu BA, Lewandrowski K, Warshaw AL, Castillo CF**. 2001. Regional effects of nafamostat, a novel potent protease and complement inhibitor, on severe necrotizing pancreatitis. Surgery **130**:175–181.

130. **Ricklin D, Lambris JD**. 2008. Compstatin: a complement inhibitor on its way to clinical application. Adv. Exp. Med. Biol. **632**:273–92.

131. **Janssen BJC, Halff EF, Lambris JD, Gros P**. 2007. Structure of compstatin in complex with complement component C3c reveals a new mechanism of complement inhibition. J. Biol. Chem. **282**:29241–7.

132. **Qu H, Ricklin D, Bai H, Chen H, Reis ES, Maciejewski M, Tzekou A, DeAngelis RA, Resuello RRG, Lupu F, Barlow PN, Lambris JD**. 2013. New analogs of the clinical complement inhibitor compstatin with subnanomolar affinity and enhanced pharmacokinetic properties. Immunobiology **218**:496–505.

133. **Risitano AM, Ricklin D, Huang Y, Reis ES, Chen H, Ricci P, Lin Z, Pascariello C, Raia M, Sica M, Vecchio L Del, Pane F, Lupu F, Notaro R, Resuello RRG, DeAngelis RA, Lambris JD**. 2014. Peptide inhibitors of C3 activation as a novel strategy of complement inhibition for the treatment of paroxysmal nocturnal hemoglobinuria. Blood **123**:2094–2101.

134. **Huber VC, Lynch JM, Bucher DJ, Le J, Metzger DW**. 2001. Fc Receptor-Mediated Phagocytosis Makes a Significant Contribution to Clearance of Influenza Virus Infections. J. Immunol. **166**:7381–7388.

135. **McEwan WA, Tam JCH, Watkinson RE, Bidgood SR, Mallery DL, James LC**. 2013. Intracellular antibody-bound pathogens stimulate immune signaling via the Fc receptor TRIM21. Nat. Immunol. **14**:327–36.

136. Smallpox Vaccine - Part 4 - Active Vaccines - Canadian Immunization Guide - Public Health Agency of Canada.

137. CDC Smallpox | FAQ About Smallpox Vaccine.

138. **Fulginiti VA, Papier A, Lane JM, Neff JM, Henderson DA**. 2003. Smallpox vaccination: a review, part I. Background, vaccination technique, normal vaccination and revaccination, and expected normal reactions. Clin. Infect. Dis. **37**:241–50.

139. **Hammarlund E, Lewis MW, Hansen SG, Strelow LI, Nelson J a, Sexton GJ, Hanifin JM, Slifka MK**. 2003. Duration of antiviral immunity after smallpox vaccination. Nat. Med. **9**:1131–7.

140. **Lawrence SJ, Lottenbach KR, Newman FK, Buller RML, Bellone CJ, Chen JJ, Cohen GH, Eisenberg RJ, Belshe RB, Stanley SL, Frey SE**. 2007. Antibody responses to vaccinia membrane proteins after smallpox vaccination. J. Infect. Dis. **196**:220–9.

141. **Adamo JE, Meseda CA, Weir JP, Merchlinsky MJ**. 2009. Smallpox vaccines induce antibodies to the immunomodulatory, secreted vaccinia virus complement control protein. J. Gen. Virol. **90**:2604–8.

142. **Benhnia MR-E-I, McCausland MM, Su H-P, Singh K, Hoffmann J, Davies DH, Felgner PL, Head S, Sette A, Garboczi DN, Crotty S**. 2008. Redundancy and plasticity of neutralizing antibody responses are cornerstone attributes of the human immune response to the smallpox vaccine. J. Virol. **82**:3751–68.

143. **Crotty S, Felgner P, Davies H, Glidewell J, Villarreal L, Ahmed R**. 2003. Cutting Edge: Long-Term B Cell Memory in Humans after Smallpox Vaccination. J. Immunol. **171**:4969–4973.

144. **el-Ad B, Roth Y, Winder a, Tochner Z, Lublin-Tennenbaum T, Katz E, Schwartz T**. 1990. The persistence of neutralizing antibodies after revaccination against smallpox. J. Infect. Dis. **161**:446–8.

145. **Nishimura C, Nomura M, Kitaoka M, Takeuchi Y, Kimura M**. 1968. Complement Antibody Requirement Appearing with Smallpox of the After Neutralizing Immunization Vaccine. Jpn. J. Microbiol. **12**:256–259.

146. **McCarthy K, Germer W.** 1952. Two heat-labile factors in normal sera which neutralize variola virus. Br. J. Exp. Pathol. **33**:529–536.

147. **Takabayashi K, Mcintosh K**. 1973. Effect of Heat-Labile Factors on the Neutralization of Vaccinia Virus by Human Sera. Infect. Immun. **8**:582–589.

148. **Reis JL, Mead D, Rodriguez LL, Brown CC**. 2009. Transmission and pathogenesis of vesicular stomatitis viruses. Brazilian J. Vet. Pathol. **2**:49–58.

149. **Tesh RB, Peralta PH, Johnson KM**. 1969. Ecologic Studies of Vesicular Stomatitis Virus. Am. J. Epidemiol. **90**:255–261.

150. **Rodriguez LL, Bunch TA, Fraire M, Llewellyn ZN**. 2000. Re-emergence of vesicular stomatitis in the western United States is associated with distinct viral genetic lineages. Virology **271**:171–81.

151. **Roberts A, Buonocore L, Price R, Rose JK, Forman J**. 1999. Attenuated Vesicular Stomatitis Viruses as Vaccine Vectors. J. Virol. **73**.

152. **Pinschewer DD, Perez M, Jeetendra E, Bächi T, Horvath E, Hengartner H, Whitt MA, Carlos J, Torre D, Zinkernagel RM**. 2004. Kinetics of protective antibodies are determined by the viral surface antigen. J. Clin. Invest. **114**:988–993.

153. **Power AT, Wang J, Falls TJ, Paterson JM, Parato KA, Lichty BD, Stojdl DF, Forsyth PAJ, Atkins H, Bell JC**. 2007. Carrier cell-based delivery of an oncolytic virus circumvents antiviral immunity. Mol. Ther. **15**:123–30.

154. **Tesfay MZ, Kirk AC, Hadac EM, Griesmann GE, Federspiel MJ, Barber GN, Henry SM, Peng K-W, Russell SJ**. 2013. PEGylation of vesicular stomatitis virus extends virus persistence in blood circulation of passively immunized mice. J. Virol. **87**:3752–9.

155. **Pauszek SJ, Barrera JDC, Goldberg T, Allende R, Rodriguez LL**. 2011. Genetic and antigenic relationships of vesicular stomatitis viruses from South America. Arch. Virol. **156**:1961–8.

156. **Sánchez-Puig JM, Sánchez L, Roy G, Blasco R**. 2004. Susceptibility of different leukocyte cell types to Vaccinia virus infection. Virol. J. **1**:10.

157. **Chahroudi A, Chavan R, Koyzr N, Waller EK, Silvestri G, Feinberg MB**. 2005. Vaccinia Virus Tropism for Primary Hematolymphoid Cells Is Determined by Restricted Expression of a Unique Virus Receptor. J. Virol. **79**:10397–10407.

158. **Yu Q, Jones B, Hu N, Chang H, Ahmad S, Liu J, Parrington M, Ostrowski M**. 2006. Comparative analysis of tropism between canarypox (ALVAC) and vaccinia viruses reveals a more restricted and preferential tropism of ALVAC for human cells of the monocytic lineage. Vaccine **24**:6376–91.

159. **Liu L, Chavan R, Feinberg MB**. 2008. Dendritic cells are preferentially targeted among hematolymphocytes by Modified Vaccinia Virus Ankara and play a key role in the induction of virus-specific T cell responses in vivo. BMC Immunol. **9**:15.

160. **Chahroudi A, Garber DA, Reeves P, Liu L, Kalman D, Feinberg MB**. 2006. Differences and similarities in viral life cycle progression and host cell physiology after infection of human dendritic cells with modified vaccinia virus Ankara and vaccinia virus. J. Virol. **80**:8469–81.

161. **Jenne L, Hauser C, Arrighi JF, Saurat JH, Hügin AW**. 2000. Poxvirus as a vector to transduce human dendritic cells for immunotherapy: abortive infection but reduced APC function. Gene Ther. **7**:1575–83.

162. **Drillien R, Spehner D, Bohbot a, Hanau D**. 2000. Vaccinia virus-related events and phenotypic changes after infection of dendritic cells derived from human monocytes. Virology **268**:471–81.

163. **Engelmayer J, Larsson M, Subklewe M, Chahroudi A, Cox WI, Steinman RM, Bhardwaj N**. 1999. Vaccinia virus inhibits the maturation of human dendritic cells: a novel mechanism of immune evasion. J. Immunol. **163**:6762–8.

164. **Humlová Z, Vokurka M, Esteban M, Melková Z**. 2002. Vaccinia virus induces apoptosis of infected macrophages. J. Gen. Virol. **83**:2821–32.

165. **Yates NL, Yammani RD, Alexander-Miller MA**. 2008. Dose-dependent lymphocyte apoptosis following respiratory infection with Vaccinia virus. Virus Res. **137**:198–205.

166. **West BC, Escheté ML, Cox ME, King JW**. 1987. Neutrophil uptake of vaccinia virus in vitro. J. Infect. Dis. **156**:597–606.

167. **Ilett EJ, Bárcena M, Errington-Mais F, Griffin S, Harrington KJ, Pandha HS, Coffey M, Selby PJ, Limpens RW a L, Mommaas M, Hoeben RC, Vile RG, Melcher AA**. 2011. Internalization of oncolytic reovirus by human dendritic cell carriers protects the virus from neutralization. Clin. Cancer Res. **17**:2767–76.

168. **Ilett EJ, Prestwich RJ, Kottke T, Errington F, Thompson JM, Harrington KJ, Pandha HS, Coffey M, Selby PJ, Vile RG, Melcher AA**. 2009. Dendritic cells and T cells deliver oncolytic reovirus for tumour killing despite pre-existing anti-viral immunity. Gene Ther. **16**:689–99.

169. **Adair RA, Roulstone V, Scott KJ, Morgan R, Nuovo GJ, Fuller M, Beirne D, West EJ, Jennings VA, Rose A, Kyula J, Fraser S, Dave R, Anthoney DA, Merrick A, Prestwich R, Aldouri A, Donnelly O, Pandha H, Coffey M, Selby P, Vile R, Toogood G, Harrington K, Melcher AA**. 2012. Cell carriage, delivery, and selective replication of an oncolytic virus in tumor in patients. Sci. Transl. Med. **4**:138ra77.

170. **Carlisle RC, Di Y, Cerny AM, Sonnen AF-P, Sim RB, Green NK, Subr V, Ulbrich K, Gilbert RJC, Fisher KD, Finberg RW, Seymour LW**. 2009. Human erythrocytes bind and inactivate type 5 adenovirus by presenting Coxsackie virus-adenovirus receptor and complement receptor 1. Blood **113**:1909–18.

171. **Wang Y, Yuan F**. 2006. Delivery of viral vectors to tumor cells: extracellular transport, systemic distribution, and strategies for improvement. Ann. Biomed. Eng. **34**:114–27.

172. **Miller AC, Russell SJ**. 2014. Heterogeneous delivery is a barrier to the translational advancement of oncolytic virotherapy for treating solid tumors. Virus Adapt. Treat. **6**:11–31.

173. **Smith E, Breznik J, Lichty BD**. 2011. Strategies to enhance viral penetration of solid tumors. Hum. Gene Ther. **22**:1053–60.

174. **Pio R, Ajona D, Lambris JD**. 2013. Complement inhibition in cancer therapy. Semin. Immunol. **25**:54–64.

175. **Li J, Orlandi R, White CN, Rosenzweig J, Zhao J, Seregni E, Morelli D, Yu Y, Meng X-Y, Zhang Z, Davidson NE, Fung ET, Chan DW**. 2005. Independent validation of candidate breast cancer serum biomarkers identified by mass spectrometry. Clin. Chem. **51**:2229–35.

176. **Fentz A-K, Spörl M, Spangenberg J, List HJ, Zornig C, Dörner A, Layer P, Juhl H, David KA**. 2007. Detection of colorectal adenoma and cancer based on transthyretin and C3a-desArg serum levels. Proteomics. Clin. Appl. **1**:536–44.

177. **Chung L, Moore K, Phillips L, Boyle FM, Marsh DJ, Baxter RC**. 2014. Novel serum protein biomarker panel revealed by mass spectrometry and its prognostic value in breast cancer. Breast Cancer Res. **16**:R63.

178. **Bjørge L, Hakulinen J, Vintermyr OK, Jarva H, Jensen TS, Iversen OE, Meri S**. 2005. Ascitic complement system in ovarian cancer. Br. J. Cancer **92**:895–905.

179. **Markiewski MM, DeAngelis RA, Benencia F, Ricklin-Lichtsteiner SK, Koutoulaki A, Gerard C, Coukos G, Lambris JD**. 2008. Modulation of the antitumor immune response by complement. Nat. Immunol. **9**:1225–35.

180. **Nozaki M, Raisler BJ, Sakurai E, Sarma JV, Barnum SR, Lambris JD, Chen Y, Zhang K, Ambati BK, Baffi JZ, Ambati J**. 2006. Drusen complement components C3a and C5a promote choroidal neovascularization. Proc. Natl. Acad. Sci. U. S. A. **103**:2328–33.

181. **Nunez-Cruz S, Gimotty PA, Guerra MW, Connolly DC, Wu Y, Deangelis RA, Lambris JD, Coukos G, Scholler N**. 2012. Genetic and Pharmacologic Inhibition of Complement Impairs Endothelial Cell Function and Ablates Ovarian Cancer Neovascularization. Neoplasia **14**:994–1004, IN1.

182. **Niculescu F, Rus H, Biesen T Van, Shin ML**. 1997. Activation of Ras and Mitogen-Activated Protein Kinase Pathway by Terminal Complement Complexes is. J. Immunol. **158**:4405–4412.

183. **Cho MS, Vasquez HG, Rupaimoole R, Pradeep S, Wu S, Zand B, Han H-D, Rodriguez-Aguayo C, Bottsford-Miller J, Huang J, Miyake T, Choi H-J, Dalton HJ, Ivan C, Baggerly K, Lopez-Berestein G, Sood AK, Afshar-Kharghan V**. 2014. Autocrine effects of tumor-derived complement. Cell Rep. **6**:1085–95.

184. **Fisher KD, Seymour LW**. 2010. HPMA copolymers for masking and retargeting of therapeutic viruses. Adv. Drug Deliv. Rev. **62**:240–5.

185. **Green NK, Herbert CW, Hale SJ, Hale a B, Mautner V, Harkins R, Hermiston T, Ulbrich K, Fisher KD, Seymour LW**. 2004. Extended plasma circulation time and decreased toxicity of polymer-coated adenovirus. Gene Ther. **11**:1256–63.

186. **Miest TS, Yaiw K-C, Frenzke M, Lampe J, Hudacek AW, Springfeld C, von Messling V, Ungerechts G, Cattaneo R**. 2011. Envelope-chimeric entry-targeted measles virus escapes neutralization and achieves oncolysis. Mol. Ther. **19**:1813–20.

187. **Hangartner L, Zinkernagel RM, Hengartner H**. 2006. Antiviral antibody responses: the two extremes of a wide spectrum. Nat. Rev. Immunol. **6**:231–43.

188. **Tober R, Banki Z, Egerer L, Muik A, Behmüller S, Kreppel F, Greczmiel U, Oxenius A, von Laer D, Kimpel J**. 2014. VSV-GP: a potent viral vaccine vector that boosts the immune response upon repeated applications. J. Virol. **88**:4897–907.

189. **Roy DG, Bell JC**. 2013. Cell carriers for oncolytic viruses : current challenges and future directions. Oncolytic Virotherapy **2103**:47–56.

190. **Liu C, Russell SJ, Peng K-W**. 2010. Systemic therapy of disseminated myeloma in passively immunized mice using measles virus-infected cell carriers. Mol. Ther. **18**:1155–64.

191. **Qiao J, Wang H, Kottke T, Diaz RM, Willmon C, Hudacek A, Thompson J, Parato K, Bell J, Naik J, Chester J, Selby P, Harrington K, Melcher A, Vile RG**. 2008. Loading of oncolytic vesicular stomatitis virus onto antigen-specific T cells enhances the efficacy of adoptive T-cell therapy of tumors. Gene Ther. **15**:604–16.

192. **Thorne SH, Negrin RS, Contag CH**. 2006. Synergistic Antitumor Effects of Immune Cell-Viral Biotherapy. Science (80-.). **311**:1780–1784.

193. **Mader EK, Maeyama Y, Lin Y, Butler GW, Russell HM, Galanis E, Russell SJ, Dietz AB, Peng K-W**. 2009. Mesenchymal stem cell carriers protect oncolytic measles viruses from antibody neutralization in an orthotopic ovarian cancer therapy model. Clin. Cancer Res. **15**:7246–55.

194. **Peng K-W, Myers R, Greenslade a, Mader E, Greiner S, Federspiel MJ, Dispenzieri a, Russell SJ**. 2013. Using clinically approved cyclophosphamide regimens to control the humoral immune response to oncolytic viruses. Gene Ther. **20**:255–61.

195. **Ikeda K, Wakimoto H, Ichikawa T, Hochberg FH, Louis DN, Antonio E**. 2000. Complement Depletion Facilitates the Infection of Multiple Brain Tumors by an Herpes Simplex Virus Mutant. J. Virol. **74**:4765–4775.

196. **Qiao J, Wang H, Kottke T, White C, Twigger K, Diaz RM, Thompson J, Selby P, de Bono J, Melcher AA, Pandha H, Coffey M, Vile R, Harrington K**. 2008. Cyclophosphamide facilitates antitumor efficacy against subcutaneous tumors following intravenous delivery of reovirus. Clin. Cancer Res. **14**:259–69.

197. **Nguyen A, Ho L, Wan Y**. 2014. Chemotherapy and Oncolytic Virotherapy: Advanced Tactics in the War against Cancer. Front. Oncol. **4**:145.

198. **Guo ZS, Parimi V, O'Malley ME, Thirunavukarasu P, Sathaiah M, Austin F, Bartlett DL**. 2010. The combination of immunosuppression and carrier cells significantly enhances the efficacy of oncolytic poxvirus in the pre-immunized host. Gene Ther. 1–11.

199. **Guse K, Sloniecka M, Diaconu I, Ottolino-Perry K, Tang N, Ng C, Le Boeuf F, Bell JC, McCart JA, Ristimäki A, Pesonen S, Cerullo V, Hemminki A**.

2010. Antiangiogenic arming of an oncolytic vaccinia virus enhances antitumor efficacy in renal cell cancer models. J. Virol. **84**:856–66.

200. **Sanfilippo CM, Blaho JA**. 2006. ICP0 gene expression is a herpes simplex virus type 1 apoptotic trigger. J. Virol. **80**:6810–21.

201. **Sobol PT, Boudreau JE, Stephenson K, Wan Y, Lichty BD, Mossman KL**. 2011. Adaptive antiviral immunity is a determinant of the therapeutic success of oncolytic virotherapy. Mol. Ther. **19**:335–44.

202. **Zhao H, Wakamiya N, Suzuki Y, Hamonko MT, Stahl GL**. 2002. Identification of human mannose binding lectin (MBL) recognition sites for novel inhibitory antibodies. Hybrid. Hybridomics **21**:25–36.

203. **Thurman JM, Kraus DM, Girardi G, Hourcade D, Kang HJ, Royer PA, Mitchell LM, Giclas PC, Salmon J, Gilkeson G, Holers VM**. 2005. A novel inhibitor of the alternative complement pathway prevents antiphospholipid antibody-induced pregnancy loss in mice. Mol. Immunol. **42**:87–97.

204. **Walsh MC, Shaffer LA, Guikema BJ, Body SC, Shernan SK, Fox AA, Collard CD, Fung M, Taylor RP, Stahl GL**. 2007. Fluorochrome-linked immunoassay for functional analysis of the mannose binding lectin complement pathway to the level of C3 cleavage. J. Immunol. Methods **323**:147–59.

205. **Bexborn F, Engberg AE, Sandholm K, Mollnes TE, Hong J, Nilsson Ekdahl K**. 2009. Hirudin versus heparin for use in whole blood in vitro biocompatibility models. J. Biomed. Mater. Res. A **89**:951–9.

206. **Meseda CA, Garcia AD, Kumar A, Mayer AE, Manischewitz J, King LR, Golding H, Merchlinsky M, Weir JP**. 2005. Enhanced immunogenicity and protective effect conferred by vaccination with combinations of modified vaccinia virus Ankara and licensed smallpox vaccine Dryvax in a mouse model. Virology **339**:164–75.

207. **Greenhalgh CJ, Hilton DJ**. 2001. Negative regulation of cytokine signaling **70**:348–356.

208. **Sherwood L**. 2011. Fundamentals of Human Physiology.

209. **White CL, Twigger KR, Vidal L, De Bono JS, Coffey M, Heinemann L, Morgan R, Merrick A, Errington F, Vile RG, Melcher AA, Pandha HS, Harrington KJ**. 2008. Characterization of the adaptive and innate immune response to intravenous oncolytic reovirus (Dearing type 3) during a phase I clinical trial. Gene Ther. **15**:911–20.

210. **Muik A, Stubbert LJ, Jahedi RZ, Geiβ Y, Kimpel J, Dold C, Tober R, Volk A, Klein S, Dietrich U, Yadollahi B, Falls T, Miletic H, Stojdl D, Bell JC, von Laer D**. 2014. Re-engineering Vesicular Stomatitis Virus to Abrogate Neurotoxicity, Circumvent Humoral Immunity, and Enhance Oncolytic Potency. Cancer Res. **74**:3567–78.

211. **Isaacs SN, Kotwal GJ, Moss B**. 1992. Vaccinia virus complement-control protein prevents antibody-dependent complement-enhanced neutralization of infectivity and contributes to virulence. Proc. Natl. Acad. Sci. U. S. A. **89**:628–32.

212. **Czajkowsky DM, Shao Z**. 2009. The human IgM pentamer is a mushroom-shaped molecule with a flexural bias. Proc. Natl. Acad. Sci. U. S. A. **106**:14960–5.

213. **Collins C, Tsui FWL, Shulman MJ**. 2002. Differential activation of human and guinea pig complement by pentameric and hexameric IgM. Eur. J. Immunol. **32**:1802–10.

214. **Diebolder CA, Beurskens FJ, de Jong RN, Koning RI, Strumane K, Lindorfer MA, Voorhorst M, Ugurlar D, Rosati S, Heck AJR, van de Winkel JGJ, Wilson IA, Koster AJ, Taylor RP, Saphire EO, Burton DR, Schuurman J, Gros P, Parren PWHI**. 2014. Complement is activated by IgG hexamers assembled at the cell surface. Science (80-.). **343**:1260–3.

215. **Mollnes TE, Garred P, Bergseth G**. 1988. Effect of time, temperature and anticoagulants on in vitro complement activation: consequences for collection and preservation of samples to be examined for complement activation. Clin. Exp. Immunol. **73**:484–8.

216. **Qu H, Magotti P, Ricklin D, Wu EL, Kourtzelis I, Wu Y-Q, Kaznessis YN, Lambris JD**. 2011. Novel analogues of the therapeutic complement inhibitor compstatin with significantly improved affinity and potency. Mol. Immunol. **48**:481–9.

217. **Werle M, Bernkop-Schnürch A**. 2006. Strategies to improve plasma half life time of peptide and protein drugs. Amino Acids **30**:351–67.

218. **Haas P-J, van Strijp J**. 2007. Anaphylatoxins Their Role in Bacterial Infection and Inlammation. Immunol. Res. **37**:161–175.

219. **Klos A, Tenner AJ, Johswich K-O, Ager RR, Reis ES, Köhl J**. 2009. The role of the anaphylatoxins in health and disease. Mol. Immunol. **46**:2753–66.

220. **Cazander G, Jukema GN, Nibbering PH**. 2012. Complement activation and inhibition in wound healing. Clin. Dev. Immunol. **2012**:534291.

221. **Martel C, Granger CB, Ghitescu M, Stebbins A, Fortier A, Armstrong PW, Bonnefoy A, Theroux P**. 2012. Pexelizumab fails to inhibit assembly of the terminal complement complex in patients with ST-elevation myocardial infarction undergoing primary percutaneous coronary intervention. Insight from a substudy of the Assessment of Pexelizumab in Acute Myocardia. Am. Heart J. **164**:43–51.

222. **Ong GL, Mattes MJ**. 1989. Mouse strains with typical mammalian levels of complement activity. J. Immunol. Methods **125**:147–58.

223. **Ebanks RO, Isenman DE**. 1996. Mouse complement component C4 is devoid of classical pathway C5 convertase subunit activity. Mol. Immunol. **33**:297–309.

224. **Ratelade J, Verkman AS**. 2014. Inhibitor(s) of the classical complement pathway in mouse serum limit the utility of mice as experimental models of neuromyelitis optica. Mol. Immunol. **62**:104–113.

225. **Kaever T, Meng X, Matho MH, Schlossman A, Li S, Sela-Culang I, Ofran Y, Buller M, Crump RW, Parker S, Frazier A, Crotty S, Zajonc DM, Peters B, Xiang Y**. 2014. Potent neutralization of vaccinia virus by divergent murine antibodies targeting a common site of vulnerability in L1 protein. J. Virol. **88**:11339–55.

226. **Owens DE, Peppas NA**. 2006. Opsonization, biodistribution, and pharmacokinetics of polymeric nanoparticles. Int. J. Pharm. **307**:93–102.

227. **He JQ, Wiesmann C, van Lookeren Campagne M**. 2008. A role of macrophage complement receptor CRIg in immune clearance and inflammation. Mol. Immunol. **45**:4041–7.

228. **Reinagel ML, Taylor RP**. 2000. Transfer of Immune Complexes from Erythrocyte CR1 to Mouse Macrophages. J. Immunol. **164**:1977–1985.

229. **Mebius RE, Kraal G**. 2005. Structure and function of the spleen. Nat. Rev. Immunol. **5**:606–16.

230. **Den Haan JMM, Kraal G**. 2012. Innate immune functions of macrophage subpopulations in the spleen. J. Innate Immun. **4**:437–45.

231. **Jenne CN, Kubes P**. 2013. Immune surveillance by the liver. Nat. Immunol. **14**:996–1006.

232. **Helmy KY, Katschke KJ, Gorgani NN, Kljavin NM, Elliott JM, Diehl L, Scales SJ, Ghilardi N, van Lookeren Campagne M**. 2006. CRIg: a macrophage complement receptor required for phagocytosis of circulating pathogens. Cell **124**:915–27.

233. **Jacobson AC, Weis JH**. 2008. Comparative Functional Evolution of Human and Mouse CR1 and CR2. J. Immunol. **181**:2953–2959.

234. **Alexander JJ, Hack BK, Cunningham PN, Quigg RJ**. 2001. A protein with characteristics of factor H is present on rodent platelets and functions as the immune adherence receptor. J. Biol. Chem. **276**:32129–35.

235. **Reagan-Shaw S, Nihal M, Ahmad N**. 2008. Dose translation from animal to human studies revisited. FASEB J. **22**:659–61.

236. **Barbee WR, Perry BD, Re N, Murgo P**. 1992. Microsphere and dilution techniques for the determination of blood flows and volumes in conscious mice. Am. J. Physiol. **263**:R728–733.

237. **Delp MD, Evans M V, Duan C, Hanna MA, Taylor CR, Chen B, La H, Maraj JJ, Kilar CR, Behnke J, Muller-delp JM, Lundquist P, Lööf J, Floby E, Johansson J, Bylund J, Hoogstraate J, Afzelius L, Andersson TB, Iii RTD, Stabley JN, Ii JMD, Ramsey MW, Danielle J, Lesniewski LA, Behnke BJ**. 1998. Effects of aging on cardiac output, regional blood flow, and body composition in Fischer-344 rats. J. Appl. Physiol. **85**:1813–1822.

238. **Gjedde SB, Gjeode A**. 1980. Organ blood flow rates and cardiac output of the BALB/c mouse. Comp. Biochem. Physiol. Part A Physiol. **67**:671–674.

239. **Takagi G, Asai K, Vatner SF, Kudej RK, Rossi F, Peppas A, Takagi I, Resuello RRG, Natividad F, Shen Y, Vatner DE**. 2003. Gender differences on the effects of aging on cardiac and peripheral adrenergic stimulation in old conscious monkeys. Am. J. Physiol. Heart Circ. Physiol. **285**:H527–534.

240. **Lee HB, Blaufox MD**. 1985. Blood Volume in the Rat The estimation of blood volume is important in studies. J. Nucl. Med. **26**:72–76.

241. **Ageyama N, Shibata H, Narita H, Hanari K, Kohno A, Ono F, Yoshikawa Y TK**. 2001. Specific gravity of whole blood in cynomolgus monkeys (Macaca fascicularis), squirrel monkeys (Saimiri sciureus), and tamarins (Saguinus labiatus) and total blood volume in cynomolgus monkeys. Contemp. Top. Lab. Anim. Sci. **40**:33–35.

242. **Kratz A, Ferraro M, Sluss PM, Lewandrowski KB**. 2004. Laboratory Reference Values. N. Engl. J. Med. **351**:1548–1563.

243. 1984. Baseline Hematology and Clinical Chemistry Values for Charles River Fischer344 Rats-CDF ® (F-344) CrlBR as a Function of Sex and Age Baseline Hematology and Clinical Chemistry Values for Charles River Fischer344 Rats-CDF ® (F-344) CrlBR as a Function. Charles River.

244. 2007. Physiological Data Summary - BALB / cJ (000651). The Jackson Laboratory.

245. **Wang H, Niu YY, Si W, Li YJ, Yan Y**. 2012. Reference data of clinical chemistry , haematology and blood coagulation parameters in juvenile cynomolgus monkeys (Macaca fascicularis). Vet. Med. (Praha). **57**:233–238.

246. **Pinkel D**. 1958. The Use of Body Surface Area as a Criterion of Drug Dosage in Cancer Chemotherapy The Use of Body Surface Area as a Criterion of Drug Dosage in Cancer Chemotherapy. Cancer Res. **18**:853–856.

247. **Pecora AL, Rizvi NR, Cohen GI, Meropol NJ, Sterman D, Marshall JL, Goldberg S, Gross P, O'Neil JD, Groene WS, Roberts MS, Rabin H, Bamat MK, Lorence RM**. 2002. Phase I Trial of Intravenous Administration of PV701, an Oncolytic Virus, in Patients With Advanced Solid Cancers. J. Clin. Oncol. **20**:2251–2266.

248. **Hotte SJ, Lorence RM, Hirte HW, Polawski SR, Bamat MK, O'Neil JD, Roberts MS, Groene WS, Major PP**. 2007. An optimized clinical regimen for the oncolytic virus PV701. Clin. Cancer Res. **13**:977–85.

249. **Lorence RM, Roberts MS, Neil JDO, Groene WS, Miller JA, Mueller SN, Bamat MK**. 2007. Phase 1 Clinical Experience Using Intravenous Administration of PV701, an Oncolytic Newcastle Disease Virus. Curr. Cancer Drug Targets 157–167.

250. **McClain DJ, Harrison S, Yeager CL, Cruz J, Ennis FA, Gibbs P, Wright MS, Summers PL, Arthur JD, Graham JA**. 1997. Immunologic Responses to Vaccinia Vaccines Administered by Different Parenteral Routes. J. Infect. Dis. **175**:756–763.

251. **Andrew ME, Coupar BE, Boyle DB**. 1989. Humoral and cell-mediated immune responses to recombinant vaccinia viruses in mice. Immunol. Cell Biol. **67**:331–7.

252. **Ovsyannikova IG, Vierkant RA, Pankratz VS, Jacobson RM, Poland GA**. 2011. Human leukocyte antigen genotypes in the genetic control of adaptive immune responses to smallpox vaccine. J. Infect. Dis. **203**:1546–55.

253. **Carroll MC**. 2000. The role of complement in B cell activation and tolerance. Adv. Immunol. **74**:61–88.

254. **Da Costa XJ, Brockman MA, Alicot E, Ma M, Fischer MB, Zhou X, Knipe DM, Carroll MC**. 1999. Humoral response to herpes simplex virus is complement-dependent. Proc. Natl. Acad. Sci. **96**:12708–12712.

255. **Gonzalez SF, Jayasekera JP, Carroll MC**. 2008. Complement and natural antibody are required in the long-term memory response to influenza virus. Vaccine **26**:I86–I93.

256. **Moss B**. 2011. Smallpox vaccines: targets of protective immunity. Immunol. Rev. **239**:8–26.

257. **Jiang X, Clark RA, Liu L, Wagers AJ, Fuhlbrigge RC, Kupper TS**. 2012. Skin infection generates non-migratory memory CD8+ T(RM) cells providing global skin immunity. Nature **483**:227–31.

258. **Georgopoulos LJ, Elgue G, Sanchez J, Dussupt V, Magotti P, Lambris JD, Tötterman TH, Maitland NJ, Nilsson B**. 2009. Preclinical evaluation of innate immunity to baculovirus gene therapy vectors in whole human blood. Mol. Immunol. **46**:2911–7.

259. **Zhu J, Martinez J, Huang X, Yang Y**. 2007. Innate immunity against vaccinia virus is mediated by TLR2 and requires TLR-independent production of IFN-beta. Blood **109**:619–25.

260. **Cohen JI, Hohman P, Fulton R, Turk S-P, Qin J, Thatcher K, Hornung RL**. 2010. Kinetics of serum cytokines after primary or repeat vaccination with the smallpox vaccine. J. Infect. Dis. **201**:1183–91.

261. **Krebs DL, Hilton DJ**. 2001. SOCS Proteins: Negative Regulators of Cytokine Signaling. Stem Cells **19**:378–387.

262. **Croker BA, Krebs DL, Zhang J-G, Wormald S, Willson TA, Stanley EG, Robb L, Greenhalgh CJ, Förster I, Clausen BE, Nicola NA, Metcalf D, Hilton DJ, Roberts AW, Alexander WS**. 2003. SOCS3 negatively regulates IL-6 signaling in vivo. Nat. Immunol. **4**:540–5.

263. **Chung C-S, Chen Y, Ayala A**. 2008. Suppressor of cytokine signaling (SOCS)-1 but not SOCS-3 inhibits MCP-1 production in mouse lung epithelial cells. FASEB J. **22**.

264. **Qin H, Niyongere SA, Lee SJ, Baker BJ, Benveniste EN**. 2008. Expression and Functional Significance of SOCS-1 and SOCS-3 in Astrocytes. J. Immunol. **181**:3167–3176.

265. **Pattison MJ, MacKenzie KF, Elcombe SE, Arthur JSC**. 2013. IFNβ autocrine feedback is required to sustain TLR induced production of MCP-1 in macrophages. FEBS Lett. **587**:1496–503.

266. **Fenner JE, Starr R, Cornish AL, Zhang J-G, Metcalf D, Schreiber RD, Sheehan K, Hilton DJ, Alexander WS, Hertzog PJ**. 2006. Suppressor of

cytokine signaling 1 regulates the immune response to infection by a unique inhibition of type I interferon activity. Nat. Immunol. **7**:33–9.

267. **Inagaki-Ohara K, Kondo T, Ito M, Yoshimura A**. 2013. SOCS, inflammation, and cancer. JAK-STAT **2**.

268. **Jennings VA, Ilett EJ, Scott KJ, West EJ, Vile R, Pandha H, Harrington K, Young A, Hall GD, Coffey M, Selby P, Errington-Mais F, Melcher A**. 2014. Lymphokine-activated killer and dendritic cell carriage enhances oncolytic reovirus therapy for ovarian cancer by overcoming antibody neutralization in ascites. Int. J. Cancer **134**:1091–101.

269. **Ilett E, Kottke T, Donnelly O, Thompson J, Willmon C, Diaz R, Zaidi S, Coffey M, Selby P, Harrington K, Pandha H, Melcher A, Vile R**. 2014. Cytokine conditioning enhances systemic delivery and therapy of an oncolytic virus. Mol. Ther. **22**:1851–63.

270. **Hook LM, Lubinski JM, Jiang M, Michael K, Friedman HM, Pangburn MK**. 2006. Herpes Simplex Virus Type 1 and 2 Glycoprotein C Prevents Complement-Mediated Neutralization Induced by Natural Immunoglobulin M Antibody Herpes Simplex Virus Type 1 and 2 Glycoprotein C Prevents Complement-Mediated Neutralization Induced by Natural Immun. J. Virol. **80**:4038–4046.

271. **Selb B, Weber B**. 1994. A study of human reovirus IgG and IgA antibodies by ELISA and Western blot. J. Virol. Methods **47**:15–25.

272. **Tai JH, Williams J V, Edwards KM, Wright PF, Crowe JE, Dermody TS**. 2005. Prevalence of reovirus-specific antibodies in young children in Nashville, Tennessee. J. Infect. Dis. **191**:1221–4.

273. **Tam JCH, Bidgood SR, McEwan WA, James LC**. 2014. Intracellular sensing of complement C3 activates cell autonomous immunity. Science (80-.). **345**:1256070–1256070.

274. **Eschli B, Zellweger RM, Wepf A, Lang KS, Quirin K, Weber J, Zinkernagel RM, Hengartner H**. 2007. Early antibodies specific for the neutralizing epitope on the receptor binding subunit of the lymphocytic choriomeningitis virus glycoprotein fail to neutralize the virus. J. Virol. **81**:11650–7.

275. **Roost H-P, Bachmann MF, Haag A, Kalinke U, Pliska V, Hengartner H, Zinkernagel RM**. 1995. Early high-affinity neutralizing anti-viral IgG responses without further overall improvements of affinity. Proc. Natl. Acad. Sci. **92**:1257–1261.

276. **Kalinke U, Bucher EM, Ernst B, Oxenius A, Roost H-P, Geley S, Kofler R, Zinkernagel RM, Hengartner H**. 1996. The Role of Somatic Mutation in the

Generation of the Protective Humoral Immune Response against Vesicular Stomatitis Virus. Immunity **5**:639–652.

277. **Zapata JC, Pauza CD, Djavani MM, Rodas JD, Moshkoff D, Bryant J, Ateh E, Garcia C, Lukashevich IS, Salvato MS**. 2011. Lymphocytic choriomeningitis virus (LCMV) infection of macaques: a model for Lassa fever. Antiviral Res. **92**:125–38.

278. **Oehen S, Hengartner H, Zinkernagel RM**. 1991. Vaccination for disease. Science (80-.). **251**:195–198.

279. **Fisher-Hoch S, Hutwagner L, Brown B, McCormick J**. 2000. Effective Vaccine for Lassa Fever. J. Virol. **74**.

280. **Knust B, Ströher U, Edison L, Albariño CG, Lovejoy J, Armeanu E, House J, Cory D, Horton C, Fowler KL, Austin J, Poe J, Humbaugh KE, Guerrero L, Campbell S, Gibbons A, Reed Z, Cannon D, Manning C, Petersen B, Metcalf D, Marsh B, Nichol ST, Rollin PE**. 2014. Lymphocytic Choriomeningitis Virus in Employees and Mice at Multipremises Feeder-Rodent. Emerg. Infect. Dis. **20**.

281. **Mercer J, Helenius A**. 2009. Virus entry by macropinocytosis. Nat. Cell Biol. **11**:510–520.

282. **Roche S, Bressanelli S, Rey FA, Gaudin Y**. 2006. Crystal structure of the low-pH form of the vesicular stomatitis virus glycoprotein G. Science **313**:187–91.

283. **Roche S, Rey FA, Gaudin Y, Bressanelli S**. 2007. Structure of the prefusion form of the vesicular stomatitis virus glycoprotein G. Science **315**:843–8.

284. **Carneiro FA, Ferradosa AS, Da Poian AT**. 2001. Low pH-induced Conformational Changes in Vesicular Stomatitis Virus Glycoprotein Involve Dramatic Structure Reorganization Low pH-induced Conformational Changes in Vesicular Stomatitis Virus Glycoprotein Involve Dramatic Structure Reorganization. J. Biol. Chem. **276**:62–67.

285. **Rojek JM, Perez M, Kunz S**. 2008. Cellular entry of lymphocytic choriomeningitis virus. J. Virol. **82**:1505–17.

286. **Di Simone C, Zandonatti MA, Buchmeier MJ**. 1994. Acidic pH Triggers LCMV Membrane Fusion Activity and Conformational Change in the Glycoprotein Spike.pdf. Virology **198**:455–465.

287. **Nagata S, Okamoto Y, Inoue T, Ueno Y, Kurata T, Chiba J**. 1992. Identification of epitopes associated with different biological activities on the glycoprotein of vesicular stomatitis virus by use of monoclonal antibodies. Arch. Virol. **127**:153–168.

Contributions of collaborators

Dr. John Lambris provided the CP40 used throughout the study. Dr. Gregory Stahl and Margaret Morrissey provided the P1H10 mouse anti-human C1q and mouse anti-human 3F8 antibodies and performed the manan-binding assay in Figure 3.4F. Dr. Joshua Thurman provided the 1379 mouse-anti human Factor B antibody. Catherine Fortin and aided in the development of the REB protocols. Julie Wells consented patients for the use of unused serum for the experiment in Figure 3.2D. Theresa Falls and Christiano Tanese de Souza aided in all the mouse and rat experiments, respectively. Kim Yates performed the cardiac punctures in the rats for the experiments shown in Figures 3.6, 3.7,3.9, 3.26 and 3.27. The neutralization assays shown in Figure 3.11A and B were performed by Dr. Sergio Acuna. Dominique Vaillant aided in the production of the virus used in the NHP experiment. The NHP experiment was performed with the help of Dr. Sergio Acuna, Dr. David Hanwell, Dr. Alyssa Goldstein, Roberto Lopez, Sandra Lafrance and Stacy Avery. The cytokine array in Figure 3.19, 3.20 and Appendix Figure 3 was performed by the Genomics Centre. The isolations of cells from which virus was quantified in Figure 3.22 was aided by Anu Ananth and Jiqing Zhang. Dr. Nicole Forbes grew and titered the reovirus and measles Edmonston virus used in Figure 3.25. Dr. Fabrice LeBoef grew and titered the virus used in Figure 3.25. Dr. Lawton Stubbert grew the virus used in experiments 3.26, 3.27 and 3.28 and performed the experiment in Figure 3.26B. Dr. Scott Findlay aided in performing statistical analyses with R.

Appendices

Appendix I- Additional Figures

Appendix Figure 1. Additional data for an animal initially treated to validate the dose

Vaccinia virus (1 x 10^8 pfu) was infused using a venous line over the course of 30 minutes. As per the treatment schedule in (A) The animals received a bolus intravenous dose of CP40 (2mg/kg) immediately prior to virus treatment as the first of the two doses in the immune state. Infectious virus in the blood was measured by plaque assay on samples taken at various time points after the end of the infusion (EOI). Blood titers for for the naïve time point (B) and the immune time points (C) and are represented as technical replicate means ±SD. Genome concentrations in the blood are shown for only the immune time point and data is represented as technical replicate means ±SD ND, not detected, LOD, limit of detection

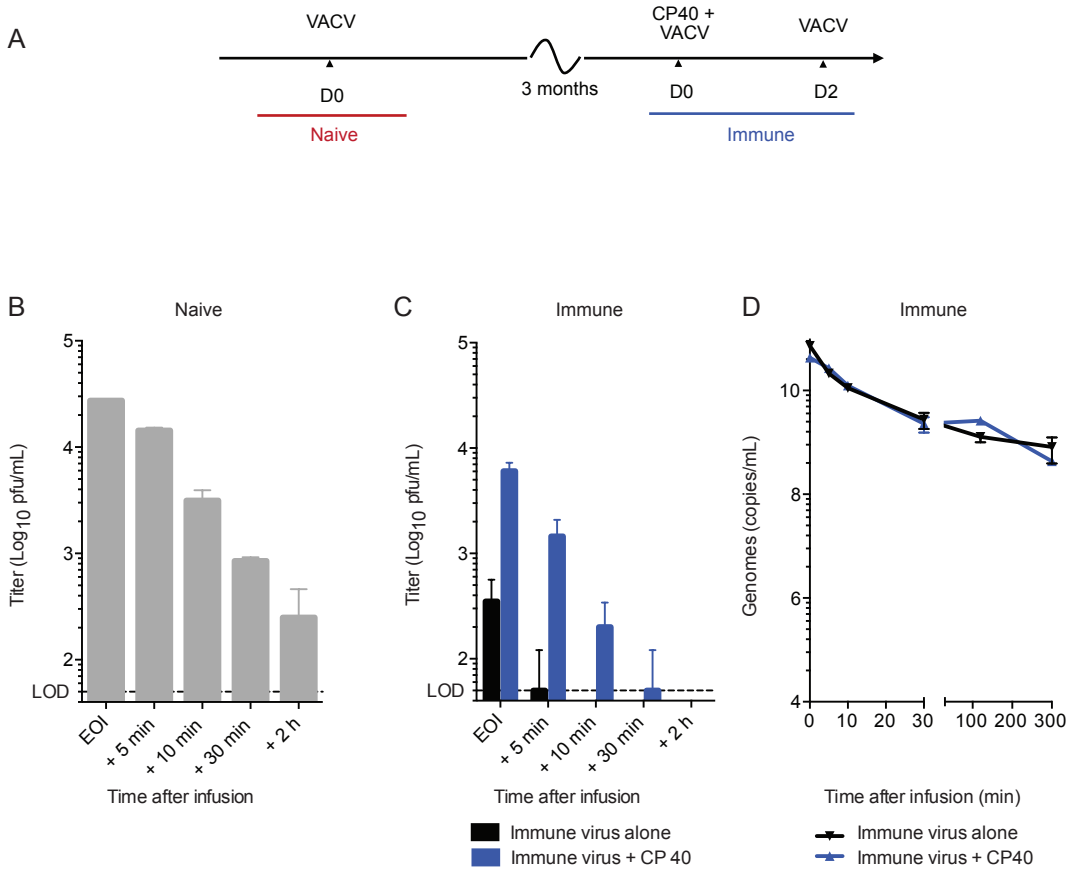
A
VACV
CP40 +
VACV
VACV
D0
3 months
D0
D2
Naive
Immune
B
Naive
Titer (Log10 pfu/mL)
5
4
3
2
LOD
EOI
+ 5 min
+ 10 min
+ 30 min
+ 2 h
Time after infusion
C
Immune
Titer (Log10 pfu/mL)
5
4
3
2
LOD
EOI
+ 5 min
+ 10 min
+ 30 min
+ 2 h
Time after infusion
Immune virus alone
Immune virus + CP 40
D
Immune
Genomes (copies/mL)
10
8
6
4
0
10
20
30
100
200
300
Time after infusion (min)
Immune virus alone
Immune virus + CP40

Appendix Figure 2 Complement inhibition hemolysis assay

(A) Determination of the volume of plasma that provides 60-70% lysis to use throughout the assay. (B) Standard curve to convert the amount of lysis, as measured by absorbance, into volume of plasma. (C) Percent inhibition is plotted for each animal relative to the pre-bleed value.

A

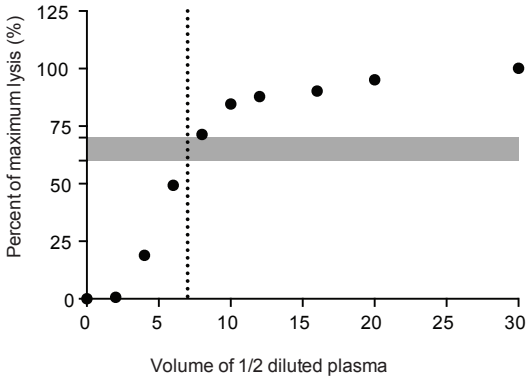
Percent of maximum lysis (%)
125
100
75
50
25
0
0
5
10
15
20
25
30
Volume of 1/2 diluted plasma

B

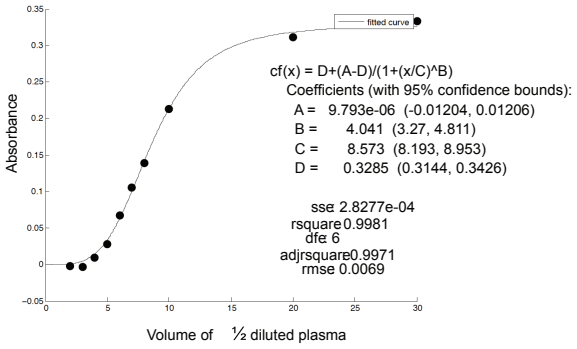
fitted curve
cf(x) = D+(A-D)/(1+(x/C)^B)
Coefficients (with 95% confidence bounds):
A = 9.793e-06 (-0.01204, 0.01206)
B = 4.041 (3.27, 4.811)
C = 8.573 (8.193, 8.953)
D = 0.3285 (0.3144, 0.3426)
sse 2.8277e-04
rsquare 0.9981
dfe 6
adjrsquare 0.9971
rmse 0.0069
Absorbance
Volume of ½ diluted plasma

C

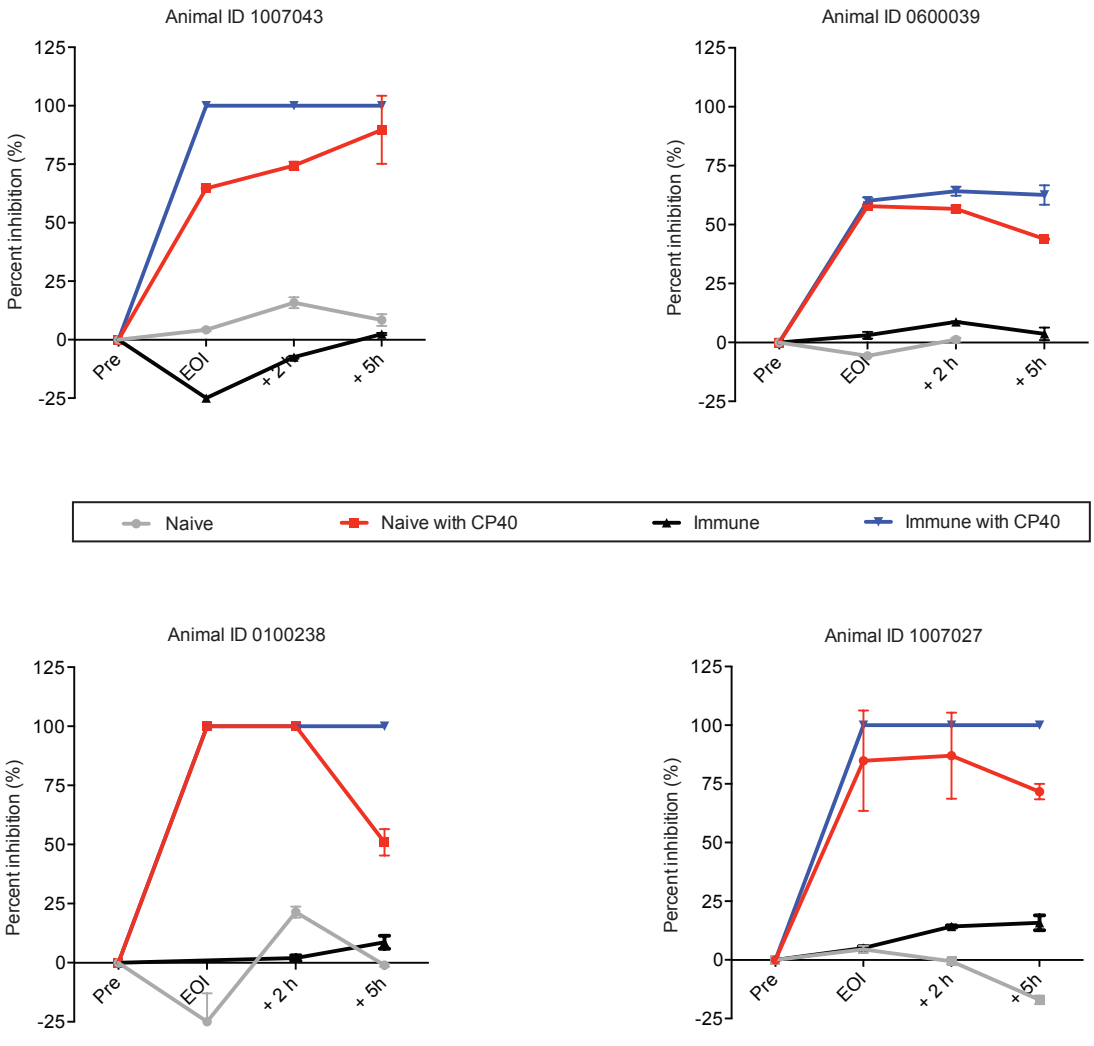
Animal ID 1007043
Animal ID 0600039
Animal ID 0100238
Animal ID 1007027
Percent inhibition (%)
125
100
75
50
25
0
-25
Pre
EOI
+ 2 h
+ 5h
Naive
Naive with CP40
Immune
Immune with CP40

Appendix Figure 3. Cytokine production following virus infusion with or without CP40 in NHPs

Blood samples were collected prior to treatment, and 2 and 5 hours after the end of the infusion. The plasma from these samples was analyzed for a panel of cytokines. (n=3 animals)

G CSF

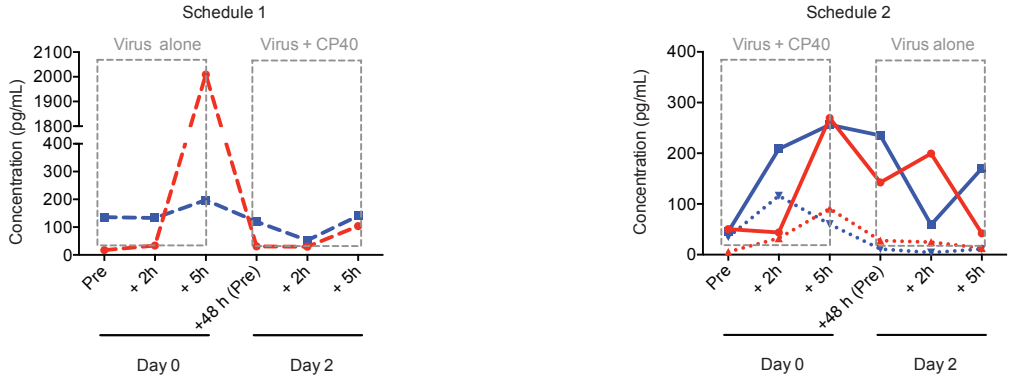

GM CSF

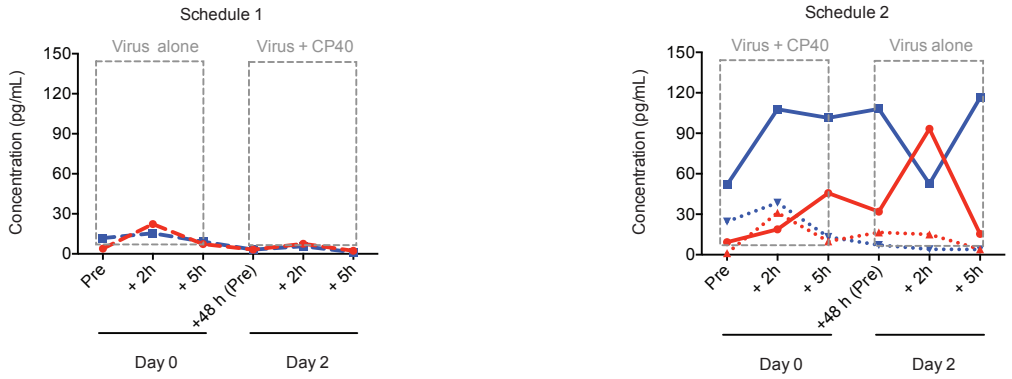

IL 1 ra

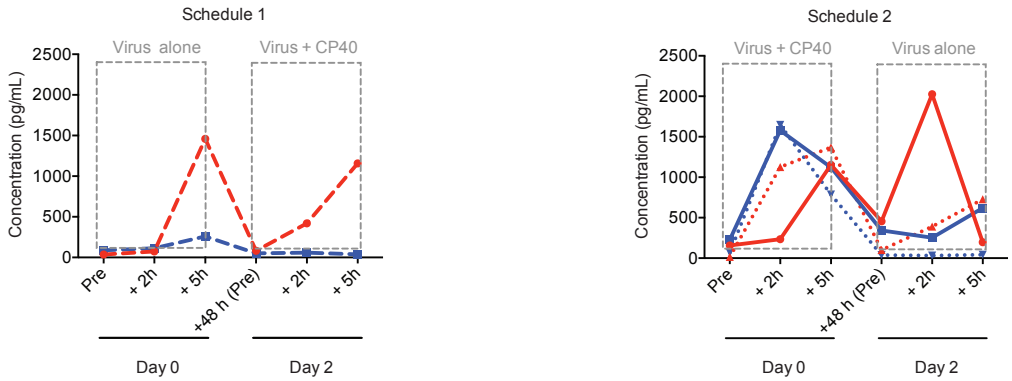

IL 2

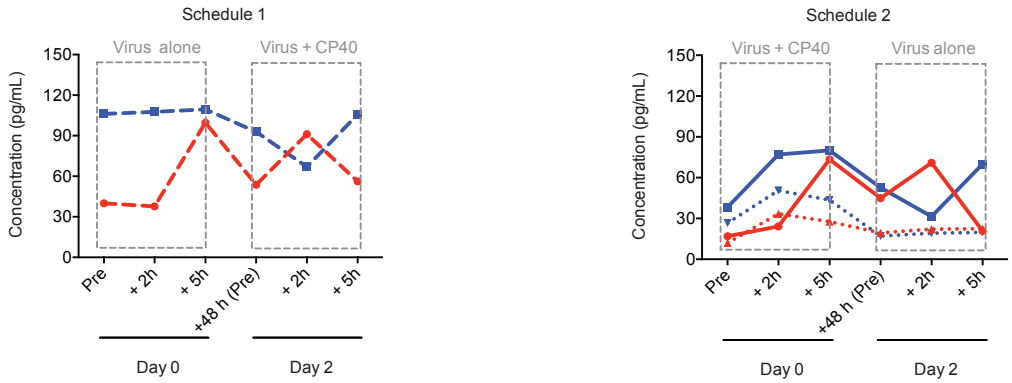

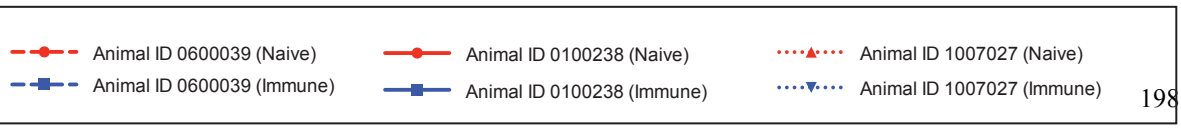

IL 4

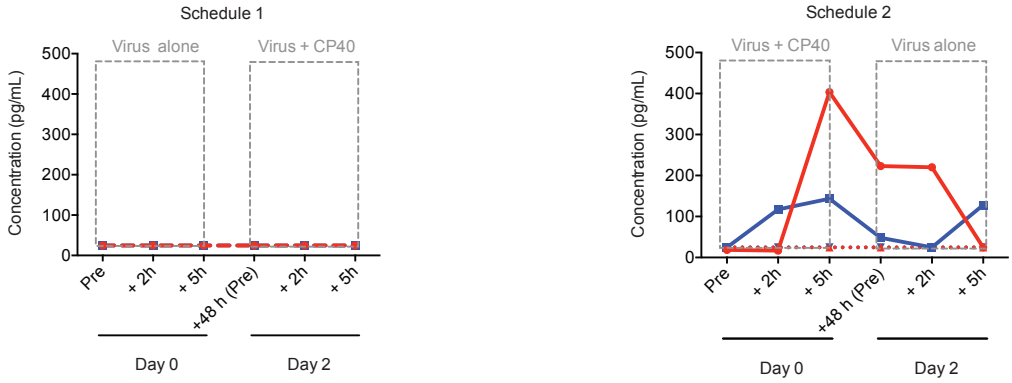

IL 5

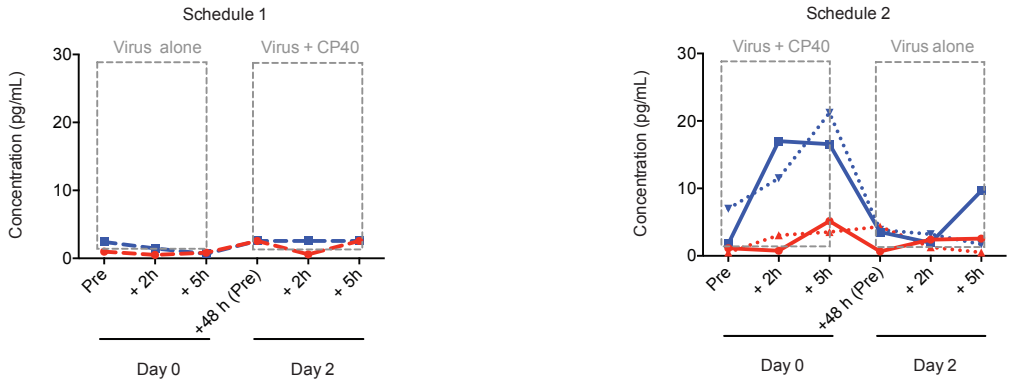

IL 8

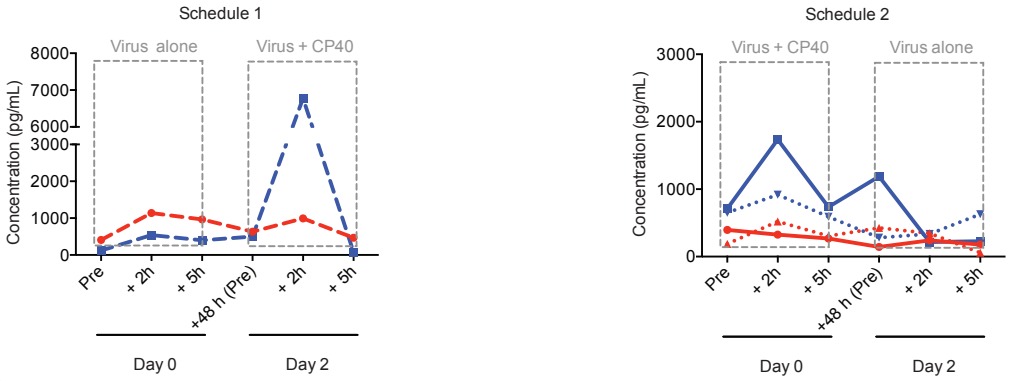

IL 10

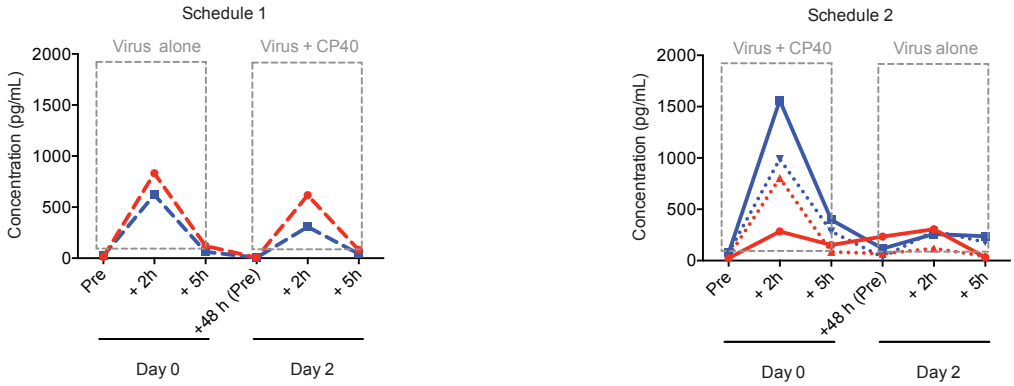

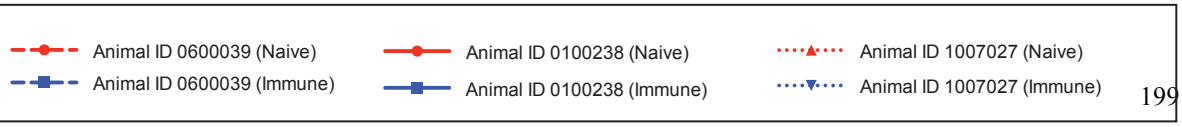

IL 12

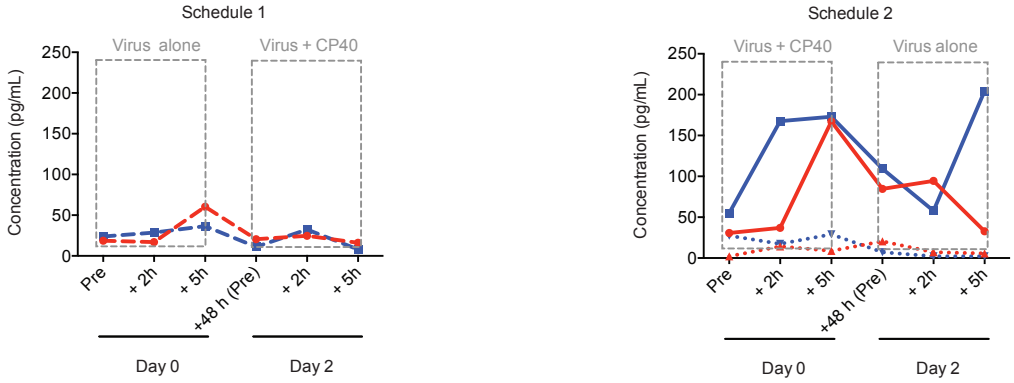

IL 13

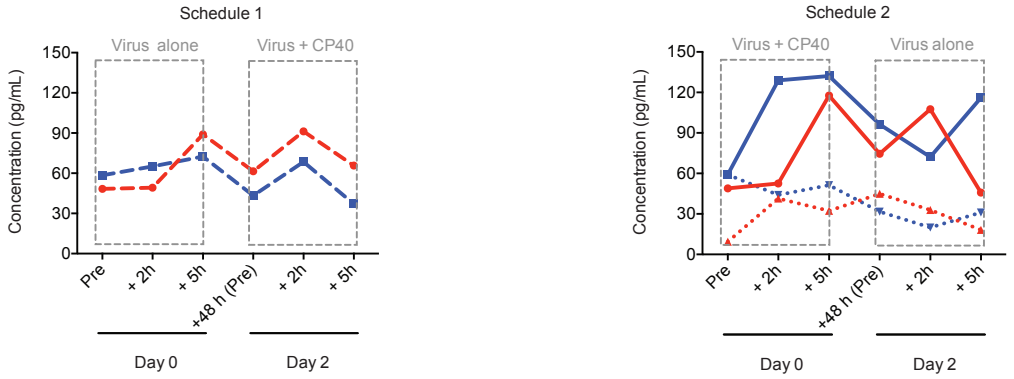

IL 15

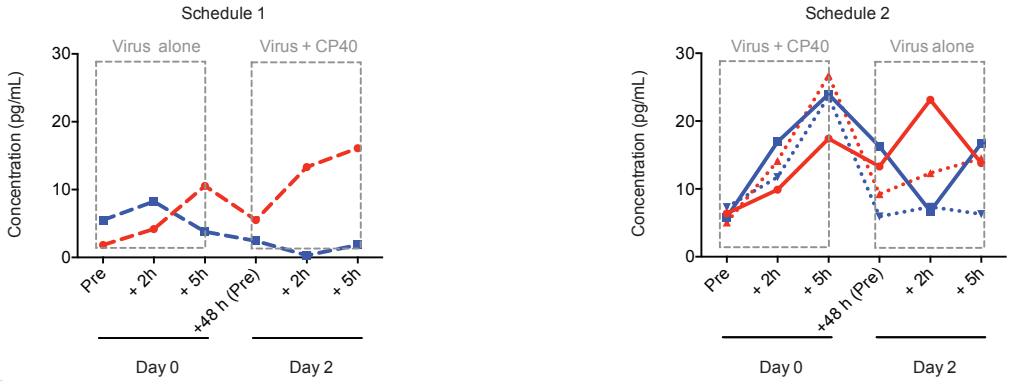

IL 17

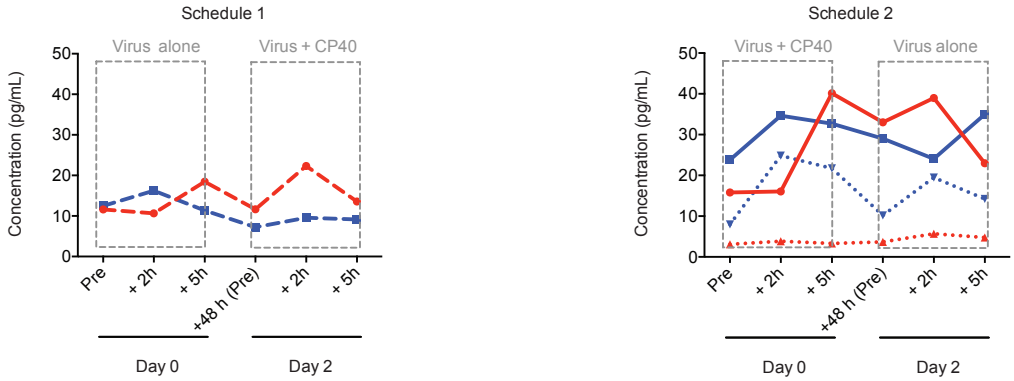

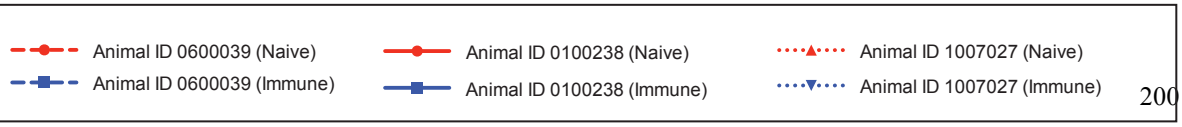

IL 18

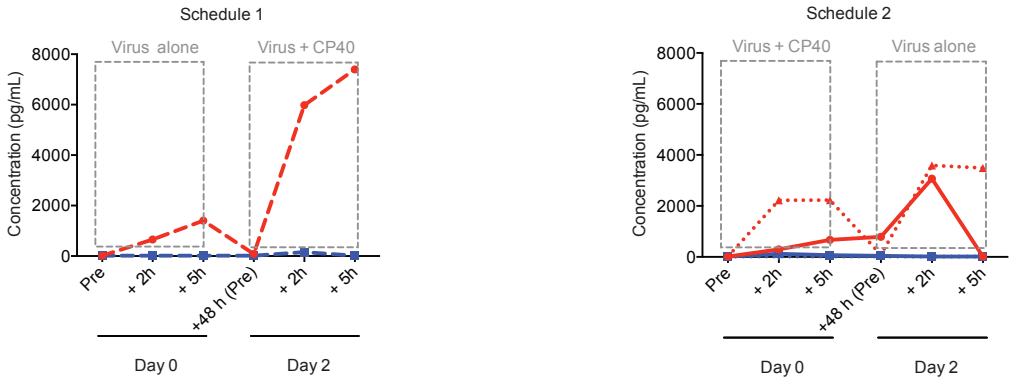

MIP 1 α

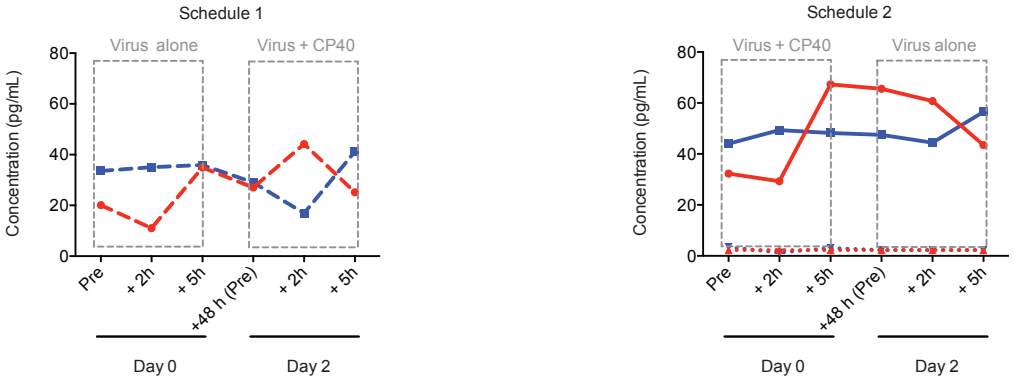

MIP 1 β

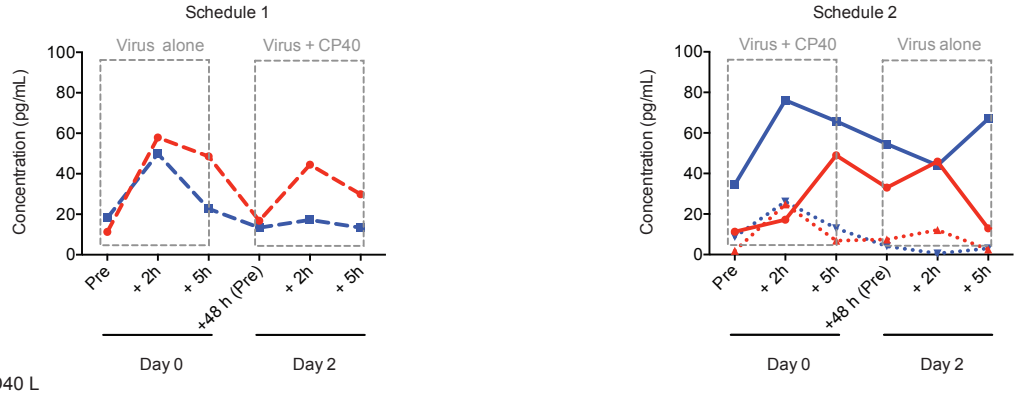

sCD40 L

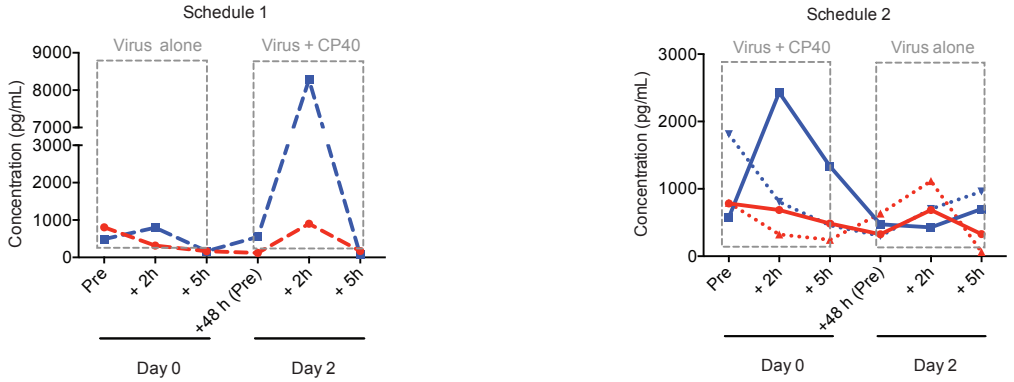

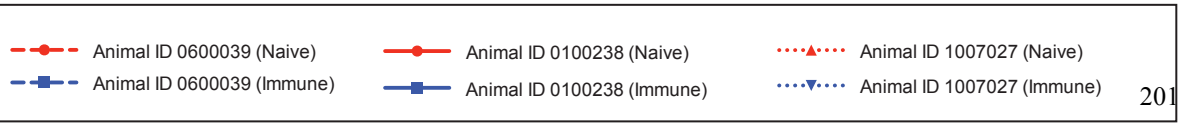

TGF α

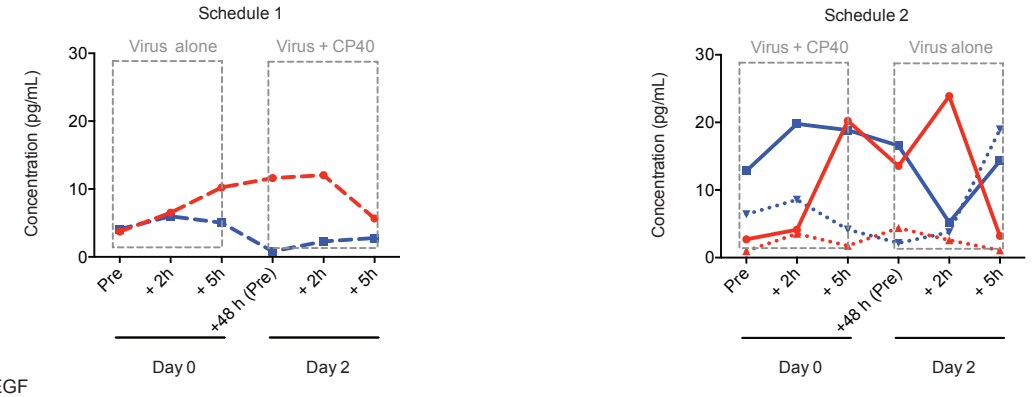
Schedule 1
Virus alone
Virus + CP40
Concentration (pg/mL)
30
20
10
0
Pre
+ 2h
+ 5h
+48 h (Pre)
+ 2h
+ 5h
Day 0
Day 2
Schedule 2
Virus + CP40
Virus alone
Concentration (pg/mL)
30
20
10
0
Pre
+ 2h
+ 5h
+48 h (Pre)
+ 2h
+ 5h
Day 0
Day 2

VEGF

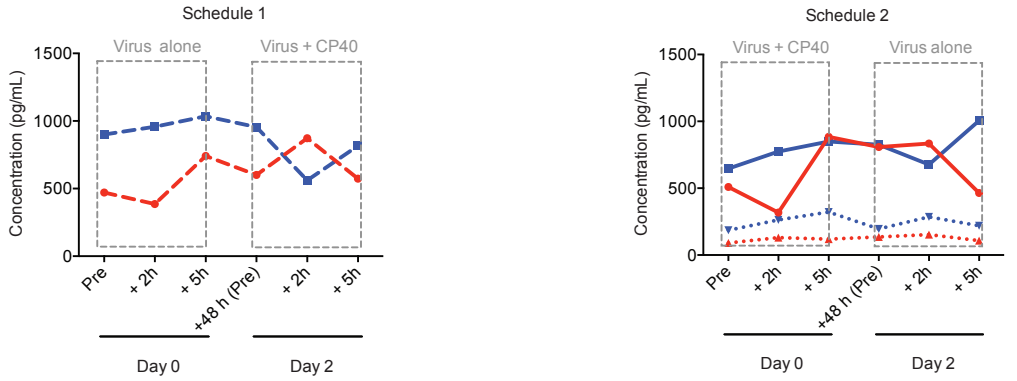
Schedule 1
Virus alone
Virus + CP40
Concentration (pg/mL)
1500
1000
500
0
Pre
+ 2h
+ 5h
+48 h (Pre)
+ 2h
+ 5h
Day 0
Day 2
Schedule 2
Virus + CP40
Virus alone
Concentration (pg/mL)
1500
1000
500
0
Pre
+ 2h
+ 5h
+48 h (Pre)
+ 2h
+ 5h
Day 0
Day 2

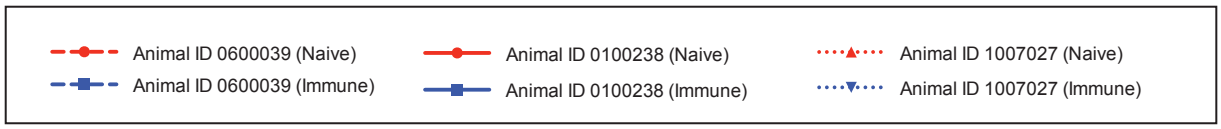
Animal ID 0600039 (Naive)
Animal ID 0600039 (Immune)
Animal ID 0100238 (Naive)
Animal ID 0100238 (Immune)
Animal ID 1007027 (Naive)
Animal ID 1007027 (Immune)

Appendix II- Complement inhibition prevents oncolytic vaccinia virus neutralization in immune humans and cynomolgus macaques

Laura Evgin[1,2], Sergio A. Acuna[3], Christiano Tanese de Souza[1], Monique Marguerie[1,2], Chantal G. Lemay[1], Carolina S. Ilkow[1], Scott C. Findlay[4], Theresa Falls[1], Kelley A. Parato[1], David Hanwell[5], Alyssa Goldstein[5], Roberto Lopez[5], Sandra Lafrance[5], Caroline J. Breitbach[6], David Kirn[6], Harold Atkins[1], Rebecca C. Auer[1], Joshua M. Thurman[7], Gregory L. Stahl[8], John D. Lambris[9], John C. Bell[1,2*†], J. Andrea McCart[3,10†]

[1]Center for Innovative Cancer Therapeutics, Ottawa Hospital Research Institute, Ottawa, ON, Canada
[2]Department of Biochemistry, Microbiology and Immunology, University of Ottawa, Ottawa, ON, Canada
[3]Toronto General Research Institute, University Health Network, Toronto, ON, Canada
[4]Department of Biology, University of Ottawa, Ottawa, ON, Canada
[5]Animal Resources Centre, University Health Network, Toronto, Canada.
[6]SillaJen Inc., Seoul South Korea
[7]Department of Medicine, University of Colorado Denver, Aurora CO, USA
[8]Center for Experimental Therapeutics and Reperfusion Injury, Harvard Institutes of Medicine, Boston, MA, USA
[9]Department of Pathology and Laboratory Medicine, University of Pennsylvania, Philadelphia, PA, USA
[10]Department of Surgery, Mount Sinai Hospital and University of Toronto, Toronto, Canada

† These authors contributed equally to this work.

*Corresponding author: John C. Bell jbell@ohri.ca

Manuscript submitted to Science Translational Medicine, November 2014

ONE SENTENCE SUMMARY

Pre-existing humoral immunity poses a significant hurdle to the systemic delivery of oncolytic vaccinia virus but may be overcome with complement inhibition.

ABSTRACT

Oncolytic viruses (OVs) have shown promising clinical activity when administered by direct intra-tumoral injection. In pre-clinical models, OVs are effective as intravenous agents but the translation of this activity to the clinic has been slow. Natural barriers in the blood including neutralizing antibodies and complement are likely going to limit the ability to repeatedly administer OVs by the intravenous route. We demonstrate here that for a prototype of the clinical vaccinia virus based product Pexa-Vec, the neutralizing activity of antibodies elicited by smallpox vaccination, as well as the anamnestic response in hyper-immune virus treated cancer patients, is strictly dependent upon the activation of complement. In a Fischer rat model, complement depletion stabilized vaccinia virus in the blood of immunized animals and correlated with improved delivery to mammary adenocarcinoma tumors. Unexpectedly, complement depletion also provided a dramatic enhancement of tumor infection when delivered by intra-tumoral injection in immunized animals. The feasibility and safety of clinically using a complement inhibitor, CP40, in combination with an oncolytic virus product was tested in a cynomolgus macaque model. Immune animals saw an average 10-fold increase in infectious virus titer at an early point after the infusion, and a prolongation of the time during which infectious virus was still detectable in the blood. Capitalizing on the complement dependence of anti-vaccinia antibody with adjunct complement inhibitors may increase the effective dose to enable successful delivery of multiple rounds of oncolytic vaccinia virus in immune hosts.

INTRODUCTION

Oncolytic viruses (OVs) are multi-mechanistic therapeutics that can cause tumor debulking by direct oncolysis, deliver therapeutic transgenes, trigger vascular disruption, and critically induce anti-tumor immunity[1]. To date the successful clinical development of OVs has been largely as loco-regional therapeutics administered by direct injection into tumor beds[2,3]. While this approach provides localized tumor destruction and the potential for the generation of systemic anti-tumor immunity[4–7], it does not take advantage of the ability of viruses to infect and destroy metastatic tumors. In pre-clinical models of systemic disease, the effectiveness of intravenous administration of OVs to virus naïve animals has been demonstrated in a variety of tumor models[8,9]. In cancer patients however, the development of OVs as intravenous agents has been slower, in large part due to concerns about being able to dose past pre-existing neutralizing antibodies or to deliver multiple doses of virus in patients developing an anti-viral immune response.

Complement is a key component of the innate immune system's first line of defense, acting to target foreign pathogens for opsonisation, neutralization, phagocytosis and clearance from the circulatory system[10]. Antibody mediated complement activation is

likely of particular importance for therapeutic vaccinia viruses as a large proportion of today's cancer patients were vaccinated during the smallpox eradication campaign. We hypothesized that inactivation of complement could lead to improved survival of oncolytic vaccinia virus in the blood of patients undergoing therapy.

The complement C3 molecule provides an attractive therapeutic target since it sits at the axis of the three activation pathways and is the gateway to the terminal complement pathway. Inhibition of C3 both quenches activation and prevents the insertion of the membrane attack complex (MAC) into the envelope of the target. Compstatin is a 13 amino acid cyclic peptide that was selected from a phage display library for binding affinity to human and non-human primate C3 and C3b[11]. Since its discovery, numerous analogs have been developed with improved pharmacodynamic and pharmacokinetic properties, with the analog CP40 emerging as the lead clinical candidate[12,13].

We provide evidence here that in hyper-immune animal models, we can improve intravenous vaccinia virus delivery to tumors following complement inhibition. Importantly, CP40 inhibits antibody mediated virus neutralization in blood samples collected from immune cancer patients. Furthermore, in immunized cynomolgus macaques, CP40 enhanced the half-life of vaccinia virus in the circulation following intravenous administration.

RESULTS

Antibody mediated vaccinia virus neutralization is complement dependent

We undertook a components analysis to assess the sensitivity of Wyeth strain vaccinia virus to neutralizing factors in whole human blood from either naïve or previously vaccinated healthy volunteers. Virus was incubated with whole blood or fractions thereof and infectious virus quantified by plaque assay. A ratio of 2×10^5 pfu/mL was used to mimic the clinical dose of 1×10^9 pfu that is required to facilitate tumor delivery in patients treated by intravenous infusion[14]. As shown in Figure 1A, the magnitude of virus neutralization was approximately equal between whole blood and plasma suggesting that the primary factors leading to loss of infectivity were plasma components. We found that even in naïve individuals, vaccinia virus was inactivated in plasma samples to some extent, but this inhibition could be eliminated by heat inactivation of complement. As expected, plasma from vaccinated individuals robustly inhibited vaccinia virus. Interestingly, heat inactivation eliminated much of the inhibition found in the plasma of immunized individuals. Similarly, using the specific complement inhibitor CP40, we were able to largely prevent the neutralization of vaccinia virus in naïve and immunized individuals. (Figure 1B).

This lead us to investigate the role that complement plays in the neutralization of vaccinia virus in cancer patients prior to therapy and two weeks post treatment with Pexa-Vec (pexastimogene devacirepvec; JX-594) (ClinicalTrials.gov Identifier NCT01394939). Serum samples collected from cancer patients prior to their first treatment and two weeks after their first infusion were heat-inactivated. Virus neutralization was assessed after incubation with this antibody with or without a replenished source of complement. As shown in Figure 1 C, Pexa-Vec boosted antibodies neutralized vaccinia virus, however this activity was blunted by complement inhibition.

We have shown previously through dose escalation of Pexa-Vec, there exists in patients natural barriers to intravenous delivery to tumor beds that can be overcome at a breakthrough dose[14]. Dose escalation *in vitro* (ranging from 2 x 10^4 pfu/mL to 2 x 10^7 pfu/mL) also demonstrated a saturation effect in both naïve and vaccinated samples (Figure 1D), however the addition of CP40 was able to recover a greater proportion of the input virus, no matter the initial dose.

We assessed the neutralizing capacity of immune plasma on other clinical candidate oncolytic viruses in the presence or absence of CP40. While complement inhibition did not lead to a reduction in viral neutralization in HSV-1 seropositive plasma, it increased the recovery of Measles Edmonston and Reovirus (Figure 1E).

Viral neutralization is mediated via the membrane attack complex

We selectively inhibited individual components of the activation pathways of the complement cascade to establish their relative impact on vaccinia virus neutralization. When either the classical or alternative pathways were inhibited in plasma from naïve donors, viral neutralization was not observed (Figure 2B,C). This indicated that both the classical or alternative pathways could lead to complement activation and viral neutralization *in vitro*. Neutralization in immune plasma was prevented with monoclonal antibodies to the classical and alternative pathways and this was maximized when used in combination, highlighting a role for the alternative pathway as a positive amplification loop (Figure 2B). Inhibition of the mannose binding lectin (MBL) pathway using an anti-MBL antibody did not have a large impact on the viability of vaccinia virus in human plasma. (Figures 2B,C) A mannose-binding lectin assay validated the functional inhibition of the MBL pathway (Supplemental Figure 1A). In both naïve and immune plasma, eculizumab, an approved C5 monoclonal antibody, abrogated almost all neutralization, implicating the terminal pathway (Figure 2D).

To determine the fate of vaccinia virus particles in the presence of anti-viral antibodies and complement, we carried out sucrose density centrifugation of virus preparations. Native viral particles subjected to centrifugation as described in Materials and Methods banded on a sucrose gradient in fractions 12 and 13 (Supplemental Figure 1B). In contrast, detergent or plasma treated viral particles were detected in fractions 1-4, consistent with complement and antibody mediated destruction of vaccinia virus.

Complement depletion of Fischer rats enhances virus delivery to tumor sites in the presence of neutralizing antibodies.

CP40 is a primate specific inhibitor, thus to test the effects of complement depletion *in vivo* in a tumor bearing animal model, we resorted to the use of cobra venom factor (CVF). To first validate that the rat model mimicked our human findings, we assessed virus neutralization *in vitro*. Vaccinia virus was shown to be sensitive to rat complement and the anti-viral antibodies were only demonstrated to be neutralizing in the presence of complement (Supplemental Figure 2A). CVF-mediated complement depletion was confirmed by immunoblot against the C3 protein (Supplemental Figure 2B). Therefore in the rat, the complement dependence of the anti-vaccinia antibodies closely mirrored the effects seen in human blood samples.

Rats were vaccinated or not and once neutralizing anti-vaccinia titers were established, animals were treated with a single dose intravenously of oncolytic vaccinia

virus. In half the animals the virus therapy was carried out following complement depletion with CVF (Figure 3A). An early time point after tail vein injection of virus (10 minutes) was chosen to simultaneously measure live virus stability in the blood and early delivery to subcutaneous mammary adenocarcinoma tumors. A greater than 100-fold mean increase in infectious virus titer was observed in the blood of vaccinated complement-depleted animals, compared to their complement-replete counterparts (Fig 3 B). A corresponding increase in delivery of infectious virus to tumors was observed in complement-depleted animals (Fig 3C). To further examine the mechanism associated with the increased detection of live virus following complement depletion, vaccinia virus genomes were quantified in tumors, blood and liver by quantitative real-time PCR (qPCR). Although titer increased dramatically following complement depletion, only a minor change was observed in viral genomes in each organ. This suggests that the distribution of virus particles remained unchanged (Fig 3D). Twenty-four hours after intravenous virus administration, infectious virus could only be recovered from subcutaneous tumors or tumour nodules in the lungs if complement was depleted at the time of virus injection (Fig 3 E). Consistent with the effects observed in the blood and tumors, a concomitant increase in delivery of infectious virus to the liver was observed 10 minutes post-injection in complement-depleted rats. However, replicating virus could not be recovered from livers 24h after virus administration, irrespective of complement status (Supplemental Figure 2C), suggesting that complement inhibition did not increase infection of normal organs. In virus naïve rats, changes in live virus stability in the blood were not observed with complement depletion after intravenous administration of virus (Supplemental Figure 2D). Similarly, infectious virus was equally recovered from tumors of complement-replete or depleted naïve rats 48 hours after treatment (Supplemental Figure 2E).

To examine whether complement and antibody exerts an important neutralizing effect in the tumor microenvironment of immune animals, rats were implanted with subcutaneous tumors and treated with vaccinia virus by intra-tumoral injection with or without complement depletion, as outlined in Figure 3F. Remarkably, tumors from complement-depleted animals contained a mean 20 and 117 fold more live virus than their complement-replete counterparts at 24 hours and 48 hours after virus administration, respectively (Figure 3G, H). In contrast, complement depletion had no effect on the infection of tumors of naïve animals following intra-tumoral injection (Supplemental Figure 2 F,G).

Transient complement inhibition in cynomolgus macaques is a safe strategy that increases the stability of vaccinia virus in the blood

We conducted a feasibility study in cynomolgus macaques to evaluate the use of CP40 to transiently inhibit complement in the context of an intravenous infusion of oncolytic vaccinia virus. Four macaques were treated according to the schedule outlined in Figure 4A. Each animal received a dose of virus as a single agent (1×10^8 pfu infused over 30 minutes), and a dose of virus with a CP40 pre-treatment (2mg/kg bolus), separated by 2 days. This regimen was first performed when the animals were naive and 4 months later when they were immune to the virus. Vaccinia virus was shown to be sensitive to non-human primate (NHP) complement and the anti-viral antibody response mounted by 3 months post virus treatment was only demonstrated to be neutralizing in

the presence of complement (Supplemental Figure 3). Animals were divided into two groups with opposite treatment schedules, such that half the animals received single agent virus first, and half received virus in combination with CP40 first. No difference was observed as a consequence of the order in which treatments were given.

Our primary objective was to determine if complement inhibition reduced antibody and complement mediated virus neutralization. Infectious virus in the blood was quantified by plaque assay. In naïve animals, the concentration of infectious virus in the blood was not significantly affected by CP40 (Figure 4C, Supplemental Figure 4A). In contrast, profound differences in the levels of circulating infectious virus were observed in immune animals when pre-treated with CP40 (Figure 4B,C). Peak titers at the end of the infusion were elevated (mean 9.93 fold increase; range 5.8-14.8) and approached levels observed when animals were naïve. While infectious virus in the blood disappeared quickly after the infusion in immune animals, this time period was prolonged with CP40. In agreement with our earlier studies using complement depletion in rats, we did not see a change in the clearance rate of viral genomes from the circulation with CP40. (Figure 4D, E, Supplemental Figure 4B). The quantification of infectious virus and total genome content in the blood for two additional animals is shown in Supplemental Figure 4A. Consistent with previously published dose finding studies[13], CP40 inhibition of complement was validated by hemolysis assay (data not shown).

While we saw the predicted effect on live virus in the blood, we did not observe adverse events that could be specifically attributable to complement inhibition. Blood chemistry was evaluated on the day of infusion at several time points before and after treatment and did not indicate renal, hepatic or pancreatic dysfunction. Complete blood counts indicated transient changes in lymphocyte, neutrophil and monocyte counts, but occurred both with and without CP40 (Supplemental Figure 5). Mild fevers were observed in some naïve animals, however the incidence of fever on the day of infusion was not increased by complement inhibition. Fevers were not observed in immune animals on the day of infusion (Supplemental Table 1). Pock lesions were observed on naïve animals but not immune animals and resolved without complications. A cytokine array was performed on plasma samples taken on the day of infusion. Although the analysis was complicated by the time frame of repeat dosing with or without CP40, there was no evidence based on cytokine expression that complement inhibition modified pro or anti-inflammatory cytokine profiles (Supplemental Figure 6).

DISCUSSION

In the present study, we demonstrate that antibody mediated complement activation leads to vaccinia virus neutralization, and that as a corollary, complement inhibition can suppress the virus neutralizing effects of pre-existing humoral immunity and lead to increased delivery of infectious virus to tumors. *In vitro* modeling of virus neutralization indicated that pre-existing immunity from smallpox vaccination presented an important hurdle, resulting in the neutralization of up to 99% of virus. Moreover, humoral immunity is a dynamic barrier to oncolytic viruses, as observed by the elevated antibody titers boosted by treatment. *In vivo*, complement depletion improved infection of tumors in immune animals when virus was delivered both systemically and intra-

tumorally. In a non-human primate model, we found CP40 complement inhibition to be a safe and efficacious method to increase the stability of virus in the blood. These findings provide a strong rationale for a complement intervention strategy in both single administrations of oncolytic vaccinia virus to pre-immune individuals and multi-dosing treatment schedules that are faced with increasing titers of antibody.

Perhaps the best evidence of the sensitivity of vaccinia virus to complement is the adaptations that the virus has evolved: the vaccinia complement protein (VCP) and the formation of the extracellular enveloped virus (EEV) virion. VCP possesses factor I co-factor activity and inhibits the formation of the C3 convertase[15]. Consequently, VCP has been shown to reduce complement-enhanced antibody-mediated neutralization *in vitro*[16]. However, infection and replication is required to produce VCP, a primarily secreted protein[17]. Vaccinia virus produces two different infectious virions: the intracellular mature virus (IMV) and the enveloped virion. The EEV particle is wrapped in an additional membrane and acquires host cell complement regulatory proteins that protect it from complement-mediated destruction[18]. However, the fragility of the EEV membrane precludes its use as an infusion product. While both these adaptations may help to traffic virus to metastatic sites following a primary local infection, they are not advantageous to an initial infusion of an oncolytic vaccinia virus

A phase I dose escalation trial of intravenously-delivered oncolytic vaccinia virus (Pexa-Vec,) demonstrated a pharmacokinetic barrier to infection of tumor sites, whereby only doses above 1.5×10^7 pfu/kg achieved detectable tumor infection[14]. The pattern of delivery was highly suggestive of a transient saturation of viral clearance mechanisms that we now believe to be in large part, complement and antibody dependent. We also observed a threshold effect *in vitro* whereby the proportion of live virus recovered was maximized by increasing the ratio of virus to volume of plasma (Figure 1D). We speculate that in a system with a fixed amount of antibody, the stoichiometric requirement of six aggregated Fc tails to bind one C1q molecule is met with decreasing frequency as the pfu per milliliter ratio increases[19]. While currently it is not clinically achievable to give doses of vaccinia virus that corresponds to the dose at which the antibody was saturated *in vitro*, viral neutralization can be prevented at any dose with complement inhibition. This was demonstrated to be feasible with the cynomolgus macaque experiment.

This type of complement intervention strategy may be applicable to other oncolytic vectors, such as Reolysin and MV-NIS (Figure 1E). While HSV-1 is sensitive to complement, and depletion has been shown to improve systemic delivery of HSV-1 to brain tumors of naïve rats[20], here we show that the antibody against HSV-1 is robustly neutralizing independent of complement. We demonstrated that the antibody from healthy human donors against Measles and Reovirus exhibits some degree of complement dependence. The general population possesses a high degree of seropositivity to these viruses, and the level of anamnestic antibody has been shown to dramatically increase following treatment with these oncolytic viruses[21,22]. Both these OV candidates are being evaluated in intravenous delivery clinical settings and may be enhanced by complement inhibition. Interim clinical results have been reported with MV-NIS for the treatment of multiple myeloma, a patient population in which the levels of functional antibody titers were shown to be very low[21]. Concurrent complement

inhibition may enable the expansion of the patient cohort to one in which live virus can be administered systemically without sustaining a prohibitive degree of neutralization.

Previous studies differ in the specific actors of the complement cascade that are reported to be required for vaccinia virus neutralization[23,24]. We felt that it was important to resolve this discrepancy in order to determine which complement inhibitors may be of use clinically. In contrast to the results of Magge et al, we demonstrated that inhibition of C1 and C3 prevented viral neutralization in both naïve and immune plasma samples. Additionally, with the use of eculizumab, we have confirmed that C5 is required for viral neutralization and that the membrane attack complex is likely responsible for virolysis (Figure 2). Our findings suggest that the C1 esterase inhibitor and eculizumab may also offer some benefit to the delivery of oncolytic vaccinia virus.

Other approaches for shielding virus from neutralization and preventing unwanted cellular interactions, like serotype exchange and pseudotyping[25–27] or polymer coating[28,29], require extensive engineering or post-production modifications. In contrast, pharmacological inhibition of complement with short half-life peptide inhibitors is an off-the-shelf strategy that gives strict temporal control over complement activity on the day of administration. The Compstatin analogs offer an optimal point of intervention in the complement cascade since they target C3 and are thus able to quench initiation and prevent further amplification[12]. Long-term complement inhibition is likely not a clinically desirable outcome. Not only could it pose a safety risk to the patient being dosed with virus, it may additionally preclude advantageous complement-mediated tumor clearance mechanisms such as antibody-mediated *complement*-dependent cancer cell cytotoxicity as has been demonstrated following Pexa-Vec treatment[30].

Numerous differences between the human and mouse complement systems have been reported that would limit the utility of the mouse model in the context of this study. Low haemolytic activity of complement from all inbred mouse strains relative to rat or human has been documented[31] and may be partially attributed to a C4 polymorphism that precludes the formation of a functional C5 convertase[32]. Most recently, an unspecified classical pathway inhibitor has been discovered in mouse serum, but not human or rat serum, that was shown to inhibit IgG-dependent complement-dependent cytotoxicity[33]. Taken together with our findings of the similarity to humans, we believe that the rat model has greater predictive value for the preclinical development of oncolytic vaccinia virus. Conclusions drawn from mice with regard to vaccinia antibody and complement must be carefully weighed with the limitations of the model[34].

In order to circumvent the neutralizing factors in the blood and increase infection of tumors, direct intra-tumoral injection has been the clinically preferred route of administration. In fact, the tumor microenvironment can be a highly perfused region and complement is known to play an important role in the neoplastic development process[35,36]. We have demonstrated that even for intra-tumoral dosing of immune animals, it is important to inhibit complement (Figure 3). These findings call in to question the degree to which intra-tumoral dosing treatment regimens are able to overcome pre-existing antibodies and suggests that the benefit of repeat dosing may be independent of oncolysis.

The results with CVF are proof of concept studies as it is not a clinical reagent. We therefore felt it important to recapitulate the effect with CP40 in a cynomolgus macaque model. In this pre-clinical model, we showed that the stability of live virus in

the blood of immune macaques could be sustained by pre-conditioning with complement inhibition (Figure 4). While we observed differences between each outbred animal, CP40 pre-treatment significantly prevented neutralization in all immune animals. Although it was not possible to study tumor delivery in this model, increased and prolonged circulating infectious titers suggests greater bioavailability to infect tumor beds. Importantly, this approach was safe as CP40 did not cause changes in the hematologic profile, blood chemistry, nor fever incidence. While numerous factors remain unexplored with regard to this type of approach, we have demonstrated that complement inhibition is a feasible concept as an adjunct to oncolytic vaccinia virus treatment.

Oncolytic viruses represent a versatile class of multi-modality therapeutics. Although local administration has produced therapeutic efficacy in the clinic, disseminated metastatic disease requires systemic dosing. In addition to presenting a barrier to intravenous administration, complement and antibody act in the tumor microenvironment to prevent the infection of cancer cells. We have demonstrated a window of opportunity whereby delivery and infection of tumors can be dramatically improved in virus immune hosts through complement inhibition strategies. We believe that adjunct complement inhibition may be essential going forward with oncolytic vaccinia virus and other oncolytic vectors that generate complement-fixing antibody.

MATERIALS AND METHODS

Study design

The overarching research objective was to determine the role of antibody and complement in the systemic delivery of oncolytic vaccinia virus. Healthy volunteers were recruited to donate blood for *in vitro* experiments. Donors were stratified into immunological groups based on self-reported vaccination status. Neutralization of vaccinia virus was examined *in vitro* to determine the importance of antibody and complement. Based on initial *in vitro* results, we hypothesized that the neutralizing effect of antibody could be largely mitigated through complement inhibition. We sought to test the feasibility and safety of these approaches in rat and cynomolgus macaque models. Rat experiments were performed at least twice with three to four animals per group. Animals were assigned randomly to treatment groups. Four cynomolgus macaques were randomly assigned to two schedule groups such that each group contained one male and one female. All animals that received the full course of treatments were included in the reported results.

Cell culture and virus. The U2OS, Vero, L929 and HeLa cell lines were purchased from the American Type Culture Collection (Manassas, VA) and maintained in complete Dulbecco's Modified Eagle's medium (HyClone, Logan, UT) supplemented with 10% fetal bovine serum (HyClone, Logan, UT). The 13762MATBIII rat mammary adenocarcinoma cell line was purchased from the American Type Culture Collection and maintained in McCoy’s 5A medium modified (ATCC, Manassas, VA) supplemented with 10% fetal bovine serum (HyClone, Logan, UT). The oncolytic Vaccinia virus Wyeth strain TK- gfp was previously described[8,37]. HSV-1 (ICP0 null mutant n212)[38,39] was a gift from Dr. Karen Mossman, McMaster University. Reolysin was a gift from Dr.

Patrick Lee (Dalhousie University). Measles Edmonston was purchased from American Type Culture Collection (Manassas, VA).

Human blood neutralization experiments This study protocol was approved by the Ottawa Hospital Research Ethics Board and all volunteers gave informed consent. Human blood was collected from healthy donors by venipuncture into glass serum collection vacutainer tubes (BD Bioscience) and treated immediately with Refludan[40] at a final concentration of 50 μg/mL. Blood was spun at 800 x g for 10 minutes to obtain plasma. Plasma aliquots were incubated for 30 minutes at 56°C to inactivate complement. Blood or fractions thereof were incubated for 1 hour at 37°C with VACV at range of doses between 2 x 10^4- 2 x 10^7 pfu/mL. The infectious virus remaining was quantified by plaque assay on U2OS cells. To investigate the complement pathway, the compstatin analog CP40[13] was pre-incubated for 15 minutes at 37°C at a final concentration of 25μM prior to virus inoculation. Alternatively, the neutralizing monoclonal antibodies 3F8[41] mouse anti-human MBL, P1H10 mouse anti-human C1q or 1379 mouse-anti human Factor B[42] or Eculizumab were pre-incubated for 15 minutes at 37°C with plasma at concentrations of 60 μg/mL, 100 μg/mL or 500 μg/mL 50 μg/mL, respectively.
In order to assess anti-Vaccinia antibody from hyper-immune individuals, leftover serum was collected from patients enrolled in JX594-CRC019 (ClinicalTrials.gov Identifier IDNCT01394939). This study protocol was approved by the Ottawa Hospital Research Ethics Board and all patients gave informed consent. The serum was heat inactivated and combined with serum free DMEM or plasma collected from a naïve donor as a source of complement and incubated with VACV at a ratio of 2 x 10^5 pfu/mL. The infectious virus remaining was quantified by plaque assay on U2OS cells. Neutralization of HSV-1, Reovirus and Measles Edmonston were performed at a ratio of 2 x 10^6 pfu/mL. Plasma samples were incubated with CP40 (25 μM) or DMEM for 15 minutes at 37°C prior to a one hour incubation at 37°C in the presence of virus. HSV-1 and Measles were titered on Veros and Reovirus titered on L929 cells.

Fluorochrome linked immunoassay (FLISA) Activation of the MBL-dependent lectin pathway was assessed in human serum incubated with mAb 3F8 at 10 μg/mL as previously described.[43]

Sucrose gradient separation of viral proteins Vaccinia virus was incubated with PBS, PBS with detergent (1% Triton X-100) or plasma from an immune donor at a ratio of 2 x 10^7 pfu/mL for 1h at 37°C. Samples were overlaid on continuous 5-75% sucrose gradients and spun at 25000 rpm in an SW41Ti rotor for 35 minutes at 4°C. The gradient was collected in 16 fractions.

Immunoblotting Plasma or viral proteins were resolved on 4-12% polyacrylamide gels (BioRad, Hercules, CA) and transferred to nitrocellulose membranes (Amersham GE Healthcare Lifesciences, Baie d'Urfe QC). Membranes were incubated for 1 hour at room temperature or at 4°C overnight with the following antibodies and dilutions: 1:100 rabbit anti-rat C3 (Cedarlane, Burlington, ON; CL7334AP); rabbit polyclonal antibody to Vaccinia (Quartett, Berlin, Germany; 1220100715). Membranes were incubated with goat anti-rabbit horseradish peroxidase-conjugated IgG (Jackson ImmunoResearch Laboratories, Inc.) for 1 hour at room temperature. Proteins were detected using

Supersignal West Pico chemiluminescent substrate (Pierce Biotechnology, Rockford, IL) followed by exposure to X-ray film (Fuji Photo Film Co, LTD, Tokyo, Japan).

Animal Studies

Rat model

Female F344 Fischer rats weighing 100-150g were purchased from Charles River (Wilmington, MA). All animals were housed in pathogen-free conditions and all studies conducted were in accordance with the guidelines of the Animal Care Veterinary Service facility of the University of Ottawa. Tumors were established by injecting 5 x 10^5- 1 x 10^6 13762 MATBIII cells subcutaneously bilaterally in the left and right flanks or 3e5 cells intravenously by tail vein injection. Tumors were treated intravenously with 1 x 10^8 pfu of Vaccinia virus and 10 minutes or 24 hours post infection, the animals were sacrificed and the tumors resected. Tumors were also treated with an intratumoral injection of 1 x 10^7 pfu and animals were sacrificed either 24 or 48 hours after administration. Blood was collected by cardiac puncture into EDTA vacutainer tubes for analysis of *in vivo* neutralization. Alternatively, blood was collected with serum tubes and treated with Refludan to assess *in vitro* neutralization. Viral neutralization was assessed *in vitro* in plasma at a concentration of 2 x 10^5 pfu/mL. For the depletion of complement, 35U of Cobra Venom Factor (CVF) (Quidel, San Diego, CA) was administered intraperitoneally 24 hours prior to virus delivery. A second dose of 35 U was administered intraperitoneally 24 hours after virus if animals were to be sacrificed 48 hours after virus administration. Tumors and livers were collected and immediately frozen. Tissues were homogenized in PBS and titrated on U2OS cells.

Cynomolgus macaque model

Healthy male and female cynomolgus macaques weighing 3 to 6 kg were obtained from Primus BioResources (Vaudreuil-Dorion QC) and Charles River (Montreal, QC). All NHP studies were performed under a protocol approved by the Animal Resource Centre, University Health Network, Toronto, ON, Canada.

To facilitate intravenous injection and blood sampling, a vascular access port was surgically implanted into the right flank with the venous line inserted into the right femoral/iliac vein. Animals were allowed to recover from surgery for several weeks prior to the initiation of the study. Macaques were randomized across schedule groups such that a male and female were assigned to each group. Animals received two doses of Vaccinia virus (1 x 10^8 pfu infused over 30 minutes) in the naïve setting (day 0 and day 2), a booster dose (1 x 10^8 pfu 2 months post naïve treatment), and two doses in the immune setting (day 0, day 2). According to their group schedule, animals received a bolus dose of CP40 (2mg/kg) immediately prior to their virus infusion either on day 0 or day 2. Blood samples were collected immediately before and at various time points after the infusion of virus (end of infusion, + 5 min, + 10 min, + 30 min, + 2h, + 5h). EDTA treated whole blood samples were frozen for subsequent analysis by qPCR and titration of infectious virus on U2OS cells. EDTA and Refludan treated blood samples were spun at 800 g for 5 minutes to obtain plasma, and immediately frozen until further analysis. Rectal temperature was measured immediately before and at various time points after the infusion of virus (end of infusion, + 5 min, + 10 min, + 30 min, + 2h, + 5h). Cell blood count (CBC) profiles were determined using a Hemavet 950FS on samples collected

immediately before the infusion of virus, at the end of the infusion, + 2h and + 5h after the infusion. Blood biochemistry was analyzed using a Vetscan VS2 on samples collected immediately before the infusion of virus, at the end of the infusion, + 2h and + 5h after the infusion.

Ex vivo neutralization Blood was collected from healthy cynomolgus macaques using the anticoagulant Refludan (50 μg/mL). Plasma was heat inactivated and combined with plasma from a naïve animal as a source of complement (ratio 5:1 naïve plasma to heat inactivated plasma). Viral neutralization was assessed *in vitro* in plasma at a concentration of 2 x 10^5 pfu/mL.Samples were incubated for 1h at 37^{o}C and infectious virus remaining quantified by plaque assay.

Cytokine array A MILLIPLEX MAP non-human primate magnetic bead cytokine array (Millipore, Bedford MA) was performed according to the manufacturer's instructions by the Princess Margaret Genomics Centre, Toronto ON. Samples were read with Luminex 100 and data was analyzed using Bio-plex Manager 6.0. OBS Concentrations were measured in pg/ml.

qPCR DNA was isolated from whole blood collected in EDTA tubes, liver or tumor samples using the DNeasy kit (Qiagen, Germantown, MD) according to the manufacture's protocol. Quantitative PCR was performed on viral DNA extracted from whole blood or tissues using the SYBR Green PCR Master Mix (Qiagen, Germantown MD) on a RotorGene RG3000A (Corbett Research). Primers targeting the E3L gene were used to quantify viral genomes (TCCGTCGATGTCTACACAGG; ATGTATCCCGCGAAAAATCA). DNA isolated from purified viral stock was used as a standard where molecular weight was used to give an estimate of the number of copies per μg of DNA.

Statistics Where possible, statistical analyses were performed on log transformed values. When data points fell below the limit of detection, the value of half the limit of detection was used for statistical comparisons however was reported as ND (not detected) for graphical purposes. Statistical analyses were performed using GraphPad Prism and the R statistical software. Two-tailed unpaired Student's t tests were performed for the comparison of two groups. Linear mixed effects models were fitted for experiments with repeated measures data using treatment condition, vaccination status or time point as fixed effects, and donor as the random effect. Model fit was compared for models generated using pooled or unpooled levels of fixed effects to determine statistical significance. *p*-values < 0.05 was considered significant *p ≤ 0.05, **p ≤ 0.01, ***p < 0.001, ****p < 0.0001.

REFERENCES

1. Kirn, D. H. & Thorne, S. H. Targeted and armed oncolytic poxviruses: a novel multi-mechanistic therapeutic class for cancer. *Nat. Rev. Cancer* **9,** 64–71 (2009).

2. Vacchelli, E., Eggermont, A., Sautès-fridman, C., Galon, J. & Zitvogel, L. Oncolytic viruses for cancer therapy Trial watch. *Oncoimmunology* **2,** (2013).

3. Miest, T. S. & Cattaneo, R. New viruses for cancer therapy: meeting clinical needs. *Nat. Rev. Microbiol.* **12,** 23–34 (2014).

4. Park, B.-H. *et al.* Use of a targeted oncolytic poxvirus, JX-594, in patients with refractory primary or metastatic liver cancer: a phase I trial. *Lancet Oncol.* **9,** 533–42 (2008).

5. Heo, J. *et al.* Randomized dose-finding clinical trial of oncolytic immunotherapeutic vaccinia JX-594 in liver cancer. *Nat. Med.* **19,** 329–36 (2013).

6. Hwang, T.-H. *et al.* A mechanistic proof-of-concept clinical trial with JX-594, a targeted multi-mechanistic oncolytic poxvirus, in patients with metastatic melanoma. *Mol. Ther.* **19,** 1913–22 (2011).

7. Ingemar Andtbacka, R. H. *et al.* OPTiM: A randomized phase III trial of talimogene laherparepvec (T-VEC) versus subcutaneous (SC) granulocyte-macrophage colony-stimulating factor (GM-CSF) for the treatment (tx) of unresected stage IIIB/C and IV melanoma. *J. Clin. Oncol.* **31,** (2013).

8. Kim, J. H. *et al.* Systemic armed oncolytic and immunologic therapy for cancer with JX-594, a targeted poxvirus expressing GM-CSF. *Mol. Ther.* **14,** 361–70 (2006).

9. Stojdl, D. F. *et al.* VSV strains with defects in their ability to shutdown innate immunity are potent systemic anti-cancer agents. *Cancer Cell* **4,** 263–75 (2003).

10. Ricklin, D., Hajishengallis, G., Yang, K. & Lambris, J. D. Complement: a key system for immune surveillance and homeostasis. *Nat. Immunol.* **11,** 785–97 (2010).

11. Ricklin, D. & Lambris, J. D. Compstatin: A Complement Inhibitor on its Way to Clinical Application. *Adv. Exp. Med. Biol.* **632,** 273–292 (2008).

12. Risitano, A. M. *et al.* Peptide inhibitors of C3 activation as a novel strategy of complement inhibition for the treatment of paroxysmal nocturnal hemoglobinuria. *Blood* **123,** 2094–2101 (2014).

13. Qu, H. *et al.* New analogs of the clinical complement inhibitor compstatin with subnanomolar affinity and enhanced pharmacokinetic properties. *Immunobiology* **218,** 496–505 (2013).

14. Breitbach, C. J. *et al.* Intravenous delivery of a multi-mechanistic cancer-targeted oncolytic poxvirus in humans. *Nature* **477,** 99–102 (2011).

15. Sahu, A., Isaacs, S. N., Soulika, A. M. & John, D. Interaction of vaccinia virus complement control protein with human complement proteins: factor I-mediated

degradation of C3b to iC3b1 inactivates the alternative complement pathway. *J. Immunol.* **160,** 5596–5604 (1998).

16. Isaacs, S. N., Kotwal, G. J. & Moss, B. Vaccinia virus complement-control protein prevents antibody-dependent complement-enhanced neutralization of infectivity and contributes to virulence. *Proc. Natl. Acad. Sci. U. S. A.* **89,** 628–32 (1992).

17. Kotwal, G. J., Isaacs, S. N., McKenzie, R., Frank, M. M. & Moss, B. Inhibition of the complement cascade by the major secretory protein of vaccinia virus. *Science* **250,** 827–30 (1990).

18. Vanderplasschen, A., Mathew, E., Hollinshead, M., Sim, R. B. & Smith, G. L. Extracellular enveloped vaccinia virus is resistant to complement because of incorporation of host complement control proteins into its envelope. *Proc. Natl. Acad. Sci. U. S. A.* **95,** 7544–9 (1998).

19. Diebolder, C. a *et al.* Complement is activated by IgG hexamers assembled at the cell surface. *Science (80-.).* **343,** 1260–3 (2014).

20. Ikeda, K. *et al.* Complement Depletion Facilitates the Infection of Multiple Brain Tumors by an Herpes Simplex Virus Mutant. *J. Virol.* **74,** 4765–4775 (2000).

21. Russell, S. J. *et al.* Remission of disseminated cancer after systemic oncolytic virotherapy. *Mayo Clin. Proc.* **89,** 926–33 (2014).

22. White, C. L. *et al.* Characterization of the adaptive and innate immune response to intravenous oncolytic reovirus (Dearing type 3) during a phase I clinical trial. *Gene Ther.* **15,** 911–20 (2008).

23. Magge, D. *et al.* Inhibitors of C5 complement enhance vaccinia virus oncolysis. *Cancer Gene Ther.* **20,** 342–50 (2013).

24. Leddy, J. P., Simons, R. L. & Douglas, R. G. Effect of Selective Complement Deficiency on the Rate of Neutralization of Enveloped Viruses by Human Sera. *J. Immunol.* **118,** 28–34 (1977).

25. Roberts, D. M. *et al.* Hexon-chimaeric adenovirus serotype 5 vectors circumvent pre-existing anti-vector immunity. *Nature* **441,** 239–43 (2006).

26. Miest, T. S. *et al.* Envelope-chimeric entry-targeted measles virus escapes neutralization and achieves oncolysis. *Mol. Ther.* **19,** 1813–20 (2011).

27. Muik, A. *et al.* Re-engineering Vesicular Stomatitis Virus to Abrogate Neurotoxicity, Circumvent Humoral Immunity, and Enhance Oncolytic Potency. *Cancer Res.* **74,** 3567–78 (2014).

28. Tesfay, M. Z. *et al.* PEGylation of vesicular stomatitis virus extends virus persistence in blood circulation of passively immunized mice. *J. Virol.* **87,** 3752–9 (2013).

29. Carlisle, R. C. *et al.* Human erythrocytes bind and inactivate type 5 adenovirus by presenting Coxsackie virus-adenovirus receptor and complement receptor 1. *Blood* **113,** 1909–1918 (2009).

30. Kim, M. K. *et al.* Oncolytic and immunotherapeutic vaccinia induces antibody-mediated complement-dependent cancer cell lysis in humans. *Sci. Transl. Med.* **5,** 185ra63 (2013).

31. Ong, G. L. & Mattes, M. J. Mouse strains with typical mammalian levels of complement activity. *J. Immunol. Methods* **125,** 147–58 (1989).

32. Ebanks, R. O. & Isenman, D. E. Mouse complement component C4 is devoid of classical pathway C5 convertase subunit activity. *Mol. Immunol.* **33,** 297–309 (1996).

33. Ratelade, J. & Verkman, a S. Inhibitor(s) of the classical complement pathway in mouse serum limit the utility of mice as experimental models of neuromyelitis optica. *Mol. Immunol.* **62,** 104–113 (2014).

34. Guo, Z. S. *et al.* The combination of immunosuppression and carrier cells significantly enhances the efficacy of oncolytic poxvirus in the pre-immunized host. *Gene Ther.* 1–11 (2010). doi:10.1038/gt.2010.104

35. Pio, R., Ajona, D. & Lambris, J. D. Complement inhibition in cancer therapy. *Semin. Immunol.* **25,** 54–64 (2013).

36. Markiewski, M. M. *et al.* Modulation of the antitumor immune response by complement. *Nat. Immunol.* **9,** 1225–35 (2008).

37. Parato, K. a *et al.* The oncolytic poxvirus JX-594 selectively replicates in and destroys cancer cells driven by genetic pathways commonly activated in cancers. *Mol. Ther.* **20,** 749–58 (2012).

38. Sanfilippo, C. M. & Blaho, J. a. ICP0 gene expression is a herpes simplex virus type 1 apoptotic trigger. *J. Virol.* **80,** 6810–21 (2006).

39. Sobol, P. T. *et al.* Adaptive antiviral immunity is a determinant of the therapeutic success of oncolytic virotherapy. *Mol. Ther.* **19,** 335–44 (2011).

40. Bexborn, F. *et al.* Hirudin versus heparin for use in whole blood in vitro biocompatibility models. *J. Biomed. Mater. Res. A* **89,** 951–9 (2009).

41. Zhao, H., Wakamiya, N., Suzuki, Y., Hamonko, M. T. & Stahl, G. L. Identification of human mannose binding lectin (MBL) recognition sites for novel inhibitory antibodies. *Hybrid. Hybridomics* **21,** 25–36 (2002).

42. Thurman, J. M. *et al.* A novel inhibitor of the alternative complement pathway prevents antiphospholipid antibody-induced pregnancy loss in mice. *Mol. Immunol.* **42,** 87–97 (2005).

43. Walsh, M. C. *et al.* Fluorochrome-linked immunoassay for functional analysis of the mannose binding lectin complement pathway to the level of C3 cleavage. *J. Immunol. Methods* **323,** 147–59 (2007).

ACKNOWLEDGEMENTS

We thank S Avery (UHN Animal Resource Centre, Toronto, ON, Canada) for assisting with non-human primate housing and experiments. We also thank K Yates and E MacDonald for technical assistance with the rat experiments. We are grateful to M Morrissey for assistance with the MBL assay. We thank D Vaillant for assistance in the preparation of virus as well as members of the Bell, Auer, Atkins and Diallo laboratories for feedback on this project.

FUNDING

J.C.B. is supported by the Terry Fox Research Foundation, the Ontario Institute for Cancer Research and the Ottawa Regional Cancer Foundation. J.A.M. is supported by the Ontario Institute for Cancer Research. J.D.L. is supported by the National Institutes of Health grants AI068730 and the European Community's Seventh Framework Programme under grant agreement no. 602699 (DIREKT) L.E. is the recipient of a Canadian Institute for Health Research Canada Graduate Scholarship.

COMPETING INTERESTS

J.D.L. is the inventor of a patent and/or patent applications that describe the use of complement inhibitors for therapeutic purposes and the founder of Amyndas Pharmaceuticals, which is developing complement inhibitors for clinical applications.

C.J.B and D.K are employees of SillaJen.

AUTHOR CONTRIBUTIONS

L.E., J.C.B., S.A.A., J.A.M., J.D.L., G.L.S., C.J.B., D.K., H.A., R.C.A., J.M.T., K.A.P., C.S.I. and C.G.L. were involved in the conception and design of experiments. L.E., M.M. and S.A.A. conducted *in vitro* experiments. C.T.S, L.E. and T.F. were involved in the rat experiments. L.E., S.A.A., D.H., A.G., R.L., S.F., J.A.M. and J.C.B. were involved in the non-human primate experiment. Statistical analysis was performed by L.E. and aided by S.C.F. The manuscript was written and reviewed by L.E., J.C.B., C.J.B, C.G.L., M.M., J.D.L, S.A.A. and J.A.M.

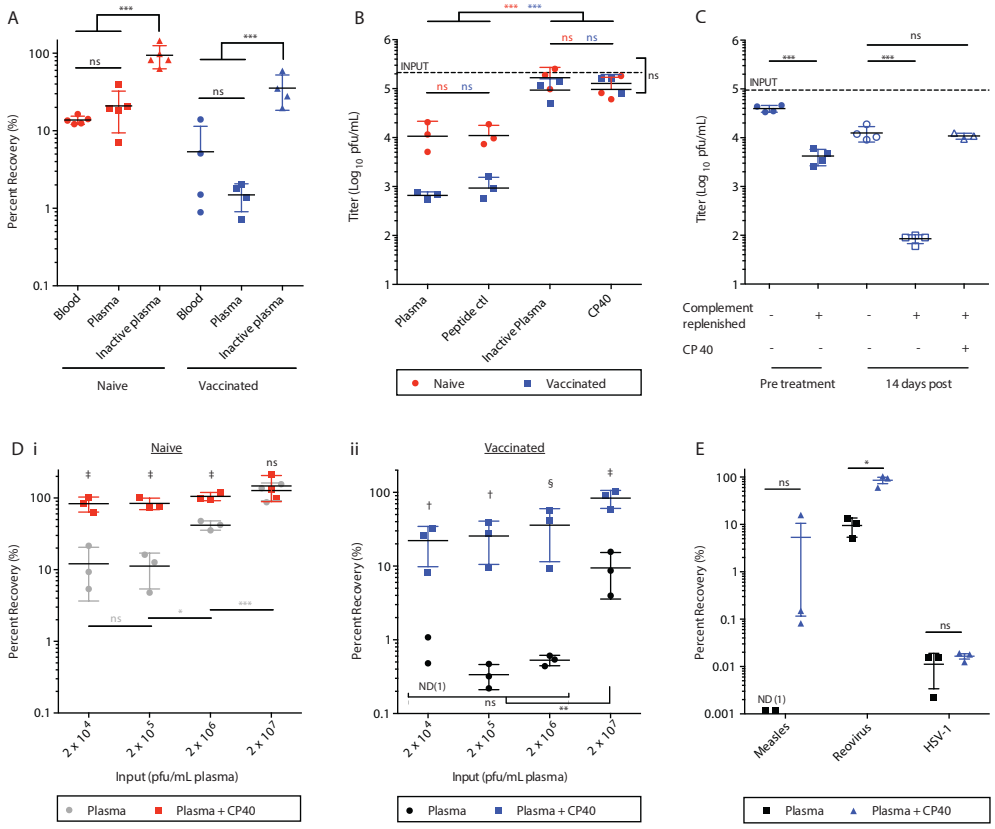
A
Percent Recovery (%)
Blood
Plasma
Inactive plasma
Naive
Vaccinated
B
Titer (Log10 pfu/mL)
INPUT
Plasma
Peptide ctl
Inactive Plasma
CP40
Naive
Vaccinated
C
Titer (Log10 pfu/mL)
INPUT
Complement replenished
CP 40
Pre treatment
14 days post
D i
Naive
Percent Recovery (%)
Input (pfu/mL plasma)
Plasma
Plasma + CP40
ii
Vaccinated
ND(1)
E
Measles
Reovirus
HSV-1
ND (1)

Figure 1.

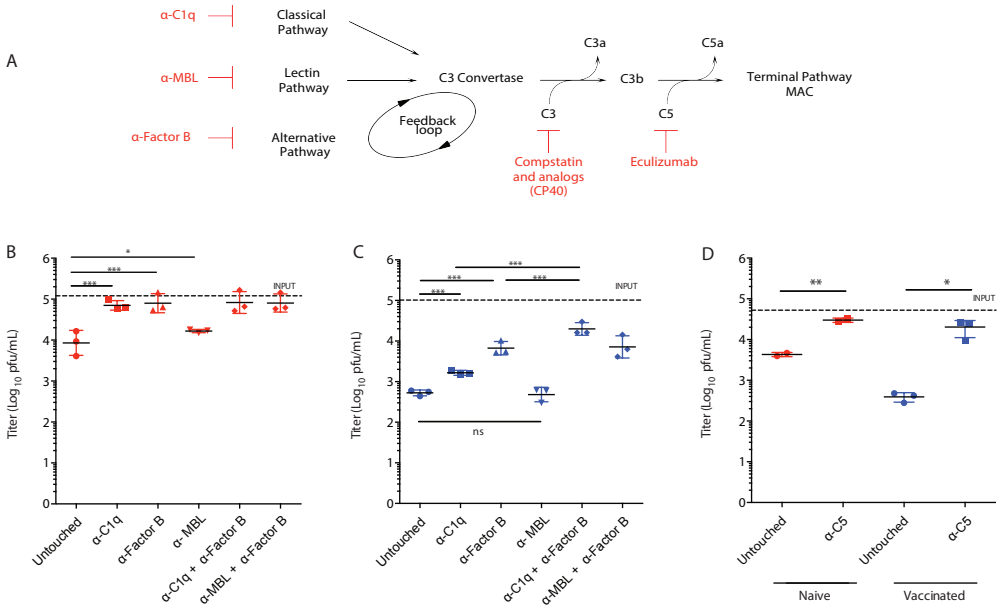
A
α-C1q
α-MBL
α-Factor B
Classical Pathway
Lectin Pathway
Alternative Pathway
C3 Convertase
Feedback loop
C3a
C3b
C5a
C3
C5
Terminal Pathway MAC
Compstatin and analogs (CP40)
Eculizumab
B
C
D
Titer (Log10 pfu/mL)
INPUT
Untouched
α-C1q
α-Factor B
α- MBL
α-C1q + α-Factor B
α-MBL + α-Factor B
ns
α-C5
Naive
Vaccinated

Figure 2.

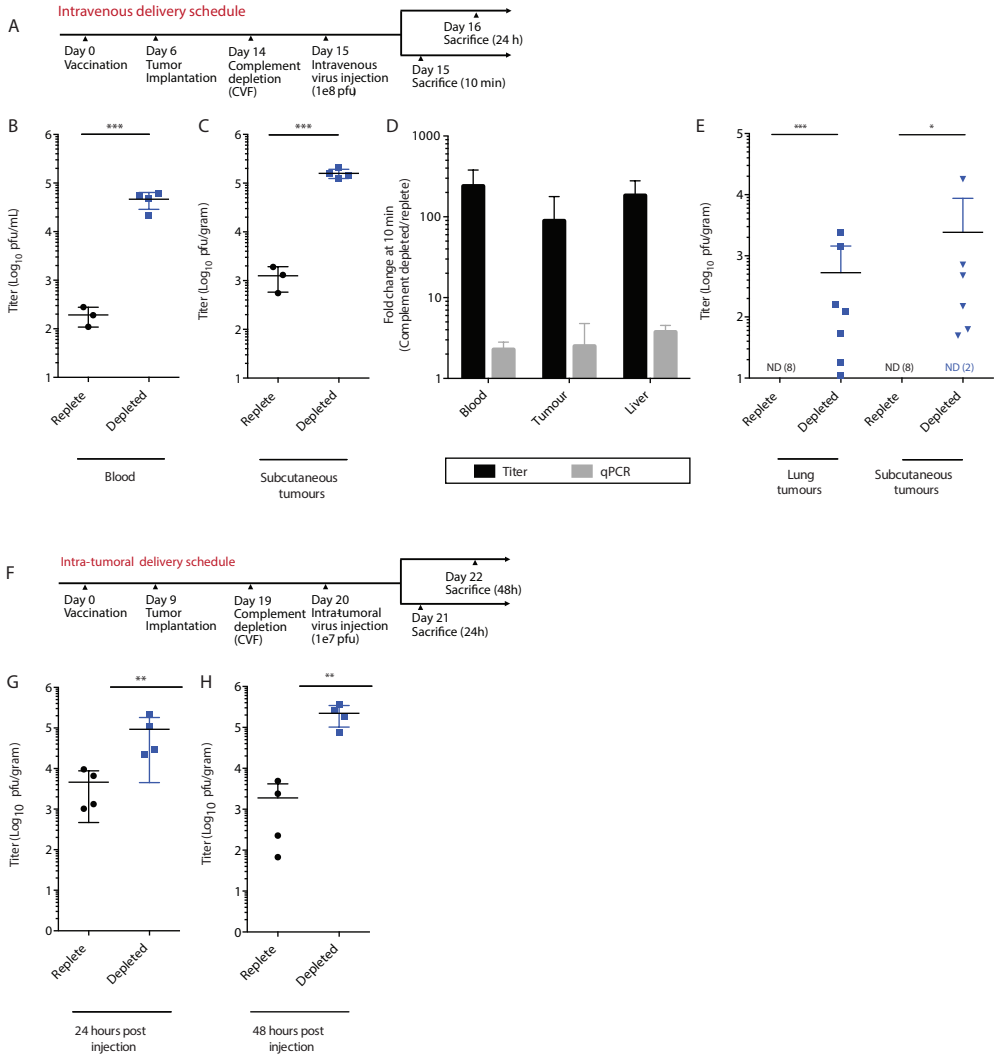
A
Intravenous delivery schedule
Day 0
Vaccination
Day 6
Tumor
Implantation
Day 14
Complement
depletion
(CVF)
Day 15
Intravenous
virus injection
(1e8 pfu
Day 16
Sacrifice (24 h)
Day 15
Sacrifice (10 min)
B
Titer (Log10 pfu/mL)
***
Replete
Depleted
Blood
C
Titer (Log10 pfu/gram)
***
Replete
Depleted
Subcutaneous
tumours
D
Fold change at 10 min
(Complement depleted/replete)
1000
100
10
1
Blood
Tumour
Liver
Titer
qPCR
E
Titer (Log10 pfu/gram)
***
*
ND (8)
ND (8)
ND (2)
Replete
Depleted
Replete
Depleted
Lung
tumours
Subcutaneous
tumours
F
Intra-tumoral delivery schedule
Day 0
Vaccination
Day 9
Tumor
Implantation
Day 19
Complement
depletion
(CVF)
Day 20
Intratumoral
virus injection
(1e7 pfu)
Day 22
Sacrifice (48h)
Day 21
Sacrifice (24h)
G
Titer (Log10 pfu/gram)
**
Replete
Depleted
24 hours post
injection
H
Titer (Log10 pfu/gram)
**
Replete
Depleted
48 hours post
injection

Figure 3.

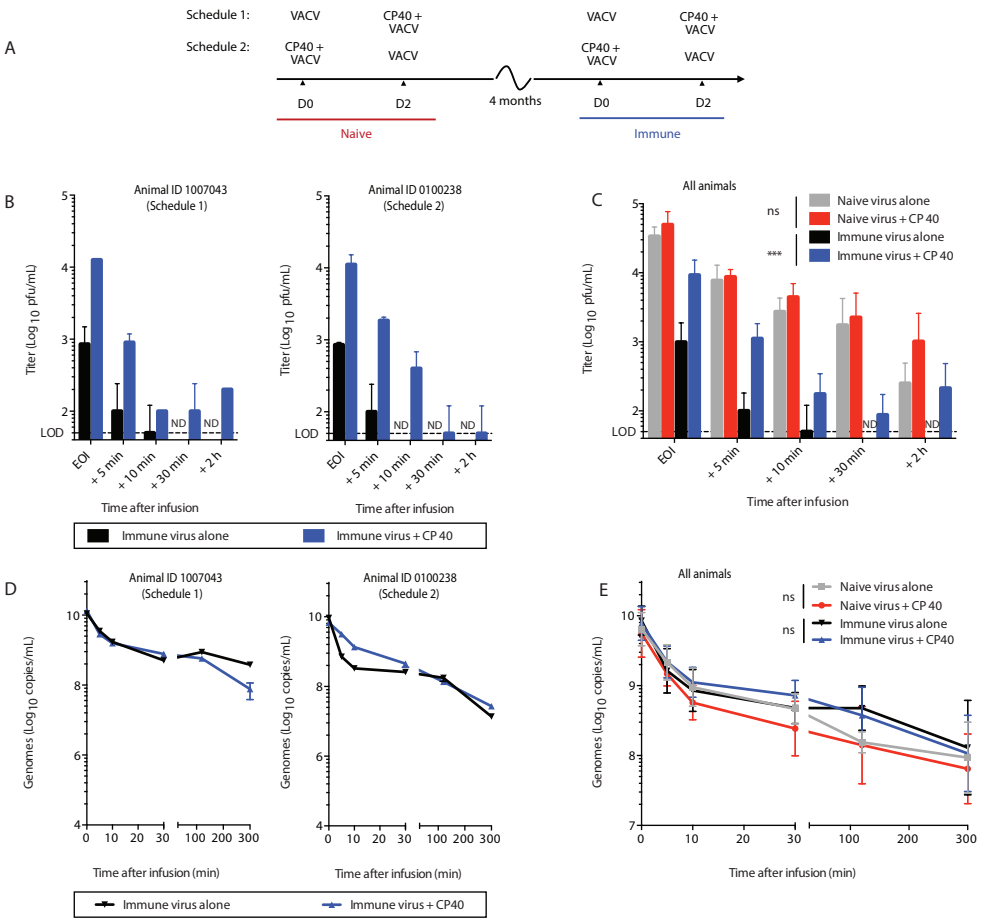
A
Schedule 1:
VACV
CP40 + VACV
VACV
CP40 + VACV
Schedule 2:
CP40 + VACV
VACV
CP40 + VACV
VACV
D0
D2
4 months
D0
D2
Naive
Immune
B
Animal ID 1007043 (Schedule 1)
Animal ID 0100238 (Schedule 2)
Titer (Log 10 pfu/mL)
LOD
ND
EOI
+ 5 min
+ 10 min
+ 30 min
+ 2 h
Time after infusion
Immune virus alone
Immune virus + CP 40
C
All animals
ns
***
Naive virus alone
Naive virus + CP 40
Immune virus alone
Immune virus + CP 40
D
Animal ID 1007043 (Schedule 1)
Animal ID 0100238 (Schedule 2)
Genomes (Log10 copies/mL)
Time after infusion (min)
Immune virus alone
Immune virus + CP40
E
All animals
ns
ns
Naive virus alone
Naive virus + CP 40
Immune virus alone
Immune virus + CP40
Time after infusion (min)

Figure 4.

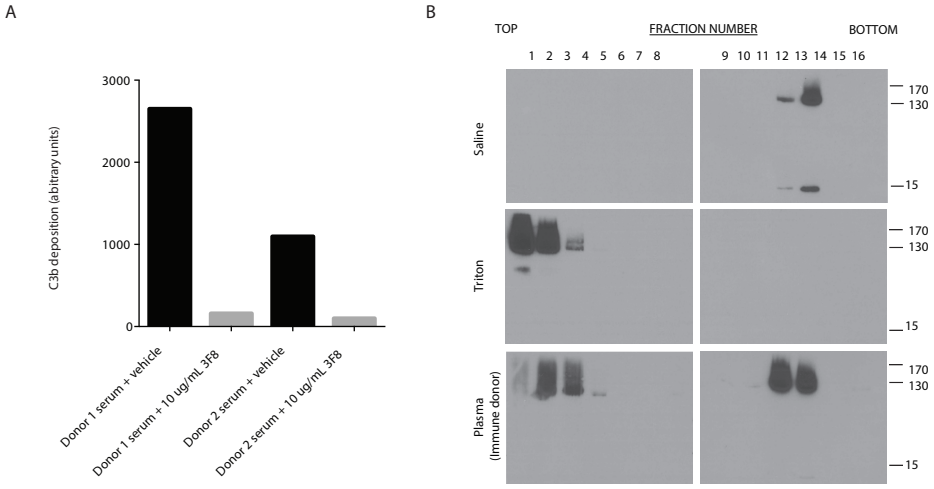

Supplemental Figure 1.

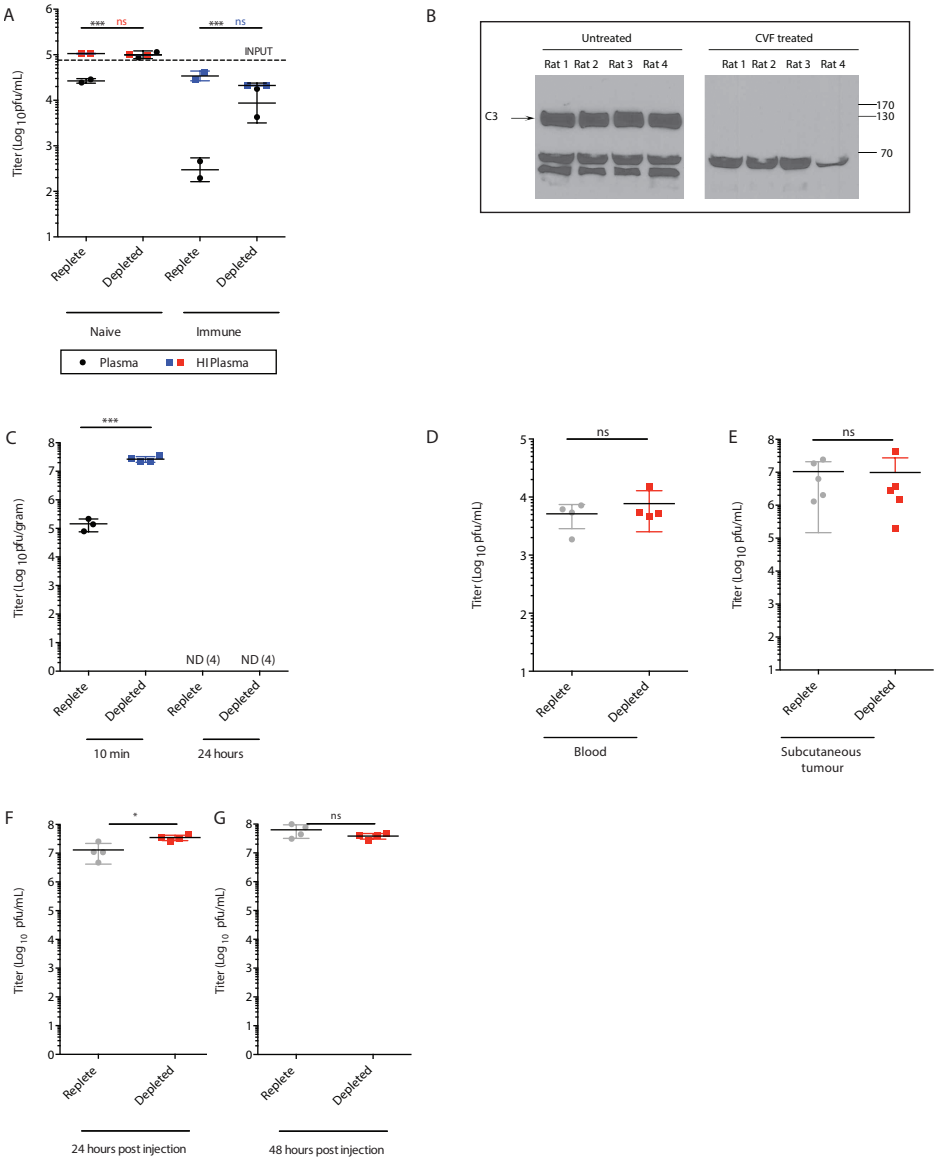

Supplemental Figure 2.

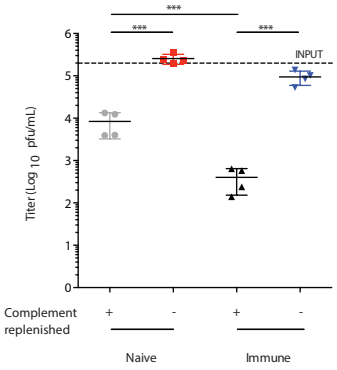

Supplemental Figure 3.

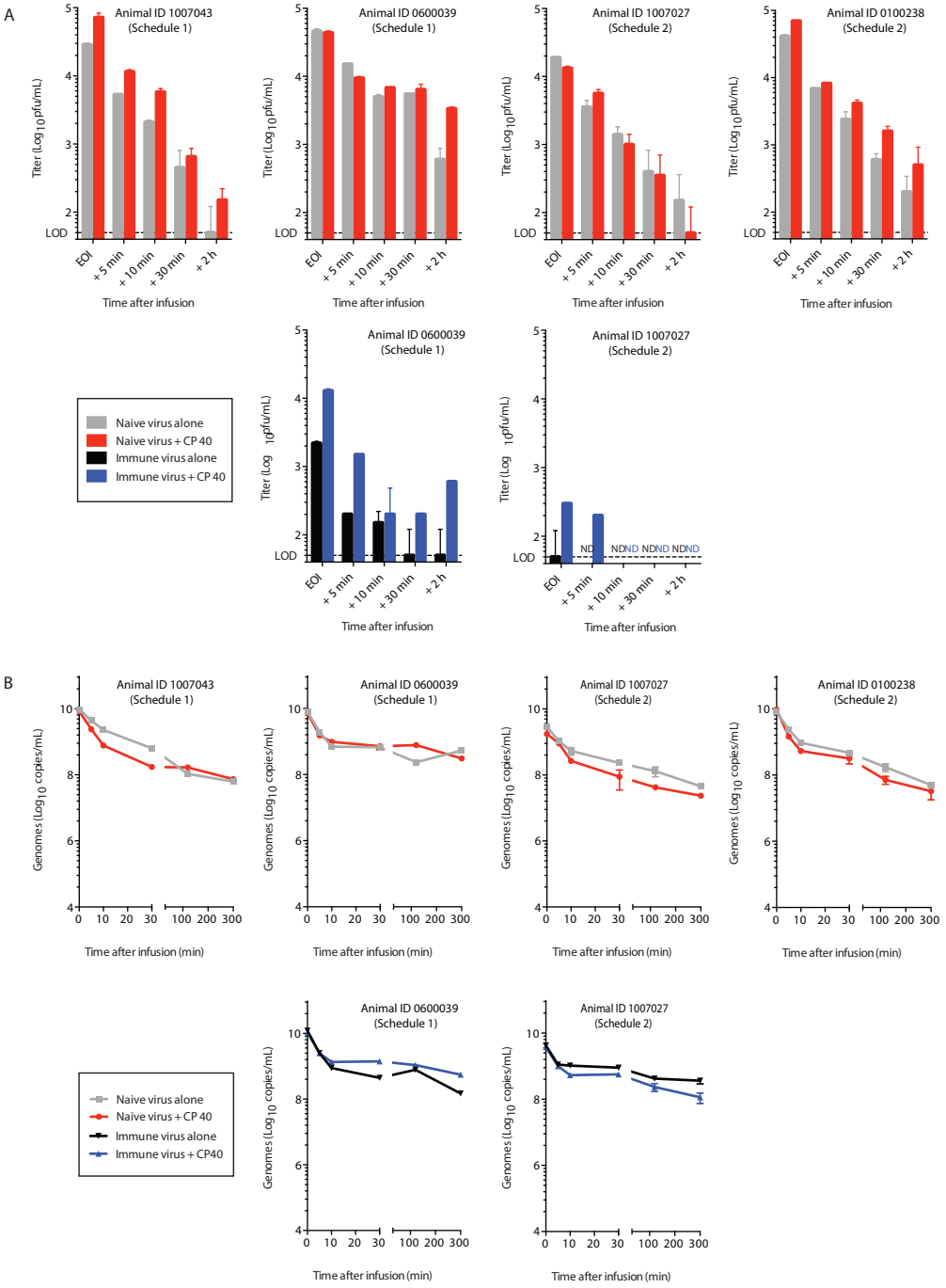

Supplemental Figure 4.

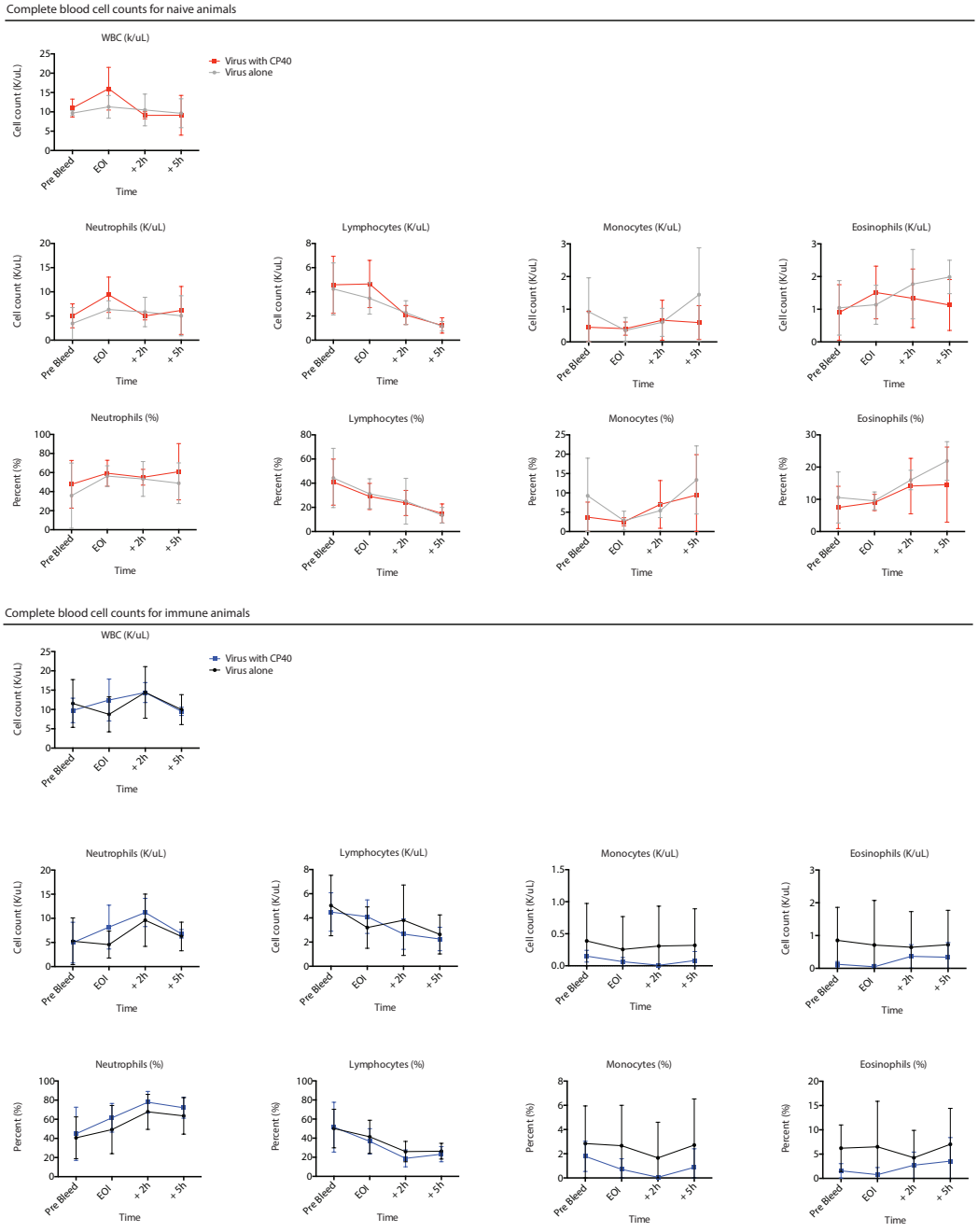

Supplemental Figure 5.

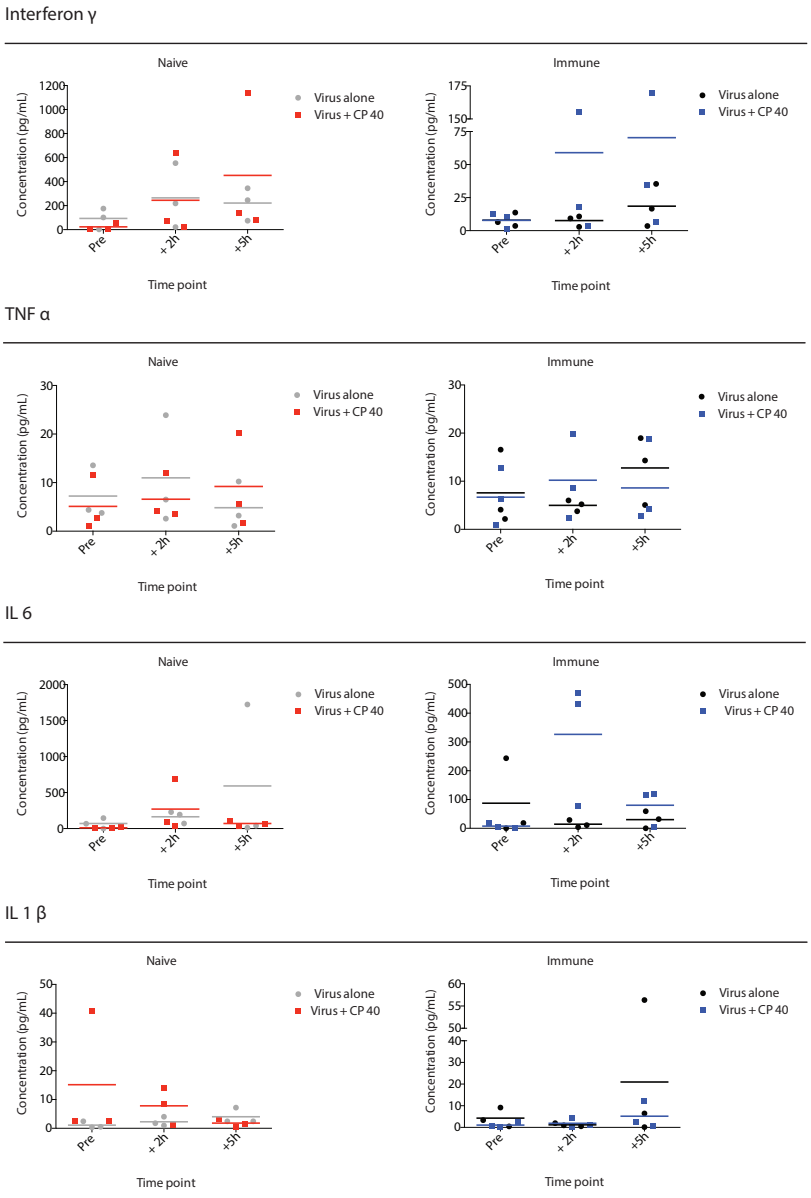

Supplemental Figure 6.

Supplemental Table. 1 Incidence of fever on the day of virus infusion

		Naïve		Immune	
Animal ID	Schedule	Virus alone	Virus + CP40	Virus alone	Virus + CP40
0600039	1	N	N	N	N
1007043	1	Y	Y	N	N
1007027	2	Y	N	N	N
0100238	2	Y	N	N	N

Supplemental Table 1.

Curriculum Vitae

LAURA EVGIN
EDUCATION

September 2009 – Present

PhD Biochemistry University of Ottawa
Thesis Supervisor: Dr. John Bell
Thesis Title: Modeling the interactions of oncolytic Vaccinia virus in the blood to achieve efficient systemic delivery
Transferred from a Masters programme to a PhD programme 2011

September 2005 – May 2009

BSc. Honours Specialization in Biochemistry University of Ottawa
Thesis Supervisor: Dr. John Bell
Thesis Title: Potent oncolytic activity of raccoonpox virus in the absence of natural pathogenicity

Awards

2012 **CIHR Canada Graduate Scholarship Doctoral Research Award**
2012 **Ontario Graduate Scholarship** (Declined)
2011 **Ontario Graduate Scholarship**
2010 **CIHR Fredrick Banting and Charles Best Canada Graduate Scholarship Master's Award**
2009 **University of Ottawa Excellence Scholarship**
2009 **Ontario Graduate Scholarship for Science and Technology**
2009 **University of Ottawa Merit Scholarship**
2008 **University of Ottawa Merit Scholarship**
2005 **University of Ottawa Admission Scholarship**

RESEARCH EXPERIENCE

PhD Candidate, University of Ottawa, Ottawa Hospital Research Institute, John Bell Lab

Description
The focus of this project has been to identify the barriers that exist to systemic oncolytic virotherapy with vaccinia virus and to develop strategies to overcome neutralizing factors in the blood.

- Extensive experience with cell culture and virology techniques (including vaccinia, HSV, rhabdoviruses, measles virus, reovirus).
- Proficiency with molecular biology techniques such as PCR, qPCR, Western blotting, ELISAs.
- Experience with complement assays, including classical and alternative hemolytic assays.
- Developed two IRB approved protocols for the collection of human blood samples.

- Worked in collaboration with experts in the complement field who provided us with reagents to dissect the mechanism of complement-mediated neutralization of Vaccinia virus.
- Established a rat model with mammary adenocarcinoma tumors to assess the impact of complement modulation strategies on systemic administration of virus.
- Designed and undertook a cynomolgus macaque experiment to evaluate the effect of a clinical candidate complement inhibitor in collaboration with Dr. Andrea McCart and Dr. John Lambris at the University Health Network in Toronto, Ontario.
- Undertook for two clinical trials an evaluation of the infectivity of Vaccinia virus and its cellular associations following intravenous administration of Pexa-Vec (JX594) to patients.

Honors thesis project, University of Ottawa, Ottawa Hospital Research Institute, John Bell Lab

Description
This project characterized raccoonpox virus as a novel oncolytic virus.

- Assessed the ability of the virus to replicate in as well as cause cytotoxicity in a panel of cell lines from the NCI-60 cell panel.
- Validated with in vitro lytic capacity of raccoonpox virus in syngeneic and xenograft mouse models of cancer.

Collaborators

Dr. Andrea McCart (University Health Network, Toronto, Ontario, Canada)
Dr. John Lambris (University of Pennsylvania, Philadelphia, Pennsylvania, USA)
Dr. Greg Stahl (Harvard University, Cambridge Massachusetts, USA)
Dr. Joshua Thurman (University of Colorado, Boulder, Colorado, USA)
Dr. Alan Melcher (University of Leeds, Leeds, UK)

PUBLICATIONS AND PRESENTATIONS

Publications
Submitted November 2014

- **Complement inhibition prevents oncolytic vaccinia virus neutralization in immune humans and cynomolgus macaques**
  Evgin L, Acuna SA, Tanese de Souza C, Marguerie M, Lemay CG, Ilkow CS, Findlay SC, Falls T, Parato KA, Hanwell D, Goldstein A, Lopez R, Lafrance S, Breitbach CJ, Kirn D, Atkins H, Auer RC, Thurman JM, Stahl GL, Lambris JD, Bell JC, McCart JA

In preparation

- **Characterization of the human innate immune effects of systemic oncolytic vaccinia virus delivery to different anatomical sites**

Published

- **Evgin L**, Vähä-Koskela M, Rintoul J, Falls T, Le Boeuf F, Barrett JW, Bell JC, Stanford MM. Potent oncolytic activity of raccoonpox virus in the absence of natural pathogenicity, Mol Ther 2010, 18(5):896-902
- Breitbach CJ, Burke J, Jonker D, Stephenson J, Haas AR, Chow LQ, Nieva J, Hwang TH, Moon A, Patt R, Pelusio A, Le Boeuf F, Burns J, **Evgin L**, De Silva N, Cyancic S,

Robertson T, Je JE, Lee YS, Parato K, Diallo JS, Fenster A, Daneshmand M, Bell JC, Kirn DH. (2011). Intravenous delivery of a multi-mechanistic cancer-targeted oncolytic poxvirus in humans, Nature 477(7362):99-102

- Muharemagic D, Zamay A, Ghobadloo SM, **Evgin L**, Savitskaya A, Bell JC, Berezovski MV. (2014) Aptamer-facilitated protection of oncolytic virus from neutralizing antibodies, Mol Ther Nucleic Acids June 3 doi: 10.1038/mtna.2014.19
- Breitbach CJ, De Silva NS, Falls TJ, Aladl U, **Evgin L**, Paterson J, Sun YY, Roy GG, Rintoul JL, Daneshmand M, Parato K, Stanford MM, Lichty BD, Fenster A, Kirn D, Atkins H, Bell JC. (2011) Targeting Tumor Vasculature With an Oncolytic Virus, Mol Ther. 19(5):886-94
- Parato KA, Breitbach CJ, Le Boeuf F, Wang J, Storbeck C, Ilkow C, Diallo JS, Falls T, Burns J, Garcia V, Kanji F, **Evgin L**, Hu K, Paradis F, Knowles S, Hwang TH, Vanderhyden BC, Auer R, Kirn DN, Bell JC. (2011) The Oncolytic Poxvirus JX594 Selectively Replicates in and Destroys Cancer Cells Driven by Genetic Pathways Commonly Activated in Cancers. Mol Ther. 20(4):749-58

Oral Presentations

2014 Overcoming Vaccinia virus neutralization in immune humans and macaques with complement inhibition
8th International Conference on Oncolytic Virus Therapeutics, Oxford UK

2014 Overcoming Vaccinia virus neutralization in immune humans and macaques with complement inhibition
Terry Fox Research Institute Annual Scientific Meeting, Montreal, Quebec

Poster Presentations

2014 Terry Fox Research Institute Annual Scientific Meeting, Montreal, Quebec.
2013 Canadian Cancer Research Conference, Toronto, Ontario
2013 Seventh International Meeting on Replicating Oncolytic Virus Therapeutics, Quebec City, Quebec
2012 XXIV International Complement Workshop, Chania, Crete, Greece
2012 XIX International Poxvirus Asfivirus and Iridovirus Symposium, Salamanca Spain
2011 The Canadian Cancer Research Conference, Toronto, Ontario
2011 The 6th International Conference on Oncolytic Viruses as Cancer Therapeutics, Las Vegas, Nevada
2010 XVIII International Poxvirus, Asfivirus and Iridovirus Symposium, Sedona, Arizona
2010 Ontario Institute for Cancer Research Meeting, Toronto, Ontario

VOLUNTEER WORK AND OTHER EXPERIENCE

Let's Talk Science *September 2009- Present*
I am currently involved with Let's Talk Science, a non-profit organization whose aim it is to inspire young people to become excited about science. I have participated in multiple demonstrations and science fairs.

Languages: English and French